UNIVERSITÉ DU QUÉBEC À MONTRÉAL

TROIS ESSAIS EN MACROÉCONOMÉTRIE

THÈSE

PRÉSENTÉE

COMME EXIGENCE PARTIELLE

DU DOCTORAT EN ÉCONOMIQUE

PAR

STÉPHANE SURPRENANT

FÉVRIER 2025

REMERCIEMENTS

Je tiens à remercier mes directeurs de recherche, Alain Guay et Dalibor Stevanovic. Vous m'avez donné l'opportunité de participer à plusieurs projets de recherche et cela a grandement contribué à enrichir mon parcours. Je tiens aussi à vous remercier pour le soutien indispensable que vous m'avez offert à chaque étape du programme. Vous avez été grandement disponibles que ce soit pour des questions rapides ou des discussions plus longues et cela même quand l'échéancier se faisait serré.

J'aimerais aussi remercier le corps professoral du département des sciences économiques. Au-delà des cours et des séminaires, vous avez créer un environnement stimulant qui invite à la réflexion, le questionnement et la discussion. J'aimerais en particulier remercier Alain Paquet avec qui j'ai eu de très nombreuses discussions tout au long de mon parcours universitaire, du baccalauréat au doctorat. Cela a toujours été et continuera d'être un grand plaisir de discuter de macroéconomie avec toi, Alain. Je remercie également tous les étudiant(e)s de maîtrise et de doctorat avec qui j'ai eu plusieurs échanges intéressants et le personnel administratif, Martine, Julie et Karine, pour leur disponibilité et leur soutien.

Je remercie aussi le conseil de recherches en sciences humaines (CRSH), le département des sciences économiques et la chaire en macroéconomie et prévisions pour leur soutien financier.

Je tiens ensuite à remercier mon père, ma mère et mon frère. Même si le parcours a été long et difficile, vous avez toujours été là pour moi durant mes études universitaires, du baccalauréat au doctorat.

Finalement, je souhaite remercier ma merveilleuse épouse, AnnShirley. Tu es entrée dans ma vie au début du programme de doctorat et tu as été là pour moi durant les examens, les travaux, les projets de recherche qui ne semblaient jamais vraiment se terminer et durant mon entrée sur le marché du travail. Merci du fond du coeur d'avoir été à mes côtés et d'être dans ma vie.

DEDICACE

À mon épouse, AnnShirley.

CONTENTS

LIST OF TABLES

LIST OF FIGURES

RÉSUMÉ

Cette thèse est composée de trois articles. Chaque article se concentre sur des problèmes différents et les résultats sont pertinents pour le travail empirique en macroéconomie.

Le premier chapitre concerne la capacité des modèles à vecteurs autorégressifs par quantile (QVAR) à prévoir les risques macroéconomiques dans plusieurs contextes. Les modèles QVAR ont été introduits par White et al. (2015), Chavleishvili and Manganelli (2021) et Ruzicka (2021) dans les contextes de prévision de la valeur en jeu (*value-at-risk*), des scénarios de prévision et de l'analyse structurelle. Par contre, leur capacité à prévoir les densités et les quantiles dans les queues de distributions n'avait pas encore été évaluée. Cet article propose de procéder à cette évaluation sur la base d'une comparaison relative à des modèles paramétriques standards dans un exercice de prévision pseudo-hors-échantillon couvrant 112 variables mensuelles aux États-Unis, ainsi qu'une période de plus de 40 ans. Les modèles QVAR font systématiquement mieux que les modèles paramétriques, particulièrement pour le marché du travail et les taux d'intérêt. De plus, l'utilisation de facteurs estimés par composantes principales comme dans Stock and Watson (2002a,b) et de facteurs quantiles introduits par Chen et al. (2021) améliore la précision des prévisions, particulièrement pour le marché du travail. Les QVAR sont donc des modèles adéquats pour la prévision de risque en macroéconomie.

Le second chapitre porte sur le problème d'identification de chocs structurels en présence de données macroéconomiques persistentes. L'approche par maximisation des parts (*Max Share*) identifie un choc en maximisant sa contribution dans la décomposition de la variance de l'erreur de prévision pour une variable cible à un horizon donné.[1] Cette méthode est souvent appliquée sur des variables en niveau (par exemple, Barsky

[1]Cela s'applique aussi sur une séquence d'horizons ou, encore, sur une bande de fréquences dans le domaine des fréquences.

and Sims (2011) ou Zeev and Khan (2015)) et cible des horizons distants afin d'éviter d'avoir à se prononcer sur la structure de cointégration du système. Nous montrons théoriquement que cette stratégie mène généralement à des estimateurs non converents. Nous illustrons dans des simulations Monte Carlo que ceci peut conduire à des biais importants et des erreurs quadratiques (*RMSE*) plus grandes à des horizons intermédiaires et longs. Une application empirique aux chocs de nouvelles (*news shocks*) sur la technologie spécifique à l'investissement (*IST*) et sur la productivité multifactorielle (*TFP*) illustre la pertinence des résultats pour le travail empirique.

Le troisième chapitre présente une grande base de données canadienne[2] et établit son utilité pour le travail empirique. La base de données a été construite pour offrir une version canadienne de la base de donnée FRED-MD (McCracken and Ng, 2016) qui est disponible publiquement pour les États-Unis et elle a été créée pour pouvoir être mise à jour régulièrement. Les millésimes (*vintages*) en temps réel sont aussi conservés afin de soutenir d'éventuels travaux de recherche. L'article montre aussi que la base de données présente une structure à facteurs latents relativement stable, qu'elle permet d'améliorer notre capacité à prévoir les points de retournements du cycle canadien et qu'elle améliore la précision des prévisions macroéconomiques. Nous montrons aussi comment la base de données peut servir pour étudier l'hétérogénéité des réponses à un choc de politique monétaire à travers le Canada.

Mots-clés: Régression quantile, risque macroéconomique, prévision par densité, prévision par quantile, facteurs quantiles, SVAR, identification par maximisation des parts et inférence, racines unitaires, racines quasi-unitaires, asymptotique, environnement riche en données, modèle à facteurs, prévision, analyse structurelle.

---

[2]La base de données est disponible publiquement et a été mise à jour à chaque mois depuis mars 2019. La version actuelle, ainsi que tous les millésimes (*vintages*) depuis mars 2019 sont disponibles ici: https://chairemacro.esg.uqam.ca/donnees/base-de-donnees-canadiennes/.

INTRODUCTION

La présente thèse est composée de trois articles où chacun porte sur une question pertinente pour le travail empirique en macroéconomie. En particulier, cette thèse couvre des problèmes liés à la prévision du risque en macroéconomie, l'identification de chocs structurels en présence de données persistentes et le travail empirique dans un environnement riche en données.

D'abord, la crise financière de 2007 et la pandémie du COVID-19 ont mis fin à la période de la Grande Modération. Ce retour de la volatilité macroéconomique dans les pays occidentaux a été accompagné d'une prolifération de travaux de recherches sur la modélisation du risque en macroéconomie. Des travaux comme ceux de Giglio et al. (2016) et Adrian et al. (2019) ont popularisé l'utilisation de régressions quantiles et ont établi qu'une hausse de stress financiers était liée à une distribution asymétrique de la croissance de la production. Plusieurs études ont ensuite évalué la capacité de divers indicateurs de stress financier dans ce type de modèles pour prévoir le risque sur la croissance de la production (par exemple, Figueres and Jarociński (2020), Adams et al. (2021) et Iseringhausen (2021)) et l'inflation (par exemple, Manzan and Zerom (2013), Manzan (2015) et López-Salido and Loria (2020)). Dans ce contexte, White et al. (2015), Chavleishvili and Manganelli (2021), Chavleishvili et al. (2021) et Ruzicka (2021) ont introduit les modèles quantiles vectoriels autorégressifs (QVAR) l'analyse dans un contexte multivarié.

Le premier chapitre contribue à cette litérature en offrant une évaluation au sens large de la capacité de prévision du risque macroéconomique des modèles QVAR. Nous procédons à une évaluation de la précision des prévisions par densité et par quantiles dans les queues de distribution des modèles QVAR à l'aide d'un exercice pseudo-hors-échantillon. Celui-ci couvre 112 variables macroéconomiques mensuelles aux États-Unis sur une période de plus de 40 ans pour des horizons de 1 à 12 mois. Nous comparons le modèle QVAR à trois modèles paramétriques standards, soit un VAR Gaussien, un VAR-GARCH et un VAR avec volatilité stochastique. Le modèle QVAR fait souvent significativement et quantitativement mieux et rarement pire que les modèles paramétriques standards. Les améliorations sont concentrées dans le marché du travail, ainsi que les taux d'intérêt et de change. Introduire des facteurs estimés par composantes principales (comme Stock and Watson (2002a,b)) ou des facteurs quantiles introduits par Chen et al. (2021) permet d'améliorer significativement la précision des prévisions de risque dans quelques cas comme pour le marché du travail. Nous concluons que le modèle QVAR est une méthode adéquate de prévision du risque macroéconomique.

Ensuite, bien que le premier chapitre se concentre sur la prévision et demande essentiellement à quel point les modèles QVAR offrent une représentation adéquate du risque macroéconomique, l'intérêt principal de leur utilisation est la possibilité qu'ils offrent d'évaluer si les chocs structurels peuvent avoir des effets différents à différents quantiles des distributions des variables macroéconomiques.

L'identification des réponses de différentes variables à des chocs structurels est un problème important en macroéconomie et peut éventuellement permettre de discriminer entre différents modèles théoriques. Cette identification est habituellement effectuée dans des modèles vectoriels autorégressifs accompagnés de divers types de restrictions. La plupart des modèles théoriques limitent le type de chocs qui peuvent avoir des effets permanents ce qui implique des relations de cointégration[3] et peut servir pour identifier des chocs structurels (par exemple, des chocs de productivité multifactorielle

[3]Des exemples sont disponibles dans King et al. (1991) et Serletis and Gogas (2014).

TFP shocks comme Gali (1999)). Par contre, ces restrictions pourraient ne pas tenir exactement dans les données et ce schéma d'identification requiert de contraindre le comportement de long terme des séries lors de l'estimation. Dans ce contexte, Francis et al. (2014) a proposé d'utiliser une approche introduite par Faust (1998) et Uhlig (2003, 2004) qui consiste à identifier un choc par la maximisation de sa contribution dans la décomposition de variance des erreurs de prévision (ce que nous appelons le *Max Share*). L'idée est donc d'échanger les restrictions de long terme qui imposent que seulements quelques chocs ont des effets non nuls à un horizon infini par la restrictions que ces chocs sont dominants à un horizon fini, mais long. L'approche est habituellement appliquée à un système estimés en niveau avec des variables possiblement cointégrées sans restrictions sur leur comportement de long terme (par exemple, Barsky et al. (2015) ou Zeev and Khan (2015)).

Le second chapitre étudie les propriétés de l'approche d'identification par maximisation des parts (*Max Share*) dans le contexte particulier où les variables employées sont persistentes[4]. Nous obtenons les distributions asymptotiques de cet estimateur et démontrons qu'il converge vers une matrice aléatoire ce qui implique que les estimateurs des vecteurs propres employés dans l'identification ainsi que les estimateurs des fonctions de réponses sont non convergents. Nous montrons dans des simulations Monte Carlo que les modèles VAR estimés en niveau dans ce contexte introduisent des biais significatifs et des erreurs quadratiques (*RMSE*) plus importantes aux horizons intermédiaires et longs comparativement à leur estimation sous des représentations stationnaires (par exemple, en différence première ou imposant la cointégration). Ceci est particulièrement important quand plusieurs chocs peuvent avoir des effets permanents. Une application empirique aux chocs de nouvelles (*news shocks*) sur la technologie spécifique à l'investissement (*IST*) et sur la productivité multifactorielle (*TFP*) illustre la pertinence des résultats pour le travail empirique.

[4]C'est-à-dire qu'elles introduisent des racines unitaires ou quasi-unitaires dans le VAR.

Finalement, que ce soit dans le contexte de la prévision ou de l'analyse structurelle, plusieurs études ont établit la valeur de pouvoir recourir à l'utilisation d'un grand ensemble de variables macroéconomiques et financières. Par exemple, Stock and Watson (2002b,a) ont proposé d'introduire des facteurs latents estimés par composantes principales comme variables explicatives dans des modèles autorégressifs à retards distribués (*autoregressive distributed lag*). Cela améliore souvent la capacité de prévision, même pour des algorithmes d'apprentissage automatique (e.g., Coulombe et al. (2021a, 2022)). Aussi, ces facteurs peuvent permettre de mieux approximer l'information disponible aux agents économiques et améliorer l'identification de chocs structurels (par exemple, Bernanke et al. (2005)). Par contre, construire une base de données macroéconomiques avec plusieurs dizaines de variables sur une période longue est un travail exigeant. Ceci peut aussi rendre difficile la mise à jour de résultats ou encore leur comparaison à travers plusieurs études puisque divers choix sont effectués lors de sa construction. McCracken and Ng (2016) ont introduit la base de données FRED-MD, une base de données mensuelles aux États-Unis qui imite la base de données employée par Stock and Watson (2002a,a), pour répondre à ce besoin.

Le troisième chapitre répond à ce besoin en introduisant une grande base de données pour le Canada sous le même principe que McCracken and Ng (2016). La base de données contient quelques centaines d'indicateurs économiques canadiens et provinciaux. Elle a été conçue afin de faciliter sa mise à jour régulière et ses millésimes (*vintages*) en temps réel sont disponibles publiquement[5]. Cette base de données permet d'éviter aux chercheurs le travail nécessaire pour prendre en compte les changements méthodologiques. Nous établissons quatre aspects utiles de cette base de données pour la recherche empirique en macroéconomie. Premièrement, la structure à facteurs explique une fraction importante de la variation observée dans les données et semblent

[5]La base de données est disponible publiquement et a été mise à jour à chaque mois depuis mars 2019. La version actuelle, ainsi que tous les millésimes (*vintages*) depuis mars 2019 sont disponibles ici: https://chairemacro.esg.uqam.ca/donnees/base-de-donnees-canadiennes/.

offrir une approche adéquate pour en réduire la dimension. Deuxièment, la base de données est utile pour prévoir les points de retournement du cycle d'affaires au Canada. Troisièmement, elle a un pouvoir prédictif substantiel pour des indicateurs macroéconomiques clés. Quartièmement, la richesse des variables incluses est exploitée pour étudier l'efficacité de la politique monétaire à travers les régions et les secteurs au Canada.

CHAPTER I

QUANTILE VARS AND MACROECONOMIC RISK FORECASTING

ABSTRACT

Recent rises in macroeconomic volatility have prompted the introduction of quantile VAR (QVAR) models for macroeconomic risk forecasting. This paper provides an extensive evaluation of the predictive performance of QVAR models in a pseudo-out-of-sample experiment spanning 112 US monthly variables over 40 years, with horizons of 1 to 12 months. We compare QVAR with three parametric benchmarks: a Gaussian VAR (VAR-N), a VAR-GARCH and a VAR with stochastic volatility (VAR-SV). QVAR frequently significantly and quantitatively improves upon parametric benchmarks and almost never performs significantly worse. Improvements are concentrated in the labor market and interest and exchange rates. Augmenting the QVAR model with factors (QFAVAR) estimated by principal components or the quantile factors significantly improves macroeconomic risk forecasting in some cases, mostly in the labor market. Generally, QVAR and QFAVAR perform equally well. We conclude that both are adequate tools for modeling macroeconomic risks.

Keywords: Quantile Regression, Macroeconomic Risk, Density Forecasting, Quantile Factors.
JEL Classification: C53, E37, C55.

1.1 Introduction

The rise in macroeconomic volatility experienced during the 2007 financial crisis and the COVID pandemic ended the Great Moderation and increased interest in modeling macroeconomic risk. Work by Giglio et al. (2016) and Adrian et al. (2019) popularized the use of quantile regressions in this context, providing evidence that financial stress leads to asymmetry in output growth. Many studies applied those methods in a single equation framework, focusing on the predictive power of financial indicators for risk to output growth (e.g., Figueres and Jarociński (2020), Adams et al. (2021) and Iseringhausen (2021)) and inflation (e.g., Manzan and Zerom (2013), Manzan (2015) and López-Salido and Loria (2020)). Others have proposed using quantile regressions as part of a structural analysis studying the effects of shocks on the conditional distribution of output growth (Loria et al., 2023) or to distinguish between shocks to upside, downside and total uncertainty (Forni et al., 2021). Against this background, several researchers (White et al. (2015), Chavleishvili and Manganelli (2021), Chavleishvili et al. (2021) and Ruzicka (2021)) have recently proposed a quantile VAR (QVAR) model for forecasting, scenario analysis, macroprudential risk management and quantile impulse responses. However, the forecasting performance of QVAR has yet to be assessed.

The use of linear quantile regression models is primarily motivated by their robustness as approximations to conditional quantiles and distributions. Economic theory can justify a wide variety of VAR processes for modeling conditional distributions[1], but all of them require committing to a particular functional form. Since linear quantile

[1]Occasionally binding collateral constraints (Aiyagari and Gertler, 1999) or a kinked Phillips curve (Benigno and Eggertsson, 2023) suggest using a threshold VAR. The model in Acemoglu and Scott (1997) imply a smooth transition process for output where the transition function emerges from firm heterogeneity as only some firms opt to invest at a given point in time. Real options arguments (Bernanke (1983) and McDonald and Siegel (1986)) and frictions to the supply of credit (e.g., (Adrian and Boyarchenko, 2012) and (Brunnermeier and Sannikov, 2014)) can motivate the use of volatility-in-means effects (e.g., Elder and Serletis (2010)).

regressions provide a weighted least squares optimal linear approximation to the true conditional quantiles (Angrist et al., 2006), they have been employed to produce forecasts or insights regarding macroeconomic risks in ways which are hopefully robust to the unknown form of the underlying data generating process.

The first contribution of this paper to provide an extensive evaluation of the predictive performance of the QVAR model. Other papers explored a similar comparison in a single equation setting between quantile regression models and AR-GARCH models (e.g., Brownlees and Souza (2021), Iseringhausen (2021) and Kipriyanov (2022)). Other papers compared quantile regression models with more sophisticated parametric VAR alternatives (e.g., Carriero et al. (2021) and Caldara et al. (2021)), but the QVAR model has yet to be compared to parametric alternatives. Throughout this paper, we target conditional densities with a focus on both tails of conditional distributions. The comparison features 112 US monthly macroeconomic variables and an out-of-sample period of over 40 years with forecasting horizons of between a month and a year. This contrasts with the typical forecasting evaluation in this literature which focuses on just a few targets. We supplement this comparative analysis with some specification tests used in the financial literature to evaluate value-at-risk models. This allows us to evaluate the 5th and 95th quantile forecasts produced by the QVAR model independently of the choice of benchmark models and to inspect the contexts in which evidence of misspecification can be found.

The forecasting experiment is built around bivariate VAR models where the target variable is paired with the National Financial Conditions Index (NFCI). This is perhaps the most interesting comparison as it is the most commonly used predictor in the growth-at-risk literature following Adrian et al. (2019). There is also some evidence that credit shocks are important drivers of macroeconomic fluctuations for a large number of variables (Boivin et al., 2020) such that financial stress is relevant to many of our target variables insofar as it captures this type of shock. On this basis, we compare QVAR with three parametric alternatives. The first alternative is a Gaussian VAR (VAR-N) which allows us to evaluate when and how much gain there is to moving beyond iid disturbances. We also include a VAR-GARCH model as in Normandin and Phaneuf (2004), Bouakez and Normandin (2010) or Bouakez et al. (2014) and a VAR-SV similar to those used by Cogley and Sargent (2005), Primiceri (2005) or Chan and Eisenstat (2018) to offer two common and relatively simple ways we can introduce parametric changes in volatility. However, unlike these authors, we do not pursue time-varying parameters in an effort to limit our deviation from the iid setting to changes in volatility. Moreover, as we explain in Section 1.2, all four models (QVAR, VAR-N, VAR-GARCH and VAR-SV) have in common that they impose a linear functional form on conditional expectations at all future horizons.

We find that QVAR provides statistically significant improvements in tail density forecasting accuracy over the VAR-N model in close to half of all variables considered and those improvements are frequently quantitatively important with reductions in density scores on the order of 10 to 30% in many cases. These are particularly important for labor market variables across all horizons considered and for interest and exchange rate at shorter horizons. QVAR also offers improvements over a VAR-GARCH and VAR-SV, albeit in fewer cases which are concentrated in those same groups of variables. More importantly, QVAR almost never does statistically significantly and substantially quantitatively worse than any of the parametric alternatives: it is therefore a robust way to model macroeconomic risk. Those results surprisingly turn out to not be driven by QVAR doing exceptionally better than the parametric alternatives during NBER recessions. Finally, specification tests do reveal evidence of misspecification. In particular, realized values which fall below or above the 5th and 95th quantile forecasts, respectively, tend to be serially correlated whereas such 'tail events' should be unpredictable under a correctly specified model.

The second contribution of this paper is to extend the analysis to a data-rich environment by augmenting QVAR models with latent factors estimated from our set of 112 target variables. Applications featuring principal component estimates (PCA) (e.g., Manzan (2015) and Coulombe et al. (2022)) and the recently introduced iterative quantile regression (IQR) estimates of quantile factors (Chen et al., 2021) have been considered in the past, but all of them involve direct forecasting models in a univariate setting. In contrast, factor augmented QVAR models jointly model the dynamic between observed variables and latent factor estimates.

We find that QFAVAR and QVAR models tend to perform equally well at forecasting macroeconomic risks across all variable categories. PCA and IQR factors may carry information which significantly overlaps much with the NFCI. However, QFAVAR models do provide statistically significant improvements in about 13% of cases, most of them in the labor market across all horizons. Specification tests reveal that introducing IQR factors into the set of variables available to QVAR reduces the frequency of misspecification and the incidence of serially correlated 'tail events.' This suggests the specifications issues reported in both cases may be due to the small set of variables we consider. We conclude that QVAR and QFAVAR models are appropriate tools for modeling macroeconomic risk.

The paper is organized as follows. Section 1.2 presents the QVAR model, details some of its properties and explains how to use it for forecasting. Section 1.3 details the forecasting experiment, the parametric alternatives and the tests used for evaluating QVAR and QFAVAR models. Section 1.4, presents and discusses the results. Section 1.5 concludes.

1.2 Quantile VAR Models

The QVAR model considered in this paper has been studied for scenario analysis and structural analysis by Chavleishvili and Manganelli (2021), Montes-Rojas (2021) and

Ruzicka (2021). For a 1 vector $\boldsymbol{y_t}$ of time series, the conditional quantile $[0\ \ 1]$ of the -th variable takes the form

$$\mathbb{Q}_{\ \ k,t}\left(\quad \tilde{\boldsymbol{x}}_t^{(k)}\right) = \sum_{\leq} \ _0 \ (\ \ ) \quad + \sum_{=1}\sum_{=1} \quad (\ \ ) \quad _{-} + \ (\ \ ) \tag{1.1}$$

where $\tilde{\boldsymbol{x}}_t^{(k)}$ contains the regressors for this equation. It is well known in this literature that quantile regressions admit a (restricted) random coefficient representation, whereby data can be simulated by uniformly sampling parameters over a grid of quantiles one equation at a time, one period at a time. This leads to

$$= \sum_{\leq} \ _0 \ (\quad) \quad + \sum_{=1}\sum_{=1} \quad (\quad) \quad _{-} + \ (\quad)$$

$$\boldsymbol{y_t} = \boldsymbol{A}_0(\boldsymbol{u}_t)\boldsymbol{y}_t + \sum_{=1} \boldsymbol{A}_j(\boldsymbol{u}_t)\boldsymbol{y}_{t-j} + \boldsymbol{\epsilon}(\boldsymbol{u}_t) \tag{1.2}$$

where $\boldsymbol{u_t}$ $[0\ \ 1]$ and $\boldsymbol{A_0(u_t)}$ is a lower triangular matrix with a null diagonal. Contemporary terms are included to ensure coefficients across equations do not depend on multiple 's, but are instead independent to eliminate the need for a notion of multivariate quantiles[2]. The triangular structure simplifies estimation and is applied to all models compared in the forecasting experiment.

Before turning to estimation and forecasting, we consider a few properties of QVAR processes. The QVAR model in (1.2) admits the following SVAR representation

$$\boldsymbol{y_t} = \bar{\boldsymbol{A}}_0\boldsymbol{y_t} + \sum_{=1} \bar{\boldsymbol{A}}_j\boldsymbol{y}_{t-j} + \bar{\boldsymbol{\epsilon}}_t \tag{1.3}$$

where $\bar{\boldsymbol{\epsilon}}_t := \left(\boldsymbol{A}_0(\boldsymbol{u}_t) \quad \bar{\boldsymbol{A}}_0(\boldsymbol{u}_t)\right) \quad + \sum_{\ =1}\left(\boldsymbol{A}_j(\boldsymbol{u}_t) \quad \bar{\boldsymbol{A}}_j\right)\boldsymbol{y}_{t-j} + \boldsymbol{\epsilon}(\boldsymbol{u}_t)$ and $\bar{\boldsymbol{A}}_j :=$

[2]The interested reader can also find a technical explanation in the Theorem 1 of Chavleishvili and Manganelli (2021).

$\mathbb{E}\left(\boldsymbol{A}_j(\boldsymbol{u}_t)\right)$ under technical conditions spelled out in Proposition 1.5 of Ruzicka (2021). This establishes that VAR and QVAR processes impose the same linear functional form for conditional expectations. Moreover, when QVAR admits a VAR representation, results in Lütkepohl (2005) concerning linear transformations of the form $\boldsymbol{F}\boldsymbol{y}_t$ apply. In particular, if a large set of variables follow a QVAR(p) process (and thus a VAR(p) process), then a subset of it will generally follow a VARMA(,) process (with possibly some heteroskedasticity or other higher order dependence). We should therefore expect that QVAR and VAR models offer similar mean forecasts under fairly general conditions.

Equation (1.3) also shows that QVAR processes capture such things as changes in conditional heteroskedasticity by allowing slope parameters to vary across quantiles. If the coefficient matrices were constant across quantiles (i.e., $\boldsymbol{A}_j(\boldsymbol{u}_t) = \bar{\boldsymbol{A}}_j$ for $= 0$), then we would have a linear model with iid shocks. This observation is also the reason why model (1.2) implies that the support of $\boldsymbol{y}_t$ must generally be bounded because otherwise quantile crossing would occur even in large samples. It is best seen in the simpler QAR(1) case (i.e., $= {}_1(\;) {}_{-1} + (\;)$) where variation in the slope parameters mean the conditional quantiles of must cross somewhere along the real line and bounding the process makes visiting this region a zero probability event[3]. When this condition is violated, the approximation QVAR provides to the conditional distribution of $\boldsymbol{y}_t$ in part of its domain may be poor[4]. However, as we explain below, the quantile regression estimator we use enjoys an optimality property which should limit this process to a small region. How much each of these points matter is an empirical question. Finally, the same univariate QAR(1) process is useful to

[3]See discussions in Koenker and Xiao (2006) and Hallin and Werker (2006) or Ruzicka (2021) for the multivariate case.

[4]Ruzicka (2021) mentions that one could mitigate this problem by using nonlinear transformations of regressions in quantile local projection setting, but this lies beyond the scope of the present paper.

intuitively understand the technical condition under which a QVAR process is ergodic, as well as both weakly and strongly stationary. In this simple case, the condition is $\mathbb{E}(\ _1(\ )^2)\quad 1$ which allows for unit and explosive roots for some subsets of conditional quantiles.

1.2.1 Estimation and Forecasting

The parameters of the QVAR process (1.1) can be estimated by linear quantile regression (Koenker and Bassett, 1978) one equation at a time for a grid of quantiles. Let $\boldsymbol{\beta}^{(\boldsymbol{k})}(\ )$ be all parameters for regression , including the intercept $(\ )$, and $\boldsymbol{x}_{\boldsymbol{t}}^{(\boldsymbol{k})} = \left(1\ \tilde{\boldsymbol{x}}_{\boldsymbol{t}}^{(\boldsymbol{k})\prime}\right)'$ be the corresponding vector of regressors. Then the estimator is given by

$$\hat{\boldsymbol{\beta}}^{(\boldsymbol{k})}(\ ) := \underset{\boldsymbol{\beta}\in\mathbb{R}^{(k+Kp)}}{\operatorname{argmin}} \sum_{=\ +1} {}_{k}\left(\qquad \boldsymbol{\beta}'\boldsymbol{x}_{\boldsymbol{t}}^{(\boldsymbol{k})}\right) \tag{1.4}$$

where ${}_k(\ ) := (\qquad \mathbb{I} \qquad)$ is the quantile loss function. Under some technical conditions which guarantee among other things that the process is strongly stationary and ergodic, Ruzicka (2021) has established the asymptotic normality of this estimator[5]. This estimator further enjoys a similar property to ordinary least squares under misspecification as it offers the optimal linear approximation to conditional quantiles in a weighted least square sense (Angrist et al., 2006). This 'robustness' property is one of the primary motivations behind its use for macroeconomic risk modeling.

In this paper, we produce all forecasts for QVAR models by simulating future sample paths from iteratively applying the random coefficient representation (1.2) using

[5]Using weights based on its asymptotic covariance matrix, $\hat{\boldsymbol{\beta}}^{(\boldsymbol{k})}(\tau_k)$ viewed as a process over $\tau_k \quad [0, 1]$ converges to a $Kp + k$-dimensional standard Brownian Bridge. The interested reader can also find some results for the quantile regression estimator under unit roots and cointegration in Koenker and Xiao (2004), Xiao (2009) or Cho et al. (2015).

estimates obtained from (1.4). Specifically, at each point in time the parameters are selected by choosing the point on the quantile grid that falls closest to a uniform random draw for each equation . Iterating this forward allows us to draw a sample path for y_{t+1} y_{t+12} and repeating this a large number of times allows us to compute a variety of statistics at each point in time (quantile forecasts, mean forecasts, etc.).

This algorithm contrasts with the approach introduced by Adrian et al. (2019) in a univariate context whereby the skewed t distribution of Azzalini and Capitanio (2003) is fitted to closely match a handful of conditional quantile forecasts produced using quantile regression estimates. On the other hand, it is closer in spirit to the method used by Chavleishvili and Manganelli (2021) for stress testing and Chavleishvili et al. (2021) for risk management in a macroprudential context as we can condition forecasts on scenarios by simply imposing predetermined sequences of quantiles. It also mirrors Ruzicka (2021)'s approach for obtaining quantile impulse responses. Considering this is how the QVAR model was introduced, we limit our attention to this approach.

An important detail concerns the choice of a grid of quantiles. We opted to use a relatively fine grid of 100 equally spaced quantiles, but note that some of those quantiles may not be well estimated. Chernozhukov et al. (2017) suggested using extreme value methods for quantiles beyond $(\quad + \quad)$ 15 where $\quad + \quad$ is the number of parameters in the last equation. For example, a bivariate QVAR with a single lag estimated on 400 observations gives us the interval $[0\ 15\quad 0\ 85]$ whereas adding a second lag reduces it to $[0\ 225\quad 0\ 775]$. Parsimony may thus be even more important when dealing with quantiles in the tails. For this reason, we follow Chavleishvili and Manganelli (2021) and Chavleishvili et al. (2021) and use a QVAR with one lag throughout the paper. This also obviates the need to implement necessarily different lag selection procedures across models. Moreover, while information criteria to choose the number of lags in each equation separately have been proposed in the literature (e.g., Koenker and Machado (1999)), there currently is no counterpart for the entire QVAR process and this question is thus left open to future research.

1.3 Forecasting Experiment

In this section, we conduct an out-of-sample forecasting experiment in which we target many monthly US variables obtained from the FRED-MD data set (McCracken and Ng, 2016) spanning the period between January 1959 to June 2022. Since all our models will also feature the National Financial Conditions Index (NFCI) which is observed from January 1971 to June 2022, we selected all target variables from FRED-MD which started at least as early as the NFCI and did not feature any missing values in the July 2022 version of the data. This leaves us with a subset of 112 target variables. To obtain many cycles of recessions and expansions, we set the start of the out-of-sample period to January of 1980, giving us 6 NBER recessions and a total of 510 periods for model comparison.

All target variables are transformed to induce stationarity[6] and we target the resulting values in $= 1$ 12 months rather than period averages as forecasts are produced iteratively through simulations for all models[7]. Finally, given our focus on forecasting tails, a difficult balance must be struck between allowing a large sample size for estimation and allowing the model to adapt to structural changes. We opted for a rolling window of 400 observations, allowing the window to initially expand to this size to include the two recessions from the early 1980s in the analysis.

---

[6]We follow McCracken and Ng (2016), except that we do not take second differences on interest rates, unemployment rates, monetary aggregates and prices as in Bernanke et al. (2005). All transformations are given in Table A.1 Appendix.

[7]Results in Coulombe et al. (2021a) suggest that averaging single period forecasts *ex post* is generally preferable to directly targeting averages when point forecasts are of primary interest, but this question lies beyond the scope of this paper.

1.3.1 Models

The forecasting experiment includes four bivariate models with the targeted variable ordered first, followed by the NFCI. These models are the QVAR, as well as three parametric alternatives: a VAR-N, a VAR-GARCH and VAR-SV. The VAR-N is a useful benchmark insofar as it is not obvious modeling moments beyond the mean is meaningful for macroeconomic data (Plagborg-Moller et al., 2020). The VAR-GARCH and VAR-SV models are interesting as common tools in the structural VAR literature which relaxes the iid assumption of the VAR-N by allowing conditional volatility to change over time. We further consider two additional variations on the baseline QVAR model by introducing latent factor and latent quantile factor estimates as regressors, a set of hitherto unexplored extensions we call a factor augmented QVAR or QFAVAR.

VAR-N This model takes the form

$$\boldsymbol{y}_{t+1} = \boldsymbol{\nu} + \boldsymbol{A}_1 \boldsymbol{y}_t + \boldsymbol{u}_{t+1} \quad \boldsymbol{u}_{t+1} \qquad (\mathbf{0} \ \boldsymbol{\Sigma}) \tag{1.5}$$

We estimate mean parameters $\boldsymbol{\nu}$ and $\boldsymbol{A}_1$ by ordinary least squares. The covariance matrix of innovations is estimated as $\hat{\boldsymbol{\Sigma}} = \sum_{=2} \hat{\boldsymbol{u}}_t \hat{\boldsymbol{u}}_t' \ (\qquad 2)$ where $= 2$, $= 1$ and $\hat{\boldsymbol{u}}_t$ are residuals.

VAR-GARCH We follow the structural VAR literature (e.g., Normandin and Phaneuf (2004); Bouakez and Normandin (2010); Bouakez et al. (2014)) and create a multivariate GARCH process by imposing that each 'structural' shock follows its own GARCH(1,1) process. Hence, we replace the normal for the vector of innovations with

$$\boldsymbol{u}_{t+1} = \boldsymbol{D}\boldsymbol{\epsilon}_{t+1} \tag{1.6}$$

$$_{+1} = \sqrt{\quad _{+1}} \quad _{+1} \qquad _{+1} \qquad (0 \ 1)$$

$$_{+1} = (1 \qquad\qquad) + \quad {}^{2} \quad +$$

where $\boldsymbol{D}$ is lower triangular to use the same restriction as in the QVAR model. We use the same parameter estimates for $\boldsymbol{\nu}$ and $\boldsymbol{A_1}$ and $\boldsymbol{\Sigma}$ as we do for the Gaussian VAR case. $\hat{\boldsymbol{D}}$ is obtained from a Cholesky factorization of $\hat{\Sigma}$. Series of 'structural residuals' $\hat{\boldsymbol{\epsilon}}_{\boldsymbol{k},\boldsymbol{t}}$ are then obtained on which individual GARCH(1,1) processes are fitted by maximum likelihood.

(Bayesian) VAR-SV We use one of the restricted models featured in Chan and Eisenstat (2018) which essentially replaces individual GARCH processes featured in the VAR-GARCH shown above by (random walk) stochastic volatility processes.

$$\begin{aligned} \boldsymbol{B_0 y}_{\ +1} &= \boldsymbol{\mu} + \boldsymbol{B_1 y} \ + \boldsymbol{\epsilon}_{\ +1} \\ _{+1} &= \exp(\quad _{+1} \ 2) \quad _{+1} \qquad _{+1} \qquad (0 \ \ 1) \\ _{+1} &= \qquad + \qquad _{+1} \qquad _{+1} \qquad (0 \ \ 1) \end{aligned} \tag{1.7}$$

We impose recursive short-run restrictions as with the QVAR and VAR-GARCH models such that $\boldsymbol{B}_0$ is set to a lower triangular matrix with a unit diagonal. It is a common choice (e.g., Cogley and Sargent (2005) and Primiceri (2005)). The model is estimated using Bayesian methods with the following priors:

$$\boldsymbol{\theta} := \left(\boldsymbol{vec}\left((\boldsymbol{\mu} \ \ \boldsymbol{B_1})'\right)' \quad {}_{0\,2\,1}\right)' \qquad (\boldsymbol{b} \quad \boldsymbol{V}\ ) \quad \boldsymbol{h_0} \qquad (\boldsymbol{b_h} \ \ \boldsymbol{V_h}) \ \text{ and } \qquad\qquad (\qquad)$$

We set $\boldsymbol{b_\theta}$ and $\boldsymbol{V_\theta}$ as a Minnesota-type prior with common hyperparameter values centered on a random walk, except for the growth rates of consumption, exchange rates and stock market indexes which we center on white noise. We center the value for $_{0\,2\,1}$ at 0 with a relatively large variance of 10 and likewise for the initial log variance ($\boldsymbol{b_h} = \boldsymbol{0}$ and $\boldsymbol{V} \ = 10$) following Chan and Eisenstat (2018). We use the shape $\quad = 5$

and scale $= 0\ 1(\quad 1)$ as Chan and Eisenstat (2018) reflecting a relatively diffuse prior centered on a small value (here, $0\ 1$).

Their Gibbs Sampling algorithm has two particular features. First of all, it jointly samples mean parameters $\boldsymbol{\theta}$ for each equation whereas other algorithms would sample free elements in $\boldsymbol{B}_0$ separately. Second of all, while it applies the common auxiliary mixture sampler proposed by Kim et al. (1998) which allows using methods for linear Gaussian state-space models, it also samples the sequence of log variances $(\boldsymbol{h}_t)_{=1}$ in a single step for each equation using the precision sampler of Chan and Hsiao (2014). These features make the algorithm fairly efficient.

QFAVAR As a means of exploring the value of a data-rich environment for macroeconomic forecasting, we introduce latent factor estimates as part of the vector of variables $\boldsymbol{y}_t$ in (1.2). This is similar in spirit to the FAVAR model of Boivin and Ng (2005), although we do not impose restrictions that would strictly justify treating the target variable and NFCI as 'observed' factors. In all cases, latent factors are recursively estimated using the in-sample data window. We collect our 112 variables into a matrix and let variable obey

$$= \boldsymbol{\lambda}_i' \boldsymbol{f}_t + \tag{1.8}$$

where $\boldsymbol{f}_t$ is a $\quad 1$ vector of factors and $\boldsymbol{\lambda}_i$ is the corresponding vector of loadings. Following common practice since Stock and Watson (2002a,b), we obtain factor estimates $\hat{\boldsymbol{f}}_t$ by principal components. We set $= 1$ factor out of concern for parsimony so our vector of time series becomes $\boldsymbol{y}_t = (\ _1 \qquad)'$. A natural alternative would be to consider doing the same thing using the quantile latent factors recently introduced by Chen et al. (2021). In this case, we have

$$\mathbb{Q}_{\ \ i,t}(\quad \boldsymbol{f_t}(\ )) = \boldsymbol{\lambda_i}(\ )'\boldsymbol{f_t}(\ ) + \quad (\ ) \tag{1.9}$$

with $(\ )$ being $(\ )$ $\quad 1$. We obtain estimates $\tilde{\boldsymbol{f}}_{\boldsymbol{t}}(\ )$ for the 5th and 95th quantiles using the IQR algorithm (Chen et al., 2021). Again, we set $(\ ) = 1$ for parsimony and use $\boldsymbol{y_t} = (\ _1 \quad (0\ 05) \quad (0\ 95) \qquad)'$.

1.3.2 Relative Forecasting Evaluation

To perform the model comparison, we follow Carriero et al. (2020) and Carriero et al. (2022) in our evaluation of density forecasts and adopt the quantile weighted continuous ranked probability score (CRPS) introduced by Gneiting and Ranjan (2011). For model and variable , define the period ahead quantile forecasts as

$$_{+} \quad (\ ) := \mathbb{Q}^{(\ )}_{t+h,v}(\quad \mathcal{F}\ )$$

and quantile scores as

$$(\ _{+} \quad (\ ) \quad _{+}\ ) := \quad (\ _{+} \quad (\ ) \quad _{+}\ ) \tag{1.10}$$

where we recall that $(\ ) := (\quad \mathbb{I} \qquad)$. For a grid of quantiles, the quantile weighted CRPS is defined as

$$(\hat{\boldsymbol{q}}_{\boldsymbol{t+h,v,m}}\ \boldsymbol{\nu} \quad _{+}\ ) = \frac{2}{\quad 1} \sum_{=1} (\ ) \quad _j(\ _{+} \quad (\ ) \quad _{+}\ ) \tag{1.11}$$

where $\boldsymbol{\nu} := (\ (\ ))\ _{=1}$ is a vector of weights and $\hat{\boldsymbol{q}}_{\boldsymbol{t+h,v,m}} := (\ _{+} \quad (\ ))\ _{=1}$ stacks quantile forecasts into a vector. Gneiting and Ranjan (2011) proposed using the function $(\ ) = (2 \quad 1)^2$ to put more weight on the tails. The use of this scoring rule is motivated by the fact that it is minimized in expectation by the true conditional density (Gneiting and Raftery, 2007).

Diebold and Mariano (1995) statistics allows us to test the null hypothesis of equal forecasting performance between models $_1$ and $_2$ using the following regression

$$(\hat{\boldsymbol{q}}_{\boldsymbol{t+h,v,m_1}}\ \boldsymbol{\nu}\quad + \quad)$$
$$(\hat{\boldsymbol{q}}_{\boldsymbol{t+h,v,m_2}}\ \boldsymbol{\nu}\quad + \quad) = \quad {}_{1}\ {}_{2} + \quad + \quad {}_{1}\ {}_{2}$$

for each forecasting horizon and variable where $_1$ $_2$ $= 0$ under the null[8]. In this context, note that $_1$ $_2$ 0 means that model $_1$ is performing better than model $_2$ (i.e., its average score is lower).

1.3.3 Absolute Forecasting Evaluation

In an effort to mitigate concerns with the choice of benchmark models, we supplement the model comparison with specification tests used in finance for evaluating value-at-risk models.

Quantile Mincer-Zarnowitz Tests Gaglianone et al. (2011) proposed a test of quantile forecast optimality in the spirit of Mincer and Zarnowitz (1969) based on a quantile regression by adapting an idea from Christoffersen et al. (2001). Let $\mathbb{Q}_{\ i,t+h}(\ \mathcal{F}\ )$ and $\mathbb{Q}_{\ i,t+h}(\ \mathcal{F}\ )$ be the -period ahead -th quantile of variable conditional on information $\mathcal{F}$ and its forecast by some model, respectively. If the model is correctly specified, we should have

$$\mathbb{Q}_{\ i,t+h}(\ \mathcal{F}\ ) = {}_0(\ ) + {}_1(\ )\mathbb{Q}_{\ i,t+h}(\ \mathcal{F}\ ) := \boldsymbol{x}_t'\boldsymbol{\alpha}(\ )$$

[8]The constant is estimated by OLS and HAC standard errors are used in all cases.

with $\boldsymbol{\alpha}(\ ) := (\ _0(\ )\ \ _1(\ ))' = (0\ 1)'$ and $\boldsymbol{x_t} := \Big(1\ \mathbb{Q}\ _{i,t+h}(\ \ \mathcal{F}\ )\Big)'$. These parameters can be estimated by a quantile regression of realized values $\ _{+}\ $ on the quantile forecasts $\mathbb{Q}\ _{i,t+h}(\ \ \mathcal{F}\ )$ at the corresponding quantile . Under mild regularity conditions, the Wald statistic testing the null of correct specification has a $\ ^2_2$ asymptotic distribution[9]. Note that simulation evidence in Gaglianone et al. (2011) suggest this test suffers from size distortion in small sample (the true size tends to be larger than the nominal size), but it tends to enjoy as much or more power than the more common alternative tests based on dummy variables such as Kupiec (1995), Christoffersen and Diebold (1998) or Engle and Manganelli (2004).

Coverage Tests We begin by defining

$$:= \mathbb{I}\Big\{\qquad \Big[\mathbb{Q}\ _{i,t+1}(0\ 05\ \mathcal{F}\ )\ \ \mathbb{Q}\ _{i,t+1}(0\ 95\ \mathcal{F}\ )\Big]\Big\}$$

as a dummy variable indicating when observations fall inside this symmetric 90% interval[10]. Following Kupiec (1995), Christoffersen and Diebold (1998) leverage the idea that a correctly specified model implies should be an iid Bernoulli variable with a $= 0\ 9$ success rate. The resulting likelihood function is thus given by

$$\mathcal{L}(\ ) = \ \ _{=1}(1\qquad)^{1-\ t}\ \ ^{t} = (1\qquad)^{\ 0}\ \ ^{\ 1}$$

where $\ _0 = \sum_{=1}(1\qquad)$ and $\ _1 = \sum_{=1}$ where is the size of the pseudo-out-of-sample period. The unconditional coverage test is based on a likelihood ratio statistic which compares this likelihood evaluated at the nominal coverage rate $= 0\ 9$ and

[9]For the implementation, we follow the authors' suggestion and use Koenker and Machado (1999)'s estimator for the covariance matrix.

[10]Since these are binary events, this is equivalent to jointly testing coverage in the 5% tail on each side of the distribution.

its sample counterpart, $= \ ^{-1}\sum_{=1}$, which is the maximum likelihood estimator. Under the null, Christoffersen and Diebold (1998) show the likelihood ratio statistic satisfies $= \ 2\log\left(\mathcal{L}(\ )\ \mathcal{L}(\ )\right) \quad {}^{2}_{1}$. The conditional coverage test changes the alternative hypothesis by modelling possible serial dependence in as a first order Markov Chain with transition matrix

$$_{1} := \begin{bmatrix} 1 & _{01} & _{01} \\ 1 & _{10} & _{11} \end{bmatrix}$$

where $= \mathbb{P}(\ _{+1} = \quad = \ )$. The likelihood function is then given by

$$\mathcal{L}(\ _{1}) = (1 \quad _{01})^{\ 00} \ {}_{01}^{01}(1 \quad _{11})^{\ 10} \ {}_{11}^{11}$$

where $:= \sum_{=2} \mathbb{I} \quad _{+1} = \quad \mathbb{I} \quad =$ counts transition cases with the maximum likelihood estimator being again the sample shares of the relevant events, i.e $_{1} =$ $_{1} \ (\ _{0} + \ _{1})$. Under the null, Christoffersen and Diebold (1998) shows the likelihood ratio statistic satisfies $= \ 2\log\left(\mathcal{L}(\ )\ \mathcal{L}(\ _{1})\right) \quad {}^{2}_{2}$. Note that for both coverage tests, we follow Christoffersen (2004) and adopt the Monte Carlo testing approach of Dufour (2006) and obtain exact finite sample p-values instead of relying on asymptotic approximations[11]. The ability to control the size of these tests exactly in small sample is an advantage they possess over the previous specification tests. However, the power of those tests varies with sample size[12] and they require non-overlapping forecasts so we only perform these tests for $= 1$. Nevertheless, as QVAR (and QFAVARs) produce forecasts iteratively, misspecification at $= 1$ would naturally propagate forward and may pose problems with quantile forecasting accuracy at longer horizons.

---

[11]The procedure is detailed in Section A.1 of the Appendix

[12]See, for example, simulation evidence in Gaglianone et al. (2011).

1.4 Discussion

As explained in the previous sections, we rely on Diebold and Mariano (1995) tests to evaluate the forecasting accuracy of the QVAR model relative to the three parametric alternatives, VAR-N, VAR-GARCH and VAR-SV, and this raises the problem of concisely reporting a very large number of results. We proceed in a manner similar to Stock and Watson (1998) who reported test rejection counts. We use Diebold and Mariano (1995) tests as a means of categorizing variables. Specifically, given that we seek to minimize the tail weighted quantile CRPS, we consider that QVAR 'wins' against a given benchmark, at a given horizon and for a given variable when it has a lower average score and the null of equal forecasting performance is rejected at 5%. QVAR 'loses' if it has a higher average quantile weighted CRPS[13] score and the null of equal forecasting performance is rejected at 5%. In all other cases, we consider that the models have equal forecasting performance. A similar idea is applied to build figures for Gaglianone et al. (2011)'s quantile extension of the Mincer-Zarnowitz test and the Christoffersen and Diebold (1998) coverage test. The same figures are presented for QFAVAR models.

1.4.1 QVAR Results

Figure 1.1 features two panels that each display the number of variables in each of the 8 groups featured in FRED-MD for which QVAR wins and loses. Group results are stacked so that the total number of wins and loses correspond to the top of area for group one. The figure shows results for each decade of the out-of-sample period and the whole out-of-sample period and for each of the parametric benchmarks. As an example of how to read the figure, consider the area plot displayed in the first row

[13] See section 1.3.2 for details.

and first column of panel A. The counts refer to the number of variables for which QVAR statistically significantly outperformed the VAR-N models in the 1980s. At horizon 3, there are about 40 variables out of 112 and about 10 of those variables are in the labor market (group 2) category. The same entry in panel B shows the VAR-N statistically significantly outperformed the QVAR for fewer than 10 variables out of 112 at all horizons.

We begin by focusing on the last column of each panel for the average relative performance across the whole out-of-sample period. For this period, panel A shows that QVAR significantly outperforms VAR-N in between 25 and 50% of cases depending on the horizon. It also significantly improves upon VAR-GARCH and VAR-SV in about 25% and 10% of cases. Importantly, panel B reveals that QVAR rarely does significantly worse than any of the three benchmark models considered, losing in around 18% of cases at an horizon of one month against VAR-GARCH and VAR-SV and in between only 5 to 10% of cases at all other horizons. Breaking down results across different categories of variables, QVAR appears to perform best relative to benchmark models when applied to the labor market (group 2) at all horizons and to interest and exchange rate (group 6), especially at shorter horizons. We note that most of the few cases where QVAR is outperformed across all benchmark models are prices (group 6). The bulk of issues of relative performances identified in the short 2020s sub-sample included in the forecasting experiment are also related to prices.

Shifting our attention across the first five columns of each panel, we can get a sense of how stable are those results. The patterns of relative performance appear to vary slightly over time, but the broad qualitative message remains the same. Across each decade, QVAR infrequently does worse than benchmark models, more frequently improves upon them and both of these observations concentrated in the same categories of variables.

Of course, Figure 1.1 does not tell us whether the statistically significant differences in performance between models are meaningfully large. To this end, Figure 1.2 displays the average log differences in scores between QVAR and VAR-GARCH and VAR-SV[14] over the whole out-of-sample period for each variable in each of the eight groups of variables in FRED-MD. Values below zero indicate that QVAR has a smaller average score than the benchmark and a rejection of the null in the corresponding Diebold and Mariano (1995) test in either direction is indicated by the color yellow. For example, take the plot in the first row and first column of panel A. It shows that there is a variable in the output and income (group 1) for which QVAR is about 15% more accurate at forecasting the tails than the VAR-GARCH model at all horizons and this difference is statistically significant at 5%.

[14]Panel B omitted the results for the oil price variable in group 7 because VAR-SV performed too poorly and it hindered visualizing the rest of the results. The random walk process for stochastic volatilities seems to be the culprit.

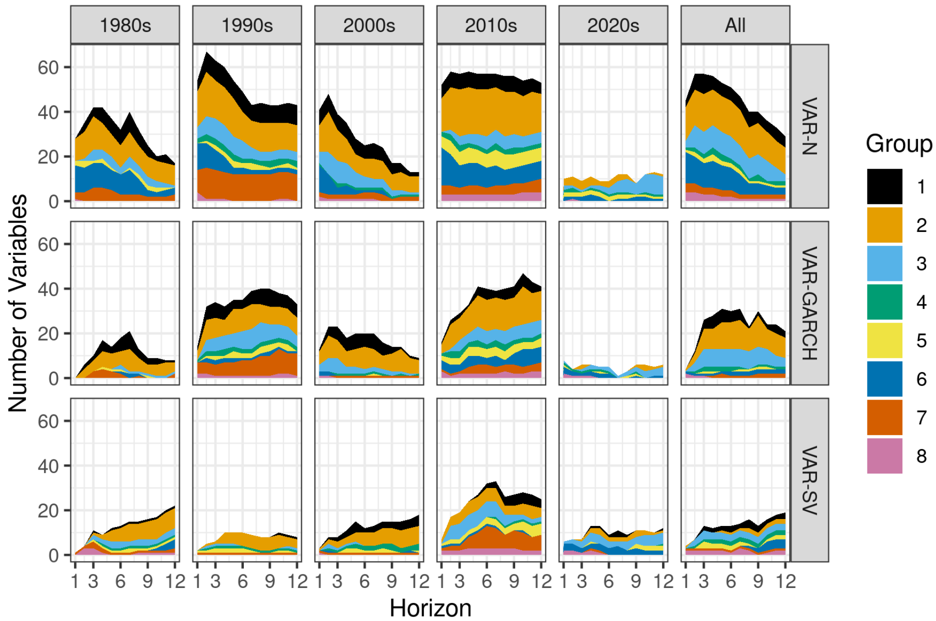

(a) Number of Cases where QVAR Beats the Benchmark

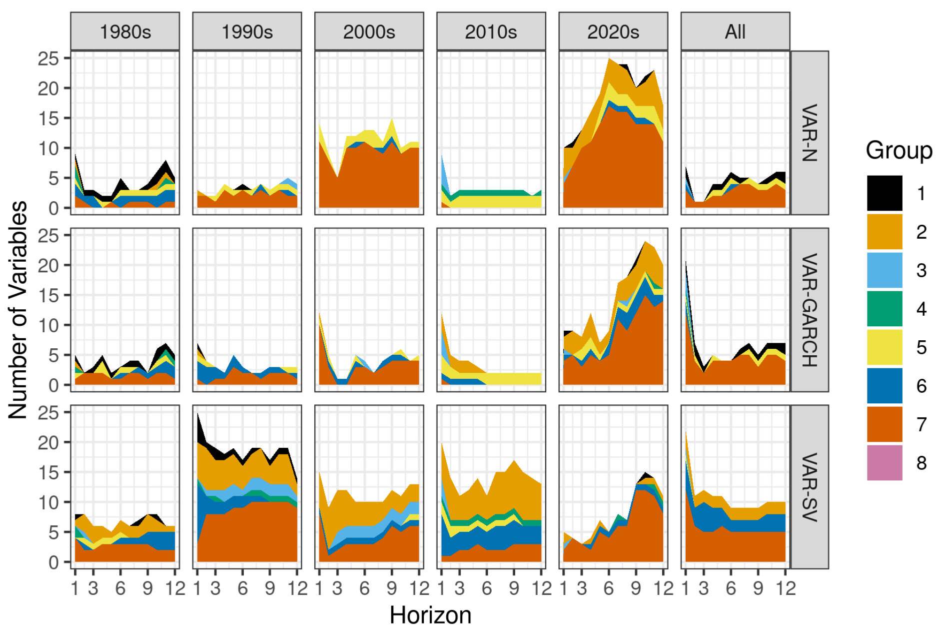

(b) Number of Cases where QVAR Loses to the Benchmark

Figure 1.1: QVAR Diebold-Mariano Tests (tail-weighted CRPS)

Note: QVAR wins (loses) when it has a lower (higher) average score and the Diebold-Mariano statistic is significant at the 5% level. Columns are periods and rows are different benchmark models. Colors indicate FRED groups: **(1)** Output and income, **(2)** Labor market, **(3)** Housing, **(4)** Consumption, orders and inventories, **(5)** Money and credit, **(6)** Interest and exchange rate, **(7)** Prices and **(8)** Stock market.

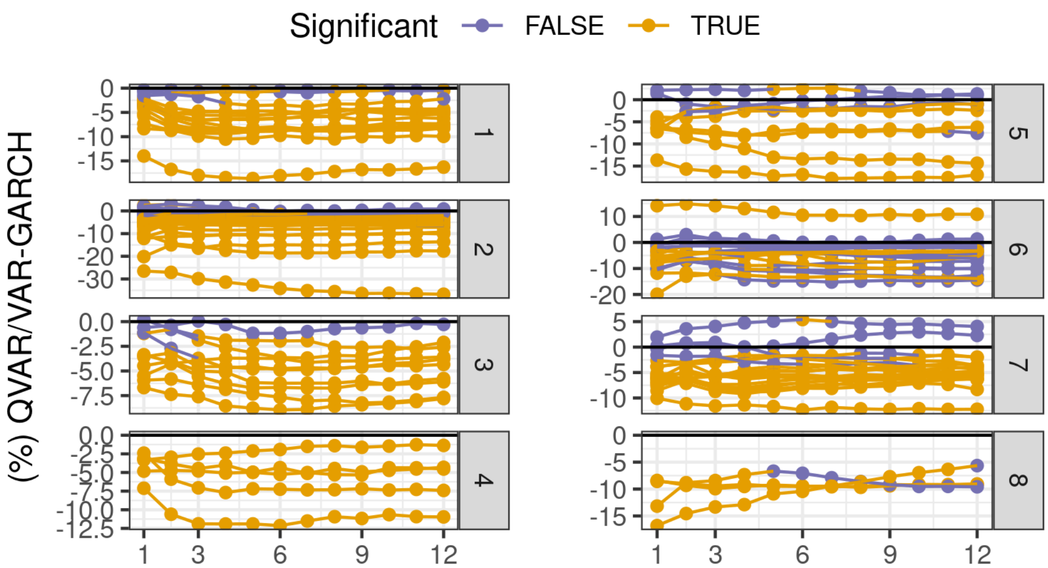

(a) QVAR and VAR-GARCH

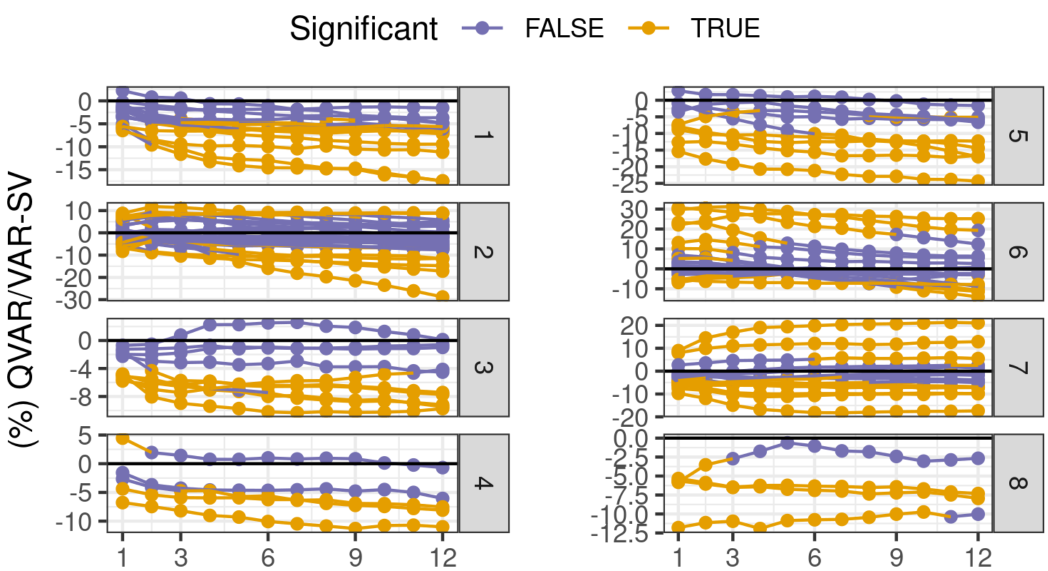

(b) QVAR and VAR-SV

Figure 1.2: QVAR Relative Scores (tail-weighted CRPS)

Note: Negative values are improvements. Yellow corresponds to rejecting the null of equal scores at 5%. Yellow corresponds to not rejecting the null of equal scores at 5%. FRED groups are: **(1)** Output and income, **(2)** Labor market, **(3)** Housing, **(4)** Consumption, orders and inventories, **(5)** Money and credit, **(6)** Interest and exchange rate, **(7)** Prices and **(8)** Stock market.

We find that the statistically significant improvements provided by QVAR over the VAR-GARCH and VAR-SV benchmarks routinely exceed 10%, even sometimes 20% or more across horizons. These gains tend to concentrate in the categories of output and income (group 1), labor market (group 2) and money and credit (group 5). Importantly, QVAR almost never does much worse than VAR-GARCH. However, it does underperform VAR-SV by statistically significant margins in excess of 10%. This can be seen in interest and exchange rates (group 6), as well as prices (group 7), even as it happens infrequently. Figure A.1 in the appendix displays the corresponding comparison between QVAR and VAR-N which is considerably more favorable: it virtually never does worse, it almost always does better, the improvements can be large or even very large and it's frequently statistically significant.

Figures 1.1, 1.2 and A.1 all point to QVAR performing relatively better against VAR-N than VAR-GARCH and VAR-SV. Moreover, this pattern seems to hold over time. Since all four models imply the same linear form for the conditional expectation of the target variable at all horizons, these result suggests that there is enough information in macroeconomic data to meaningfully capture variation in conditional volatility. Overall, these figures also offer evidence in favor of the purported robustness of QVAR in the sense that it tends to perform as well or better, but almost never much worse than competing parametric alternatives.

Perhaps surprisingly, Figure 1.3 reveals that this good relative performance of QVAR is generally not driven by recessions. When a forecasted value is realized in what the NBER later determines to be a recession month, QVAR performance is statistically indistinguishable from that of benchmark models in between 75 and 85% of cases depending on the model and horizon. There is a slightly greater advantage during recessions against the VAR-SV than the VAR-N and VAR-GARCH models at longer horizons. Given that this pattern does not hold against VAR-GARCH, this may owe to the fact the random walk in stochastic volatility may overstate the persistence of uncertainty in those circumstances. This finding points to the presence of important variation in macroeconomic risks during periods of economic expansion that aren't as well captured by the parametric alternatives we considered. One possible explanation is that the binary discrete approximation to what is an otherwise continuous state variable we call "the business cycle" is neglecting meaningful information and more than two states should be considered. Alternatively, we can also note that the concept of a recession is fuzzy and the NBER recession dates are up to debate.

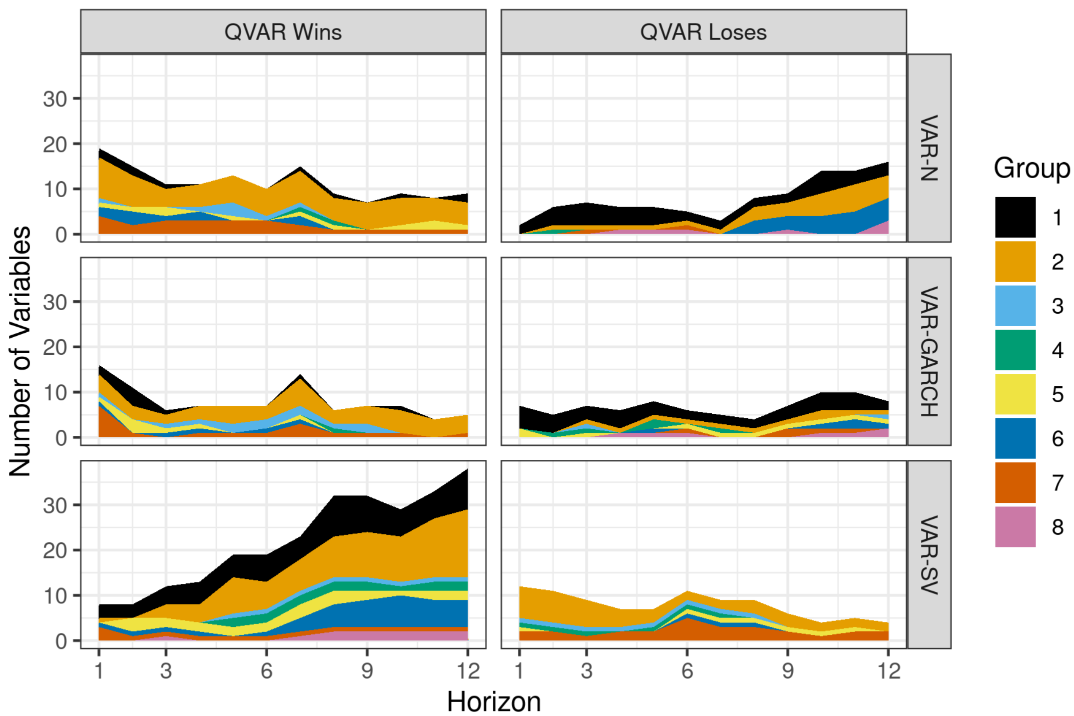

Figure 1.3: QVAR Recesssion Comparison (tail-weighted CRPS)

Note: QVAR wins (loses) when it has a lower (higher) average score and the Diebold-Mariano statistic is significant at the 5% level. Rows are different benchmark models. Colors indicate FRED groups: **(1)** Output and income, **(2)** Labor market, **(3)** Housing, **(4)** Consumption, orders and inventories, **(5)** Money and credit, **(6)** Interest and exchange rate, **(7)** Prices and **(8)** Stock market.

We now turn to specification tests. Figure 1.4 displays results for the quantile Mincer-Zarnowitz tests of Gaglianone et al. (2011) for forecasts at the 5th and 95th quantiles separately. The figure counts the number of variables for which the null hypothesis of a correctly specified quantile forecast cannot be rejected at a level of 5% and breaks these results down for each decade in the out-of-sample period, as well as the whole period, and each group of variables in FRED-MD. As an example of how to read the figure, the area plot in the column of the first row shows that at a horizon of 1 and 2 months, we cannot reject the hypothesis that the QVAR forecast is well specified at 5% during the 1980s for about 75 out of 112 variables. This is also true for over 20 labor market variables (group 2).

Looking across all columns and rows, we see that the null hypothesis of optimal quantile forecasts cannot be rejected for between 25 and 50% of cases, depending on the horizon and period covered. However, we consistently find greater evidence of misspecification at longer than shorter horizons. Of all variable types, the test again singles out labor market (group 2) and interest and exchange rate (group 6) variables as cases where the model performs particularly well. This picture is also relatively stable over time.

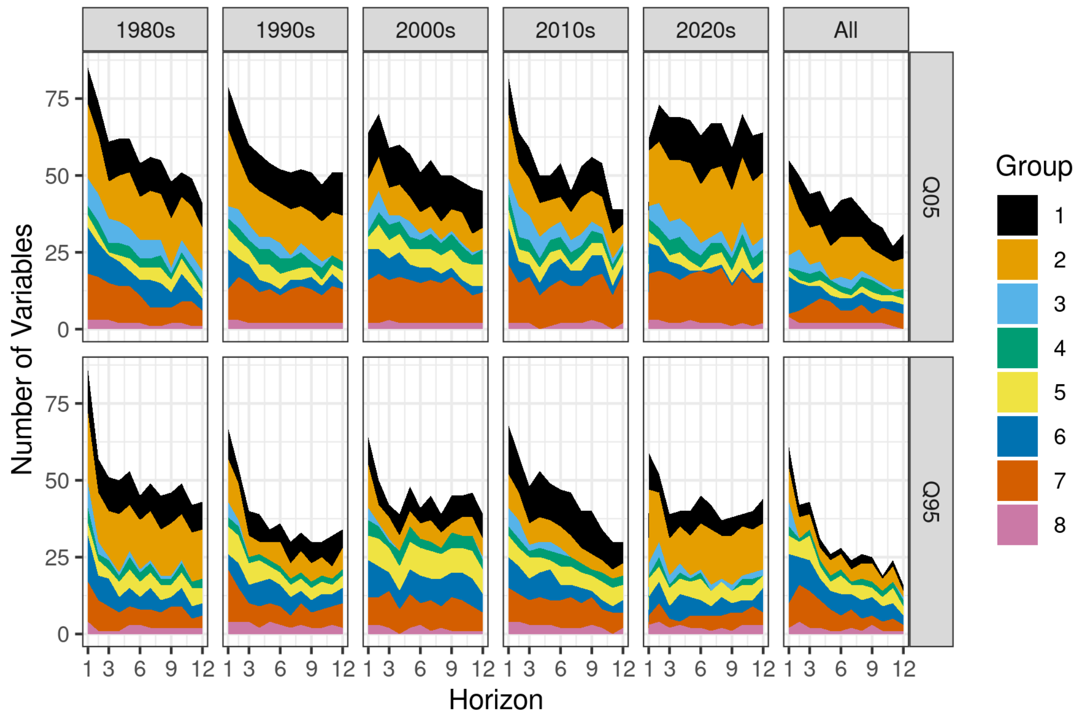

Figure 1.4: Number of Optimal QVAR Forecasts

Note: Number of cases where we obtain a non rejection of the null of optimal forecast at 5% for the Gaglianone et al. (2011) test. Columns are periods and rows are the 5th (Q05) and 95th (Q95) quantile forecasts, respectively. Colors indicate FRED groups: **(1)** Output and income, **(2)** Labor market, **(3)** Housing, **(4)** Consumption, orders and inventories, **(5)** Money and credit, **(6)** Interest and exchange rate, **(7)** Prices and **(8)** Stock market.

Results for coverage tests are presented in Figure 1.5. We here focus on one month ahead 5th and 95th quantile forecasts[15], so an observation that falls outside of the 90% interval between them will be our notion of a 'tail event.' If QVAR is correctly specified, the unconditional probability of a tail event would be 10%. That's the null of the unconditional coverage tests. Moreover, 'tail events' should be 'unpredictable' and, in particular, they shouldn't be serially correlated. The null of correct conditional coverage jointly tests both of these restrictions. The figure shows the shares of non rejection

[15]Recall that the tests are carried out only for horizon $h = 1$ for reasons discussed in Section 1.3.

of the null for each of those tests for each group of variables and each decade of the out-of-sample period.

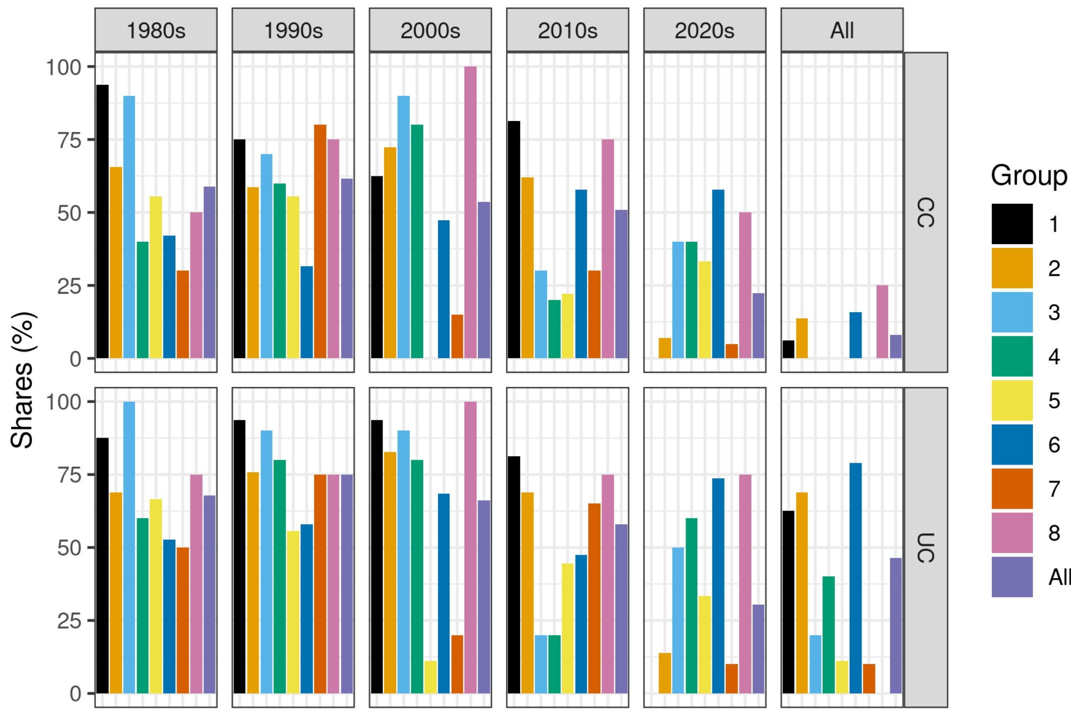

Figure 1.5: Unconditional and Conditional Coverage Tests on QVAR (90% Interval)

Note: Shares of non rejection of the null at 5% using Monte Carlo p-values (Dufour, 2006). UC is the unconditional coverage test and CC is the conditional covargae test. Columns are periods. Colors indicate FRED groups: **(1)** Output and income, **(2)** Labor market, **(3)** Housing, **(4)** Consumption, orders and inventories, **(5)** Money and credit, **(6)** Interest and exchange rate, **(7)** Prices and **(8)** Stock market and **(All)** 112 variables.

The last column results for the whole pseudo-out-of-sample period. We can see in the bottom row that the test fails to reject the null of correct unconditional coverage in almost 50% of cases and, likewise, for more than half of output and income (group 1), labor market (group 2) and interest and exchange rates (group 6). However, we can see that the null of correct conditional coverage is rejected over 90% of times across all variable groups. This means that on average QVAR quantile forecasts lead to a correct probability of 10% for observing tail events, but that it leads to tail events that are serially correlated. Since forecasts at longer horizons are produced iteratively, this may explain the consistent pattern in Figure 1.4 where the null of optimal quantile forecasts can always be rejected more frequently at longer than shorter horizons.

1.4.2 QFAVAR Results

Figure 1.6 presents the results for the Diebold and Mariano (1995) tests comparing both QFAVAR models with the QVAR model. The last column of both panels show that on average over the whole pseudo-out-of-sample period, QVAR and both QFAVAR models have statistically indistinguishable tail density forecasting performances in between 85 to 90% of cases depending on the horizon and the type of factor included. More differences can be noticed during the 1990s and 2010s where the addition of either PCA or IQR factors improves performance for prices (group 7) in particular. We will recall that the few cases in which QVAR is significantly outperformed by VAR-SV with relatively large magnitudes are concentrated in this category.

Figure 1.7 displays the average log differences in scores, as well as whether these differences are statistically significant. As QFAVAR models serve as benchmarks in these comparisons, adding factors is found to be helpful when the values displayed are positive. We can see that the changes in accuracy resulting from the addition of either type of factors are relatively small with the vast majority being under 5% in either direction. This corroborates the main finding from the previous figure and suggests that adding factors usually doesn't substantially affect tail density forecasting accuracy. That being said, panel A does show a few moderate improvements obtained from the addition of a PCA factor in interest and exchange rates (group 6) and prices (group 7) variables. At the same time, introducing a PCA factor can be costly as we can see in panel A with some moderately negative values in money and credit (group 5), as well as in some of the interest and exchange rate (group 6) variables.

Perhaps where differences are most striking is during NBER recessions as can be seen in Figure 1.8. QFAVAR models outperform QVAR in between 12 and 18% of cases depending on the horizon and type of factors considered. It also appears to be rarely costly to add factors when the realized value turns out to fall during a recession. It is especially visible with the labor market (group 2) where adding a PCA factor helps at all horizons, while the IQR factors seem to be most helpful at shorter horizons.

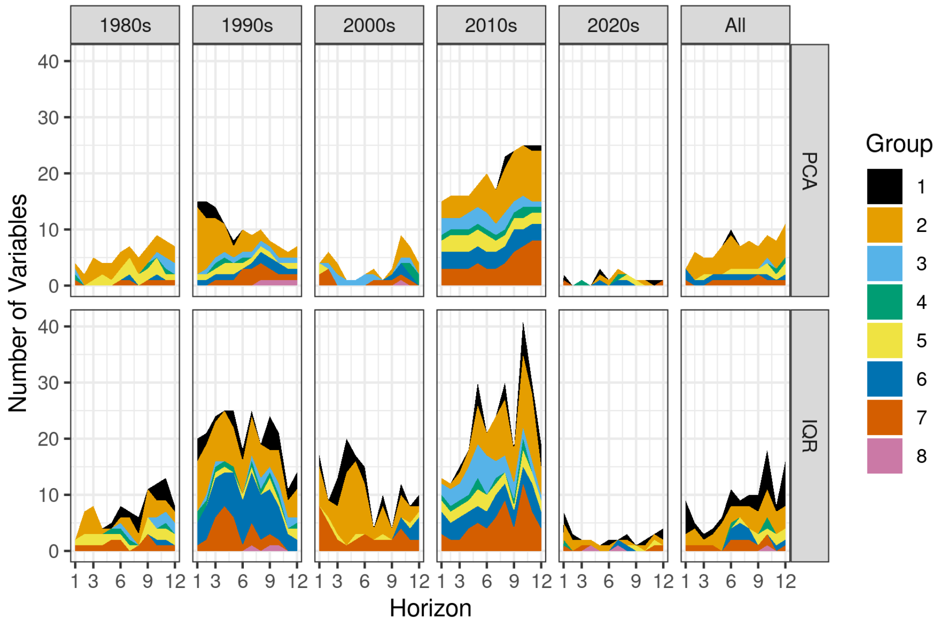

(a) Number of Cases where QVAR Loses to QFAVAR

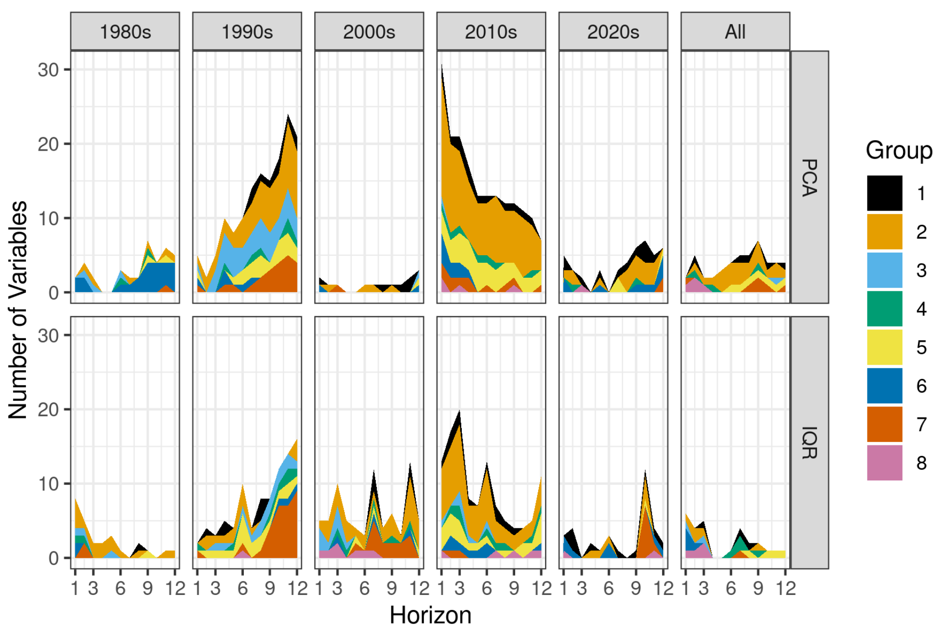

(b) Number of Cases where QVAR Beats QFAVAR

Figure 1.6: QFAVAR Diebold-Mariano Tests (tail-weighted CRPS)

QVAR wins (loses) when it has a lower (higher) average score and the Diebold-Mariano statistic is significant at the 5% level. Columns are periods and rows are different benchmark models. Colors indicate FRED groups: **(1)** Output and income, **(2)** Labor market, **(3)** Housing, **(4)** Consumption, orders and inventories, **(5)** Money and credit, **(6)** Interest and exchange rate, **(7)** Prices and **(8)** Stock market.

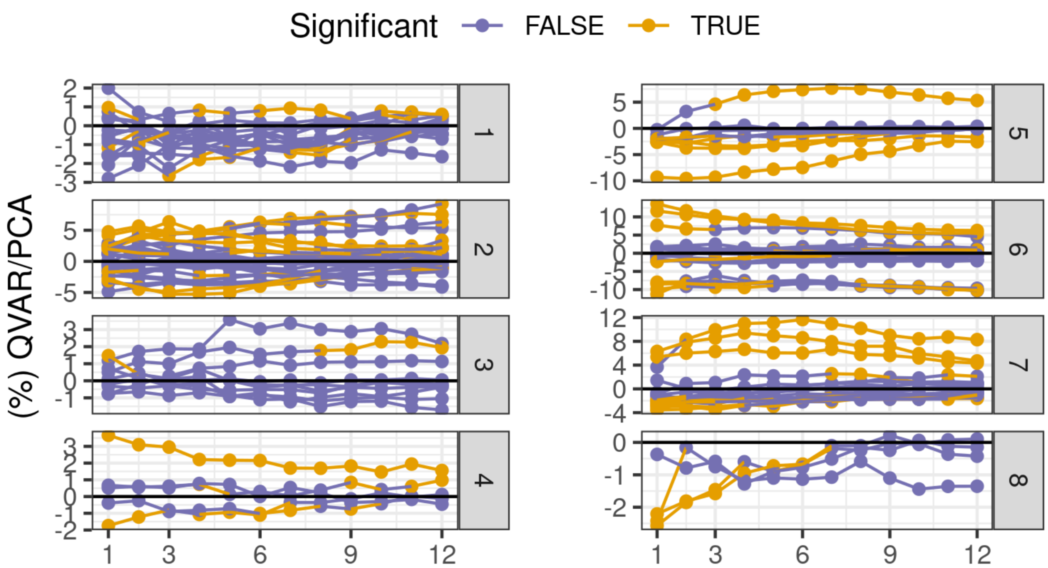

(a) QVAR and QFAVAR (PCA)

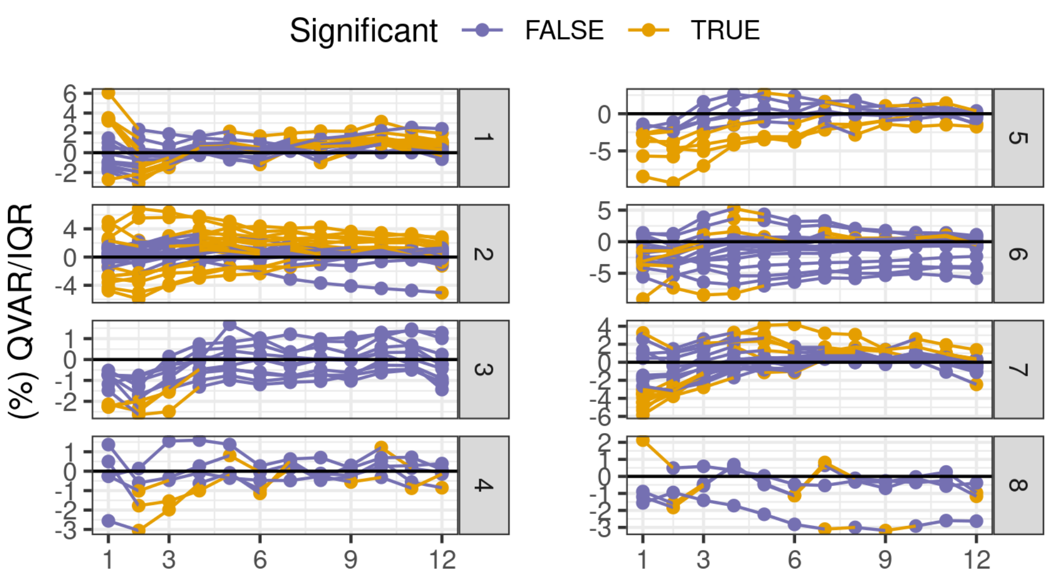

(b) QVAR and QFAVAR (IQR)

Figure 1.7: QFAVAR Relative Scores (tail-weighted CRPS)

Note: Positive values are improvements over QVAR. Yellow corresponds to rejecting the null of equal scores at 5%. Yellow corresponds to not rejecting the null of equal scores at 5%. FRED groups are: **(1)** Output and income, **(2)** Labor market, **(3)** Housing, **(4)** Consumption, orders and inventories, **(5)** Money and credit, **(6)** Interest and exchange rate, **(7)** Prices and **(8)** Stock market.

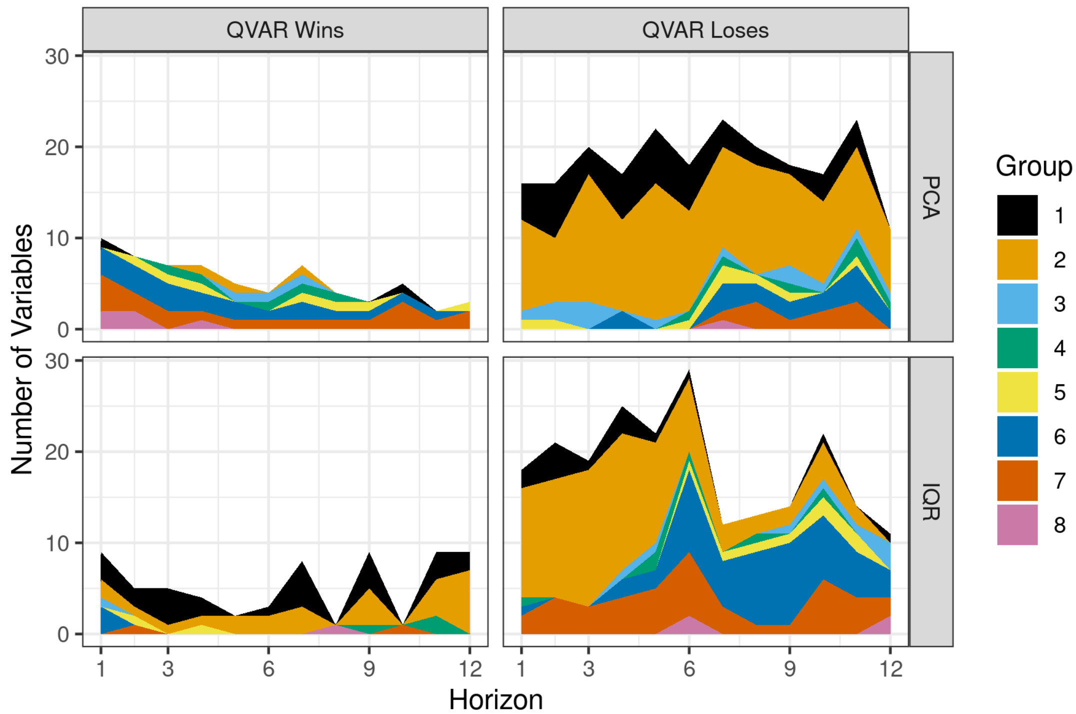

Figure 1.8: QVAR and QFAVAR Recesssion Comparison (tail-weighted CRPS)

Note: QVAR wins (loses) when it has a lower (higher) average score and the Diebold-Mariano statistic is significant at the 5% level. Rows are different benchmark models. Colors indicate FRED groups: **(1)** Output and income, **(2)** Labor market, **(3)** Housing, **(4)** Consumption, orders and inventories, **(5)** Money and credit, **(6)** Interest and exchange rate, **(7)** Prices and **(8)** Stock market.

Introducing latent factor estimated by either PCA or IQR in the set of variables used by QVAR to produce forecast has little effect on its tail forecasting accuracy. However, there remains the question of whether we can find evidence that QFAVAR models tend to be less frequently misspecified than the QVAR model. Figure 1.9 displays the number of cases where the null of a correctly specified quantile forecast at the 5th and 95th quantiles could not be rejected at the 5% level. We can see in the last column that using IQR factors rather than a PCA factor results in slightly fewer rejections at both quantiles over all horizons across the whole pseudo-out-of-sample period. Adding factors do not meaningfully impact the conclusions we previously reached for the QVAR model, nor their stability over time, except that including either PCA and IQR factors slightly reduces the number of rejections.

Finally, Figure 1.5 present the shares of non rejection of the null hypothesis of correct unconditional and conditional coverage, respectively, for both QFAVAR models. On average across variable categories and time, introducing a PCA factor slightly increases the cases in which the model is found to have incorrect coverage. Moreover, it does not address the issue of excessive clustering of violations of the 5th and 95th conditional quantile bounds. Two notable exceptions are with interest and exchange rates (group 6) and the stock market (group 8) where both the issues with coverage and clustering are improved. The story is quite different when we introduce IQR factors. This QFAVAR model is found to have correct unconditional and conditional coverage more frequently across time and variable categories. This provides some suggestive evidence that factors which specifically target tail behavior in large data sets carries useful some information that allows improving the timing of changes in risk such that the model less frequently leads to serially correlated tail events (i.e., observations that lie in the tails of its forecasts). This would be worth exploring in future research.

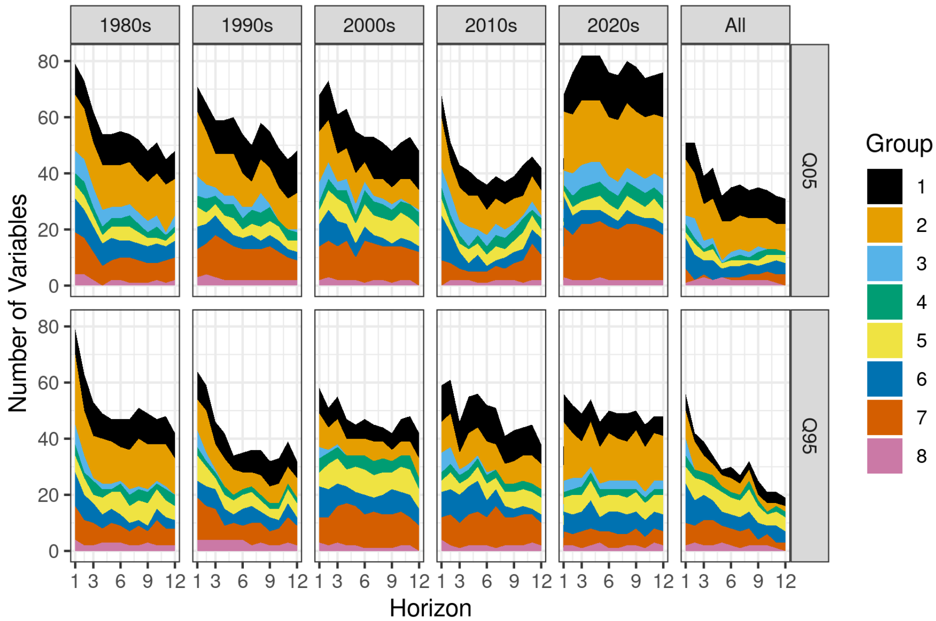

(a) Number of Optimal QFAVAR (PCA) Forecasts

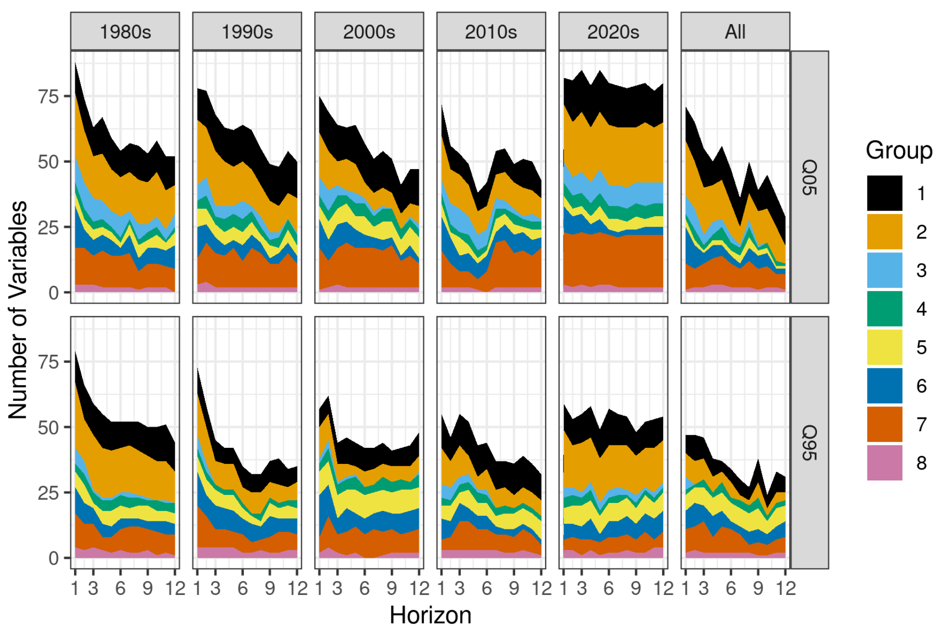

(b) Number of Optimal QFAVAR (IQR) Forecasts

Figure 1.9: QFAVAR Relative Scores (tail-weighted CRPS)

Note: Number of cases where we obtain a non rejection of the null of optimal forecast at 5% for the Gaglianone et al. (2011) test. Columns are periods and rows are the 5th (Q05) and 95th (Q95) quantile forecasts, respectively. Colors indicate FRED groups: **(1)** Output and income, **(2)** Labor market, **(3)** Housing, **(4)** Consumption, orders and inventories, **(5)** Money and credit, **(6)** Interest and exchange rate, **(7)** Prices and **(8)** Stock market.

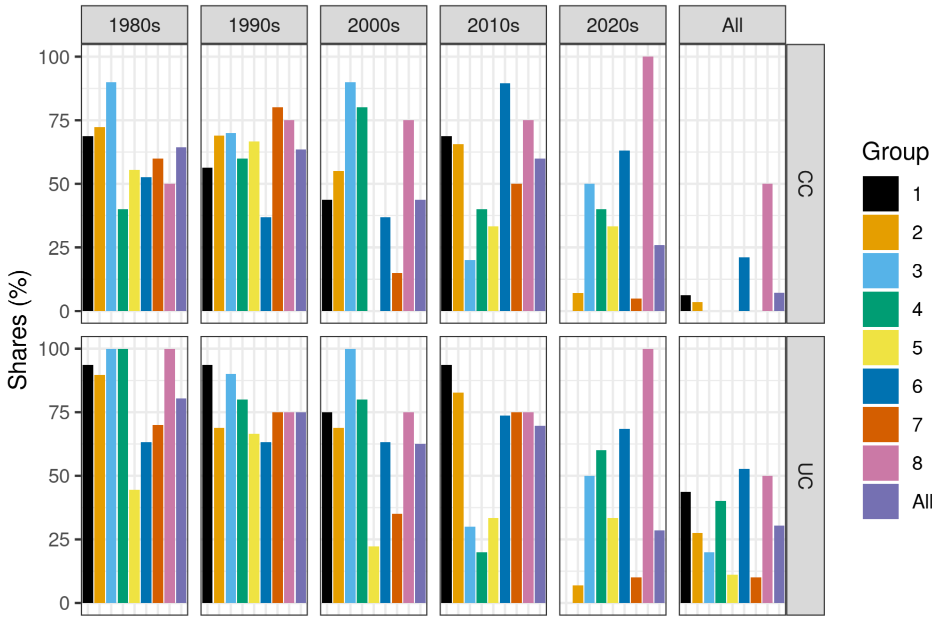

(a) PCA Factor

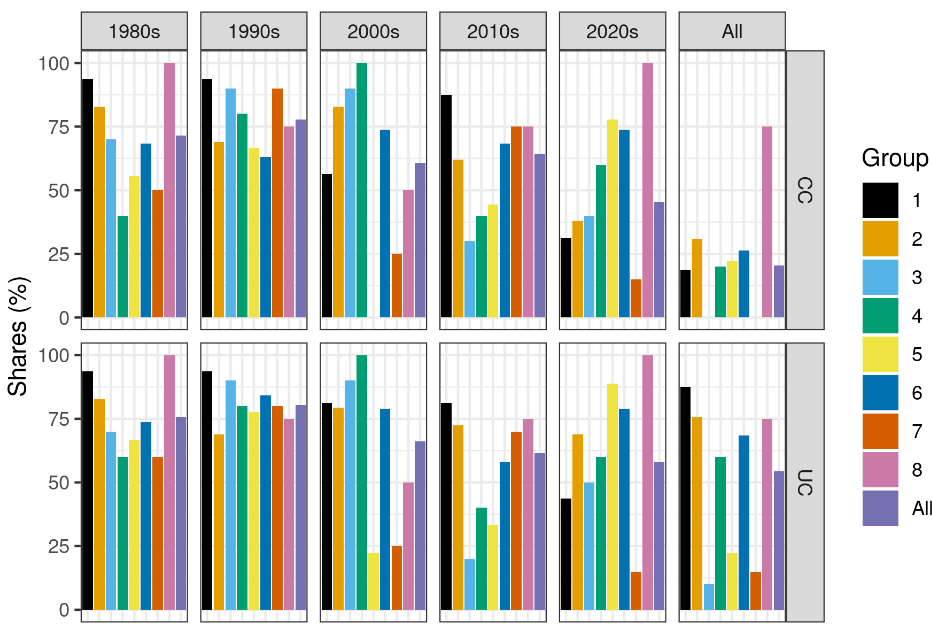

(b) IQR Factors

Figure 1.10: Unconditional and Conditional Coverage Tests on QFAVARs (90% Interval)

Note: Shares of non rejection of the null at 5% using Monte Carlo p-values (Dufour, 2006). UC is the unconditional coverage test and CC is the conditional covargae test. Columns are periods. Colors indicate FRED groups: **(1)** Output and income, **(2)** Labor market, **(3)** Housing, **(4)** Consumption, orders and inventories, **(5)** Money and credit, **(6)** Interest and exchange rate, **(7)** Prices and **(8)** Stock market and **(All)** 112 variables.

1.5 Conclusion

In this paper, we evaluated the performance of the QVAR model for forecasting macroeconomic risk. To this end, we conducted a large out-of-sample forecasting experiment on US monthly variables using VAR-N, VAR-GARCH and VAR-SV models as parametric benchmarks. All models were specified as bivariate models featuring the target variables and the NFCI.

We found that QVAR provides significant improvements in tail density forecasting accuracy over the VAR-N model in close to half of all variables considered and those improvements are frequently quantitatively important, reaching between 10 and 30% in many cases. QVAR also offers improvements over a VAR-GARCH and VAR-SV, albeit in fewer cases. For all three benchmark models, improvements are concentrated in the labor market as well as interest and exchange rate variables. However, we also found evidence that observations which fall in the tails of QVAR forecasts tend to be serially correlated, which points to misspecification.

We then extended QVAR to a data-rich environment by introducing PCA and IQR factors as additional predictors. The resulting QFAVAR model significantly improves upon the QVAR model for forecasting macroeconomic risks in 13% of our target variables. Most of the improvements are tied to labor market variables. Interestingly, adding IQR factors also reduces the incidence of serial correlations with observations that fall in the tails of density forecasts. This suggests the specification issue with QVAR may be alleviated by adding information in the model and that IQR factors, in particular, carry information that helps improve the timing of predicted changes in macroeconomic risks.

In summary, we find that QVAR and QFAVAR models are adequate tools for modeling macroeconomic risk. This is relevant from a macroprudential risk management perspective, as in Chavleishvili et al. (2021), since the relevance of conclusions drawn from such studies requires reliable and accurate models of risk.

CHAPTER II

MAX SHARE IDENTIFICATION FOR STRUCTURAL VARS IN LEVELS: THERE IS NO FREE LUNCH

ABSTRACT[1]

This paper examines the implications of using VARs in levels under the Max Share identification approach when variables exhibit unit or near-unit roots. We derive the asymptotic distributions of the Max Share estimator, demonstrating that it converges to a random matrix, resulting in inconsistent reduced-form impulse responses and eigenvector estimates for structural shock identification. Monte Carlo simulations highlight that VAR models in levels can exhibit significant bias and higher RMSEs at intermediate and long horizons compared to stationary representations (e.g., first-difference VARs or VECMs), particularly in the presence of multiple permanent shocks. An empirical application focusing on investment-specific technology and TFP news shocks underscores the sensitivity of results to the nonstationarity of variables and the identification order of structural shocks when using VARs in levels.

Keywords: SVARs, Max Share identification and inference, unit roots, near-unit roots and asymptotics

JEL Classification: C32, C50.

[1]This Chapter is a paper written with Professor Alain Guay and Professor Florian Pelgrin.

2.1 Introduction

Structural VARs are now routinely applied in empirical macro research to assess and understand the key mechanisms in macroeconomics, such as the impact of technology shocks or the primary drivers of business fluctuations. Building upon the seminal works of Sims (1980b,a), moving from atheoretical/unrestricted VAR models to structural VAR models requires making identifying assumptions grounded on economic theory and related priors—VAR results cannot be interpreted independently of a more structural macroeconomic model (Cooley and Leroy, 1985; Bernanke, 1986).

Recent contributions have often concentrated on forecast error variance decompositions of some target variables, known as the *Max Share identification*, to pinpoint one structural shock (Faust, 1998; Uhlig, 2004) or multiple structural shocks (e.g., Zeev and Khan (2015); Carriero and Volpicella (2024)). For example, this approach identifies technology shocks as those explaining the most significant proportion of the forecast error variance decomposition of labor productivity at ten-year period (Francis et al., 2014). Applications include identifying technology shocks (DiCecio and Owyang, 2012), news shocks (Barsky and Sims, 2011; Kurmann and Otrok, 2013; Forni et al., 2014; Kurmann and Sims, 2021; Bouakez and Kemoe, 2023; Kilian et al., 2023), neutral and investment specific shocks (Chen and Wemy, 2015; Zeev and Khan, 2015), credit shocks (Mumtaz et al., 2018), inflation target shocks (Mumtaz and Theodoridis, 2023), sentiment shocks (Fève and Guay, 2019; Levchenko and Pandalai-Nayar, 2020; Benhima and Cordonier, 2022) and main business cycle shocks (Angeletos et al., 2020).

A common practice in these contributions involves estimating unrestricted VARs *in levels* even when roots may be at or near unity. For instance, the structural identification of technological news shocks relies on a TFP (Total Factor Productivity) measure (e.g., Fernald (2014)), which inherently has an exact unit root due to its construction.[2] Additionally, other macroeconomic variables of interest, such as the relative price of investment goods to consumption and real personal consumption expenditures per capita, may exhibit trending behaviors and potentially near-unit root processes. Some of these variables may also be cointegrated, indicating the presence of common stochastic trends.

The rationale for specifying models *in levels* is that individual regression coefficients can be consistently estimated in any unrestricted VAR model *in levels*, regardless of the potential presence of unit roots and cointegration, as long as the model includes an intercept and sufficient lags, as indicated by Sims et al. (1990). Kilian and Lütkepohl (2017) highlight that the uncertainty regarding the presence of unit roots justifies this approach, as VAR models *in levels* encompass both integrated VAR models and stationary models without a trend. Furthermore, uncertainty about the presence of unit roots in the variables and cointegration relationships between these unit root variables can lead to misspecification and thus inconsistent estimates when using pre-test procedures to transform some variables in the multivariate dynamic representation.

Finally, the Max Share approach involves selecting a truncated forecast error variance horizon to capture short-to-medium or long-run cycles, typically representing a substantial fraction of the sample size. For instance, with quarterly observations spanning 60 years, a truncated horizon of 40 quarters (or 60 or 80 quarters) constitutes a significant part of the sample size. Consequently, the rate at which the maximal truncated horizon increases relative to the sample size is crucial in the asymptotic analysis of the Max Share approach, especially for the impulse response and forecast error variance decomposition estimators.

Unfortunately, combining the estimation of VARs *in levels* with a substantial horizon-

[2]Starting from quarterly estimates of TFP growth (or the first-difference of the logarithm of TFP), one can derive the level (non-stationary) series, typically with initial levels normalized to zero.

to-sample size ratio can result in undesirable statistical properties for impulse responses and forecast error variance decompositions. Phillips (1998) demonstrates that estimated impulse responses and forecast error decompositions are inconsistent at all but the shortest horizons when some unit root processes or local-to-unity processes are present. These estimates tend to converge to random matrices rather than the true impulse responses, despite the consistent estimation of individual autoregressive VAR parameters (Sims et al., 1990).

The results of Phillips (1998) have several implications for the Max Share approach. Most notably, the Max Share identification relies on finding the largest eigenvalue(s) of the Max Share matrix derived from the forecast error variance decomposition, and thus the associated eigenvector(s). Inconsistent estimates of the forecast error variance decomposition impacts the eigendecomposition of this matrix, influencing the distribution of the maximum eigenvalue and the corresponding eigenvector. The severity of this issue naturally depends on the forecast error variance horizon. As a result, including nonstationary variables in unrestricted VARs *in levels* may lead to the identification of a hybrid shock rather than a primitive shock, potentially causing a confounding effect.[3]

Thus, when using the Max Share approach, there is a trade-off between employing a *nonstationary* representation, such as an unrestricted VAR *in levels* with some unit or near-unit roots, and a *stationary* representation, such as a VECM in the presence of common trends or an unrestricted VAR with some first-differenced variables. Indeed, there is no "free lunch"; estimating unrestricted VARs *in levels* may result in inconsistent estimates of structural shocks and impulse responses. Conversely, estimating

[3]See Dieppe et al. (2021) and Francis and Kindberg-Hanlon (2022) for additional discussion on confounding effects with the Max Share approach. They provide evidence that the identification performance of the Max Share procedure is poor when shocks other than the target of interest significantly contribute to the forecast error variance decomposition at the targeted horizon, thus confounding the estimation. In contrast, we outline the consequences of estimating VARs in levels in the presence of confounding effects, as for instance two dominant permanent structural shocks.

a VECM (or a VAR with variables in differences) may suffer from misspecification issues due to pre-test procedures.

Therefore, it is crucial to thoroughly understand the consequences of using variables *in levels* for the Max Share identification approach in the presence of unit-root or near-unit-root processes. The contributions of this paper are as follows: First, we derive the asymptotic results for the estimator of the Max Share matrix, its eigenvalues, and the corresponding eigenvectors in the presence of (weakly) stationary variables. This analysis is conducted in three cases of interest: maximizing the objective function over a given maximal horizon (e.g., Kurmann and Sims (2021)), over a range of horizons (e.g., Zeev and Khan (2015)), or over a frequency interval (e.g., Angeletos et al. (2020)). Notably, the asymptotic distributions of the Max Share estimator, the eigenvalues, and the associated eigenvectors have not been previously proposed in the literature.

Second, building upon the seminal work of Phillips (1998), we derive the Max Share asymptotics with roots at or near unity. Specifically, when the horizon is a fixed fraction of the sample size, we show that the estimator of the Max Share matrix is inconsistent when the unrestricted VAR is estimated *in levels*, converging instead to a random matrix that is a continuous average of a matrix quadratic form in the limiting (reduced-form) impulse responses. Consequently, the estimators of both the largest eigenvalue and the associated eigenvector are also inconsistent, tending towards a random variable/vector. We illustrate our results using a bivariate structural VAR in four relevant cases for applied macroeconomics: (i) the first variable is a unit root process while the second one is weakly stationary, (ii) both variables possess a unit root without cointegration, (iii) both variables are cointegrated and (iv) the first variable has a unit root while the second one is a near-to-unity stochastic process.

Third, we conduct Monte Carlo simulations using a flexible bivariate data-generating process (DGP) that accommodates a unit-root process, a highly persistent process, and a potential confounding effect between two permanent structural shocks. Through these simulations, we compare the performance of a *stationary* representation, achieved by appropriately transforming the variables of the DGP, with a VAR *in levels*. We use OLS-based estimates for the stationary specification, as well as OLS-based estimates, bias-corrected estimates (Pope, 1990), and bootstrapped estimates (Kilian, 1998a; Inoue and Kilian, 2002a) for the *level* specification, across different impulse response horizons and truncated forecast error variance horizons.[4]

In this respect, we highlight the following key insights:

1. **Structural impulse responses**: Structural impulse responses derived from VAR models in *levels* show a significant loss in terms of bias and RMSE properties at intermediate and long horizons compared to those from the stationary representation of VAR models (e.g., first-difference specification), despite performing similarly at (very) short horizons.

2. **Bias Correction and estimation methods**: Bias-corrected, bootstrap, or Bayesian methods can reduce the bias in OLS-based impulse response estimates in unrestricted VARs in *levels*. However, these methods may increase RMSEs and generally perform worse than estimates derived from a *stationary* representation (e.g., *first-difference* model).

3. **Confounding effects**: The presence of a potential confounding effect, such as two permanent shocks, further amplifies the discrepancies between *first-difference* estimates and *level*-based estimates.

Finally, we illustrate our theoretical and simulation results through an application that identifies two permanent shocks, namely an investment-specific technology and TFP

[4]Bayesian estimates using Minnesota priors and estimates from short-run identification are also available upon request.

news shocks, using the Max-share approach (See Fisher (2006); Chen and Wemy (2015); Zeev and Khan (2015); Kurmann and Sims (2021)). Results critically depend on the integration order of the variables, and thus the chosen specification in level or in first-difference, and the identification order of structural shocks. Notably, in the specification using *level* variables, the impulse response functions differ substantially depending on whether the TFP measure or the relative price of consumption-to-investment is placed first. However, it vanishes when stationary transformations of the variables are performed.

Both theoretical and empirical results underscore that the application of the Max-share approach using variables *in levels*, especially when some of the variables are characterized by unit or near unit root processes (and possibly cointegration relationships), can have detrimental effects on the identification of structural shocks and their corresponding impulse response functions. These issues are exacerbated when a long forecast error variance horizon is chosen and multiple permanent shocks are present. Therefore, it is strongly recommended to also report the corresponding results using stationary transformations of the variables, such as with a VECM or a VAR with first-differenced variables.

The rest of the paper is organized as follows. Section 2.2 reviews notation and presents the Max-share identification strategy. Section 2.3 presents the asymptotic results in the presence of (weakly) stationary variables and extends the results to cases where unrestricted VAR models are estimated in levels and there are some roots at, or near, unity. Section 2.4 provides Monte Carlo simulations, while Section 2.5 discusses an empirical application regarding the identification of investment-specific and technology long-term shocks. The last section contains concluding comments and future extensions. Proofs are gathered in Appendix B.

2.2 Max share identification of structural VAR models

In this section, we first introduce preliminary notation and provide an overview of the Max Share approach.

2.2.1 Notation

Let $= ({}_1 \quad)'$ be a N-vector time series generated by the following th order vector autoregressive model in *levels*:

$$= \sum_{=1} \quad _{-} + \quad = \; (\;\;) \; _{-1} + \tag{2.1}$$

where is the lag operator, the ( ) autoregressive matrices are fixed, $=$ $({}_1 \quad)'$ is a -dimensional weak white noise with $\mathbb{E}[\quad] = 0 \; _{\times 1}$ and $\mathbb{E}[\quad '] =$. The reduced-form (2.1) is initialized at $= \quad + 1 \quad 0$ and we let these initial values be any random vectors including constants.The presence of deterministic regressors does not affect our main results and thus we proceed without them to keep the derivations as simple as possible.

The reduced-form VAR can also be written in companion form as:

$$= \quad _{-1} + \tag{2.2}$$

where $= (\; ' \qquad '_{-} \;)'$, $= (\; ' \; 0 \qquad 0)'$, and

$$= \begin{bmatrix} {}_1 & {}_2 & & {}_{-1} & \\ & 0 & & 0 & 0 \\ \vdots & \vdots & \ddots & \vdots & \vdots \\ 0 & 0 & & & 0 \end{bmatrix} \tag{2.3}$$

Up to some initial conditions, the vector moving average (VMA) representation of the reduced-form VAR is then defined by:

$$= \sum_{=0}^{-1} \quad _{-} \tag{2.4}$$

and one can retrieve the reduced-form VMA representation of :

$$= \sum_{=0}^{-1} \quad _{-} \tag{2.5}$$

where $_0$ is the identity matrix of order , denoted by I , and $= \sum_{=1} \quad _{-}$. Notably, equation 2.5 can be decomposed as follows:

$$= \sum_{=0}^{-1} \quad _{-} = \sum_{=0}^{*} \quad _{-} + \sum_{= ^*+1}^{-1} \quad _{-} \tag{2.6}$$

This decomposition of the VMA representation is useful to study the impulse response and forecast error variance asymptotics in nonstationary VARs (Phillips, 1998). In particular, it is worth emphasizing, for a small fixed *, the estimates of the impulse response matrices have asymptotic normal distributions (as in the stationary case) even in the presence of unit root or nearly unit root processes. In contrast, the estimates of impulse-response matrices of the second right-hand side term, which are those associated to a lead time that can be written formally as $=$ where 0 a fixed fraction of the sample, are inconsistent for all . More specifically, the limits are random variables with unit root or local-to-unity distributions.

The structural VAR model can be written as:

$$_0 \quad = \sum_{=1} \quad _{-} + \quad = \; (\;) \; _{-1} + \tag{2.7}$$

where is an 1 random vector of structural shocks with $\mathbb{E}[\ ] = 0$ and $\mathbb{E}[\ \ ']=$. A common identification assumption is $=$. Taking equations (2.4) and (2.7), the error terms of the reduced-form model are a linear combination of structural shocks:[5]

$$= \ _0^{-1} \ = \ _0 \tag{2.8}$$

with $_0^{-1}\ (\ ) = \ (\ )$. The structural VMA representation is then defined by:

$$= \sum_{=0}^{\infty} \ _0^{-1} \ _{-} = \sum_{=0}^{\infty} \ _{-}$$

where $= \ _0^{-1} = \ _0$. Using equation (2.8), one has $= \ _0^{-1}\ _0^{-1\prime} = \ _0\ _0^{\prime}$. Let $_{\mathrm{tr}}$ denote the lower triangular Cholesky decomposition of (with the diagonal elements normalized to be positive), and let be a orthogonal matrix. Since $^{\prime} = \ ^{\prime} = \mathrm{I}$ and hence $(\ _{\mathrm{tr}}\ )(\ _{\mathrm{tr}}\ )^{\prime} = \ _{\mathrm{tr}}\ _{\mathrm{tr}}^{\prime}$, the set of possible solutions for $_0^{-1}$ can be written as $_{\mathrm{tr}}$. Then identification involves pinning down some or all columns of .

Finally, Equation (2.1) can also be equivalently written in levels and differences format as:

$$= \ _{-1} + \ (\ ) \ _{-1} + \tag{2.9}$$

where $=\ (1)$, $= \sum_{=1}^{-1} \ ^{-1}$ with $= \sum_{=\ +1}$, and $= (\ _1\ \ _2\ )^{\prime}$. Assumptions regarding nonstationary components and the presence of cointegration (i.e., the dimension of the cointegrating space and the form of the cointegration vectors) will be specified in Assumption 2.3.2. Furthermore, the formulation (2.9) proves to be

[5] For a more general presentation, see Amisano and Giannini (1997), Kilian (2013) and Kilian and Lütkepohl (2017).

useful when deriving the asymptotic properties of the Max Share matrix estimator.

2.2.2 Max share approach

Starting from the seminal contributions of Faust (1998) and Uhlig (2003, 2004), the Max Share identification scheme focuses on maximizing the contribution of a (structural) shock to the forecast-error variance of a given variable at a long but finite horizon, say . To illustrate it, consider the bivariate structural VAR model of Gali (1999) that attributes variation in U.S. labour productivity and hours worked to a technology shock and a non-technology shock. The first structural shock, labelled as a technology shock, can be identified by maximizing its contribution to the forecast-error variance of labor productivity (Francis et al., 2014).

Using the VMA representation of the reduced-form VAR, the starting point is to define the -step-ahead forecast error for as a function of realized reduced-form errors:

$$_{+} \quad \mathbb{E}\,[\ _{+}\ ] = \sum_{=0}^{-1} \quad _{+\,-} \tag{2.10}$$

Accordingly, the h-step-ahead forecast-error variance matrix is given by:

$$\mathtt{MSE}(\ ) = \sum_{=0}^{-1} \quad {}' = \sum_{=0}^{-1} \ _{\mathrm{tr}} \quad {}' \ {}'_{\mathrm{tr}} \ {}' \tag{2.11}$$

Then the share of forecast-error variance of a given variable that is attributed to a given shock at horizon is:

$$(\ ) = \frac{{}' \quad (\ )}{{}'\mathtt{MSE}(\ )} = \frac{{}' \ {}' \quad (\ )}{{}'\mathtt{MSE}(\ )} \tag{2.12}$$

where is the -th column vector of the identity matrix, $=$ is the -th column of the orthogonal matrix , and $(\ )$ is the Max Share matrix at horizon for the variable :

$$(\ ) = \sum_{=0}^{-1} {}'_{\mathrm{tr}} \; ' \quad ' \quad {}_{\mathrm{tr}} = \sum_{=0}^{-1} \; ' \tag{2.13}$$

with $= \; ' \quad {}_{\mathrm{tr}}$ the -th row of ${}_{\mathrm{tr}}$. According to the decomposition of the VMA representation (2.6), the Max Share matrix depends not only on the impulse responses at short-run horizons but also on those at longer horizons when constitutes a substantial fraction of the sample size.

We consider the first structural shock $= 1$, which is identified by solving, for a given horizon , the following maximization of the *Max Share statistic* with respect to ${}_1$:

$${}_1 \; (\ ) = \underset{1}{\mathtt{argmax}} \; \frac{{}'_1 \; (\ ) \; {}_1}{{}'\mathtt{MSE}(\ )} \tag{2.14}$$

subject to ${}'_1 \; {}_1 = 1$.[6] Note that the solution, denoted by ${}_1 \; (\ )$, is conditional upon the selection of a truncated forecast error variance horizon . Following Faust (1998) and Uhlig (2003, 2004), it can be shown that ${}_1$ is the eigenvector associated to the largest eigenvalue of the Max Share matrix or, equivalently, is the first principal component:

$$(\ ) \; {}_1 \; (\ ) = \; {}_{\max} \; {}_1 \; (\ ) \tag{2.15}$$

Thus, the structural IRFs from the identified shock are given by:

$${}_{\cdot 1} \; (\ ) = \; {}_{\mathrm{tr}} \; {}_1 \; (\ ) \tag{2.16}$$

where ${}_{\cdot 1}$ is the first column of the impulse response matrix . The identified shocks and the corresponding IFRs then depend on the finite sample and the asymptotic prop-

[6]Without loss of generality, note that further structural constraints can be added, such as the absence of contemporaneous effect of a structural shock (e.g., Zeev and Khan (2015); Bouakez and Kemoe (2023)).

erties of the Max Share matrix for a given horizon (i.e., ( )), as well as the largest eigenvalue $_{\max}$ and the associated eigenvector $_1$. As aforementioned and according to the VMA decomposition (2.6), the Max Share matrix depends not only on the impulse responses at short-run horizons but also on those at longer horizons when constitutes a substantial fraction of the sample size. The next section examines the asymptotic properties of these elements.

As a final remark, other Max Share matrices have been considered in the literature. On the one hand, as stated in Uhlig (2003) and Barsky and Sims (2011), one can also consider an *accumulated* Max Share approch, i.e., the (partial) sum of the contributions of a given structural shock to the forecast-error variance of a given variable between two finite horizons, say $\underline{\ }$ and $\bar{\ }$ (with $\bar{\ }$ $\underline{\ }$). Notably, the accumulated Max Share matrix, denoted by $(\underline{\ }\ \bar{\ })$, is then given by:

$$(\underline{\ }\ \bar{\ }) = \sum_{=\underline{\ }}^{\bar{\ }} \frac{(\ )}{{}'\mathrm{MSE}(\ )} = \sum_{=\underline{\ }}^{\bar{\ }} \frac{\sum_{=0}^{-1} \quad {}'}{\sum_{=0}^{-1} \quad {}'}$$

In this expression, the weight decreases for $= \underline{\ } \quad \bar{\ }$, and thus the accumulated Max Share matrix places more weight on short horizons than long horizons. Similarly to the non-accumulated Max Share approach, the first structural shock $= 1$ is identified by maximizing, for a given horizon interval $[\underline{\ };\bar{\ }]$, the following Max Share statistics with respect to $_1$:

$$_1^{(\ )} = \underset{1}{\mathrm{argmax}} \quad {}_1' \left(\sum_{=\underline{\ }}^{\bar{\ }} \frac{(\ )}{{}'\mathrm{MSE}(\ )} \right) \ _1 \tag{2.17}$$

subject to ${}_1' \ _1 = 1$.

On the other hand, building on DiCecio and Owyang (2012), Francis et al. (2014) and Angeletos et al. (2020), the Max Share approach in the frequency domain aims to maximize the contribution of a given structural shock to the spectral density of a given variable over a frequency interval, say $[\_;\bar{\ }]$. Provided the multivariate spectral density, denoted by , is well-defined $[\ ;\ ]$, one has:

$$(\ ) = \frac{1}{2}\overline{(\ (\ ))}\quad (\ (\ ))$$

where $\bar{\ }$ denotes the complex conjugate transpose of . Therefore, the Max share statistics in the frequency domain, that is the contribution to the spectral density of a given variable attributable to a given shock , say $= 1$, over a frequency band $[\_;\bar{\ }]$ is defined by:

$$\frac{{}'_1\ (\_;\bar{\ })\ {}_1}{{}'(\_\ \bar{\ })} \tag{2.18}$$

where the frequency Max Share matrix over the frequency band $[\_;\bar{\ }]$ is:

$$(\_;\bar{\ }) = 2\mathrm{Re}\int_{\_}^{\bar{\ }} \overline{\ (\exp(\ ))}\quad (\exp(\ )) \tag{2.19}$$

where $(\exp(\ )) = [\ (\exp(\ ))\ {}_{\mathrm{tr}}] = \left[\sum_{=0}^{\infty}\ (\exp(\ ))\ {}_{\mathrm{tr}}\right]$ and $\mathtt{Re}$ is the real part of any complex. The identification and interpretation of the first structural shock then proceeds as in the case of the *non-accumulated* Max Share approach at a given horizon . In the frequency domain, the Max Share matrix relies on the infinite sum of the (reduced-form) impulse responses irrespective of the frequency interval. A truncated sum may weaken the statistical performances in the presence of persistent stochastic processes.[7]

---

[7]Note that the multivariate spectral density is no longer defined at $\omega = 0$ in the presence of unit or near-unit root processes.

2.3 Max Share asymptotics

This section delves into the asymptotic properties of the Max Share estimator. We start by examining the asymptotic distribution of the estimator for the Max Share matrix in the context of a weakly stationary multivariate process . These results are also valid for VAR models *in levels* with a fixed in the VMA decomposition (2.6), i.e., for short horizons. Next, we characterize the asymptotic distribution of the (maximal) eigenvalues and their corresponding eigenvectors. We then provide the asymptotic distribution of the Max Share estimator in the presence of roots at or near unity. As highlighted by the decomposition (2.6), the small sample properties of the Max Share approach based on a VAR *in levels* stem from the finite-sample approximations associated with these two asymptotic behaviors.

2.3.1 Max Share asymptotics with weakly stationary processes

We suppose that:

Assumption 2.3.1 (Stationary Case)

(a) *is an i.i.d. process with zero mean, covariance matrix* 0 *and finite fourth cumulants;*

(b) *The determinantal equation* $\sum_{=1} \quad = 0$ *has roots outside the unit circle.*

Following Lütkepohl (2005) and using the Delta method, the asymptotic distribution of the estimator of the Max Share matrix at a fixed horizon is then given in Theorem 2 3 1

Theorem 2.3.1 *Let Assumption 2.3.1 hold and let $= vec([\ _1\ ])$, $= vech(\ )$, $= (\ _{+1}\ )$ $\mathbb{R}^{\times(\ -\ )}$, and $(0) :=$ $[(\ (\ ))(\ (\ ))']$. Then, as , the estimator of the Max Share matrix $(\ )$, denoted $\widehat{\ }(\ )$, at a fixed and finite forecast error variance horizon is weakly consistent and is asymptotically normally distributed:*

$$\overline{\ }\, vec\left(\widehat{\ }(\ ) \quad (\ )\right) \quad \mathcal{N}(0 \quad (\ ))$$

with

$$(\ ) = \begin{bmatrix} \tilde{}(\ ) & (\ ) \end{bmatrix} \begin{bmatrix} (0)^{-1} & 0 \\ 0 & 2\ ^{+}(\ \ )\ ^{+\prime} \end{bmatrix} \begin{bmatrix} {}'_{\tilde{}}(\ ) \\ {}'(\ ) \end{bmatrix}$$

where $^{+} := (\ '\ )^{-1}\ '$ is the Moore-Penrose generalized inverse of an appropriate $^2 \quad (\ + 1)\ 2$ duplication matrix, and the gradients $\tilde{}(\ )$ and $(\ )$ are defined in Appendix B.

Proof: See Appendix B.

This Theorem can be easily adapted to apply to the *accumulated* Max Share approach (Uhlig, 2003; Barsky and Sims, 2011), which involves summing the contributions of the th structural shock to the forecast error variance of the th variable between two finite horizons. It can also be extended to the Max Share approach in the *frequency* domain (DiCecio and Owyang (2012); Angeletos et al. (2020).[8]

We can now provide the asymptotic distribution of the eigenvalues of $(\ )$. We start

[8]Appendix B provides the results in the case of the accumulated Max Share matrix (respectively, the non-accumulated frequency-based Max Share approach).

from the spectral decomposition of ( ):

$$( ) = ( ) ( ) ( )' \qquad (2.20)$$

where ( ) is the diagonal matrix associated with the ordered eigenvalues ( ), $= 1$, and ( ) is the corresponding matrix of (orthonormal) eigenvectors. By convention, we assume that the eigenvalues are always arranged in algebraically non-increasing order:

$$_{\max}( ) \quad _1( ) \quad _2( ) \qquad ( ) \quad _{\min}( )$$

Since ( ) is not necessarily of full rank, suppose that the first eigenvalues are different from zero, and thus the last eigenvalues are equal to zero. Accordingly, the orthonormal matrix ( ) can be partitioned as $( ) = \left[\quad ( ) \quad _{-}( ) \right]$, where $( ) = \left[\ _1( ) \quad _{2:}( ) \right]$, with $_1( )$ being the eigenvector associated with $_{\max}( )$, $_{2:}( )$ the matrix of eigenvectors associated with $_2( )$ ( ), and $_{-}( )$ the matrix of eigenvectors associated with the smallest eigenvalues $_{+1}( )$ $_{\min}( )$. Notably,

$$_{\max}( ) = {}'_1 ( ) \quad ( ) \ _1 \ ( )$$
$$_{2:}( ) = \mathrm{vec}(\ {}'_{2:} ( ) \quad ( ) \ _{2:} ( ))$$

Combining this decomposition with Theorem 2.3.1, the asymptotic distribution of the eigenvalues follows.

Theorem 2.3.2 *Let Assumption 2.3.1 hold. Then, the (ordered) eigenvalue estimators* ( ), *which solve the spectral decomposition (equation 2.20) for* $\widehat{\ }$ ( ), *are weakly consistent estimators of* ( ), $= 1$. *Furthermore, the asymptotic distribution* *of* $\widehat{\ }_{\max}\ (\ )$ *at a fixed and finite forecast error variance horizon is given by:*

$$\bar{\ }\left(\widehat{\ }_{\max}\ (\ )\quad {}_{\max}(\ )\right)\qquad (0\ (\ {}_{1}\ (\ )\quad {}_{1}\ (\ ))'\ (\ )(\ {}_{1}\ (\ )\quad {}_{1}\ (\ )))$$

where $(\ )$ *is the asymptotic variance-covariance matrix of* $\bar{\ }vec\left(\widehat{\ }\ (\ )\quad (\ )\right)$ *as given in Theorem 2.3.1. Additionally, the asymptotic distribution of* $\widehat{\ }_{2:}\ = \left(\widehat{\ }_{2}\ (\ )\quad \widehat{\ }\ (\ )\right)'$ *is:*

$$\bar{\ }\left(\widehat{\ }_{2:}\ (\ )\quad {}_{2:}(\ )\right)\qquad (0\ (\ {}_{2:}(\ )\quad {}_{2:}(\ ))'\ (\ )(\ {}_{2:}(\ )\quad {}_{2:}(\ )))$$

Proof: See Appendix B.

There are three points worth noting. First, the weak convergence of the eigenvalue estimator stems from the continuity property. Specifically, this implies that $(\ )\quad (\ )$ for $= 1$ and $(\ )\quad 0$ for $= \ + 1$. Second, a consistent estimate of the asymptotic variance-covariance matrix of the largest eigenvalue relies on a consistent estimate of both $(\ )$ and the eigenvector associated with ${}_{\max}(\ )$. This creates two sources of uncertainty in finite samples. Third, it is straightforward to show that the asymptotic distribution of the largest eigenvalue (and of ${}_{2:}\ (\ )$, respectively) in the case of the *accumulated* or frequency-based Max Share approach has the same expression as in Theorem 2.3.2, except for the appropriate asymptotic variance-covariance matrix defined in the Appendix B.

Finally, we derive the asymptotic distribution of the eigenvector associated with the maximal eigenvalue, as well as the joint distribution of the $\ 1$ eigenvectors associated with the remaining $\ 1$ largest (nonzero) eigenvalues, denoted by ${}_{2:}\ (\ )$. For simplicity, ${}_{1}\ (\ )$ is abbreviated as ${}_{1}(\ )$, and the results apply to any variable $= 1$.

Theorem 2.3.3 *Let Assumption 2.3.1 hold. Suppose that* $_{\max}(\ )$ $_2(\ ) +$ *for* 0*, i.e., the maximum eigenvalue of* $(\ )$ *is well-separated from the second highest eigenvalue. Then,*

i) $\widehat{\ }_1 \ (\ )$ $_1(\ )$ *and the asymptotic distribution of* $\widehat{\ }_1 \ (\ )$ *is:*

$$\overline{\ } (\widehat{\ }_1 \ (\ ) \quad _1(\ )) \qquad (0 \quad _1(\ ))$$

where $_1(\ ) = (\ {}_1'(\ ) \qquad) \ {}_1'(\ ) \ (\ ) \ _1(\ )(\ _1(\ ) \qquad)$*, with* $_1(\ ) = \sum_{=2}(\ _{\max}(\ ) \quad (\ ))^{-1} \ _1(\ ) \quad {}'_j(h)$*, and* $_j(\ ) = \ (\ ) \ '(\ )$ *is the eigen-projection associated with* $(\ )$*;*

ii) $\widehat{\ }_{2:} \ (\ )$ $_{2:} (\ )$ *and the asymptotic distribution of* $\mathrm{vec}(\widehat{\ }_{2:} \ )(\ )$ *is:*

$$\overline{\ } \left(\mathrm{vec}(\widehat{\ }_{2:} \ (\ )) \quad \mathrm{vec}(\ _{2:} (\ ))\right) \qquad (0 \quad _{2:r}(\ ))$$

where $_{2:r}(\ ) = (\ {}'_{2:} (\ ) \qquad) \ {}_2'(\ ) \ (\ ) \ _2(\ )(\ _{2:} (\ ) \qquad)$*, with* $_2(\ ) = \sum_{=2} \sum_{\neq} (\ (\ ) \quad (\ ))^{-1} \ _j(\ ) \quad {}'_i(\ )$*.*

Proof: See Appendix B.

As consequences of the above results, considering the expression of the structural IRFs using the first (identified) structural shock associated with the largest eigenvalue (equation 2.16), the estimates of structural IRFs depend on the reduced-form estimates $\ $, the lower-triangular factor from the Cholesky decomposition, and the eigenvector $_1$, which are nonlinear functions of the estimates of the autoregressive parameters. In the weakly stationary case, all these estimates converge in probability to their respective true values, implying that the structural IRFs associated with the largest eigenvalue are weakly consistent.[9]

[9]See Lütkepohl (2005) for the asymptotic properties of the reduced-form moving average coef-

In the special case where the error terms of the reduced-form VAR are normally distributed, and according to Anderson (1963), the expression of $_1$ is given by:

$$_1(\ ) = \ _{2:}(\ )\left(\tilde{}(\ )\right)^2 \ {}'_{2:}(\ )$$

where

$$\tilde{}(\ ) = \begin{bmatrix} (\ _1(\ )\ \ _2(\ ))^{1\ 2}\ (\ _1(\ )\ \ \ _2(\ )) & & 0 \\ \vdots & \ddots & \vdots \\ 0 & & (\ _1(\ )\ \ (\ ))^{1\ 2}\ (\ _1(\ )\ \ \ (\ )) \end{bmatrix}$$

In the general case, the expression of $_1(\ )$ (respectively, $_{2:r}(\ )$) depends on $_1(\ )$ (respectively, $_2$). Specifically, $_1(\ )$ is a linear combination of the Kronecker products between the eigenprojection associated with the maximal eigenvalue $_{\max}(\ )$, denoted by $_1(\ )$, and those associated with each other eigenvalue $(\ )$, denoted by $_j(\ )$. The weight of each Kronecker product is determined by the discrepancy between $_{\max}(\ )$ and $(\ )$, specifically by $_{\max}(\ )\ \ _2(\ )$, that is, the difference between the two largest eigenvalues. When these two eigenvalues are roughly of the same magnitude, the presence of at least two driving structural shocks cannot be ruled out, causing $_1(\ )$ to become arbitrarily large. Thus, an examination of the empirical eigenvalues is necessary.

2.3.2 Max Share asymptotics with some roots at, or near, unity

We now discuss the asymptotics of the Max Share estimator in the presence of nearly unit root and/or nonstationary processes when the VAR model is estimated *in levels*. In the spirit of Phillips (1998), our primary interest is on the behaviour of when

ficients in the stationary case.

the sample size goes to infinity and the horizon is a fixed fraction of , that is, $=$.[10]

Consider the general specification in levels and differences:

$$= \quad {}_{-1} + \quad (\quad) \quad {}_{-1} +$$

We construct the orthogonal matrix $= [\;\; {}_{\perp} \;\;]$ where ${}_{\perp}$ is an $(\quad)$ orthogonal full rank matrix containing the unit roots or near unit roots linear combinations of and is an orthogonal full rank matrix containing the stationary linear combinations of .

Following Phillips (1998), we assume that:

Assumption 2.3.2

(a) *is an i.i.d. process with zero mean, covariance matrix* 0 *and finite fourth cumulants;*

(b) *The determinantal equation* $\sum_{=1} \quad = 0$ *has roots on or outside the unit circle;*

(c) $= \; {}_{\perp} \exp(\; {}^{-1} \;) \; {}'_{\perp} + \quad {}' + \quad {}'$, *where* $\mathbb{R}^{\times}$ *and* $0 \quad \operatorname{rank}(\;) = \operatorname{rank}(\;) =$. *Without loss of generality, is orthonormal, and* $\mathbb{R}^{\times}$ *is a constant matrix;*

(d) *The matrix* ${}'_{\perp} (\qquad (1)) \; {}_{\perp}$ *is nonsingular and* ${}_{\perp} \quad {}_{\perp} \quad \mathbb{R}^{\times}$ *with* $=$ *are the orthogonal complements of and , respectively.*

---

[10] One could also consider the case where both h and T go to infinity such that $h/T \quad 0$. However, it is less relevant from a macroeconomic perspective.

The standard condition **(a)** is necessary for deriving the asymptotic variance matrix. Condition **(b)** allows for the inclusion of both stationary and nonstationary components. Condition **(c)** encompasses the unit root and local-to-unity cases. Specifically, the matrix can be interpreted as a noncentrality parameter matrix (see Phillips (1998)).[11] Moreover, note that $=\ '$ in the presence of unit roots and cointegration. Lastly, condition **(d)** specifies that the stochastic process is driven by random walks and/or nearly integrated processes. Consequently, the linear combinations $'_{\perp}$ exhibit unit roots or near unit roots (or a mixture of both), while $'$ remains stationary.

Interestingly, Assumption 2.3.2 covers several cases of interest. Notably, empirical macroeconomic applications often focus on one of the following four cases.

- **Case 1:** Some variables have a unit root while other variables are weakly stationary. For instance, in the bivariate case, one variable possesses a unit root (e.g., a TFP measure) and the other is stationary with an autoregressive coefficient (e.g., a financial spread), say $= 9$. In this case, $= 1$, $= 1$, and $= [0 \quad 1]'$.

- **Case 2:** All variables in the vector possess a unit root without cointegration (Lütkepohl and Velinov, 2016). Accordingly, $_{\perp} =$, is the null matrix, and $(\ ^{-1}\ ) =$.

- **Case 3:** All variables possess a unit root but there are cointegration relationships (e.g., the baseline quarterly model of King et al. (1991)), $(\ ^{-1}\ ) =$, and $=\ '$.

- **Case 4:** Some variables have a unit root (e.g., a TFP measure) and other variables have near unit roots (e.g., hours worked). In particular, can be a diagonal matrix in which some series may be I(1) processes corresponding to the components

[11] An alternative and asymptotically equivalent approach is to replace the matrix exponential representation with deviations from I_s of the form $I_s + T^{-1}\Gamma$.

with $\quad = 0$, and some series may be stable processes with near unit roots (that is, $\quad 0$).[12] The matrix $\quad$ can be partitioned such that the first diagonal elements correspond to the I(1) variables and the remaining elements correspond to the nearly integrated variables.

We are now in a position to present the asymptotics of the impulse responses and the Max Share matrix in the presence of unit or near-unit roots when the unrestricted (reduced-form) VAR is estimated *in levels*. To avoid any confusion, note that in the sequel, we use the index $\quad$ (respectively, the notation $\quad$) to denote the impulse response horizon or lead time (respectively, the forecast error variance horizon).

Theorem 2.3.4 *Consider the reduced-form VAR in levels (equation 2.1). Let Assumption 2.3.2 hold, and let* $\quad [0 \;\; 1]$. *Then,*

i) If the lead time $\quad = \quad$*, where* $\quad 0$ *is a fixed fraction of the sample, the limiting reduced-form impulse response matrix* $\quad$ *is nonzero as* $\quad$*:*

$$\quad = \;{}_{\perp} \exp(\quad {}_{\Gamma}) \; {}' \tag{2.21}$$

ii) If $\quad = \quad$*, where* $\quad 0$ *is a fixed fraction of the sample, then the limiting non-accumulated Max Share matrix and the h-step-ahead forecast-error variance matrix at horizon* $\quad$ *are random as* $\quad$*:*

$$ {}^{-1}\widehat{\quad} \;(\quad) \qquad {}^{-1}\int_0 \quad {}'_{tr} \quad \exp(\quad {}'_{\Gamma}) \;{}'_{\perp} \quad {}' \;{}_{\perp}\exp(\quad {}_{\Gamma}) \;{}' \quad {}_{tr} \qquad (\quad {}_{\Gamma}) \tag{2.22}$$

$$ {}^{-1}MSE(\quad) \qquad {}^{-1}\int_0 \quad {}_{\perp}\exp(\quad {}_{\Gamma}) \;{}' \qquad \exp(\quad {}'_{\Gamma}) \;{}'_{\perp} \tag{2.23}$$

---

[12] Note that if Γ has some nonzero off-diagonal elements, one can have series that are near integrated of different orders.

where denotes weak convergence. The formal definitions of the matrices $_{\perp}$, *, and* $_{\Gamma}$*, which is a matrix function of a mixture of unit-root or local-to-unity distributions (or a mixture of both distributions), are given in Appendix B.*

Proof: These results follow directly from Lemma 2.2 and Theorem 3.1 in Phillips (1998).

Part (i) of Theorem 2.3.4 asserts that the limiting response matrices of the moving average (reduced-form) representation lie in the range of $_{\perp}$ in the presence of roots at or near unity. This implies that the limiting impulse responses, denoted as , are nonzero exclusively for nonstationary variables possessing unit roots or near unit roots, specifically for $'_{\perp}$, particularly when the lead time constitutes a significant fraction of the sample size. Moreover, the matrix captures the permanent impact of the reduced-form innovations on $'_{\perp}$.

Importantly, result (i) shows that for $=$ where 0 is a fixed fraction of the sample, the impulse response matrices in the moving average representation for the VAR *in levels* are inconsistent except at the very shortest horizons. More precisely, the limits of the impulse response matrices become random variables rather than true values. The presence of unit roots and/or nearly unit roots accelerates the convergence of OLS estimates and leads to (super-)consistency in OLS regressions in levels (see Sims et al. (1990)). Specifically, as explained by Phillips (1998), impulse response functions do not converge faster in some directions, defined from the range of $_{\perp}$, but rather carry the effects of (near) unit roots indefinitely as the lead time increases. It is important to note that (near) unit roots are estimated with some degree of error, and this error not only persists but also accumulates as , with the impulse response horizon constituting a non-negligible fraction of the sample size.

The second result (ii) of Theorem 2.3.4 establishes that the estimator of the Max Share

$\widehat{\ }\ (\ )$ matrix becomes inconsistent and converges to a random matrix, when the unrestricted VAR is estimated in levels. This inconsistency arises because $\widehat{\ }\ (\ )$ depends on the reduced-form impulse response estimates at medium-to-long horizons (equations 2.6 and 2.13). Specifically, this random matrix represents a continuous average of a (matrix) quadratic form, derived from the limiting (reduced-form) impulse responses (equation 2.22). Consequently, the estimators of the corresponding eigenvalues and eigenvectors are also inconsistent, failing to converge to their true values.

Similarly, the mean squared error converges to a random variable, which is a continuous average of a quadratic form derived from the limiting reduced-form impulse responses. Interestingly, the Max Share statistic can converge weakly in probability to a non-random matrix when the forecast error variance horizon is a fixed fraction of the sample size and diverges to infinity, that is, the mixture of unit root or local-to-unity distributions does not contribute to the limiting Max Share statistic. For instance, this occurs in the first experiment of our Monte Carlo simulations. Meanwhile, finite-sample approximations can be severely distorted relative to the limiting distribution.

Given that structural IRFs from the identified Max Share shock are given by equation (2.16), the presence of some roots at, or near, unity has three significant implications. Firstly, according to Theorem 2.3.4(i), structural impulse responses, which are fundamentally functions of the reduced-form impulse responses, are inconsistent when roots are at or near unity. Their limits are altered by the distribution of the unit root or near unit root processes. Secondly, as stated in Theorem 2.3.4(ii), structural impulse response functions are also inconsistent due to the estimation of the eigenvector $_1\ (\ )$. Specifically, with a medium- to long-term Max Share identification scheme, the (inconsistent) estimate of $_1\ (\ )$, derived from an inconsistent estimate of the Max Share matrix, affects all structural impulse response matrices. This impact is not limited to those with a lead time extending beyond a fixed fraction of the sample size but also contaminates the entire structural IRF matrices. Thirdly, in combination with the inherent inconsistency of the reduced-form impulse response matrices, non-normal asymptotics generally prevail. This results in non-normal random limits, even in the presence of stationary components within the VAR specification. Therefore, the structural IRFs are influenced by the stochastic nature of the eigenvector estimates and the nonstationarity embedded within the unrestricted VAR model *in levels*.

2.4 Monte Carlo simulations

This section provides some Monte Carlo simulations to study the performances of the Max-share procedure in the presence of misspecification regarding the integration order. We assume that the data generating process (DGP) is a bivariate VAR model:

$$\begin{pmatrix} \;\;_{1} \\ _{2} \end{pmatrix} = \begin{pmatrix} _{11} & _{12}+ \\ _{21} & _{22} \end{pmatrix} \begin{pmatrix} _{1\;-1} \\ _{2\;-1} \end{pmatrix} + \begin{pmatrix} 0 & _{12} \\ 0 & 0 \end{pmatrix} \begin{pmatrix} _{1\;-2} \\ _{2\;-2} \end{pmatrix} + \begin{pmatrix} _{1} \\ _{2} \end{pmatrix} \tag{2.24}$$

with

$$= \begin{pmatrix} 1 & _{12} \\ _{21} & 1 \end{pmatrix} \begin{pmatrix} _{1} \\ _{2} \end{pmatrix}$$

where $\quad (0 \quad _2)$ is a bivariate vector of structural shocks.

The parameter controls the number of permanent structural shocks and the magnitude of the permanent effect of the second shock $_2$ on the first variable $_1$. When $= 0$, only the first structural shock has a permanent impact on the first variable. To some extent, the corresponding specification can be viewed as the one often encountered in the macroeconomic literature to identify a permanent shock, for example, the identification of a technology shock with some measures of (labor or total) productivity and hours worked (see Section 2.5).[13] When $= 0$, the two structural shocks have a permanent effect on the first variable (e.g., Fisher (2006)). In other words, the identification of the first structural shock can be contaminated by the second permanent structural shock, meaning the two permanent shocks can be confounded. Taking the transformation of the first variable, this specification is labeled the *first-difference* model.

On the other hand, the corresponding specification *in levels* is given by:

$$\begin{aligned} \begin{pmatrix} {}_{1} \\ {}_{2} \end{pmatrix} &= \begin{pmatrix} 1 + {}_{11} & {}_{12} + \\ {}_{21} & {}_{22} \end{pmatrix} \begin{pmatrix} {}_{1\ -1} \\ {}_{2\ -1} \end{pmatrix} \\ &+ \begin{pmatrix} {}_{11} & {}_{12} \\ {}_{21} & 0 \end{pmatrix} \begin{pmatrix} {}_{1\ -2} \\ {}_{2\ -2} \end{pmatrix} + \end{aligned} \tag{2.25}$$

In both cases, we can also consider a situation in which the second variable ${}_{2}$ is nearly integrated, that is, ${}_{22} = \exp(\quad)$ with $\quad 0$. To summarize, ${}_{1}$ is integrated of order one and is either specified in first-difference or in level, and ${}_{2}$ is either weakly stationary or nearly integrated in our Monte Carlo simulations. In the sequel, we assume that ${}_{11} = 0$. Appendix B provides the derivation of the asymptotic distribution of the Max Share matrix $\widehat{\ }_{1}\ (\ )$ for different configurations of this DGP.

Using equation (2.24), we generate 10,000 samples of size $= 240$ observations, a common sample size in applied macroeconomic research. To control for initial condition effects, we include 200 pre-sampled observations that are subsequently discarded during estimation. In each replication, we set the lag order to its true value, whether considering $(\ \ {}_{1}\ \ {}_{2}\ )'$ or $(\ {}_{1}\ \ {}_{2}\ )'$, ensuring that our results are free from lag

[13]It is worth emphasizing that the VAR(1) specification (the first set of experiments) is the DGP of Gospodinov et al. (2013) and Chevillon et al. (2020), whereas the VAR(2) (the second set of experiments) corresponds to that of Gospodinov (2010) and Gospodinov et al. (2011).

order misspecification issues. [14] For each replication, we perform OLS estimation for both the *first difference* (equation 2.24) and *level* (equation 2.25) VAR specifications. Additionally, for the level-based specification, we apply the analytical correction proposed by Pope (1990) and a bootstrap procedure (Kilian, 1998b; Inoue and Kilian, 2002b).[15] Subsequently, we identify two structural shocks using the Max Share approach, which involves maximizing the contribution of the first structural shock to the h-step ahead forecast error variance of the first variable $_1$ or $_1$ (equation 2.14). We explore different truncated forecast error variance horizons for the Max Share criterion, including $= 0$, 40, and 80 quarters. Notably, when $= 0$, the Max Share approach simplifies to a Cholesky decomposition of the variance-covariance matrix of the innovations .

The results are evaluated across three dimensions. Firstly, after computing the (cumulative) mean bias and root mean squared error (RMSE) for selected lead times ($= 0$, 4, 8, and 40 quarters), we analyze the average impulse response functions of the -th variable due to the -th structural shock at each lead time , using a forecast error variance horizon of $= 0$ 40, or 80 for the Max Share matrix. These average impulse response functions are denoted as $\overline{\texttt{IRF}}$ ( ) and are compared against the true impulse response function $\texttt{IRF}$. Note that we only report the impulse responses for the first structural shock for sake of conciseness: detailed tables regarding the bias and RMSE, along with further evidence for the second structural shock, are provided in Appendix B. Secondly, we calculate the contemporaneous correlation between the estimated structural shocks and the true structural shocks, denoted by $\texttt{corr}($ $)$ for $= 1$ 2, as well as the contemporaneous correlation between estimated structural shocks and true complemen-

[14]Several robustness exercises, available upon request, were conducted to control for lag order selection, all of which confirm the consistency of our results.

[15]Bayesian estimation with Minnesota unit root priors and consideration of short-run restrictions were also conducted, although detailed results are not presented here, but are available upon request.

tary structural shocks, denoted by $\texttt{corr}(\qquad)$ for $\;=\;$. Lastly, we analyze the empirical distribution of the first (and second) element of the eigenvector $_1$, denoted by $_{1\,1}(\ )$ (and $_{2\,1}(\ )$), associated with the maximal eigenvalue of the Max Share matrix.

In our *initial experiment*, we assume that $(\ _1\ \ _2)'$ is modeled as a VAR(1) system with parameters $(\ _{11}\ \ _{12}\ \ _{21}\ \ _{22}\ \ _{12}\ \ _{21}\ ) = (0\ \ 0\ \ 0\,2\ \ 0\,96\ \ 0\ \ 0\,5\ \ 0)$. Since $_{11} = \ _{12} = \ = 0$, $_1$ follows a random walk, while the second variable is a (persistent) stationary process driven by $\ $. This configuration corresponds to **Case 1** as described in Section 2.3. Furthermore, with $\ = 0$, only the first structural shock has a lasting impact on the first variable. As depicted in Figure 2.1 for $\ = 0$, there is no contemporaneous bias observed in the average structural impulse response function (IRF) estimates, denoted by $\overline{\texttt{IRF}}_{11\,0}(0)$ and $\overline{\texttt{IRF}}_{21\,0}(0)$, regardless of how the nonstationary variable $_1$ is handled. This absence of bias is consistent with the fact that the Max Share identification method is here essentially equivalent to a recursive Cholesky identification approach. As demonstrated by Phillips (1998), IRFs are then consistently estimated at short horizons $\ $, where $\ =\ $ represents a small fraction of the sample size.

Figure 2.1: Impulse response effects of the first structural shock based on a contemporaneous (h = 0) Max-Share identification (experiment 1)

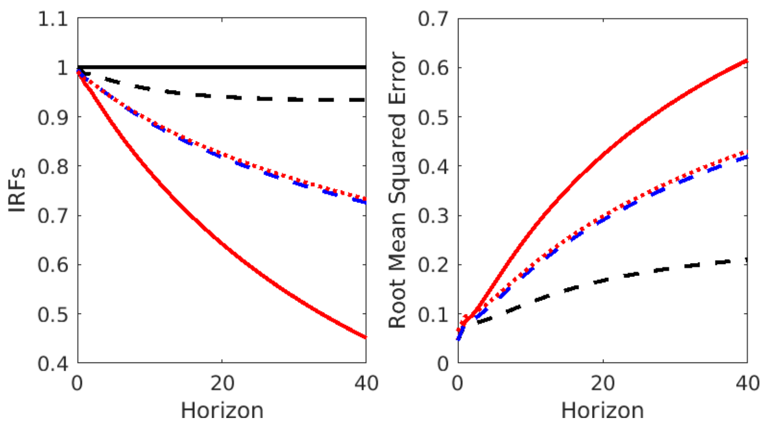

(a) Variable 1

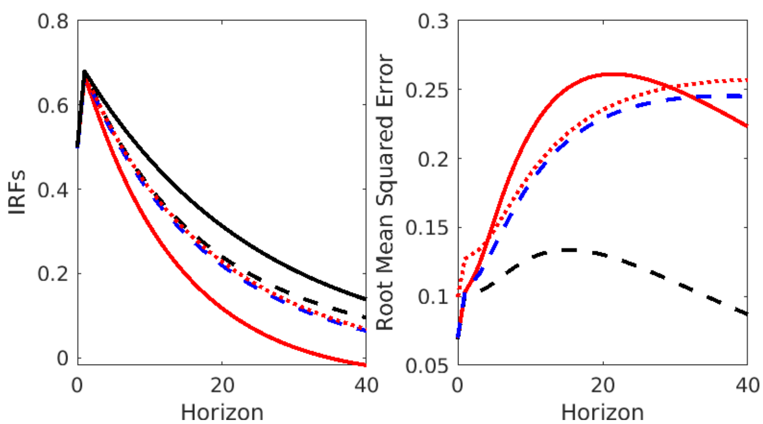

(b) Variable 2

Notes: The black solid line represents the true IRF, $\mathtt{IRF}_{11,i}$ and $\mathtt{IRF}_{21,i}$ for $i = 0,\quad, 40$, whereas the dashed line, the red solid line, the blue dashed line, and the red dotted line represent the average IRF estimates, $\overline{\mathtt{IRF}}_{11,i}(0)$ and$\overline{\mathtt{IRF}}_{11,i}(0)$, inherited from the first-difference specification, the level specification, the bias-correction method of Pope, and a bootstrap procedure, respectively.

As the lead time of structural impulse response functions (IRFs) increases, the bias and root mean squared error (RMSE) of $\overline{\mathtt{IRF}}_{11}\quad(0)$ increase significantly when the reduced-form VAR is estimated in levels. Specifically, the (average) bias of the impulse response function of the first variable to the first structural shock, $\overline{\mathtt{IRF}}_{11}$ (0), is approximately 0.05 at $= 20$ and 0.07 at $= 40$ for the *first-difference* VAR, whereas these biases are notably higher at 0.35 and 0.55, respectively, for the VAR *in levels*. Meanwhile, with the exception of the shortest horizons, the RMSE of the level-based specifications rises rapidly compared to the first-difference specification, showing a multiplication factor of two or even three at medium-to-long horizons.

Interestingly, both Pope's correction and the bootstrap method exhibit similar bias reduction performances, halving the bias compared to the (uncorrected) VAR *in levels*. However, the (average) bias remains substantial, around 0.15 and 0.3 at $= 20$ and 40, respectively. This bias reduction comes at the cost of a slight RMSE increase at the shortest horizons (4), followed by a much larger RMSE at medium-to-long horizons compared to the corresponding performances of the *first-difference* specification.

Furthermore, similar patterns are observed when analyzing the (average) impulse response function of the second variable to the first structural shock, as well as the corresponding RMSE at each horizon. Starting from 4, a notable discrepancy in bias performances between the first-difference and the level-based specifications is observed regarding $\overline{\mathtt{IRF}}_{21}$. This relative performance is even more pronounced when examining the RMSE. Indeed, using Pope's correction or the bootstrap procedure effectively reduces the (average) bias to levels comparable to the *first-difference* specification but comes with a multiplication factor (for the RMSE) greater than two at medium-to-long horizons.

Figure 2.2: Impulse response effects of the first structural shock based on a *non-accumulated* Max-Share identification with $= 40$ (experiment 1)

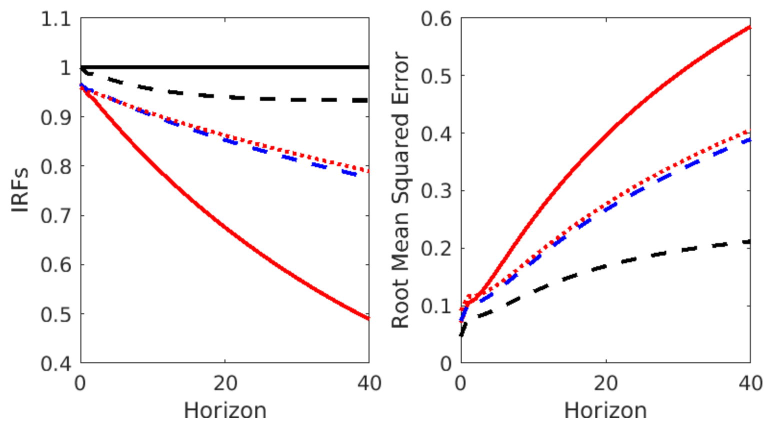

(a) Variable 1

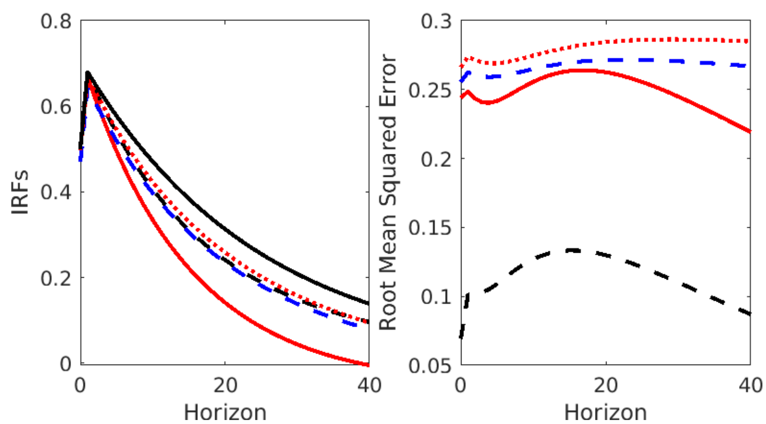

(b) Variable 2

Notes: The black solid line represents the true IRF, $\texttt{IRF}_{11,i}$ and $\texttt{IRF}_{21,i}$ for $i = 0,$, 40, whereas the dashed line, the red solid line, the blue dashed line, and the red dotted line represent the average IRF estimates, $\overline{\texttt{IRF}}_{11,i}(0)$ and$\overline{\texttt{IRF}}_{11,i}(0)$, inherited from the first-difference specification, the level specification, the bias-correction method of Pope, and a bootstrap procedure, respectively.

Figure 2.3: Impulse response effects of the first structural shock based on a *non-accumulated* Max-Share identification with $= 80$ (experiment 1)

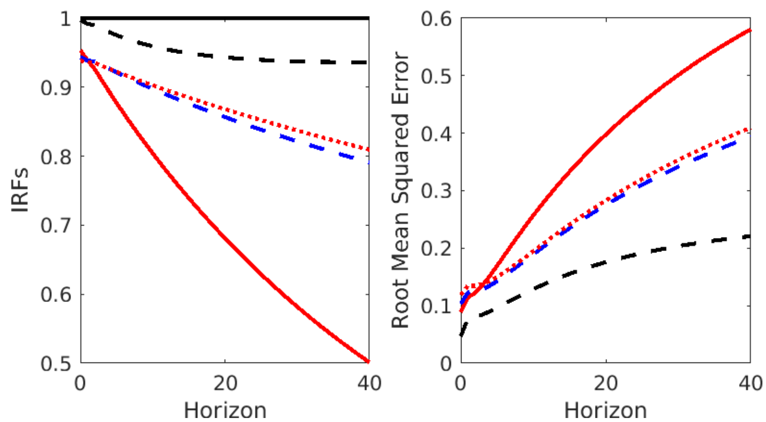

(a) Variable 1

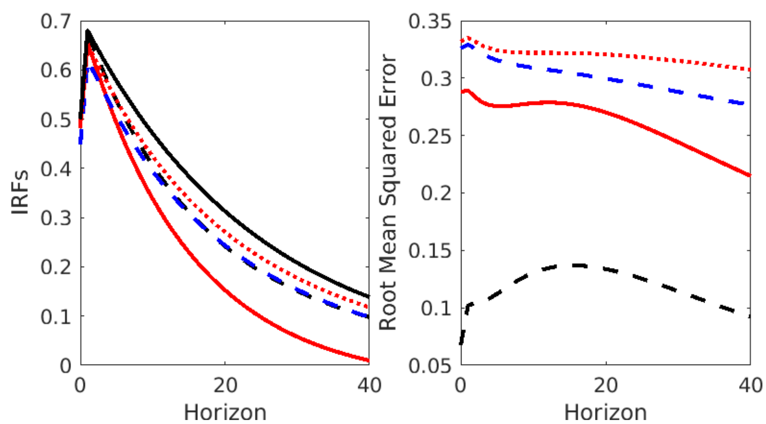

(b) Variable 2

Notes: The black solid line represents the true IRF, $\mathtt{IRF}_{11,i}$ and $\mathtt{IRF}_{21,i}$ for $i = 0,$ $, 40$, whereas the dashed line, the red solid line, the blue dashed line, and the red dotted line represent the average IRF estimates, $\overline{\mathtt{IRF}}_{11,i}(0)$ and$\overline{\mathtt{IRF}}_{11,i}(0)$, inherited from the first-difference specification, the level specification, the bias-correction method of Pope, and a bootstrap procedure, respectively.

As illustrated in Figure 2.2 and Figure 2.3, an increase in the forecast error variance horizon within the Max Share procedure unveils three main features. First, consistent with the findings of Theorem 2.3.4, a contemporaneous bias in the impulse response function of the first variable, resulting from the first structural shock, emerges when level-based methods are used. Additionally, neither Pope's correction nor standard bootstrap techniques fully mitigate this bias, particularly at the shortest impulse response horizons . When analyzing the effect of the first structural shock on the second variable, $\overline{\texttt{IRF}}_{21}$, both bias-correction methods display minimal (average) bias and perform comparably to the first-difference method, albeit at the cost of lower efficiency. The uncertainty associated with level-based structural IRF estimates for the second variable increases with the forecast error variance horizon . Specifically, the RMSE for bias-corrected methods is higher than that inherited from ordinary least squares estimation of the VAR in levels when considering the IRF of the second variable due to the first structural shock. Conversely, for the IRF of the first variable, the RMSE from bias-corrected methods is lower.

Examining the eigenvector corresponding to the maximal eigenvalue, Figure 2.4 displays the distributions of its two elements when the forecast error variance horizon is 40 or 80 quarters. When employing the *first-difference* specification, the distribution of the first element of the eigenvector exhibits a pronounced peak around the true value of the first unit vector element. In contrast, all estimation methods using the *level* specification result in a significantly greater dispersion for the first element, with values ranging between 0.6 and 1. The distributions for the second element of the eigenvector, while approximately symmetric around the true value of 0, span a broad interval from -1 to 1.

These results can be rationalized by analyzing the asymptotic distribution of the Max Share statistic. According to the derivations presented in Appendix B, the asymptotic distribution of the Max Share matrix is characterized as a random matrix expressed by:

$$ {}^{-1}\widehat{\ }_{1}\ (\ ) \qquad \frac{1}{\ }\begin{bmatrix}1 & 0\\ 0 & 0\end{bmatrix}\int_0 \exp(2\ \ ) \tag{2.26}$$

Figure 2.4: Distributions of the eigenvector elements associated to the largest eigenvalue (experiment 1)

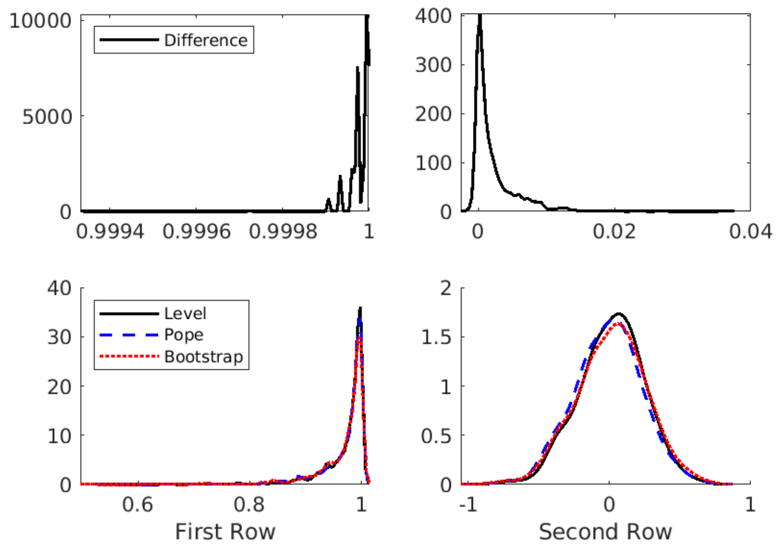

(a) h = 40

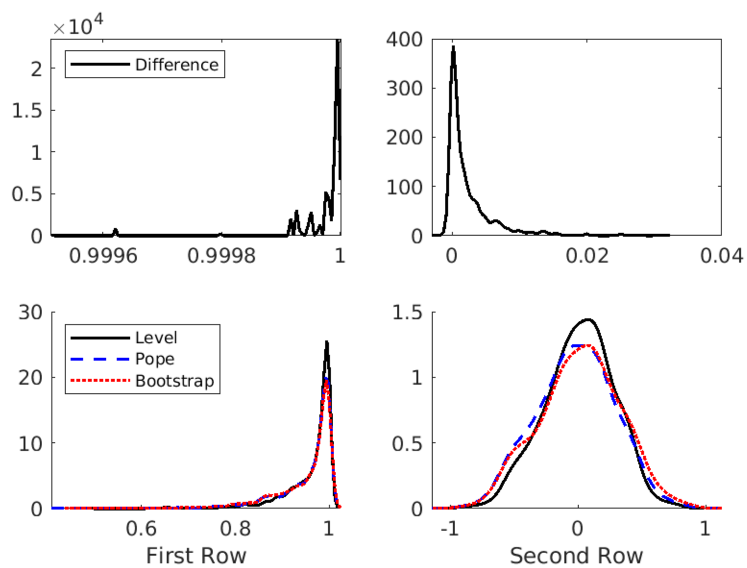

(b) h = 80

(1) The top (respectively, bottom) panel illustrates the distribution of the two elements $v_{1,1}(h)$ and $v_{2,1}(h)$ of the eigenvector associated with the largest eigenvalue when the forecast error variance horizon is set to $h = 40$ (respectively, $h = 80$). (2) For each horizon, the two upper subfigures depict the distributions of the eigenvector elements (black solid line) when considering the *first-difference* model. The two lower subfigures display the distributions of the OLS-based estimates (black solid line), bias-corrected estimates (blue dashed line), and the bootstrapped estimates (red solid line) of the *level* specification.

with $\int_0 \exp(2 \quad) \quad = \frac{1}{2}[\exp(2 \quad) \quad 1]$ where the real random variable has a unit root distribution. Moreover, the asymptotic distribution of the mean squared error is given by:

$$^{-1} \; {}_1'\mathtt{MSE}(\;)\;_1 \qquad \frac{1}{\;} \int_0 \exp(2 \quad)$$

These two results imply that the Max Share statistic is weakly convergent, i.e.

$$\frac{{}_1' \;(\;)\;_1}{{}_1'\mathtt{MSE}(\;)\;_1} \qquad \begin{bmatrix} 1 & 0 \\ 0 & 0 \end{bmatrix} \tag{2.27}$$

In this case, the limit of the Max Share statistic is consistent, and the limits in (weak) probability of the eigenvalue estimators are one and zero, respectively. Moreover, the limit of the eigenvector estimator associated with the maximal eigenvalue is the vector $[1 \;\; 0]'$. This aligns with the simulation results depicted in Figure 2.4. Additionally, given the definition of the structural impulse response functions outlined in equation (2.16), the impact on these functions also depends on the distribution of the reduced-form impulse responses . As outlined in Theorem 2.3.4, the latter is given by:

$$\begin{bmatrix} \exp(\quad) & 0 \\ 0 & 0 \end{bmatrix}$$

This distribution has a random limit, characterized by the exponential of the scalar unit root distribution, which notably exhibits left-skewness that intensifies with increasing values of .[16] For instance, with $= \frac{40}{240}$, our Monte Carlo simulations indicate that the resulting asymmetry in the distributions of the reduced-form impulse response functions (IRFs) is pronounced, featuring a significant negative skewness coefficient. This

[16]See also Figure 1(a) of Phillips (1998).

asymmetry mirrors that typically observed in unit-root distributions.[17]

Figure 2.5: Impulse response effects of the first structural shock based on a *non-accumulated* Max-Share identification with $= 40$ (experiment 2)

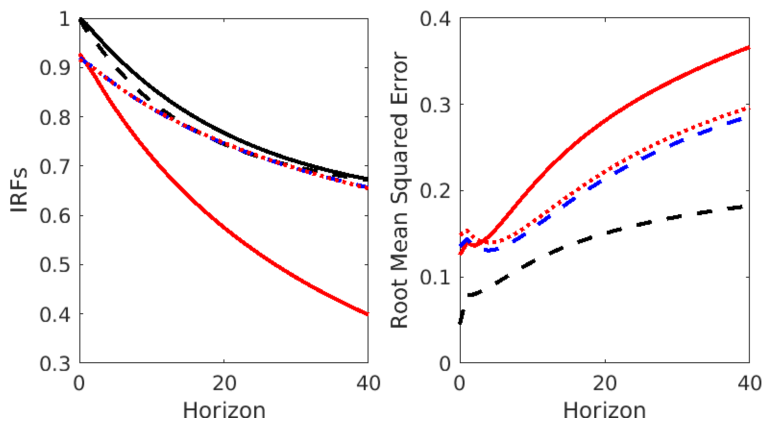

(a) Variable 1

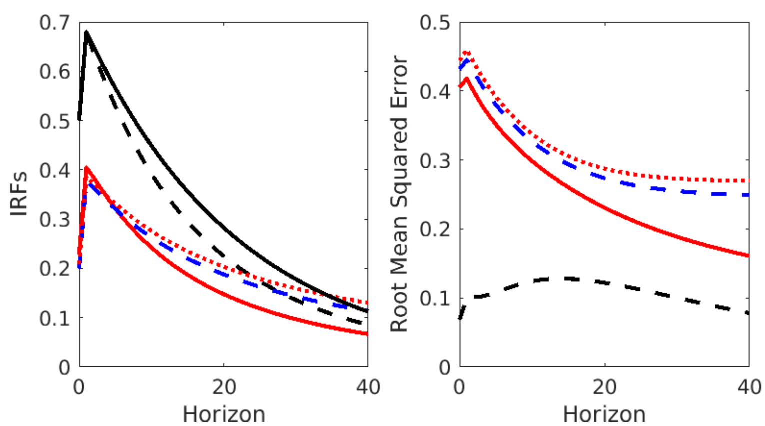

(b) Variable 2

The black solid line represents the true IRF, $\mathtt{IRF}_{11,i}$ and $\mathtt{IRF}_{21,i}$ for $i = 0, \quad , 40$, whereas the dashed line, the red solid line, the blue dashed line, and the red dotted line represent the average IRF estimates, $\overline{\mathtt{IRF}}_{11,i}(0)$ and$\overline{\mathtt{IRF}}_{11,i}(0)$, inherited from the first-difference specification, the level specification, the bias-correction method of Pope, and a bootstrap procedure, respectively.

[17]Note that the asymmetry results from the nonnormal limit theory (Phillips, 1998).

Figure 2.6: Distributions of the eigenvector elements associated to the largest eigenvalue (experiment 1)

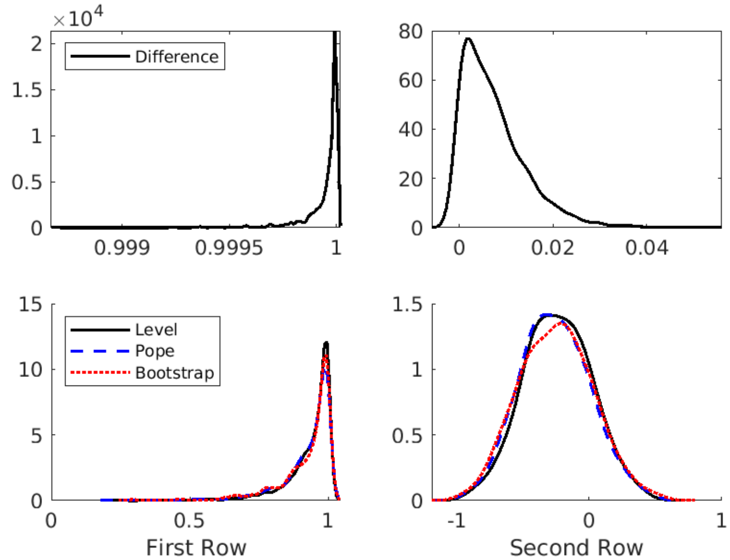

(a) h = 40

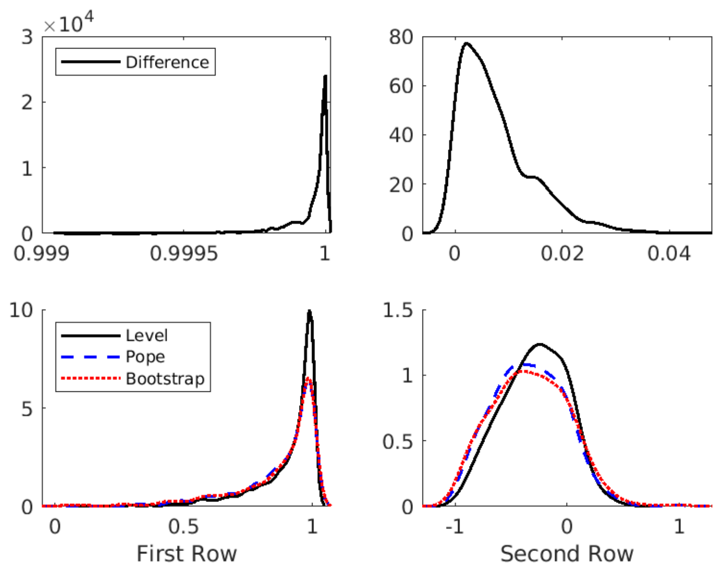

(b) h = 80

Notes: (1) The top (respectively, bottom) panel illustrates the distribution of the two elements $v_{1,1}(h)$ and $v_{2,1}(h)$ of the eigenvector associated with the largest eigenvalue when the forecast error variance horizon is set to $h = 40$ (respectively, $h = 80$). (2) For each horizon, the two upper subfigures depict the distributions of the eigenvector elements (black solid line) when considering the *first-difference* model. The two lower subfigures display the distributions of the OLS-based estimates (black solid line), bias-corrected estimates (blue dashed line), and the bootstrapped estimates (red solid line) of the *level* specification.

For our *second experiment*, we maintain the same parameter vector as in the initial experiment. However, we now assume that both structural shocks have a permanent effect on the first variable ($=\quad 0\;025 = 0$), potentially leading to a confounding effect. Several noteworthy observations arise from Figure 2.5. Firstly, consistent with Experiment 1, impulse response estimates derived from the first-difference method consistently outperform those from the level specification across all lead times, demonstrating superior bias and RMSE properties.[18] Secondly, as the forecast error variance horizon increases, we observe significant differences, particularly regarding the impact of the first structural shock on the second variable. This suggests that the Max Share identification method may partially confound the two permanent structural shocks.

This interpretation is further supported by the correlation analysis between each estimated structural shock and the true complementary structural shock (see Tables B.1 and B.2 in Appendix B). Specifically, we note that these (absolute) correlations hover around 25% for level-based impulse response estimates, whereas they are negligible when using the first-difference specification. Additionally, we observe an average 10% decrease in the correlation between each estimated structural shock and the true one for OLS-based, bias-corrected, and bootstrapped estimates derived from the level specification. In contrast, these correlations remain unchanged and close to 100% in the case of the *first-difference* specification.

Thirdly, we observe that the RMSE generally increases as the forecast error variance horizon extends in the Max Share procedure, particularly noticeable at the shortest impulse response horizons for level-based estimates. Fourthly, consistent with the results detailed in Appendix B, two main features emerge regarding the distribution of the eigenvector elements (see Figure 2.6). On the one hand, using the *first-difference* specification in the presence of two persistent structural shocks results in distributions that

[18]Figures B.3 and B.4 display results for $h = 0$ and $h = 80$, respectively, in Appendix B.

remain nearly invariant compared to those in the first experiment. On the other hand, employing the specification *in levels* broadens the support of the two distributions. Notably, the distribution of the second eigenvector element exhibits a right-skewed pattern, with a negative mean and median estimate of $_{2\,1}$ around -0.5, significantly deviating from the true value of 0. Increasing the forecast error variance horizon from 40 to 80 quarters further exacerbates this issue. This can be understood by examining the asymptotic distribution of $\widehat{\ }_1\ (\ )$ given by:

$$^{-1}\widehat{\ }_1\ (\ ) \qquad \frac{1}{\ } \begin{bmatrix} 0\ 3735 & 0\ 3395 \\ 0\ 3395 & 0\ 3086 \end{bmatrix} \int_0 \exp(2 \qquad)$$

Comparing with the expression of the asymptotic distribution of the Max Share matrix estimator in equation 2.26, one main difference is that the matrix $'_{\mathrm{tr}} \quad '_{\perp}\ _1\ _1\ _{\perp}\ '$ given in the right-hand side now possesses four nonzero elements due to the presence of two permanent structural shocks, thus $\ = 0$. It turns out that the finite sample estimation of these elements further contributes to increased uncertainty, compounding the finite sample approximation of nonnormal, asymmetric asymptotics associated with the unit-root distribution. [19]

For our last two reported experiments, we focus on **Case 4** (Section 2.3), where $(\ _1\ \ _2\ )'$ is modeled as a VAR(1) system with parameter $(\ _{11}\ \ _{12}\ \ _{21}\ \ _{22}\ \ _{12}\ \ _{21}) = (0\ \ 0\ 2\ \ 0\ 2\ \ 0\ 99\ \ 0\ \ 0\ 5)$ and $\ = 0$ (*experiment 3*) or -0.025 (*experiment 4*). The second variable is modeled as a near-unit root process. In the case of a forecasting error variance horizon of 40 quarters, Figures 2.7 and 2.8 report the average impulse responses and the RMSE for $\ = 0$ and $\ = \ \ 0\ 025$,

---

[19]Interestingly, when we apply the Max Share matrix estimator with a horizon beginning at 20 instead of zero and a maximal horizon of 80, the medians of the first eigenvector are close to those of the asymptotic matrix given above.

respectively.[20] Several points are worth noting. The presence of a near-unit root second variable substantially increases the bias of impulse response estimates, even in the case of the first-difference specification. In particular, the bias is more pronounced for greater impulse response horizons and $= 0$ or 40 quarters when studying the effect of the first structural shock on the second variable (lower panels in Figure 7 and 8) in the presence or absence of a confounding effect. Meanwhile, the level-based estimates of $\overline{\texttt{IRF}}_{21}$ exhibit, as in our second experiment, a large contemporaneous bias, combined with large RMSEs. With only one permanent structural shock ($= 0$), the occurrence of a near-unit root for $_2$ results in contemporaneous correlations (in absolute value) $\texttt{corr}(\quad)$ of 15% for the two structural shocks. In the case of two permanent structural shocks, these correlations increase to around 60% for $= 40$, while those between the -th estimated level-based structural shock and the true one, $\texttt{corr}(\quad)$, drop to 74% ($= 40$) and 60% ($= 80$). Consistent with previous results, in the case of first-difference estimates, the correlations $\texttt{corr}(\quad)$ for $= 1\ 2$ remain close to 100%, and those between and for $=$ are close to zero.

The rationale behind the structural IRF results remains consistent with the findings of the first two experiments. On the one hand, using the derivations detailed in Appendix B, the asymptotic distribution of the Max Share matrix is given by:

$$^{-1}\widehat{\ }_1\ (\ )\qquad \frac{1}{\ }\int_0 \begin{bmatrix} 0\ 8615 & 0\ 6808 \\ 0\ 2 & 0\ 9615 \end{bmatrix} \exp(\ '_\Gamma)\ _1\ '_1 \exp(\ _\Gamma) \begin{bmatrix} 0\ 8615 & 0\ 2 \\ 0\ 6808 & 0\ 9615 \end{bmatrix}$$

where $_\Gamma$ denotes a matrix function representing a mixture of unit root and local-to-unity distributions and $= \begin{bmatrix} 0 & _1 \\ 0 & _2 \end{bmatrix}$, with $= 0$ (*experiment 3*) or $= \quad 025$ (*experiment 4*), $= \frac{1}{\ }$, and $_1$ characterizes the root near unity (see Assumption 3.2).

[20]Results for $h = 0$ and 80 are also available in the supplementary material.

The finite sample approximation of this more complex asymptotic distribution, which is nonnormal and asymmetric, significantly impacts the eigenvector associated to the largest eigenvalue.

Figure 2.7: Impulse response effects of the first structural shock based on a *non-accumulated* Max-Share identification with $= 40$ (experiment 3)

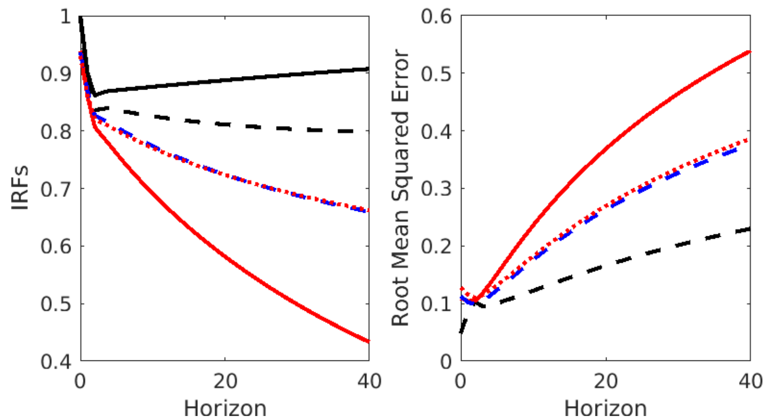

(a) Variable 1

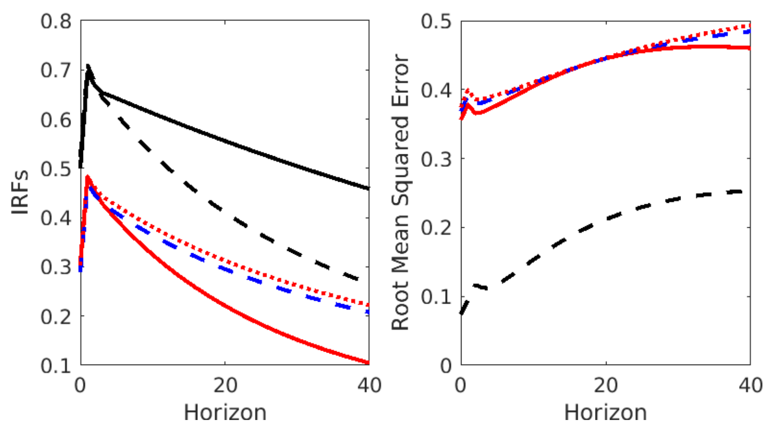

(b) Variable 2

Notes: The black solid line represents the true IRF, $\mathtt{IRF}_{11,i}$ and $\mathtt{IRF}_{21,i}$ for $i = 0,\quad, 40$, whereas the dashed line, the red solid line, the blue dashed line, and the red dotted line represent the average IRF estimates, $\overline{\mathtt{IRF}}_{11,i}(0)$ and$\overline{\mathtt{IRF}}_{11,i}(0)$, inherited from the first-difference specification, the level specification, the bias-correction method of Pope, and a bootstrap procedure, respectively.

Figure 2.8: Impulse response effects of the first structural shock based on a *non-accumulated* Max-Share identification with $\ = 40$ (experiment 4)

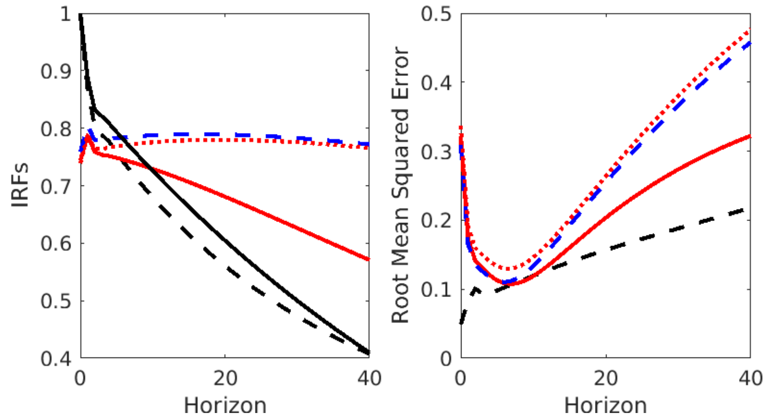

(a) Variable 1

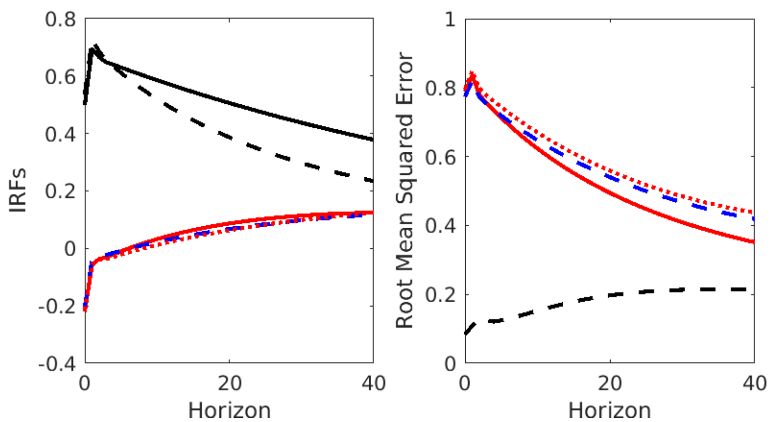

(b) Variable 2

Notes: The black solid line represents the true IRF, $\mathtt{IRF}_{11,i}$ and $\mathtt{IRF}_{21,i}$ for $i = 0, \quad , 40$, whereas the dashed line, the red solid line, the blue dashed line, and the red dotted line represent the average IRF estimates, $\overline{\mathtt{IRF}}_{11,i}(0)$ and$\overline{\mathtt{IRF}}_{11,i}(0)$, inherited from the first-difference specification, the level specification, the bias-correction method of Pope, and a bootstrap procedure, respectively.

On the other hand, this effect is compounded with the estimation of the reduced-form impulse responses whose asymptotic distribution, as indicated by Theorem 2.3.4, is given in both cases by:

$$\exp(\quad \Gamma) \begin{bmatrix} 0\ 9615 & 0\ 2 \\ 0\ 2 & 0\ 9615 \end{bmatrix}$$

where $\exp(\quad \Gamma)$ is a $2 \quad 2$ matrix. Consequently, the elements of the structural IRFs of the first variable, as identified by the Max Share approach, are adversely affected by the relationship (2.16).

Regarding the finite sample distribution of the two elements of the eigenvector associated with the maximal eigenvalue, the simulation results from the first two experiments are further exacerbated in the context of both a near-unit root for the second variable and a possible confounding effect ($\quad = 0$) (see Figures 9 and 10). Specifically, the distributions of level-based estimates of the eigenvector elements exhibit either a left-skewed shape (for the first eigenvector element) or a right-skewed shape (for the second eigenvector element) when $\quad = 40$, with only minor concentration around the true value. As the forecast error variance horizon increases, both distributions undergo significant distortions in the presence of both a unit root and a near-unit root in the unrestricted VAR *in levels*. In particular, when $\quad = \quad 0\ 025$, the distribution of the first eigenvector element displays an inverted U-shape with a broad range, while the distribution of the second eigenvector element is bimodal, with values predominantly clustered around either -1 or 1. [21]

---

[21] The bimodal distribution can be understood with the following argument: let $A = \begin{bmatrix} 1+\varepsilon & 0 \\ 0 & 1 \quad \varepsilon \end{bmatrix}$, where $\varepsilon > 0$ is small enough. A has two eigenvalues $\lambda_{\max} = 1+\varepsilon$ and $\lambda_{\min} = 1 \quad \varepsilon$. One eigenvector associated with the largest (respectively, smallest) eigenvalue is the first (respectively, second) basis vector of $\mathbb{R}^2$, $v_1 = \begin{bmatrix} 1 \\ 0 \end{bmatrix}$ (respectively, $v_2 = \begin{bmatrix} 0 \\ 1 \end{bmatrix}$). Consider a small perturbation of A, $A_\varepsilon = A + \epsilon \begin{bmatrix} \quad 1 & 1 \\ 1 & \quad 1 \end{bmatrix}$. The two eigenvalues remain unchanged, while (using the same normalization as in the initial matrix) one eigenvector associated with $\lambda_{\max}$ is the sum vector of $\mathbb{R}^2$, $v_1 = \begin{bmatrix} 1 \\ 1 \end{bmatrix}$ and

In conclusion, given the prevalence of such a data-generating process (DGP) in macroeconomic applications, these simulation experiments highlight several interesting insights. First, structural impulse responses derived from VAR models in *levels* show a substantial loss in terms of bias and RMSE properties at intermediate and long horizons. This contrasts with those obtained from the first-difference specification. Second, while bias-corrected, bootstrap and Bayesian methods mitigate the bias issue, they still perform worse than estimates from a *stationary* representation, especially in terms of RMSE. Third, the presence of a potential confounding effect, such as two permanent shocks, exacerbates the discrepancies between *first-difference* estimates and *level*-based estimates. This further underscores the need for caution when interpreting results from unrestricted VAR models *in levels*.

$v_2 = \begin{bmatrix} 1 \\ 1 \end{bmatrix}$.

Figure 2.9: Distributions of the eigenvector elements associated to the largest eigenvalue (experiment 3)

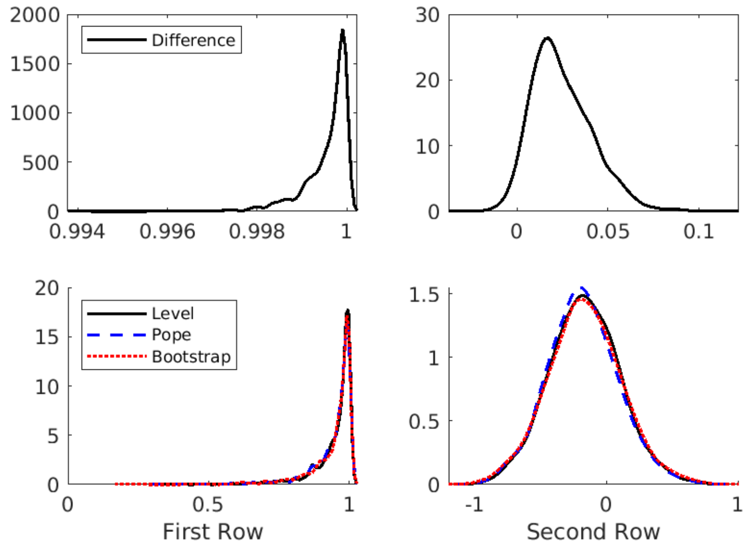

(a) h = 40

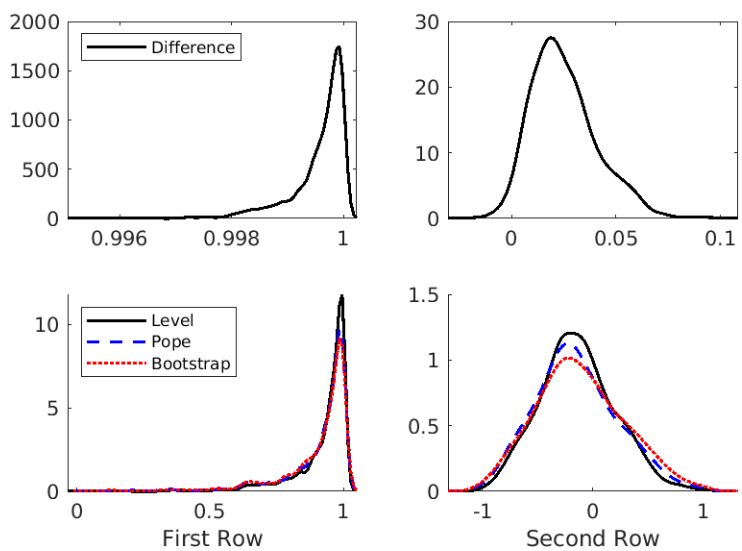

(b) h = 80

Notes: (1) The top (respectively, bottom) panel illustrates the distribution of the two elements $v_{1,1}(h)$ and $v_{2,1}(h)$ of the eigenvector associated with the largest eigenvalue when the forecast error variance horizon is set to $h = 40$ (respectively, $h = 80$). (2) For each horizon, the two upper subfigures depict the distributions of the eigenvector elements (black solid line) when considering the *first-difference* model. The two lower subfigures display the distributions of the OLS-based estimates (black solid line), bias-corrected estimates (blue dashed line), and the bootstrapped estimates (red solid line) of the *level* specification.

Figure 2.10: Distributions of the eigenvector elements associated to the largest eigenvalue (experiment 4)

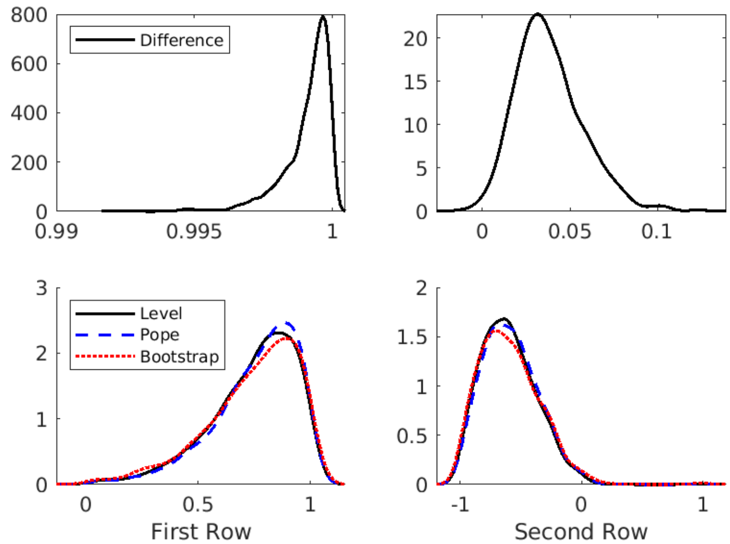

(a) h = 40

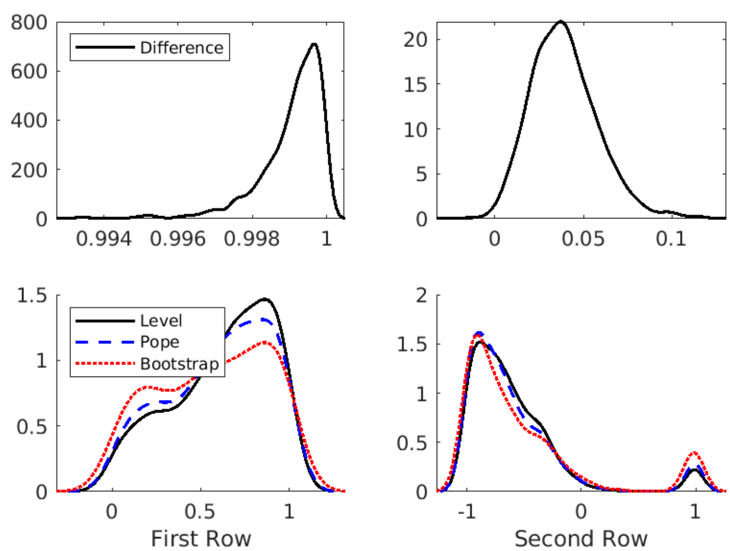

(b) h = 80

Notes: (1) The top (respectively, bottom) panel illustrates the distribution of the two elements $v_{1,1}(h)$ and $v_{2,1}(h)$ of the eigenvector associated with the largest eigenvalue when the forecast error variance horizon is set to $h = 40$ (respectively, $h = 80$). (2) For each horizon, the two upper subfigures depict the distributions of the eigenvector elements (black solid line) when considering the *first-difference* model. The two lower subfigures display the distributions of the OLS-based estimates (black solid line), bias-corrected estimates (blue dashed line), and the bootstrapped estimates (red solid line) of the *level* specification.

2.5 Empirical application

Our empirical application underscores the potential issues arising from relying solely on VAR models *in levels*, consistent with our theoretical and simulations results. We draw upon the study of Zeev and Khan Zeev and Khan (2015), who used Max Share identification to investigate the nature of investment-specific technology (IST) news shocks. Interestingly, their unrestricted VAR specification, which includes both IST and TFP variables in levels, highlights two possible sources of long-run fluctuations, potentially leading to a confounding effect.

We consider a reduced-form VAR with five (log-) variables for the US economy from 1959Q1 to 2019Q4:

$$= (\log \mathrm{TFP} \quad \log \mathrm{IST} \quad \log \qquad \log \qquad \log \qquad)'$$

The first variable is the real time, quarterly series on total factor productivity (TFP) adjusted for variations in factor utilization, constructed by Fernald (2014). Our benchmark measure of IST is the inverse of the real price of investment, which is defined as the ratio of the investment deflator and the consumption deflator. The consumption deflator encompasses nondurable and service consumption from the National Income and Product Account (NIPA) whereas the investment deflator corresponds to private fixed investment and durable consumption. Following Whelan (2002), we make use of a Fisher index to get chain-aggregated data.[22] Consumption is measured as the sum of nondurables and services and is converted to per capita terms by dividing by the civilian noninstitutionalized population aged 16 and over. The real series is then obtained by using the corresponding chain-weighted deflator. The hours series is log of total

[22]The IST series is nearly identical when using the Törnqvist-Theil discrete time approximation to a Divisia index.

hours worked in the nonfarm business sector adjusted for the civilian noninstitutionalized population aged 16 and over. Finally, inflation is measured as the percentage change in the GDP deflator.

Our identification strategy assumes two sources of persistent fluctuations in the system, which we define as TFP and IST news shocks. In line with Kurmann and Sims (2021), we sequentially apply the Max Share approach of Francis et al. (2014) to identify two structural permanent shocks. The truncated forecast error variance horizon is set to $=$ 80 quarters. Let $_0$ represent the lower triangular Cholesky factor of the reduced-form covariance matrix , and be an orthonormal matrix such that all impact matrices are given by $_0 =$ $_0$. The first structural shock is identified by solving:

$$_1(\ ) = \underset{_1}{\text{argmax}} \ \frac{{}'_1 \ {}_1(\ ) \ {}_1}{{}'_1\mathtt{MSE}(\ ) \ {}_1} \quad \text{s.t.} \quad {}'_1 \ {}_1 = 1$$

where $_1$ is the first column of the matrix . This vector $_1$ is the linear combination that best explains future movements in TFP over a horizon , that is, the linear combination that maximally contributed to TFP future forecast error variance.[23] The second structural shock is identified similarly, under the additional condition that this shock is orthogonal to the first structural shock:

$$_2(\ ) = \underset{_2}{\text{argmax}} \ \frac{{}'_2 \ {}_2(\ ) \ {}_2}{{}'_2\mathtt{MSE}(\ ) \ {}_2} \quad \text{s.t.} \quad {}'_2 \ {}_2 = 1 \quad \text{and} \quad {}'_2 \ {}_1 = 0$$

where $_2$ is the second column of the matrix . This vector $_2$ primarily accounts for the long-term fluctuations in IST. Consequently, the first two columns of $_0$ encompass the TFP and IST news shocks. To ensure the robustness of our identification strategy, we reverse the order of identification, where $_1$ represents IST and $_2$ represents TFP.

[23] As pointed out by Kurmann and Sims (2021) for the TFP shock, imposing short-run restrictions, such as zero impact restrictions used by Barsky and Sims (2011), may lead to misleading outcomes due to the imperfect measurement of factor utilization. Therefore, we refrain from such identifying restrictions on TFP and IST permanent shocks.

In our empirical analysis, we employ two specifications. First, we estimate an unrestricted reduced-form VAR *in levels* with four lags, which is standard practise for quarterly data. Second, we estimate a VECM to account for potential unit roots and long-run relationships. Unit root tests provide evidence that the first three variables—TFP, IST, and consumption– are non-stationary. Moreover, economic theory suggests that consumption shares a stochastic trend with both TFP and IST.

More specifically, Johansen (1995)'s cointegration tests, using both trace and maximum eigenvalue test-statistics, reject the null hypothesis of a cointegration rank of two or less, but not of three or less. This result implies that the data is consistent with the presence of two stochastic trends, suggesting no more than one cointegrating relationship among TFP, IST, and consumption, assuming total hours worked and inflation are covariance stationary. Conversely, the Engle-Granger test rejects the null hypothesis of cointegration between any combinations of these three variables. To reconcile these conflicting pre-test results, we report results based on a single cointegration vector, although our findings remain robust even under the assumption of no cointegration, such as when estimating a VAR with the three non-stationary variables in their first differences. This dual approach, employing both a VECM and a first-differenced VAR, is again intended to provide a comprehensive understanding of the underlying dynamics while enhancing the robustness of our results against varying assumptions regarding the cointegration structure.

Figure 2.11 illustrates the structural impulse response functions (top panel) and the forecast error variance shares (bottom panel) due to the structural TFP shock on each variable under both identification strategies. Figure 2.12 provides a similar presentation for the structural IST shock. Notably, the IRFs and FEVD shares for the TFP shocks differ significantly depending on the identification ordering. For instance, while both orderings agree that a TFP shock increases hours worked (except at impact), the VAR *in levels* yields a distinct response and attributes a substantially larger share in the variance decomposition of hours worked to the TFP shock. Specifically, TFP shocks account for nearly 60% of the variance decomposition of hours worked after 10 quarters when identified first, but only 20% when identified second. Thus, when TFP shocks are identified first, they are seen as the main driver of fluctuations in hours worked, a conclusion that should be moderated when these shocks are identified second.

The differences are even more pronounced with IST shocks, as depicted in Figure 2.12. When the VAR *in levels* is employed, hours worked decline for several quarters following the impact of IST shocks when identified conditional on TFP shocks. If IST shocks are identified first, they explain a significant portion of fluctuations in hours worked and consumption. However, when identified second, their impact on these fluctuations is considerably less significant. This suggests that, in the second identification scheme, IST shocks may not be a primary driver of business cycles.

This analysis provides evidence that applying the Max Share approach to VAR *in levels* at a distant horizon can lead to conflicting results, likely due to the confounding of the two permanent shocks, as seen in our simulation experiments. By explicitly accounting for the stochastic trends using a VECM, the impact of the identification order is substantially reduced. As detailed in the Appendix B, this impact becomes almost negligible when employing a reduced-form VAR model with the first three variables in differences. Regardless of the stationary transformation or the identification order, the impulse response functions and the forecast error variance shares remain consistent for the two structural shocks. Importantly, neither TFP nor IST shocks emerge as the primary drivers of fluctuations in hours worked.

Figure 2.11: TFP shock

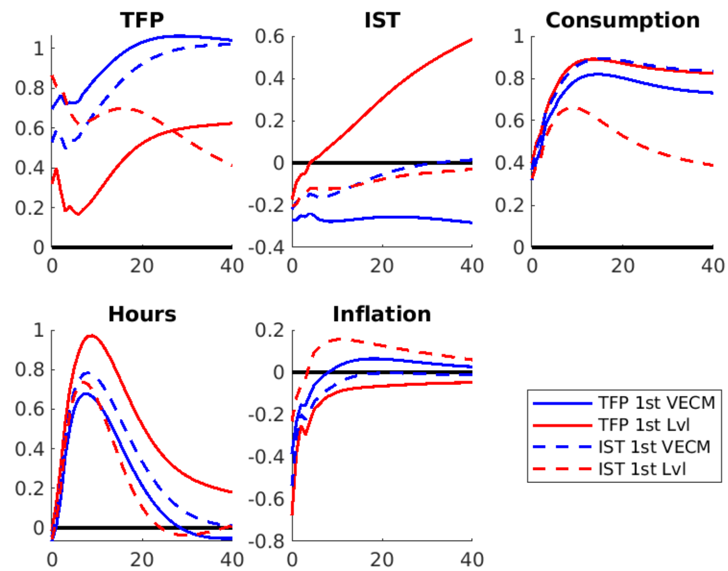

(a) Structural Impulse Responses

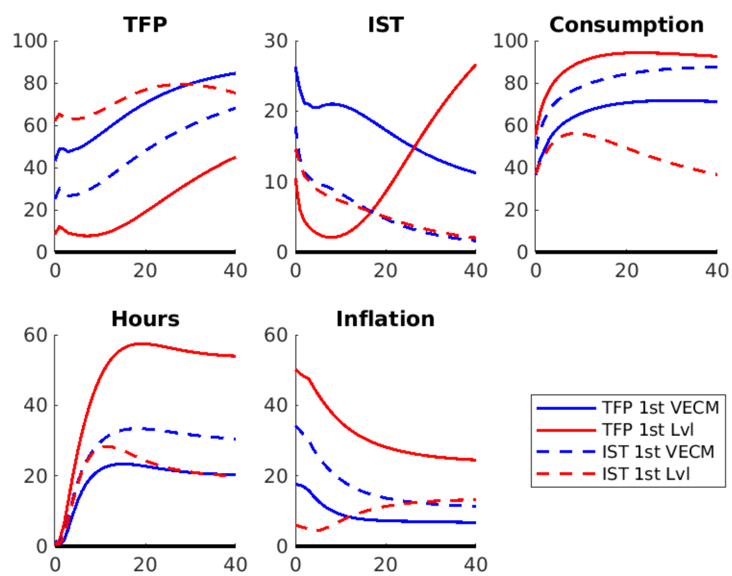

(b) Forecast Error Variance Decomposition

Notes: (1) Red color corresponds to level-based estimates. Blue color corresponds to "first-difference" estimates. (2) A solid line indicates the TFP shock is identified before the IST shock. A dashed line indicates the IST shock is identified before the TFP shock.

Figure 2.12: IST shock

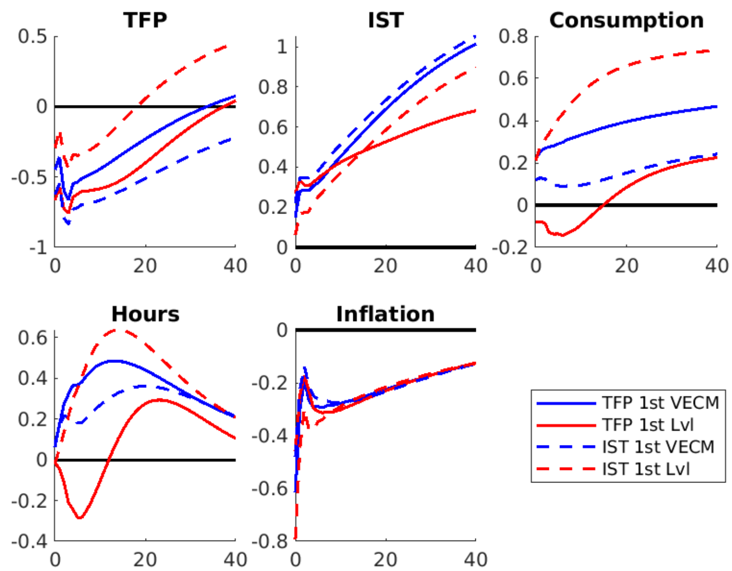

(a) Structural Impulse Responses

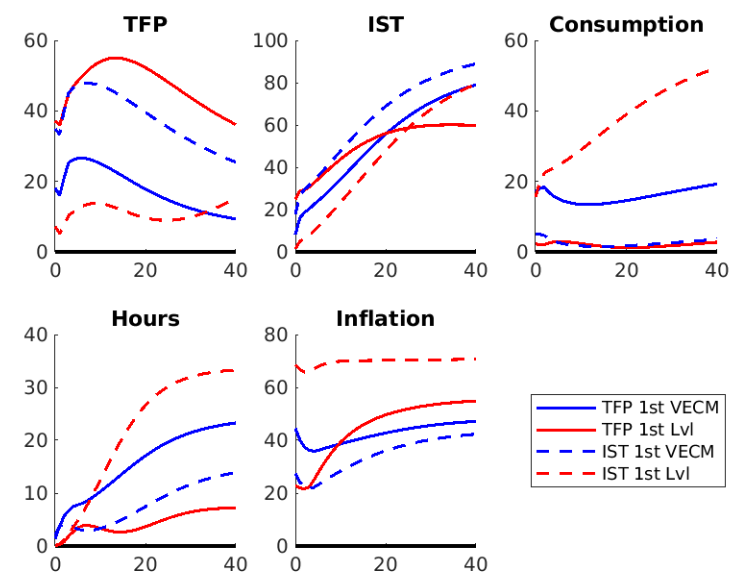

(b) Variance Decomposition

Notes: (1) Red color corresponds to level-based estimates. Blue color corresponds to VECM- based estimates. (2) A solid line indicates the TFP shock is identified before the IST shock. A dashed line indicates the IST shock is identified before the TFP shock.

Finally, this empirical application underscores the potential pitfalls of relying solely on VAR *in levels*. While this application does not settle the debate on whether TFP or IST shocks are pivotal for business cycles, it highlights the sensitivity of results when using a VAR *in levels* in the presence of persistent processes with roots at or near unity. This emphasizes the importance of also estimating stationary representations, such as a reduced-form VECM or a reduced-form VAR with certain variables in differences, to accurately capture the dynamics of structural shocks and enhance the robustness of macroeconomic analysis.

2.6 Conclusion

This paper critically explores the implications of using VAR models *in levels* for the Max Share identification approach, particularly in the presence of unit or near-unit root processes. Our theoretical and empirical analyses provide several key insights. First, structural impulse responses from level-based VARs exhibit significant bias and higher RMSE at intermediate and long horizons compared to those from stationary representations, despite performing similarly at very short horizons. Second, while bias-corrected, bootstrap, and Bayesian methods reduce some bias, they tend to increase RMSE and do not consistently outperform stationary specifications, such as first-difference models. Third, the presence of multiple permanent shocks exacerbates discrepancies between estimates from level-based and differenced VARs, potentially leading to confounding effects and unreliable identification of structural shocks.

These findings emphasize the importance of using stationary transformations, such as VECMs or differencing, and reporting the corresponding results to ensure reliable identification of structural shocks and impulse responses. Such transformations help mitigate the risk of identifying hybrid shocks instead of primitive shocks. While unrestricted VARs *in levels* can be useful under uncertainty about unit roots and cointegration, it is advisable to complement this approach with *stationary* model estimates, like the adaptive automated VECM estimation procedure proposed by Liao and Phillips (2015), which effectively handles unknown cointegrating rank structures and transient lag dynamic orders, or to conduct a thorough VECM robustness analysis in a stepwise manner.

CHAPTER III

A LARGE CANADIAN DATABASE FOR MACROECONOMIC ANALYSIS

ABSTRACT[1]

This paper provides a large-scale Canadian macroeconomic database and shows its usefulness for empirical macroeconomic analysis. The dataset contains hundreds of Canadian and provincial economic indicators. It is designed to be updated regularly and real-time vintages are publicly available. It relieves users to deal with data changes and methodological revisions. We show four useful features of this dataset for macroeconomic research. First, the factor structure explains a sizeable part of the variation of the dataset and appears as an appropriate means of dimension reduction. Second, the dataset is useful to capture turning points of the Canadian business cycle. Third, it has substantial predictive power when forecasting key macroeconomic indicators. Fourth, the richness of the panel is used to study the effectiveness of monetary policy across regions and sectors.

Keywords: Big Data, Factor Model, Forecasting, Structural Analysis.
JEL classification: C55, C82, E32

---

[1]This Chapter is a paper written with Olivier Fortin-Gagnon, Maxime Leroux and Professor Dalibor Stevanovic. It has been published in 2022 in the Canadian Journal of Economics, 55(4), p. 1799-1833. https://onlinelibrary.wiley.com/doi/abs/10.1111/caje.12618.

3.1 Introduction

Large datasets are now very popular in empirical macroeconomic research. Stock and Watson (2002a,b) have initiated the breakthrough by providing the econometric theory and showing the benefits in terms of macroeconomic forecasting, while Bernanke et al. (2005) have inspired the literature on impulse response analysis in the so-called data-rich environment. Since then, many theoretical and empirical improvements have been made, see Stock and Watson (2016) for a recent overview. Most of this literature is built on US datasets. Therefore, McCracken and Ng (2016, 2020) proposed a standardized version of a large monthly and quarterly US datasets that are regularly updated and publicly available at the FRED (Federal Reserve Economic Data) website. No such developments have been made with Canadian macroeconomic data, so the objective of this work is to fill the gap and provide a user-friendly version of a large Canadian dataset suitable for many types of macroeconomic research. Since Canada is an example of a small open economy, this dataset will also be of interest for a wide range of applications in international economics.

In this paper, we construct a large-scale Canadian macroeconomic database in monthly frequency and show how it can be useful for empirical macroeconomic analysis with several illustrative examples. The dataset contains hundreds of Canadian and provincial raw economic indicators observed from 1914. It is designed to be updated regularly in real time through StatCan databases and is publicly available.[2] It relieves users to deal with data changes and methodological revisions. We provide a balanced and stationary panel starting from 1981 that is suitable for work in business cycle fluctuations. The quarterly panel is available as well, and is essentially constructed by averaging the monthly series and adding the GDP and its components that are only observable at quarterly frequency. In this paper we only study the monthly panel.

---

[2]Data can be accessed here: http://www.stevanovic.uqam.ca/DS_LCMD.html.

Early attempts to construct large Canadian macroeconomic datasets are Gosselin and Tkacz (2001) and Galbraith and Tkacz (2007). Boivin et al. (2010) updated and merged data from those previous studies yielding a panel that covered the period 1969 - 2008 and had 348 monthly and 87 quarterly series. Then, Bedock and Stevanovic (2017) constructed a new dataset of 124 monthly variables observed from 1981 to 2012. Their selection of series was based on the Canadian counterparts of US data used in Boivin and Ng (2005). More recently, Sties (2017) has built a much smaller monthly dataset containing mostly financial series and few real activity indicators. Stephen Gordon has also been updating some relevant Canadian indicators[3], while the Bank of Canada released its Staff Economic Projections database, as documented in Champagne et al. (2018, 2020).[4] Our data selection is inspired by McCracken and Ng (2016) when it comes to major groups of economic variables. Given that Canada is a small open economy, the dataset contains many international trade, financial flows and natural resource indicators.

We illustrate several useful features of this dataset for macroeconomic research. **First**, we show that our panel is likely to present a factor structure and that common factors explain a sizable portion of variation in Canadian and provincial aggregate series. The principal component analysis of the dataset identifies few driving forces of the Canadian economy such as GDP in business and financial sectors, term structure, exchange rates, unemployment duration, international transaction net flows and oil production. **Second**, the dataset is useful to capture turning points of the Canadian business cycle. Using Probit, Lasso and factor models we show that this dataset has substantial explanatory power in addition to the standard term spread predictor. **Third**, the dataset provides information to substantially improve the predictive accuracy when forecast-

[3]See Project Link at https://www.ecn.ulaval.ca/s̃gor.

[4]Data are available here: https://www.bankofcanada.ca/rates/staff-economic-projections/.

ing key real macroeconomic indicators. Factor and sparse models, random forests and regularized complete subset regressions show good performance in forecasting real activity variables such as industrial production, employment and unemployment rate, as well as CPI and Core CPI inflation. In the case of credit market aggregates, only the regularized complete subset regressions and random forests are resilient, while practically no model improves the predictive accuracy for housing starts and building permits. **Fourth**, the dataset can serve for structural impulse response analysis. We document heterogenous effects of monetary policy on different sectors of the Canadian economy and across regions. The passage to inflation targeting since 1992 coincides with a decrease in those differences, but some regional heterogeneity still pertains and may pose a challenge for the Bank of Canada in its role to further stabilize the economy.

The rest of the paper is organized as follows. Section 3.2 describes the construction of datasets and performs the factor analysis. Section 3.3 shows the informational content of this dataset in detecting recession dates. In Section 3.4 we conduct a pseudo-out-of-sample forecasting exercise to test the capability of the dataset to help predicting main Canadian macroeconomic variables. Section 3.5 performs an impulse response analysis and Section 3.6 concludes.

3.2 Datasets

In this section, we start by describing the construction of the dataset and, in particular, how we deal with several issues related to availability and statistical properties of the data. We then explore the factor structure of this dataset.

3.2.1 Construction of datasets

The Canadian monthly database comprises eight different groups of variables: production, labor, housing, manufacturers' inventories and orders, money and credit, international trade and financial flows, prices and stock markets. Whenever available, we included regional data covering the Atlantic provinces, Québec, Ontario, the Prairies and British Columbia, as well as provincial data. The complete list of series is available in the data appendix C.2. We decided to include a large number of housing market series since the housing cycle is an important feature of the business cycle (Leamer, 2015). In addition, given that Canada is a small open economy, we added more international trade, financial flows and natural resource indicators than one usually finds in the US applications.

In building this database, several problems are encountered. Some tables have unfortunately been discontinued and the new tables seldom go sufficiently far back in time to afford us a sizeable time frame. Therefore, we combine old and new time series to cope with this problem. This happens with data on production, housing, orders and imports and exports. For instance, GDP data for the period starting in January 1981 and ending today is split across two tables: 379-0027, going from 1981/01 to 2012/01 and 379-0031, starting only on 1997/01. There exist several procedures to combine two time series that share an overlapping period. de la Escosura (2016) reviews three splicing procedures and introduces a new one of his own. As he notes, this aspect of data analysis generally receives little attention with researchers often going for what he calls retropolation whereby the new time series is re-projected using the growth rates of the old time series. If the oldest observation of the new series is made at time , the retropolated series over the previous time interval is given by:

$$:= \left(\frac{}{} \right) \tag{3.1}$$

This corresponds to assigning all the measurement adjustment to the level of the old time series. However, by construction, all increasing time series will be retrospectively skewed upward. As de la Escosura (2016) notes, this is an undesirable feature if we are studying long-term growth, although it is mostly accurate over long time periods and in economies undergoing deep structural change, such as developing economies. Linear and non-linear interpolation schemes would, on the other hand, force the levels of the new series at and of the old series at some other reference date, to be preserved, which means assigning all the modification to the observed growth rates of the old time series in between both references dates.[5]

The choice of a splicing method therefore depends on the application and the beliefs of the researchers concerning what is best measured. In the construction of this database, we privilege the retropolation approach because we prefer to leave observed growth rates intact. For some series, this involves making hardly any changes as we can see in Figure 3.1.

For imports and export series, there usually was a need to aggregate old series before splicing since old and new trade data do not share a common classification system. In the example provided below of exported consumption goods, we aggregate section 2 data on food, feed, beverages and tobacco, major group 4.23 on textile fabricated materials, and major group 5.11 on other consumption goods to approximate the consumer good class of the North American Product Classification System (NAPCS). As is evident from the examples provided in Figure 3.1, viewing the old time series as noisy indexes of new time series seems justified by the high correlations in the overlapping periods.

[5]Interpolation schemes spare observed levels at specific dates, at the expense of modifying growth rates, the dates being strategically chosen because measurements are believed to be more accurate. Moreno (2014) also proposed a mixed splicing method that allows for a middle ground to be chosen by the researcher through a tuning parameter.

Figure 3.1: Examples of data splicing

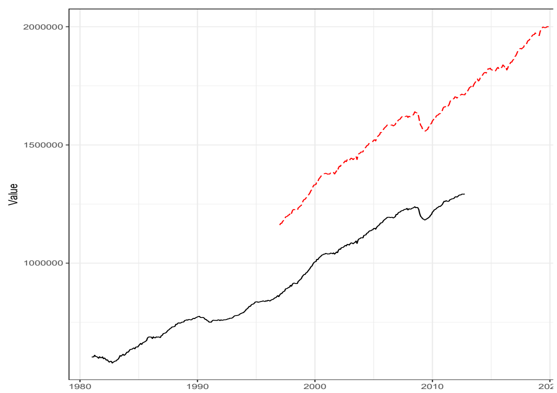

(a) Gross domestic product (Canada)

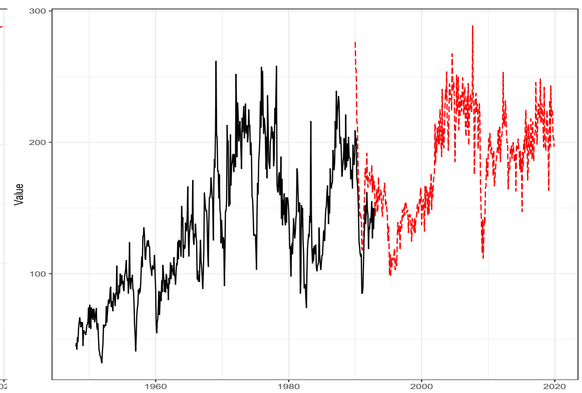

(b) Housing starts (units, Canada)

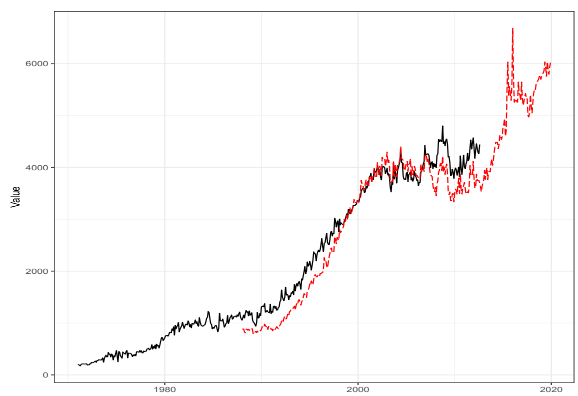

(c) Exports of consumer goods (Canada)

Note: Old series are in black, while new (actual) series are in red.

Another problem concerns the seasonal behavior of a few important labor market time series, unemployment duration and initial claims, as they are not readily available in a seasonally adjusted format. To deal with this, we use the SEATS model based decomposition method that is provided along the X11 type capabilities of the ARIMA-X13-SEATS program of the US Census Bureau[6]. As a sanity check on the viability of the

[6]This approach relies on a factorization of the AR lag polynomial of an ARIMA model whereby different roots of the polynomial can be assigned, respectively, to trend, transitory and seasonal components based on the fact each component will exhibit a different signature in the frequency domain. The ARIMA model is selected based on the automatic selection procedure provided by the program which

procedure, the Kruskal-Wallis test (Kruskal and Wallis (1952)) for seasonal behavior is conducted both prior to and after the seasonal adjustment is performed. The result of the Kruskal-Wallis tests are shown in table C.1 in Appendix C.1. The tests imply a rejection of the absence of seasonal behavior prior to the adjustments, but do not allow for rejection of the null hypothesis after the adjustments have been made as anticipated. Figures C.1-C.2, in Appendix C.1.1, show the behavior of the model based adjustment procedure for a few of unemployment duration and initial claims series.

Most of the series included in the database must be transformed to induce stationarity. We roughly follow McCracken and Ng (2016) and Bedock and Stevanovic (2017): most I(1) series are transformed in the first difference of logarithms, a first difference of levels is applied to unemployment rates and interest rates, first difference of logarithms is used for all price indexes, and housing data is featured in logarithms. Transformation codes are reported in the data appendix.[7]

Our last concern is to balance the resulting panel since some series have missing observations. We opted to apply an expectation-maximization algorithm by assuming a factor model to fill in the blanks as in Stock and Watson (2002b) and McCracken and Ng (2016). We initialize the algorithm by replacing missing observations with their unconditional mean and then proceed to estimate a factor model by principal component. The fitted values of this model are used to replace missing observations. Examples of missing values include export and import series since the old tables went back only to 1988/01.

---

relies on minimizing the BIC. For the implementation details, the reader is referred to the user manual of the US Census Bureau ARIMA-X13-SEATS program. Reader is referred to US Census Bureau (2017) X-13ARIMA-SEATS Reference Manual, available at https://www.census.gov/ts/x13as/docX13AS.pdf

[7]Some of those transformations are questionable, e.g. keeping unemployment or interest rates in levels rather than applying first differences. We provide raw data as well so users can apply any transformation of their choice. This can potentially improve predictability as in Coulombe et al. (2021a).

The resulting balanced and stationary panel is used in the rest of this paper.[8] We will consider only aggregate Canadian data in sections 3.3 and 3.4, while the richness of the provincial data will be explored in the section 3.5. The number of variables is likely to change over time as new data become available or some existing series end. In this paper, the Canadian data set contains 116 variables, while adding the provincial data gives a panel of 386 time series.

3.2.2 Number of Factors

Estimating the number of factors is an empirical challenge. Usually the first step is to plot the eigenvalues of the correlation matrix of data (scree plot) as well as the average explanatory power of consecutive principal components (trace). These are reported in Figure 3.2 for both panels: aggregate data only (CAN) and aggregate plus provincial data (CAN+Prov). The results are typical for macroeconomic panels. There is no clear cut separation among eigenvalues, and the explanatory power grows slowly with the number of factors. However, we remark that in the case of the Canadian panel 10 principal components explain almost 50% of variance of all variables, which is quite satisfactory. This suggests that the factor representation of the Canadian macroeconomy is an appropriate means of dimension reduction. Adding hundreds of regional time series reduces the explanatory power of the common factors which is not surprising. Considering groups of highly correlated variables tends to deteriorate the ability of principal components to recover the factor space (Boivin and Ng, 2006).

Many statistical decision procedures have been proposed to select the number of factors (see Takongmo and Stevanovic (2016) for a review). Table 3.1 reports the number of factors estimated by the following methods: (BN02) Bai and Ng (2002) $_2$ informa-

[8] This dataset ends on 2019M12 and have been constructed from March 2020 vintage. Changes can occur across vintages when some series become unavailable, such as the CERI_new: Canadian-Dollar Effective Exchange Rate Index.

tion criterion; (ABC) modified version of (BN02) by Alessi et al. (2010); (ON) Onatski (2010) test based on the empirical distribution of eigenvalues; (AH) Ahn and Horenstein (2013) eigenvalue ratio test; (HL) Hallin and Liška (2007) test for the number of dynamic factors; (BN07) Bai and Ng (2007) test for the number of dynamic factors; and finally (AW) Amengual and Watson (2007) information criterion for the number of dynamic factors. (ON) and (AH) are known to be very conservative – and sensitive to the presence of weaker factor structures – and they indeed identify only few sources of common variation. (BN02) and (ABC) suggest 6 static factors for the aggregate panel and 5 to 6 in the case of the panel augmented by the regional series. The number of dynamic factors is estimated between 4 and 6 according to (HL), (BN07) and (AW).

It is also common in the literature to verify the stability of the factor structure in terms of the number of common components. Figure 3.3 plots the number of factors selected recursively by Bai and Ng (2002) and Hallin and Liška (2007) methods.[9] We observe that the number of static and dynamic factors is generally increasing since 1990, a similar pattern found with other large macroeconomic datasets (McCracken and Ng, 2016; Coulombe et al., 2021b). Many explanations on the time-varying nature of the number of factors are plausible: structural changes in terms of the correlation structure, presence of group-specific factors, finite-sample sensitivity of selection procedures, and so on. We are not investigating those possibilities but practitioners should be aware of this instability.

3.2.3 Estimated Factors

The factors estimated over the full sample by principal components are depicted in Figures 3.4 and 3.5 alongside their main series identified by the corresponding largest

[9]These are the most commonly used procedures to select the numbers of static and dynamic factors respectively. We use the expanding window in the recursive procedure.

Figure 3.2: Eigenvalues and explanatory power of factors

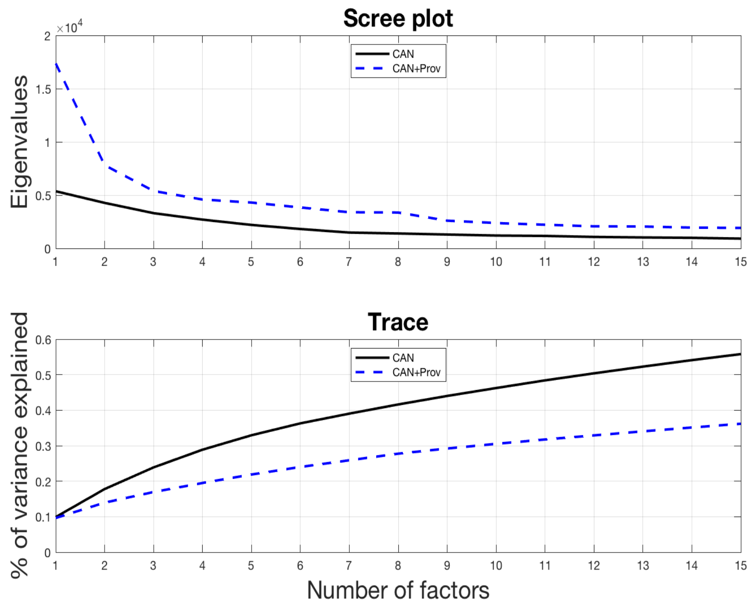

Note: This figure plots the eigenvalues of the correlation matrix of data and the average explanatory power of consecutive factors.

Table 3.1: Estimating the number of factors in CAN_MD

	Canada	Canada + Provinces
BN02	6	5
ABC	6	6
ON	0	2
AH	2	1
HL	4	4
BN07	4	6
AW	4	4

Note: This table lists the number static and dynamic factors estimated by various statistical procedures.

loading for each factor. The first factor closely tracks the evolution of real activity in Canada measured by GDP growth in the business sector, therefore capturing much of the movements related to business cycle frequencies.

The variable best explained by the second factor is the production in the finance, real estate and insurance sectors. The third factor is related to Treasury bonds of maturi-

Figure 3.3: Number of factors over time

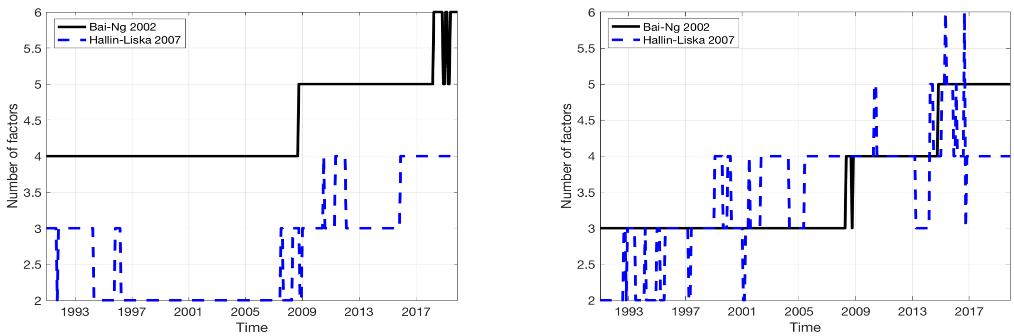

(a) Canada

(b) Canada + Provinces

Note: This figure plots the number of factors selected recursively since 1981 by the Bai and Ng (2002) IC_{p2} information criterion and by the test of Hallin and Liška (2007).

ties 1-3 years, while the USD to CAD exchange rate movements seem to dominate the fourth factor. Another strong characteristic of the strength of the business cycle, unemployment average duration, is the most correlated variable with the fifth factor. The sixth factor is related to net flows in securities with United States and the seventh to the spread between the 1-3Y Treasury bonds and the short-term bank rate. Finally, the Alberta oil production growth is driving the eighth factor. In addition to real activity variables, the importance of exchange rates, international transactions and oil production confirms the intuition that a small open economy business cycle should be heavily exposed to international markets. The stability of factors' interpretation is analyzed in section C.1.2 of the Appendix.

3.3 Predicting Recessions

In this section we verify the ability of the dataset in analyzing the Canadian business cycle. To begin, we need an operational definition of a recession. We assume peaks and troughs are observed and they coincide with the dates from Cross and Bergevin (2012). Since 1981, the C.D. Howe committee has identified three recessions: June

Figure 3.4: Factors 1 to 4 and their main series

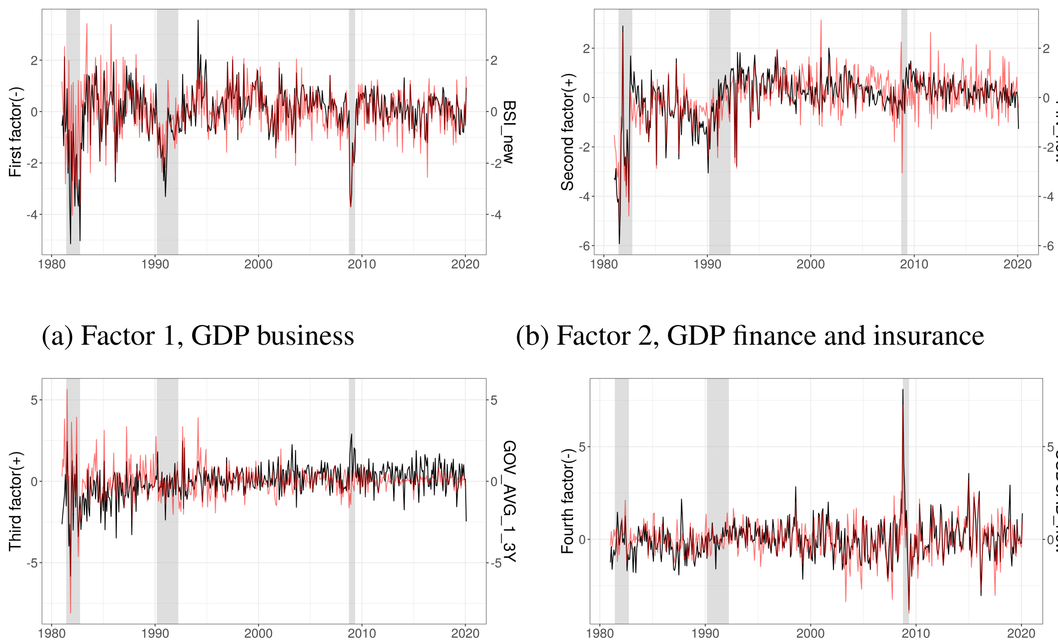

(a) Factor 1, GDP business

(b) Factor 2, GDP finance and insurance

(c) Factor 3, Governmental bonds 1-3 years

(d) Factor 4, Exchange rate CADUSD

Note: Factors are displayed in black and their main components in red. Factors have been estimated over the full sample and the chosen rotation is indicated by (+) or (-). Factors and series have been reduced by their respective standard deviation.

1981 - October 1982, March 1990 - April 1992 and October 2008 - May 2009. Hence, these are fairly rare events in our dataset so we will not be able to do a pseudo-out-of-sample forecasting evaluation. We will focus only on the in-sample capability to correctly identify the turning points and to discover important leading indicators of the business cycle.

We adopt the static Probit to model the probability of recession since this is the standard approach in the literature. Let be a latent lead indicator:

$$= \quad + \quad + \tag{3.2}$$

Figure 3.5: Factors 5 to 8 and their main series

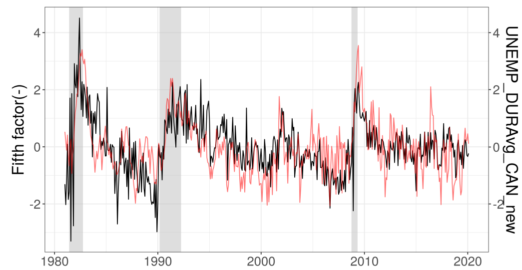

(a) Factor 5, Unemployment average duration

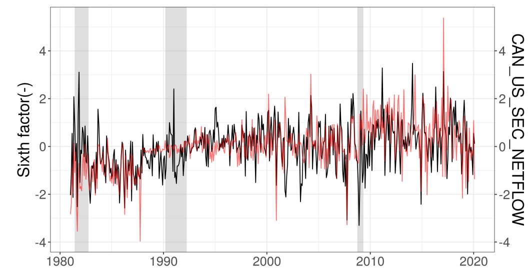

(b) Factor 6, Canadian securities, United States, Net flows

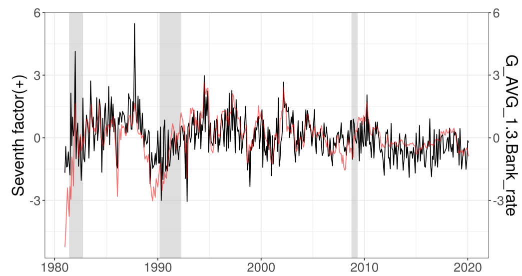

(c) Factor 7, Government bonds (1-3 years) - Bank rate

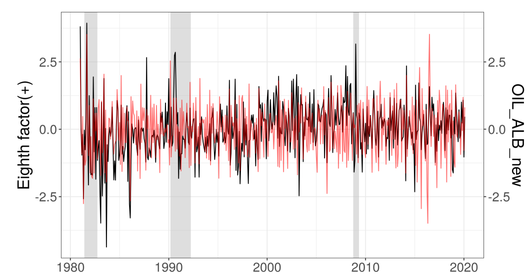

(d) Factor 8, Crude oil production in Alberta

Note: Factors are displayed in black and their main components in red. Factors have been estimated over the full sample and the chosen rotation is indicated by (+) or (-). Factors and series have been reduced by their respective standard deviation.

where is an -dimensional predictors' set, $(0 \;\; 1)$, and which satisfies:

$$
{}_{+} = \left\{ \begin{array}{ll} 1 & \text{if} \qquad 0 \\ 0 & \text{otherwise} \end{array} \right\}
$$

where is the forecasting horizon. Since Estrella and Mishkin (1998) it is standard practice to consider the slope of the yield curve as the only predictor. It is usually proxied by the term spread (TS) which is the difference between the 10-year and 3-month Treasury bills. This is our benchmark model. Therefore, the probability of recession is

$$
\mathrm{P}(\;\; {}_{+} \; = 1 \qquad) = \;\; (\quad + \qquad) \tag{3.3}
$$

Then, we consider two ways of including the information from our large macroeconomic dataset in predicting business cycle turning points. The first is the static Probit where instead of we consider factors estimated as principal components of :

$$= \quad + \quad + \tag{3.4}$$

$$= \quad + \tag{3.5}$$

The probability of recession is then

$$\mathrm{P}(\ _{+} = 1 \ ) = \ (\ + \ ) \tag{3.6}$$

This is a two-step procedure. First, principal components are constructed. Second, the Probit model is estimated with those factors as inputs. Note that this is considered as *dense* modelling since all series in are first used to construct .

Another popular way to include a large number of predictors is through a Lasso model. Following Sties (2017), we use the Logit Lasso model:

$$\mathrm{P}(\ _{+} = 1 \ ) = \frac{^{(\ _h + \ _h \ _t)}}{1 + \ ^{(\ + \ _h \ _t)}} \tag{3.7}$$

with

$$\arg\min_{h \ h} \left[\quad + \sum_{=1} \quad \right]$$

This is known as *sparse* modeling since many elements of are set to zero. The hyperparameter is selected by cross-validation. As opposed to the factor Probit model (3.6), this is a one-step procedure.

Those three models are evaluated through the Estrella and McFadden pseudo- ^{2}s, the quadratic probability score (QPS), and the log probability score (LPS). The forecasting

Figure 3.6: Predicting recessions: full sample probabilities

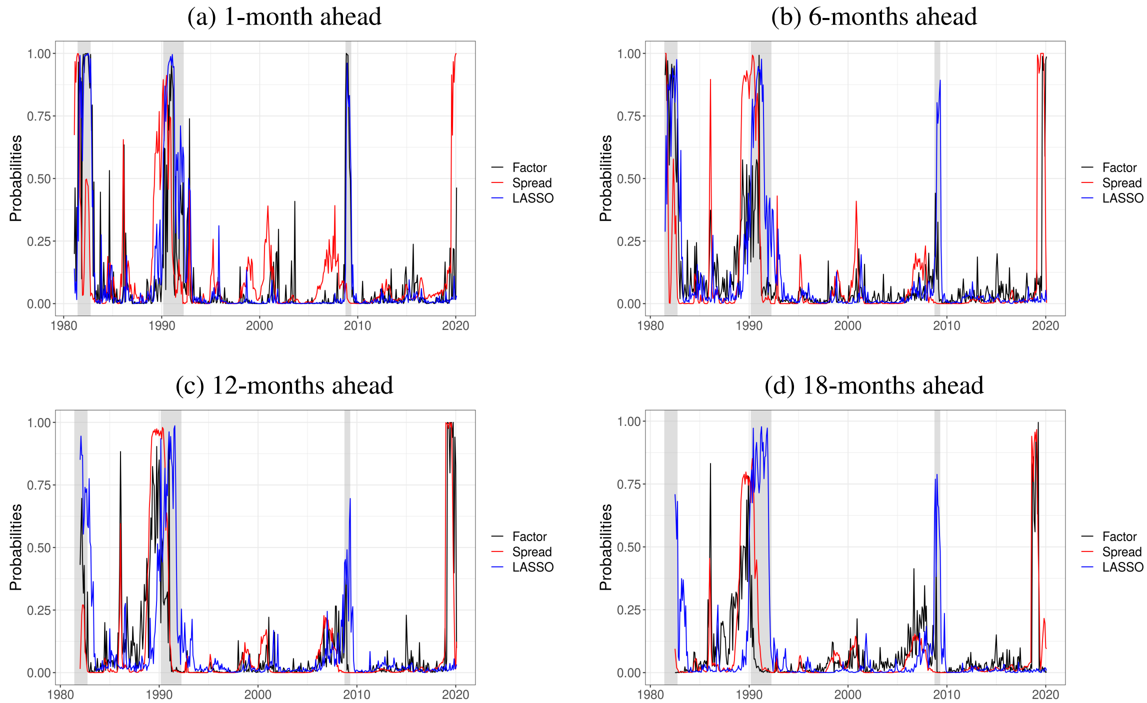

Note: This Figure reports the estimated probabilities of recessions from all three models and for horizons 1, 6, 12 and 18 months ahead. The shaded areas correspond to C.D. Howe recession dates.

horizons are 1 to 18 months. Figure 3.6 shows the full-sample estimated probabilities for horizons 1, 6, 12 and 18 months ahead. Overall, all three models produce high probabilities during the C.D. Howe recession dates. Spread and factor Probit models produce more volatile probabilities and present a lot of 'false' signals.[10] Some of them are interpretable. The peak in 1987 is caused by the stock market crash, while the 2001 increase in recession probability reflects the U.S. recession. The increase at the end of sample is associated to the inversion of the term structure slope. On the other hand, the Lasso model probabilities are much smoother across all horizons.

[10]We call a false signal when the estimated probability is high while the C.D. Howe did not classify that observation as a recession. Of course, this false signal may also reveal some economic disturbances that were not pervasive or big enough to be judged as recession by the committee.

Figure 3.7: Predicting recessions: goodness of fit

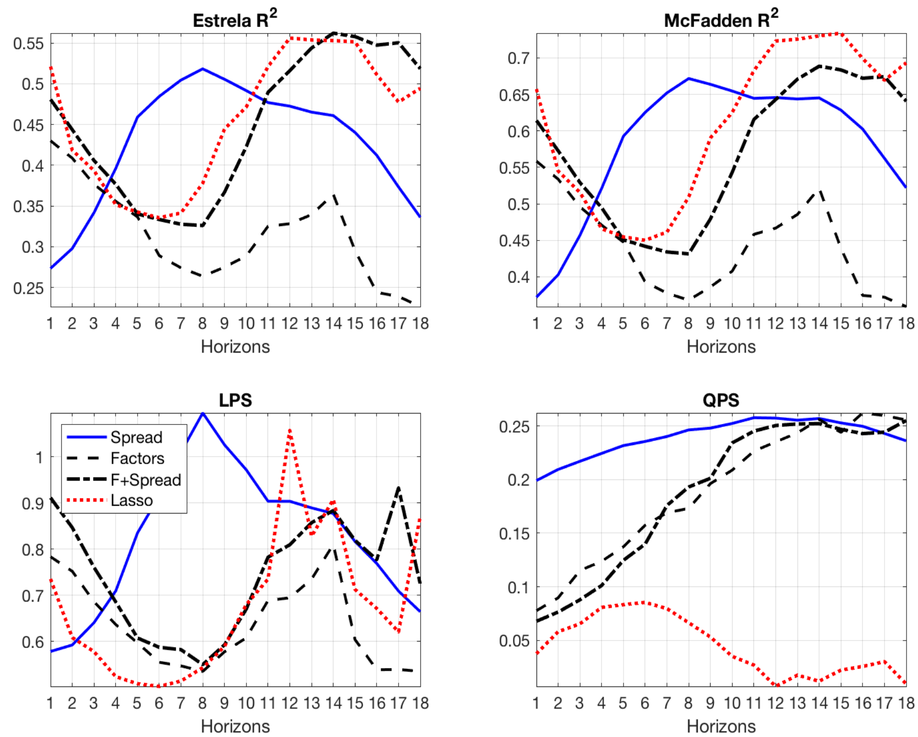

Note: This Figure shows several in-sample goodness-of-fit measures for all three models and for all horizons.

Figure 3.7 shows goodness of fit measures across horizons for all three models. In terms of pseudo- ^{2}, Spread model performance is maximized around 8-month ahead which has been already reported in the literature at least for the US economy. Factors have better explanatory power at short horizons, while Lasso and the Spread model augmented by factors (F+Spread) improve at longer horizons. In terms of LPS and QPS, the Lasso model is preferred to the Probit alternatives, especially in case of the quadratic probability score.

Table 3.2 reports the 10 most important series of selected by Lasso procedure for horizons 1, 6, 12 and 18 months ahead. One month ahead, the most important predictor is the initial claims, followed by a term spread and average unemployment duration.

Table 3.2: Predicting recessions: top 10 series in Lasso

	h=1	h=6	h=12	h=18
1	CLAIMS_CAN	G_AVG_5.10.Bank_rate	G_AVG_5.10.Bank_rate	G_AVG_10p.TBILL_3M
2	G_AVG_5.10.Bank_rate	CLAIMS_CAN	CRED_MORT	CRED_HOUS
3	UNEMP_DURAvg_CAN_new	IPPI_MACH_CAN	TBILL_6M.Bank_rate	N_DUR_INV_RAT_new
4	TSX_CLO	TBILL_6M.Bank_rate	NHOUSE_P_CAN	WTISPLC
5	EMP_CAN	PC_3M.Bank_rate	RT_new	G_AVG_5.10.Bank_rate
6	TSX_HI	TSX_CLO	FIN_new	CLAIMS_CAN
7	BSI_new	PC_PAPER_1M	BANK_RATE_L	FOR_SEC_NETFLOW
8	NHOUSE_P_CAN	CPI_SERV_CAN	CPI_DUR_CAN	USDCAD_new
9	EMP_CONS_CAN	NHOUSE_P_CAN	GBPCAD_new	NHOUSE_P_CAN
10	PC_3M.Bank_rate	IPPI_METAL_CAN	RES_IMF	EMP_MANU_CAN

Note: This table reports 10 most important predictors selected by Lasso.

Employment and stock market indicators are also relevant. Claims and spreads are still the most important at the 6-month horizon, and few price indices enter the top 10. As expected, spreads are the most decisive predictor at the 12 and 18-month horizons, followed by credit aggregates. Interestingly, the oil price arrives fourth at the longest horizon.

Overall, the analysis in this section shows that our dataset provides valuable information, compressed by factors or selected by Lasso, for monitoring the Canadian business cycle. In terms of individual predictors, we find that term spreads are very resilient, followed by the labor market and stock market indicators for short horizons, and credit aggregates for longer horizons.

3.4 Forecasting Economic Activity

In order to explore the potential for predictive modelling of the CAN-MD database, we perform a standard out-of-sample forecasting exercise. Let be the variable of interest. If is stationary, the goal is to forecast its average over periods:

$$ {}^{(\ )}_{+} = (1200 \quad) \sum_{=1} \quad + \tag{3.8}$$

where $\ln$. If is an I(1) series, then we forecast the average annualized growth rate as in Stock and Watson (2002b) and McCracken and Ng (2016):

$$ {}^{(\ )}_{+} = (1200 \quad)\ln(\ _{+} \quad) \tag{3.9} $$

3.4.1 Forecasting Models

A large number of forecasting techniques have been proposed to deal with big macroeconomic datasets, see Kotchoni et al. (2019) and Coulombe et al. (2022) for a review and comparison. The goal of this section is to verify whether the CAN-MD dataset has some relevant and significant forecasting power in predicting key Canadian macroeconomic series, and not to find the best models. Therefore, we will use only a subset of data-rich methods based on dimension reduction, sparse modeling and model averaging.

Autoregressive Direct (ARD) The benchmark time series model is the *autoregressive direct* (ARD) model, which is specified as:

$$ {}^{(\ )}_{+} = {}^{(\ )} + \sum_{=1}^{h_y} {}^{(\ )} \quad _{-\ +1} + \quad _{+} \qquad = 1 \tag{3.10} $$

where $\ln$ $\ln$ $_{-1}$, 1 and . A direct prediction of ${}^{(\ )}_{+}$ is deduced from the model above as follows:

$$ {}^{(\ )}_{+\ |} = {}^{(\ )} + \sum_{=1}^{h_y} {}^{(\ )} \quad _{-\ +1} $$

where ${}^{(\ )}$ and ${}^{(\ )}$ are OLS estimators of ${}^{(\ )}$ and ${}^{(\ )}$. The optimal is selected using the Bayesian Information Criterion (BIC).

Diffusion Indices (ARDI) The first data-rich model is the (direct) autoregression augmented with diffusion indices from Stock and Watson (2002b):

$$
\begin{aligned}
{}^{(\ )}_{+} &= {}^{(\ )} + \sum_{=1}^{h_y} {}^{(\ )} {}_{-\ +1} + \sum_{=1}^{h_f} {}_{-\ +1} {}^{(\ )} + {}_{+} \qquad = 1 && (3.11)\\
&= \quad + && (3.12)
\end{aligned}
$$

where is the -dimensional large informational set, are $^{(\ )}$ static factors, and the superscript stands for the value of when forecasting periods ahead. This the dimension-reduction workhorse model that has been heavily used for macroeconomic forecasting. The optimal values of hyperparameters , , and $^{(\ )}$ are simultaneously selected by BIC from 1 6 grids for the number of lags and 1 10 for the number of factors. The -step ahead forecast is obtained as:

$$
{}^{(\ )}_{+\ |} = {}^{(\ )} + \sum_{=1}^{h_y} \hat{}^{(\ )} {}_{-\ +1} + \sum_{=1}^{h_f} {}_{-\ +1} \hat{}^{(\ )}
$$

The feasible ARDI model is obtained after estimating as the first $^{(\ )}$ principal components of .[11]

Penalized regressions An alternative shrinkage scheme to the factor model is the penalized regression:

$$
= \operatorname{argmin} \left\{ \sum_{=1} \left({}^{(\ )}_{+} \quad \sum_{=1}^{Z} \quad \right)^2 + \sum_{=1}^{Z} \quad \right\} \qquad 0 \qquad (3.13)
$$

where 0 is the hyperparameter controlling the strength of the regularization and is a collection of predictors from two distinct cases: (i) observables

[11]See Stock and Watson (2002a) for technical details on the estimation of F_t as well as their asymptotic properties.

$:= [\quad - \quad {}^{y}_{=0} \quad - \quad {}^{x}_{=0}]$; (ii) ARDI $:= [\quad - \quad {}^{y}_{=0} \quad - \quad {}^{f}_{=0}]$.. We consider two special cases. If $= 2$, (3.13) becomes the Ridge estimators (Hoerl and Kennard, 1970):

$$= (\ ' \ + \quad {}_{Z})^{-1} \ ' \tag{3.14}$$

where is the matrix of predictors, and is the target vector. If $= 1$, we obtain Lasso estimator (Least Absolute Shrinkage Selection Operator) of Tibshirani (1996)

$$= \operatorname{argmin} \left\{ \sum_{=1} \left(\ {}^{(\ )}_{+} \ \sum_{=1}^{Z} \ \right)^2 + \sum_{=1}^{Z} \ \right\} \tag{3.15}$$

Lasso is the representative of the *sparse* class of models where the predictive regression is estimated at the same time as variable selection is performed. In the presence of correlated predictors, Lasso tends to discard variables having less predictive impact, inducing an inconsistent model selection. Two solutions have been proposed. The first is the Elastic Net of Zou and Hastie (2005):

$$\_ \quad = \operatorname{argmin} \left\{ \sum_{=1} \left(\ {}^{(\ )}_{+} \ \sum_{=1}^{Z} \ \right)^2 + \sum_{=1}^{Z} \left(\quad + (1 \quad) \ ^2 \right) \right\} \tag{3.16}$$

with $= [0 \ \ 1]$. Fixing to 1 or 0 generates Lasso or Ridge respectively. The second alternative is the Adaptive Lasso of Zou (2006):

$$\_ \quad = \operatorname{argmin} \left\{ \sum_{=1} \left(\ {}^{(\ )}_{+} \ \sum_{=1}^{Z} \ \right)^2 + \sum_{=1}^{Z} \ \right\} \tag{3.17}$$

where $= \frac{1}{|\tilde{\ }_i|^{\gamma}}$ are weights previously obtained from a consistent estimator and 0. Here, is obtained by Ridge and we fix $= 1$. Hyperparameters and are selected by cross-validation. The corresponding forecasting models are labelled by Ridge-X, Lasso-X, Elastic-Net-X, and Adaptive Lasso in the case of observable predictors, and ARDI, Ridge, ARDI, Lasso, ARDI, Elastic-Net, and ARDI,Adaptive-Lasso in the case of being populated by lags of and estimated factors. In 'X' models, the number of lags are $=\ =6$, while in factor space models we used $=\ =6$ and $=10$ for every .

Random forests The previous models are linear in both parameters and predictors. A growing literature on machine learning methods for macroeconomic forecasting is documenting the importance of nonlinearities, see Coulombe et al. (2022) for details and review. One of the most promising, yet computationally feasible, methods to introduce nonlinearity in the predictive equation is to use regression trees.

The idea is to split sequentially the space of , as defined above, into several regions and model the response by the mean of $^{(\ )}_{+}$ in each region. The process continues according to some stopping rule. The details of the recursive algorithm can be found in Hastie et al. (2009). Then, the tree regression forecast has the following form:

$$(\ ) = \sum_{=1} \mathrm{I}_{(\ \in\ _m)} \tag{3.18}$$

where is the number of terminal nodes, are node means, and $_1$ represents a partition of feature space. In the diffusion indices setup, the regression tree would estimate a nonlinear relationship linking factors and their lags to $^{(\ )}_{+}$. Once the tree structure is known, it can be related to a linear regression with dummy variables and their interactions.

However, the recursive tree fitting process is prone to overfitting. The most popular solution was proposed in Breiman (2001): Random Forests. This consists in growing many trees on subsamples (or nonparametric bootstrap samples) of observations. Further randomization of underlying trees is obtained by considering a random subset of regressors for each potential split. An important hyperparameter to be selected is the number of variables to be considered at each split, which is fixed to one third of the sample cross-section size. The minimum number of observations in every terminal node is set to 5. These are default values in Matlab. The forecasts of the estimated regression trees are then averaged together to make one single "ensemble" prediction of the targeted variable.[12] Depending on , two random forests models are used: RF-X (on observables) and RFARDI (on factors). The former has been successfully applied in Medeiros et al. (2019), while the RFARDI model has been one of the best models in Coulombe et al. (2022).

Regularized Data-Rich Model Averaging Kotchoni et al. (2019) proposed a new class of data-rich model averaging techniques that combines pre-selection and regularization with the complete subset regressions (CSR) of Elliott et al. (2013). The idea of CSR is to generate a large number of predictions based on different subsets of and then construct the final forecast as the simple average of the individual forecasts:

$$ {}^{(\ )}_{+} = + + + \tag{3.19}$$

$$ {}^{(\ )}_{+|} = \frac{\sum_{=1} {}^{(\ )}_{+|}}{} \tag{3.20}$$

where contains series for each model $= 1$.

Kotchoni et al. (2019) proposed to preselect a subset of relevant predictors (first step) before applying the CSR algorithm (second step). This model is labelled Targeted CSR (**T-CSR**). The initial step is meant to discipline the behavior of the CSR algorithm ex ante. The idea is to pre-select a subset * of the series in , that are relevant for forecasting ${}^{(\ )}_{+}$ as in Bai and Ng (2008). Then, CSR is applied on *. In particular, we use hard thresholding to construct *. A univariate predictive regression is done

[12] In this paper, we consider 500 trees, which is usually more than enough to get a stabilized prediction (that will not change with the addition of another tree).

for each predictor :

$$ {}^{(\ )}_{+} = \ + \sum_{=0}^{3} \ _{-} + \ + \tag{3.21} $$

The subset * is obtained by gathering those series whose coefficients have the -stat larger than the critical value : $^{*} =$, with $= 1\ 65$. We consider T-CSR with three choices for the hyperparamter : 5, 10, and 20 regressors, labelled T-CRS,5, T-CSR,10, and T-CSR,20 respectively. The total number of models is fixed at 2500.

3.4.2 Pseudo-Out-of-Sample Experiment Design

The pseudo-out-of-sample period is 1990:01 - 2019:12. The forecasting horizons considered are 1, 3, 6, and 12 months. All models are estimated with the expanding window. The results using the rolling window approach are reported in the appendix C.1.3. The hyperparameters are re-optimized every 24 months. When needed, 5-fold cross-validation is used. We consider the following variables: industrial production, employment, unemployment rate, consumer price index, core consumer price index, credit aggregates (total, business, and household), housing starts, and building permits. These are typical macroeconomic aggregates that have been forecasted in the previous literature. All the series are modelled as I(1), hence we forecast the annualized growth rates. The forecasting performance of the above models will be compared on the basis of the Root Mean Square Prediction Error (RMSPE) as is often the case in forecasting literature. Other metrics could be used but for the sake of simplicity and under space constraints we stick to the most common one.

3.4.3 Results

Tables 3.3 - 3.6 summarize the results. We report the value of RMSPE ratio with respect to the reference ARD model as well as the p-value of Diebold-Mariano test. We group the variables in three categories: real activity (industrial production, employment, and unemployment rate), inflation (CPI and core CPI), credit market (total, business, and household), and housing market (housing starts, and house price).

Using our large database improves substantially the prediction power for real activity series. For instance, when forecasting industrial production one month ahead, almost all models outperform significantly the autoregressive reference and the winner is the random forest using all the observables, RF-X. For $= 3$, improvements are even larger and the best model, Ridge-X, decreases the RMSE by 8%. At longer horizons, most of the models show significant ameliorations with ARDI estimated by Adaptive Lasso improving the accuracy by 15% at the one-year horizon. In the case of employment growth, ARDI,Elastic-Net is the best at short horizons. Interestingly, the forecasting power decreases at long horizons for this series. In the case of the unemployment rate, most of the models produce significantly better results than the autoregressive benchmark.

Table 3.4 shows that using the large panel greatly improves the prediction of inflation series. RF-X is in general the most resilient model which is in line with Medeiros et al. (2019). Probably the most important horizon when forecasting inflation is the one year ahead and the regularized data-rich averaging model T-CSR outperforms the autoregressive benchmark by 24 and 13% for total and core inflation respectively.

Table 3.3: Forecasting real activity

	Industrial Production				Employment				Unemployment			
Models	h=1	h=3	h=6	h=12	h=1	h=3	h=6	h=12	h=1	h=3	h=6	h=12
AR,BIC (RMSE)	0.010	0.006	0.005	0.004	0.002	0.001	0.001	0.001	0.186	0.109	0.088	0.073
ARDI,BIC	0.98**	0.94***	0.98	0.91*	0.97***	1.00	1.08*	1.31**	0.97*	0.93	0.91*	1.07
Elastic-Net-X	0.96***	0.94**	0.97	1.03	0.96**	0.98	1.14	1.42***	1.02	0.93*	0.99	1.20**
Ridge-X	0.95***	0.92**	0.91**	0.89**	0.96*	0.95	1.07	1.13	0.96***	0.90***	0.89**	1.00
Lasso-X	0.96***	0.94**	0.99	1.03	0.96**	0.98	1.11	1.42***	1.01	0.88***	0.96	1.21**
Adaptive-Lasso-X	0.98	0.96	0.98	1.04	0.96**	0.98	1.12	1.43***	0.99	0.91**	0.95	1.18*
RF-X	0.94***	0.95	0.96	0.94	0.95**	0.98	1.10	1.04	0.96***	0.91***	0.96	0.94
ARDI,Elastic-Net	0.95***	0.93**	0.90***	0.86**	0.95***	0.93**	1.12*	1.38***	0.97*	0.94	1.07	1.09
ARDI,Ridge	0.96**	0.94*	0.94**	0.87***	1.04	0.99	1.10*	1.21**	0.96***	0.93*	0.95	1.02
ARDI,Lasso	0.96***	0.94**	0.90***	0.86**	0.95***	0.94*	0.99	1.31**	0.96**	0.98	1.03	1.07
ARDI,Adaptive-Lasso	0.96***	0.94**	0.90**	0.85**	0.95***	0.94*	1.04	1.30**	0.96***	0.98	1.01	1.01
RFARDI	0.96***	0.95	0.94*	0.89***	0.95***	0.96	1.03	1.12**	0.94***	0.89***	0.90***	0.93*
T-CSR5	0.97***	0.94***	0.94***	0.90***	0.97***	0.95***	0.98	1.06	0.98**	0.92***	0.91***	0.91**
T-CSR10	0.97**	0.93***	0.94**	0.89**	0.97**	0.95**	1.00	1.16*	0.98	0.92***	0.91**	0.97
T-CSR20	0.99	0.94**	0.96	0.93*	0.98	0.97	1.05	1.32**	1.00	0.94**	0.95	1.10

Note: This table reports the ratio of the root mean squared predictive error (RMSPE) with respect to the reference ARD model and the results of the Diebold-Mariano test with *10%, **5%, ***1%.

Table 3.4: Forecasting inflation

	CPI				Core CPI			
Models	h=1	h=3	h=6	h=12	h=1	h=3	h=6	h=12
AR,BIC (RMSE)	0.004	0.003	0.002	0.001	0.003	0.002	0.001	0.001
ARDI,BIC	0.98	0.93***	0.86***	0.81***	1.00	0.95	0.95	0.96
Elastic-Net-X	0.93***	0.91***	0.85***	0.84**	0.92***	0.93**	0.91**	0.92
Ridge-X	0.95***	0.90***	0.85***	0.83***	0.96**	0.93**	0.92**	1.04
Lasso-X	0.94***	0.91***	0.86***	0.79***	0.94***	0.94*	0.92**	0.88*
Adaptive-Lasso-X	0.94***	0.92***	0.85***	0.79***	0.93***	0.92**	0.91**	0.88
RF-X	<u>0.93</u>***	<u>0.88</u>***	0.86***	0.92	<u>0.91</u>***	<u>0.86</u>***	<u>0.89</u>***	0.95
ARDI,Elastic-Net	0.98**	0.95*	0.90**	0.84**	0.98	0.98	0.97	0.97
ARDI,Ridge	0.98	0.94**	0.90**	1.01	0.99	1.02	0.98	1.06
ARDI,Lasso	0.99	0.91***	0.84***	0.79***	0.97*	0.95**	0.92**	0.90
ARDI,Adaptive-Lasso	0.97**	0.91***	0.84***	0.79***	0.98	0.94*	0.90**	0.91
RFARDI	0.95***	0.89***	<u>0.82</u>***	0.88**	0.95***	0.91***	0.89***	1.03
T-CSR5	0.95***	0.92***	0.87***	0.87***	0.96***	0.97**	0.96**	0.97
T-CSR10	0.94***	0.91***	0.83***	0.79***	0.95***	0.94***	0.92**	0.91*
T-CSR20	0.95**	0.92***	0.86***	<u>0.76</u>***	0.97	0.94**	0.92**	<u>0.87</u>**

Note: See table 3.3.

Table 3.5: Forecasting credit markets

Models	Total Credit h=1	Total Credit h=3	Total Credit h=6	Total Credit h=12	Business Credit h=1	Business Credit h=3	Business Credit h=6	Business Credit h=12	Consumption Credit h=1	Consumption Credit h=3	Consumption Credit h=6	Consumption Credit h=12
AR,BIC (RMSE)	0.002	0.001	0.001	0.002	0.003	0.002	0.002	0.002	0.003	0.002	0.002	0.002
ARDI,BIC	1.04**	1.08**	1.11**	1.20***	1.01	1.00	1.00	1.00	1.05***	1.09**	1.13**	1.27***
Elastic-Net-X	1.01	1.04	1.13**	1.13**	1.03	1.01	1.02	1.08	1.11***	1.18***	1.22***	1.34***
Ridge-X	1.14***	1.19***	1.24***	1.28***	1.08**	1.13***	1.16***	1.08	1.21***	1.26***	1.34***	1.27***
Lasso-X	1.04*	1.03	1.14***	1.15**	1.04**	1.01	1.03	1.07	1.12***	1.18***	1.22***	1.33***
Adaptive-Lasso-X	1.02	1.03	1.13**	1.15**	1.04*	1.01	1.01	1.07	1.11***	1.20***	1.25***	1.32***
RF-X	1.02	1.14***	1.27***	1.27***	1.04**	1.13***	1.23***	1.21***	1.03	1.09**	1.19***	1.25***
ARDI,Elastic-Net	1.03	1.08*	1.10*	1.13*	1.02	1.00	1.00	0.96	1.07***	1.08*	1.13**	1.23***
ARDI,Ridge	1.19***	1.25***	1.36***	1.15**	1.10***	1.08*	1.09	1.12**	1.17***	1.25***	1.25***	1.26***
ARDI,Lasso	1.00	1.02	1.03	1.08	1.02	0.97	0.97	0.96	1.07***	1.10**	1.18**	1.23***
ARDI,Adaptive-Lasso	1.00	1.02	1.03	1.08	1.02	0.98	0.96	0.96	1.07***	1.10**	1.17**	1.24***
RFARDI	0.99	1.04	1.10**	1.11**	1.02	1.04*	1.10**	1.10**	1.02	1.01	1.05	1.08*
T-CSR5	1.00	0.98	0.99	1.00	1.00	0.98	0.93**	0.90**	1.00	0.99	1.01	1.05
T-CSR10	1.02	0.97	1.01	1.04	1.02	0.98	0.92**	0.89**	1.02	1.02	1.05	1.11**
T-CSR20	1.07***	0.99	1.04	1.11*	1.07***	1.01	0.94*	0.91*	1.07**	1.06*	1.12**	1.19**

Note: See table 3.3.

Table 3.6: Forecasting the housing market

Models	Housing Starts h=1	h=3	h=6	h=12	Building Permits h=1	h=3	h=6	h=12
AR,BIC (RMSE)	0.090	0.040	0.026	0.017	0.079	0.032	0.020	0.013
ARDI,BIC	1.00***	1.00	0.99	0.96	1.00	1.02	1.02*	1.11**
Elastic-Net-X	1.04**	1.03	1.05***	1.21***	1.05***	1.04**	1.07**	1.16**
Ridge-X	1.06***	1.01	1.01	1.04	1.07***	1.06***	1.04**	1.09
Lasso-X	1.02*	1.01	1.02*	1.16***	1.04***	1.04**	1.07**	1.17**
Adaptive-Lasso-X	1.02*	1.03**	1.03**	1.16***	1.04***	1.05***	1.05**	1.26***
RF-X	1.04***	1.01	1.03***	1.06**	1.04***	1.04*	1.06	1.05
ARDI,Elastic-Net	1.03**	1.02	0.99	0.99	1.04***	1.05***	1.07***	1.09
ARDI,Ridge	1.05***	1.01	1.00	1.02	1.07***	1.05***	1.04**	1.04*
ARDI,Lasso	1.01*	1.00	1.00	1.00	1.04***	1.03**	1.03***	1.09
ARDI,Adaptive-Lasso	1.02***	1.02*	1.00	1.00	1.03***	1.05***	1.02**	1.11
RFARDI	1.03***	1.02*	1.04*	1.07**	1.03**	1.04**	1.06**	1.08**
T-CSR5	0.99	1.00	1.00	0.99	0.99	1.01	1.03	1.04
T-CSR10	1.00	1.01	1.03	1.05	1.00	1.03	1.07*	1.11*
T-CSR20	1.04*	1.04*	1.09**	1.19***	1.04**	1.07*	1.18**	1.25**

Note: See table 3.3.

The results for the credit market, presented in the table 3.5, are mixed. In the case of total credit growth, the best models are RFARDI and T-CSR, but improvements are small and insignificant. T-CSR10 ameliorates substantially forecasting power for the business credit at horizons 6 and 12, by as much as 8 and 11% respectively.

Finally, table 3.6 reports the results for the housing market. It shows that predicting housing starts and building permits growths is a very difficult task. Virtually none of our models improves significantly upon the autoregressive benchmark.

Up to now we have studied the average performance over the whole 1990-2019 period. Giacomini and Rossi (2010) propose a test to compare the out-of-sample forecasting performance of two competing models in the presence of instabilities. Figure 3.8 shows the results. We report the comparison between selected data-rich models and the autoregressive benchmark. Following the Monte Carlo results in Giacomini and Rossi

(2010), the moving average of the standardized difference of MSPEs is produced with a window that uses 30% of the out-of-sample period. The critical value of 10% is used. Positive values of the test statistic reflect a better performance of a competing model, which becomes significant if above the critical value. For real activity series, the performance is relatively stable across horizons and variables. For industrial production, there is a ditch in the performance around 2005 but it fully recovers by the end of the sample. In the case of inflation, the forecasting power generally improves over time except for the core inflation at one-year horizon. The fluctuation test is quite stable for credit markets at short horizons but indicate a lot of instability when predicting housing starts and building permits.

Figure 3.8: Forecasting performance over time: fluctuation test

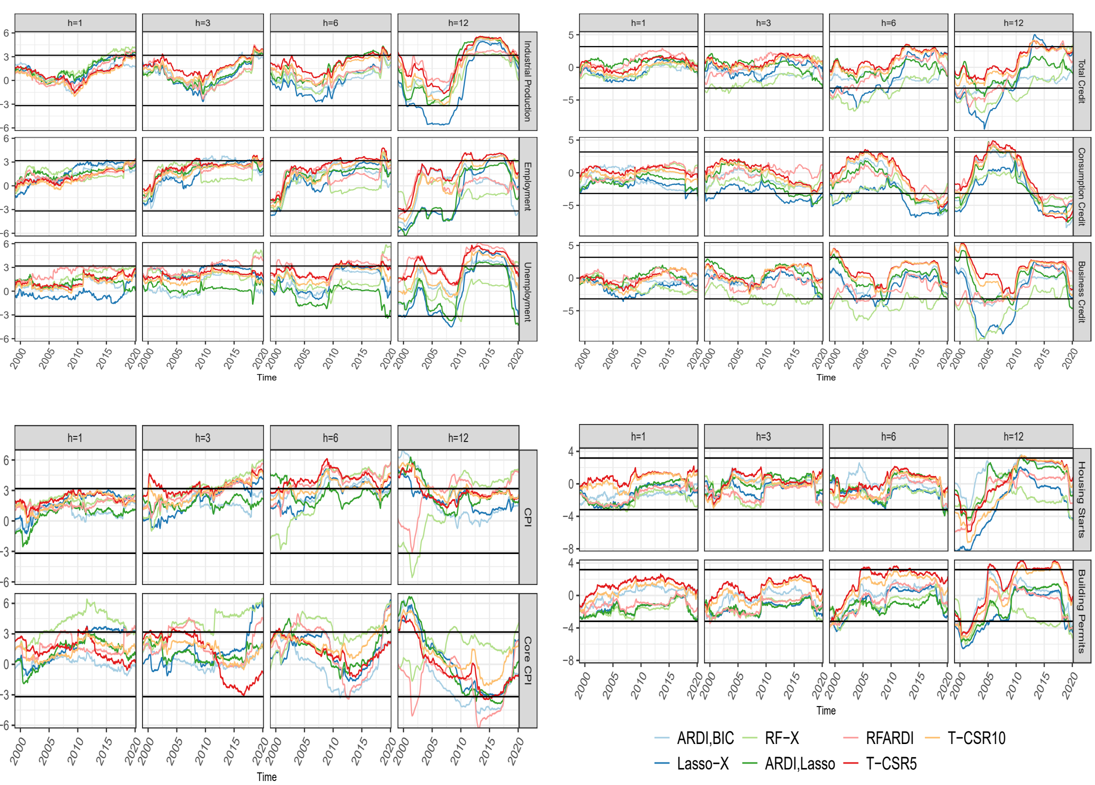

Note: The figure shows the Giacomini-Rossi fluctuation test for best RMSPE models against the ARD benchmark. Solide lines correspond to 10% critical value.

In the above analysis the expanding window approach has been used, which is less robust to frequent structural breaks, but more efficient since more observations are available to estimate the parameters. When the rolling window is used, we find relatively similar results except that the distribution of best models by variable and horizon is different. For instance, the standard ARDI is in general the most resilient model when predicting real activity variables. In case of credit markets, the T-CSR5 model improves significantly the predictive accuracy for most of the horizons and variables. The results are available in tables C.4-C.7 and in figure C.5.

Our monthly and quarterly datasets have already been successfully used in other forecasting exercises. Coulombe et al. (2022) have shown that machine learning methods relying on (nonparametric) nonlinearities can improve the forecasting accuracy of Canadian macroeconomic variables when paired with large datasets such as CAN-MD and CAN-QD.

3.5 Measuring heterogenous effects of monetary policy

In this section we take advantage of the richness of the cross section of CAN-MD database to study the regional and sectoral effects of monetary policy.[13] The Bank of Canada's goal of economic stabilization throughout Canada is not equivalent to economic stability in all of Canada's provinces at the same time. This can be an issue in all monetary unions; a cure for the union can become a curse for some of its members if their business cycles are not synchronized (Micossi, 2015). Our goal in this section is not to introduce new estimation methodologies but to show how CAN-MD can be used to explore regional and sectoral effects of shocks on key macroeconomic aggregates

[13] Note that our CAN-MD and CAN-QD datasets have been recently used in Moran et al. (2022) who constructed a measure of Canadian macroeconomic uncertainty and studied their effects in the context of Covid-19 pandemic.

and their components.[14]

To estimate the impulse response functions (IRFs) of key macroeconomic variables to monetary policy shocks we follow Champagne and Sekkel (2018) and use local projections with their constructed monetary policy shocks.[15] Their shock is constructed following the narrative approach of Romer and Romer (2004) that uses the monetary policy framework to decompose rate changes in systematic and exogenous components. Each rate change is composed of the Bank of Canada's systematic reaction function to current and expected economic conditions and of the monetary policy shocks. To identify the latter, Champagne and Sekkel (2018) use real-time information available during meetings of the Governing Council preceding the interest rate announcement to purge the rate changes of the systematic component.

We estimate IRFs for price, labor market, and housing market series for Canada, Ontario, Québec, Manitoba, Saskatchewan, British Columbia, Alberta, New Brunswick, Nova Scotia, and Newfoundland.[16] Table 3.7 lists the selected series. These variables are among key indicators for the conduct of the monetary policy in Canada and are available for provinces.

[14]The study of the regional effects of monetary policy has a long history. Dominguez-Torres and Hierro (2019) provide a thorough review of the literature. Kronick and Ambler (2019) estimate regional effects of monetary policy shocks but only on inflation and unemployment. We go further by considering the components of inflation, the housing market, and sectoral employment.

[15]See Dufour and Renault (1998), Òscar Jordà (2005), and Plagborg-Møller and Wolf (2019) for details on local projections as means of estimating IRFs. We opted for a direct approach via local projections instead of the simultaneous approach like a Factor-Augmented VAR as in Bernanke et al. (2005) because the structural shock here is already identified and hence considered as an exogenous variable. The alternative would be to add ϵ_t as an exogenous variable in the VAR process specified on the above control variables. Here, given a very large number of provincial variables (hence correlation clusters that can affect the estimation of common factors, (Boivin and Ng, 2006)) we prefer to estimate IRFs with a direct approach and not impose factor model restrictions (Stevanovic, 2015).

[16]Prince Edward Island is left out of this analysis since some of the series considered were problematic.

Table 3.7: Variables of interest for the impulse response analysis

Prices	Labor market	Housing market
CPI_total	Total_EMP	Build_permit_total
CPI_core	Services_EMP	Build_permit_ind
CPI_goods	Resources_EMP	Build_permit_comm
CPI_services	Const_EMP	Housing_start
CPI_durables	Sales_EMP	
CPI_health	Finance_EMP	
CPI_clothing	Manufacturing_EMP	
CPI_shelter	Unemployment	

Note: IRFs of these series are estimated for Canada and all provinces but Prince Edward Island.

For all provinces and all series we estimate the following regressions:

$$ {}_{+} \quad = \quad + \quad (\ ) \ {}_{-1} \quad + \quad + \ {}_{+} \tag{3.22} $$

where denotes the variable of interest as listed in Table 3.7, $_{-1}$ contains control variables, is the already identified monetary policy shock series, and $=$ 0 1 48. We follow closely Champagne and Sekkel (2018) in the variables used as controls in $_{-1}$; when estimating the IRFs for Canada we include real GDP growth rate, CPI growth rate, and the growth rate of series , monetary policy shock lags but instead of using the growth rate of commodity prices as they do we instead include the first four principal components extracted from CAN-MD.[17] When estimating the IRFs of provinces, we use the same controls as for Canada but augment the set with the core CPI inflation rate and unemployment rate of the province to capture provincial business cycles. In all cases we use 4 lags of control variables and 48 lags of the monetary policy shocks. The full sample time span is 1981M01 - 2015M10 and we also consider the estimation during the inflation targeting (IT) period that starts in 1992M01.

[17] Bernanke et al. (2005) show that using principal components can solve the price puzzle found on US data without having to rely on commodity prices as an ad hoc way of correcting the puzzle. Boivin et al. (2010) apply a similar approach on Canadian data and also find that it solves many puzzles found in the literature as it better approximates the Central Bank's information set.

Given a limited number of observations and a large number of lags in controls, we do not consider estimating (3.22) during the pre-IT period only. is then the effect of the monetary policy shocks months ahead, for series and province .

There is a fair amount of heterogeneity across regions, sectors, and time and thus we choose to resume and quantify the main sources of heterogeneity in IRFs with the following fixed effect model:

$$= + + + \tag{3.23}$$

where the left hand side is the gap between province's estimated IRFs for series at a given horizon ( ) and the same series for Canada ( ), while and are the provincial and series fixed effects.[18] Figure 3.9 shows the results in terms of explained heterogeneity for both full sample and IT period using the ^{2} from the fixed-effect regressions.

Results of the first column (All series) come from the estimation of equation (3.23) using the IRFs of all series from Table 3.7, i.e. all sectors (prices, labor, and housing), all their components (or subsectors) and for all provinces. The second (Aggregate series) performs the same analysis using only the IRFs for core CPI, unemployment, total employment, housing starts, and total building permits, hence the component-specific variation is averaged out. In the former case, the sectorial (and component-specific) source of heterogeneity in IRFs are more important than regional ones. The total ^{2} rises slightly since the inflation targeting shift in the monetary policy. When only aggregate variables are used, the picture is similar for the full sample, but for the IT-period we observe that regional heterogeneity becomes more important within two years after the shock.

[18] Selected IRFs are reported in the appendix C.1.4.

Figure 3.9: Total heterogeneity explained by sectors and provinces

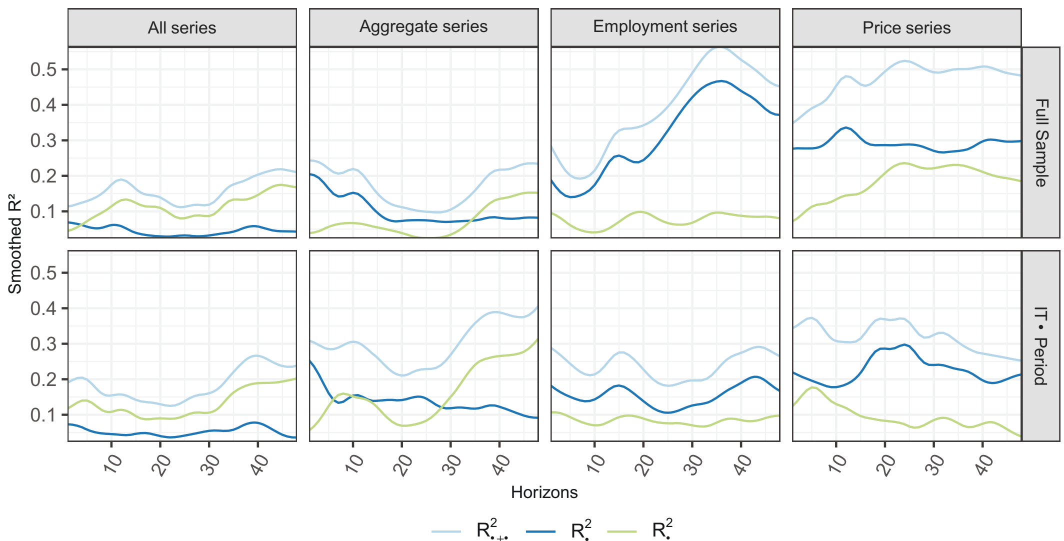

Note: The light blue line show the total smoothed R^2 from equation (3.23) while the dark blue and green lines respectively show the smoothed R^2 using only provincial and sectorial fixed effects.

To investigate this heterogeneity at a more granular level, we perform the same analysis on employment and price series' IRFs separately. The results are reported in the third and fourth columns respectively. Those graphs reveal that provincial unobserved heterogeneity is the most important ingredient to explain the gaps in IRFs. Comparing full sample and inflation targeting periods shows that the importance of both sources of heterogeneity has decreased with the change in monetary policy, which could be interpreted as a result of monetary policy effectiveness to stabilize the economy and to synchronize the business cycle fluctuations across the country (Mihov, 2001; Boivin and Giannoni, 2006).

We now explore the average differences for employment and CPI series in separate analysis. In other words, for every group of series formed from employment sub-sectors and CPI sub-components, we estimate the following fixed-effect model

$$\hat{\beta}_{h,s,p} = \Phi^{CAN}_{h,Bench.} + \theta_{h,p} + \phi_{h,s} + e_{h,s,p}, \tag{3.24}$$

where is the IRF of either Canadian total employment or Core CPI, while and are the province and sub-sector (sub-component) -specific fixed effects.

Figure 3.10 shows the estimated fixed effects coefficients for sectorial employment and CPI components for Canada and across provinces.[19] This figure reports the IRFs of the benchmark in the leftmost column and fixed effect estimates and thereafter. For example, let's look at the leftmost two entries in the top panel: the IRF of total employment in Canada and the fixed effects associated with the response of employment in the service industry . The average response of service employment is also negative since the sum of 0 and 0 is negative. The same panel also reveals that the response has the same sign and is much stronger in the Atlantic provinces (0) and that it eventually turns positive in the Prairies (0 at longer horizons).

In the case of employment for the full sample, we remark that the construction sector responds more to monetary policy shocks than total employment, as well as Ontario, Québec, and few Atlantic provinces, while the opposite is true for the west part of Canada with smaller and less persistent responses of employment. Since 1992, the heterogeneity across provinces and sectors is dampened, except for employment in the resource sector which exhibits a clear increase over the entire IRF horizon. These results are broadly in line with Jansen et al. (2013) who find that firms in the construction sector in the United States are more affected by changes in interest rates while those in the mining sector are better off following a tightening of monetary policy.

The second part of figure 3.10 explores regional and sectorial heterogeneity in the response of prices. In the full sample, the responses to monetary policy shocks for most

[19] Dedola and Lippi (2005) and Peersman and Smets (2005) have documented cross-industry heterogeneities to monetary policy shocks using industrial output in France, Germany, Italy, the UK, the US, and the Euro zone, while Fares and Srour (2001) have explored the cross-industry heterogeneity for Canada.

provinces are weaker than for Canada, while Ontario is more affected. In terms of sub-components, the heterogeneity is mostly observed in durable goods which virtually do not respond with going the opposite direction of . After the change in monetary policy in 1992, the regional differences are much smaller and the response for durable goods is even less important. This lower response of durable good prices is consistent with the idea that their consumption is highly interest rate sensitive and has a central role in monetary policy transmission (Erceg and Levin, 2006; Barsky et al., 2007; Cantelmo and Melina, 2018).

Overall, this analysis has documented a presence of a fair amount of heterogeneity across sectors, regions, and time in the effects and transmission of the monetary policy in Canada. If inflation targeting has helped to decrease those differences, still some regional heterogeneity pertains and may pose a challenge for the Bank of Canada in its role to further stabilize the economy.

Figure 3.10: Heterogeneity across sectors and provinces

(a) Employment

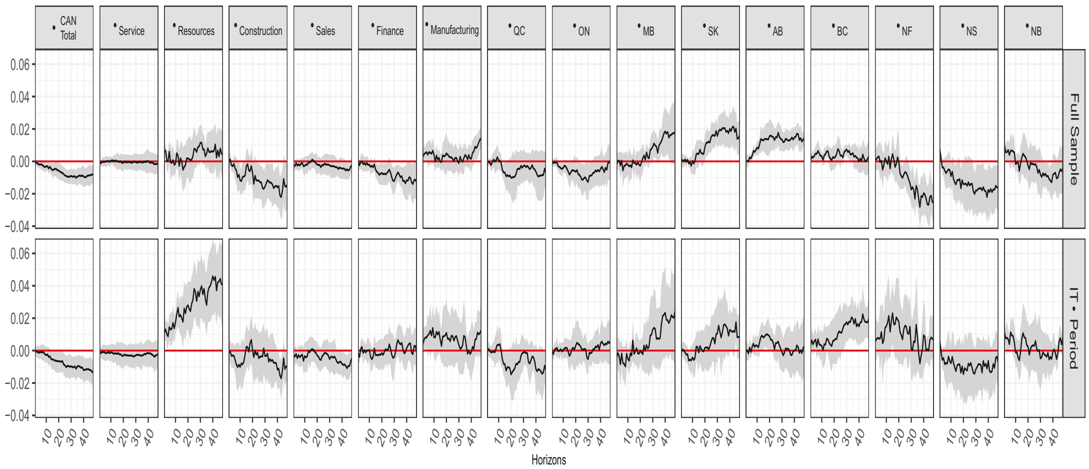

(b) Inflation

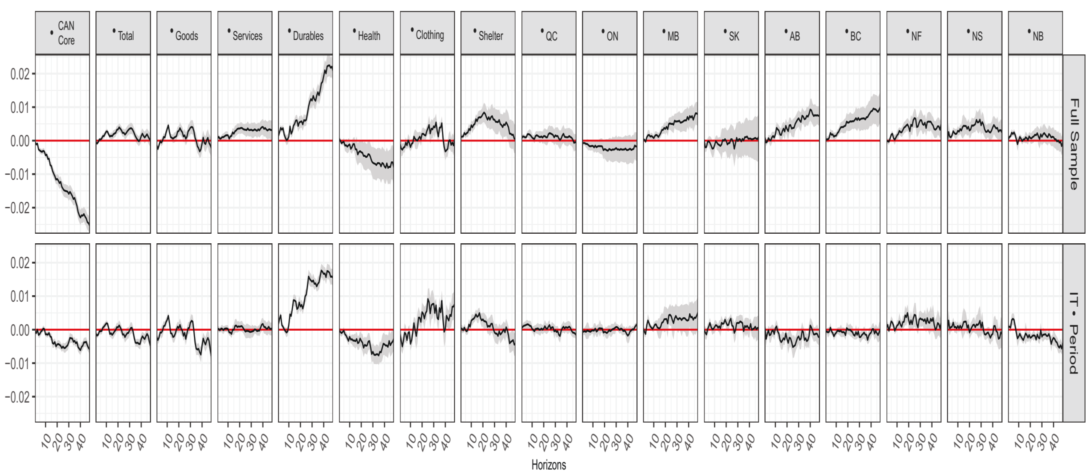

Note: This figure shows the estimated fixed effect coefficients from equation (3.24) along with the 90% confidence bands constructed using heteroskedastic consistent standard errors.

3.6 Conclusion

In this paper we proposed a large-scale Canadian macroeconomic database containing hundreds of Canadian and provincial economic indicators. It is designed to be updated regularly through the StatCan database and is publicly available. Real-time vintages are collected as well. It relieves users from dealing with data changes and methodological revisions and we provide an already balanced and stationary panel starting in 1981.

Four important features of the dataset have been explored. First, we studied the factor structure and found that common factors explain a sizable portion of variation in Canadian and provincial aggregate series. Few driving forces of the Canadian economy have been identified, such as GDP in business and financial sectors, term structure, exchange rates, unemployment duration, and international transaction net flows and oil production. Second, the dataset has been applied to the prediction of turning points for the Canadian business cycle. Using Probit, Lasso, and factor models we showed that this dataset has substantial explanatory power in addition to the standard term spread predictor.

Third, using the dataset has substantially improved the predictive accuracy when forecasting key real macroeconomic indicators. Factor and sparse models, random forests, and regularized complete subset regressions showed good performance in forecasting real activity variables such as industrial production, employment and unemployment rate, as well as CPI and Core CPI inflation.

Finally, we studied heterogenous effects of monetary policy on different sectors of the Canadian economy and across regions. Results suggested that the passage to inflation targeting since 1992 coincides with a decrease in those differences, but some regional heterogeneity still pertains and may pose a challenge for the Bank of Canada in its role to further stabilize the economy.

CONCLUSION

Cette thèse porte sur trois problèmes pertinents au travail empirique en macroéconomie soit la prévision du risque en macroéconomie, l'identification de chocs structurels en présence de données persistentes et l'analyse macroéconomique dans un environnement riche en données.

Dans le premier chapitre, nous exploitons un exercice de prévision pseudo-hors-échantillon afin d'évaluer le modèle QVAR pour les prévisions par quantiles et par densités dans les queues de distribution. L'exercice couvre un grand nombre de variables macroéconomiques aux États-Unis sur quelques décennies pour des horizons de 1 à 12 mois et inclut une comparaison avec des modèles VAR standards. Nous trouvons que le modèle QVAR fait souvent significativement et quantitativement mieux et rarement pire que les modèles VAR considérés. Le modèle fait particulièrement bien pour le marché du travail et les taux d'intérêt et de change. Nous avons aussi considéré l'ajout de facteurs estimés par composantes principales, ainsi que des facteurs quantiles et trouvons que ceci améliore la capacité de prévision dans certains cas comme pour le marché du travail. Ces résultats suggèrent que le modèle QVAR offrent une représentation adéquate du risque macroéconomique. Cela suggèrent que la motivation originale de les appliquer à des questions de nature structurelles pourraient générer des résultats informatifs.

Dans le second chapitre, nous abordons l'identification de chocs structurels par la maximisation des parts (*Max Share*) lorsque le modèle VAR est estimé en niveau sur des variables persistentes. Nous établissons théoriquement que l'estimateur résultant est non convergent et montrons dans des simulations Monte Carlo que ceci peut causer des biais importants et augmenter les erreurs quadratiques (*RMSE*) lorsqu'on cible des horizons intermédiaires et longs. Nous illustrons la pertinence des résultats pour le travail empirique dans une application empirique aux chocs de nouvelles (*news shocks*) sur la technologie spécifique à l'investissement (*IST*) et sur la productivité multifactorielle (*TFP*). Ces résultats montrent que la pratique commune d'estimer en niveau et de recourir à la maximisation des parts pour éviter de se prononcer sur le comportement de long terme du système n'est pas justifiée. Ces résultats suggèrent d'utiliser des représentations stationnaires pour s'assurer de la robustesse des résultats obtenus en niveau. Des méthodes d'apprentissage automatique (par exemple, Liao and Phillips (2015) ou Liang and Schienle (2019)) permettant la sélection conjointe du rang de cointégration et du nombre de retards sont des avenues prometteuses pour effectuer ce type d'analyse de robustesse.

Dans le troisième chapitre, nous introduisons une grande base de données macroéconomiques mensuelles pour le Canada. La base de données contient quelques centaines d'indicateurs économiques canadiens et provinciaux. Elle a été conçue afin de faciliter sa mise à jour régulière et ses millésimes (*vintages*) en temps réel sont disponibles publiquement. Nous établissons que la base de données présente une structure à facteurs latents relativement stable et qu'elle permet d'améliorer la prévision des points de retournement du cycle économique canadien, ainsi que la prévision d'indicateurs macroéconomiques clés. Nous montrons finalement comment la base de données peut servir pour étudier l'hétérogénéité des réponses à la politique monétaire à travers les différents secteurs et régions au Canada.

En somme, ces articles contribuent au travail en macroéconomie en montrant que les modèles QVAR permettent de bien modéliser le risque macroéconomique, l'identification de chocs structurels par maximisation des parts (*Max Share*) dans des modèles VAR estimés en niveau sur des données persistentes posent des problèmes jusqu'ici négligés et suggèrent de considérer systématiquement leur robustesse et en offrant une grande base de données macroéconomiques mensuelles pour le Canada à partir de laquelle nous pouvons appliquer des méthodes qui exploitent la richesse des données pour améliorer les prévisions ou approfondir l'analyse structurelle.

APPENDIX A

QUANTILE VARS AND MACROECONOMIC RISK FORECASTING

A.1 Monte Carlo Tests

The idea behind the Dufour (2006) Monte Carlo testing framework is that exact finite sample p-values can be obtained even when an analytic formula for the distribution of a test statistic under the null is unavailable provided we can simulate it. In our case, we draw samples of observations of $(0\ 9)$ and compute likelihood ratio statistics for $=1$. If $_0$ is the corresponding statistic we computed on the actual data, then the p-value is given by

$$(\quad _0) = \frac{(\quad _0) + 1}{+1}$$

where $(\quad _0) = \sum_{=1} \mathbb{I} \qquad _0$. As noted by Christoffersen (2004), the distribution is discrete such that ties can happen and need to be handled. They propose breaking ties by drawing $+1$ uniform random variables $[0\ 1]$ where $=$ 0 and using

$$(\quad _0) = 1 \quad \frac{1}{}\sum_{=1} \mathbb{I} \qquad _0 + \frac{1}{}\sum_{=1} \mathbb{I} \quad = \quad _0 \ \mathbb{I} \qquad _0$$

in the above formula.

A.2 Additional Results

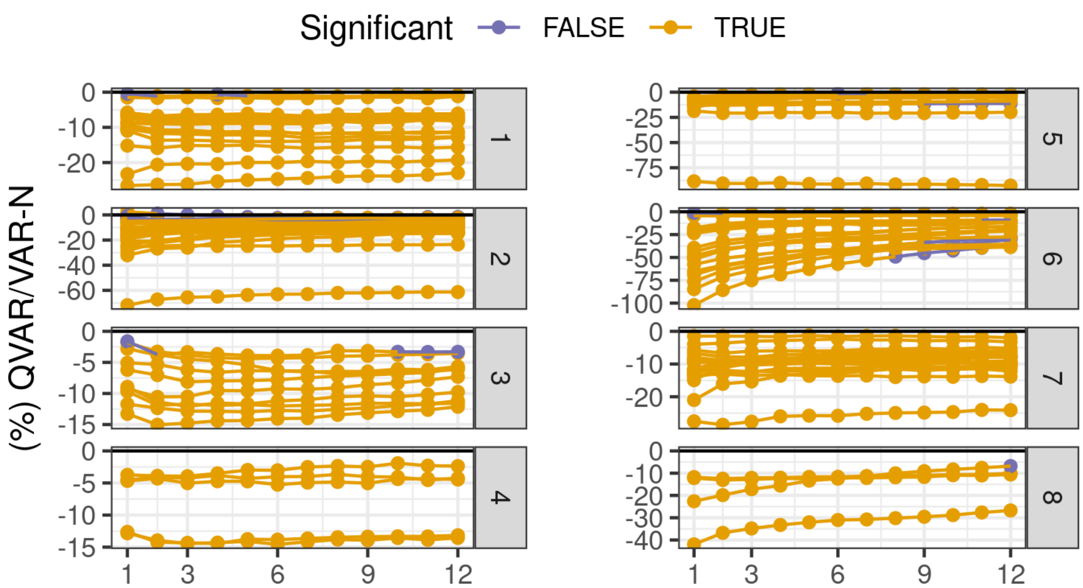

Figure A.1: QVAR and VAR-N Relative Scores (tail-weighted CRPS)

Note: Negative values are improvements. Yellow corresponds to rejecting the null of equal scores at 5%. Yellow corresponds to not rejecting the null of equal scores at 5%. FRED groups are: **(1)** Output and income, **(2)** Labor market, **(3)** Housing, **(4)** Consumption, orders and inventories, **(5)** Money and credit, **(6)** Interest and exchange rate, **(7)** Prices and **(8)** Stock market.

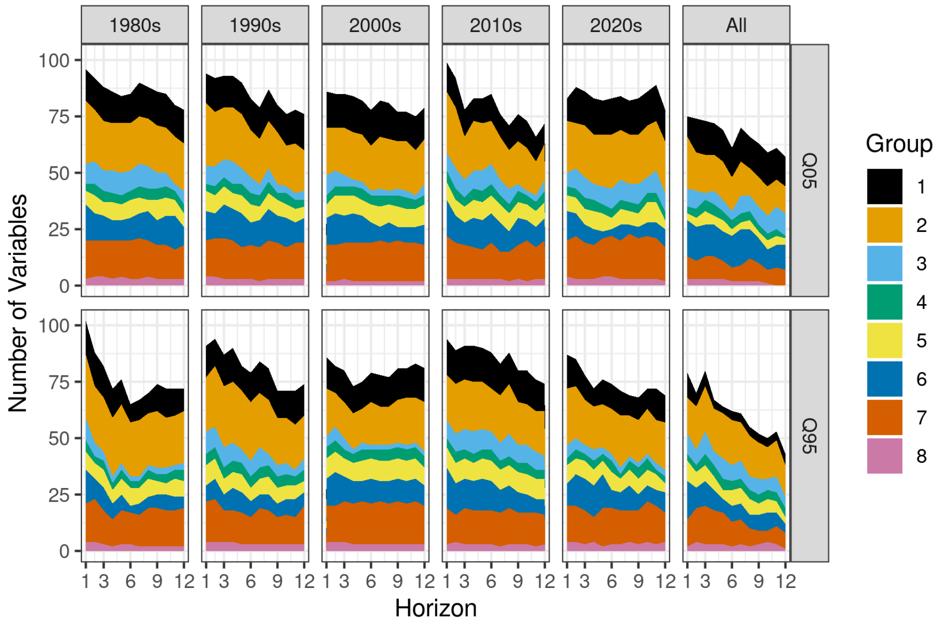

(a) Null Constant

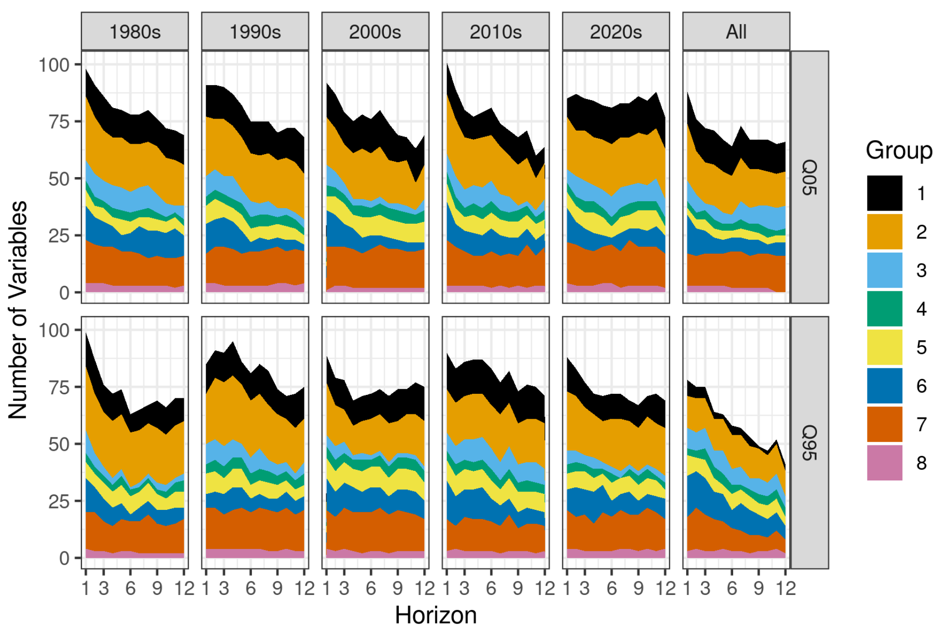

(b) Unit Slope

Figure A.2: Number of Optimal QVAR Forecasts

Note: Number of cases where we obtain a non rejection of the null at 5% for the Gaglianone et al. (2011) test. Columns are periods and rows are the 5th (Q05) and 95th (Q95) quantile forecasts, respectively. Colors indicate FRED groups: **(1)** Output and income, **(2)** Labor market, **(3)** Housing, **(4)** Consumption, orders and inventories, **(5)** Money and credit, **(6)** Interest and exchange rate, **(7)** Prices and **(8)** Stock market.

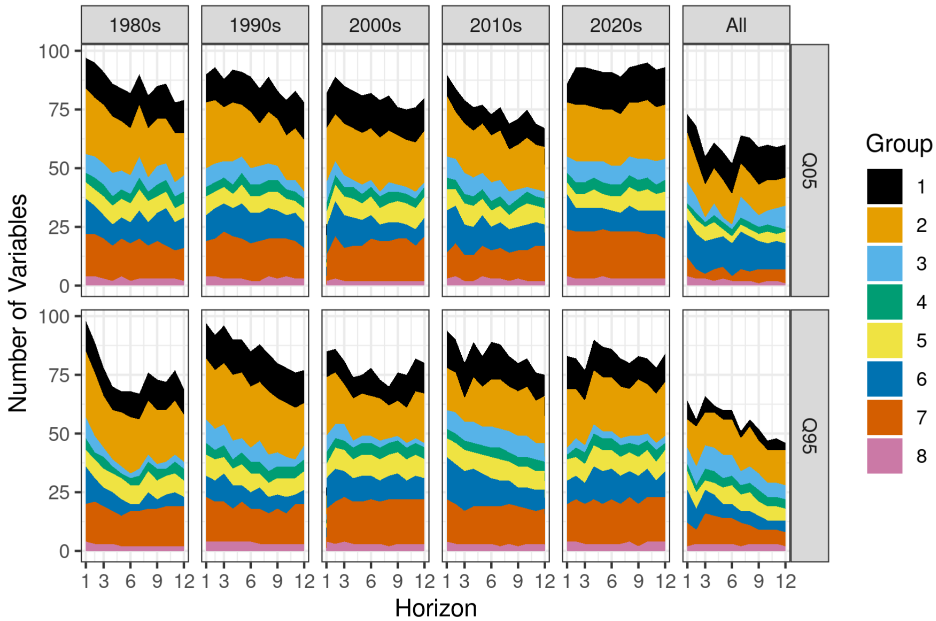

(a) Null Constant

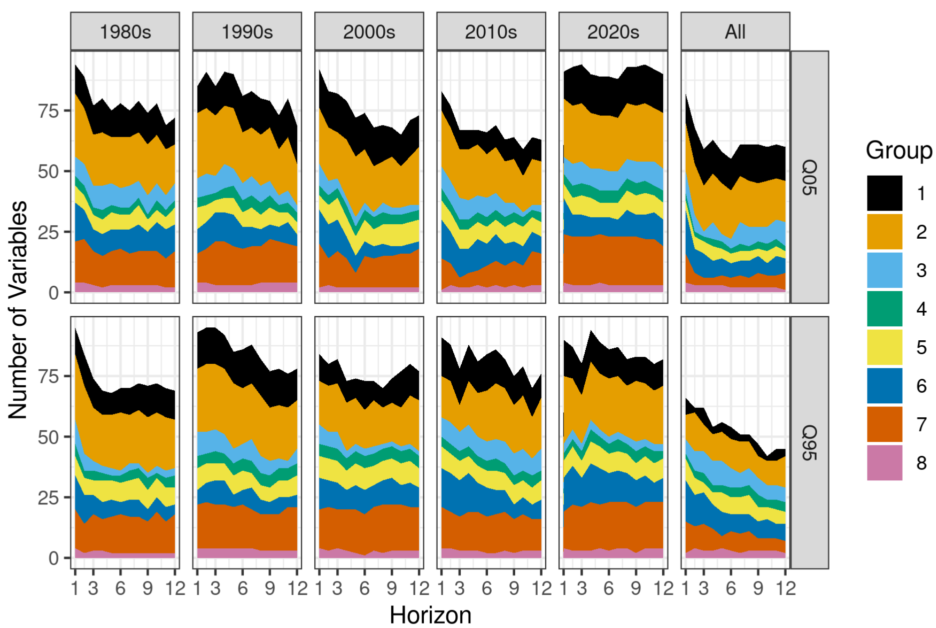

(b) Unit Slope

Figure A.3: Number of Optimal QFAVAR (PCA) Forecasts

Note: Number of cases where we obtain a non rejection of the null at 5% for the Gaglianone et al. (2011) test. Columns are periods and rows are the 5th (Q05) and 95th (Q95) quantile forecasts, respectively. Colors indicate FRED groups: **(1)** Output and income, **(2)** Labor market, **(3)** Housing, **(4)** Consumption, orders and inventories, **(5)** Money and credit, **(6)** Interest and exchange rate, **(7)** Prices and **(8)** Stock market.

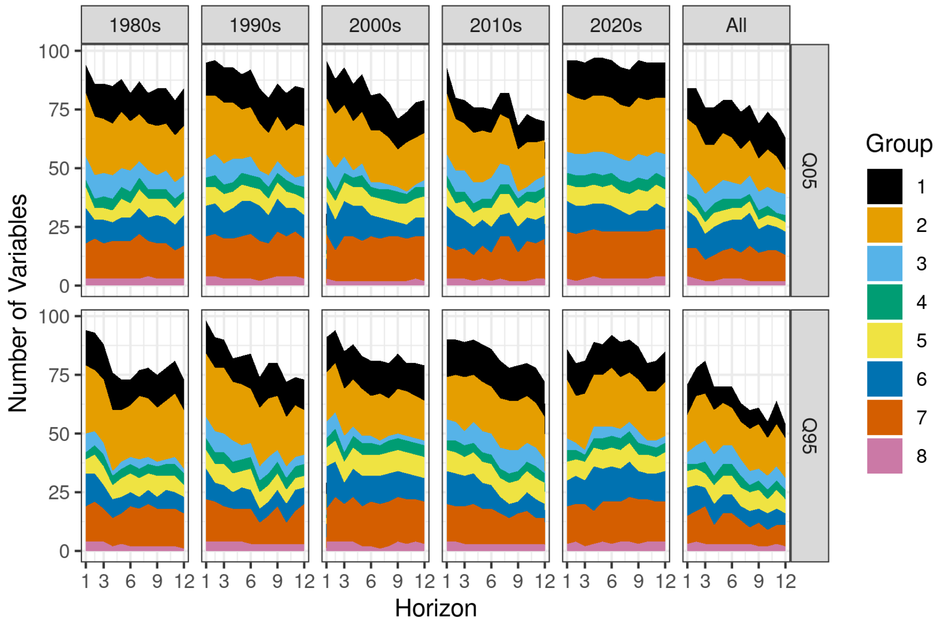

(a) Null Constant

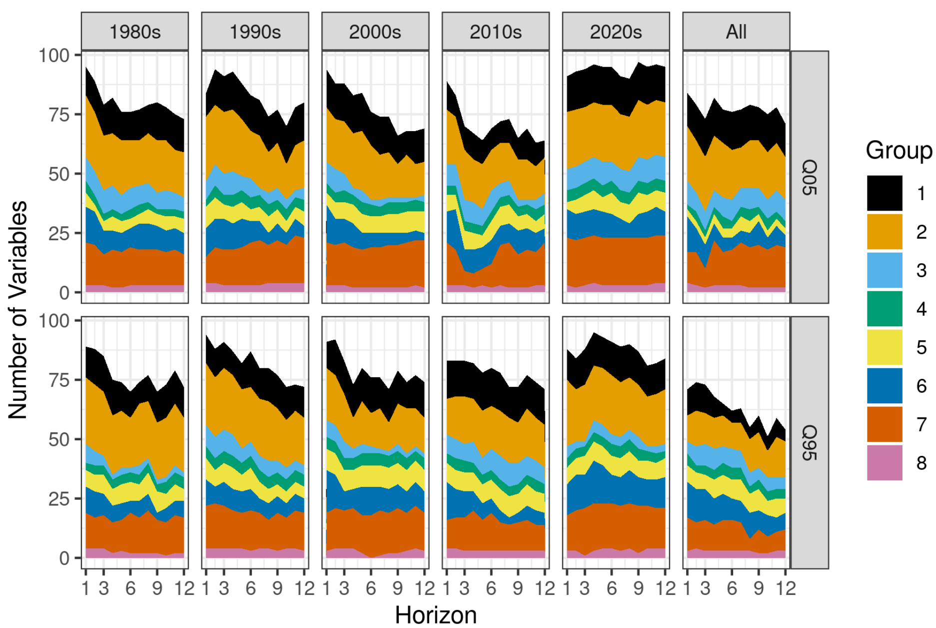

(b) Unit Slope

Figure A.4: Number of Optimal QFAVAR (IQR) Forecasts

Note: Number of cases where we obtain a non rejection of the null at 5% for the Gaglianone et al. (2011) test. Columns are periods and rows are the 5th (Q05) and 95th (Q95) quantile forecasts, respectively. Colors indicate FRED groups: **(1)** Output and income, **(2)** Labor market, **(3)** Housing, **(4)** Consumption, orders and inventories, **(5)** Money and credit, **(6)** Interest and exchange rate, **(7)** Prices and **(8)** Stock market.

A.3 Data Transformation

As in the reference documentation of FRED-MD, the transformation codes are (1) , (2) , (3) ^{2} , (4) , (5) , (6) ^{2} and (7) $_{-1}$ 1.

Table A.1: Data Transformation

ID	Description	Used	FRED
RPI	Real Personal Income	5	5
W875RX1	Real personal income ex transfer receipts	5	5
INDPRO	IP Index	5	5
IPFPNSS	IP: Final Products and Nonindustrial Supplies	5	5
IPFINAL	IP: Final Products (Market Group)	5	5
IPCONGD	IP: Consumer Goods	5	5
IPDCONGD	IP: Durable Consumer Goods	5	5
IPNCONGD	IP: Nondurable Consumer Goods	5	5
IPBUSEQ	IP: Business Equipment	5	5
IPMAT	IP: Materials	5	5
IPDMAT	IP: Durable Materials	5	5
IPNMAT	IP: Nondurable Materials	5	5
IPMANSICS	IP: Manufacturing (SIC)	5	5
IPB51222s	IP: Residential Utilities	5	5
IPFUELS	IP: Fuels	5	5
CUMFNS	Capacity Utilization: Manufacturing	1	2
HWI	Help-Wanted Index for United States	5	2
HWIURATIO	Ratio of Help Wanted/No. Unemployed	4	2
CLF16OV	Civilian Labor Force	5	5
CE16OV	Civilian Employment	5	5
UNRATE	Civilian Unemployment Rate	1	2
UEMPMEAN	Average Duration of Unemployment (Weeks)	1	2
UEMPLT5	Civilians Unemployed - Less Than 5 Weeks	1	5
UEMP5TO14	Civilians Unemployed for 5-14 Weeks	1	5
UEMP15OV	Civilians Unemployed - 15 Weeks & Over	1	5

Table A.1. Data Transformation (Continued)

ID	Description	Used	FRED
UEMP15T26	Civilians Unemployed for 15-26 Weeks	1	5
UEMP27OV	Civilians Unemployed for 27 Weeks and Over	1	5
CLAIMSx	Initial Claims	5	5
PAYEMS	All Employees: Total nonfarm	5	5
USGOOD	All Employees: Goods-Producing Industries	5	5
CES1021000001	All Employees: Mining and Logging: Mining	5	5
USCONS	All Employees: Construction	5	5
MANEMP	All Employees: Manufacturing	5	5
DMANEMP	All Employees: Durable goods	5	5
NDMANEMP	All Employees: Nondurable goods	5	5
SRVPRD	All Employees: Service-Providing Industries	5	5
USTPU	All Employees: Trade, Transportation & Utilities	5	5
USWTRADE	All Employees: Wholesale Trade	5	5
USTRADE	All Employees: Retail Trade	5	5
USFIRE	All Employees: Financial Activities	5	5
USGOVT	All Employees: Government	5	5
CES0600000007	Avg Weekly Hours : Goods-Producing	1	1
AWOTMAN	Avg Weekly Overtime Hours : Manufacturing	1	2
AWHMAN	Avg Weekly Hours : Manufacturing	1	1
CES0600000008	Avg Hourly Earnings : Goods-Producing	5	6
CES2000000008	Avg Hourly Earnings : Construction	5	6
CES3000000008	Avg Hourly Earnings : Manufacturing	5	6
HOUST	Housing Starts: Total New Privately Owned	4	4
HOUSTNE	Housing Starts, Northeast	4	4
HOUSTMW	Housing Starts, Midwest	4	4
HOUSTS	Housing Starts, South	4	4
HOUSTW	Housing Starts, West	4	4
PERMIT	New Private Housing Permits (SAAR)	4	4
PERMITNE	New Private Housing Permits, Northeast (SAAR)	4	4
PERMITMW	New Private Housing Permits, Midwest (SAAR)	4	4

Table A.1. Data Transformation (Continued)

ID	Description	Used	FRED
PERMITS	New Private Housing Permits, South (SAAR)	4	4
PERMITW	New Private Housing Permits, West (SAAR)	4	4
DPCERA3M086SBEA	Real personal consumption expenditures	5	5
CMRMTSPLx	Real Manu. and Trade Industries Sales	5	5
RETAILx	Retail and Food Services Sales	5	5
ACOGNO	New Orders for Consumer Goods	5	5
AMDMNOx	New Orders for Durable Goods	5	5
ANDENOx	New Orders for Nondefense Capital Goods	5	5
AMDMUOx	Unfilled Orders for Durable Goods	5	5
BUSINVx	Total Business Inventories	5	5
ISRATIOx	Total Business: Inventories to Sales Ratio	2	2
UMCSENTx	Consumer Sentiment Index	2	2
M1SL	M1 Money Stock	5	6
M2SL	M2 Money Stock	5	6
M2REAL	Real M2 Money Stock	5	5
BOGMBASE	Monetary Base	5	6
TOTRESNS	Total Reserves of Depository Institutions	5	6
NONBORRES	Reserves Of Depository Institutions	7	7
BUSLOANS	Commercial and Industrial Loans	5	6
REALLN	Real Estate Loans at All Commercial Banks	5	6
NONREVSL	Total Nonrevolving Credit	5	6
CONSPI	Nonrevolving consumer credit to Personal Income	5	2
DTCOLNVHFNM	Consumer Motor Vehicle Loans Outstanding	5	6
DTCTHFNM	Total Consumer Loans and Leases Outstanding	5	6
INVEST	Securities in Bank Credit at All Commercial Banks	5	6
FEDFUNDS	Effective Federal Funds Rate	1	2
CP3Mx	3-Month AA Financial Commercial Paper Rate	1	2
TB3MS	3-Month Treasury Bill:	1	2
TB6MS	6-Month Treasury Bill:	1	2
GS1	1-Year Treasury Rate	1	2

Table A.1. Data Transformation (Continued)

ID	Description	Used	FRED
GS5	5-Year Treasury Rate	1	2
GS10	10-Year Treasury Rate	1	2
AAA	Moody's Seasoned Aaa Corporate Bond Yield	1	2
BAA	Moody's Seasoned Baa Corporate Bond Yield	1	2
COMPAPFFx	3-Month Commercial Paper Minus FEDFUNDS	1	1
TB3SMFFM	3-Month Treasury C Minus FEDFUNDS	1	1
TB6SMFFM	6-Month Treasury C Minus FEDFUNDS	1	1
T1YFFM	1-Year Treasury C Minus FEDFUNDS	1	1
T5YFFM	5-Year Treasury C Minus FEDFUNDS	1	1
T10YFFM	10-Year Treasury C Minus FEDFUNDS	1	1
AAAFFM	Moody's Aaa Corporate Bond Minus FEDFUNDS	1	1
BAAFFM	Moody's Baa Corporate Bond Minus FEDFUNDS	1	1
TWEXAFEGSMTHx	Trade Weighted U.S. Dollar Index	5	5
EXSZUSx	Switzerland / U.S. Foreign Exchange Rate	5	5
EXJPUSx	Japan / U.S. Foreign Exchange Rate	5	5
EXUSUKx	U.S. / U.K. Foreign Exchange Rate	5	5
EXCAUSx	Canada / U.S. Foreign Exchange Rate	5	5
WPSFD49207	PPI: Finished Goods	5	6
WPSFD49502	PPI: Finished Consumer Goods	5	6
WPSID61	PPI: Intermediate Materials	5	6
WPSID62	PPI: Crude Materials	5	6
OILPRICEx	Crude Oil, spliced WTI and Cushing	5	6
PPICMM	PPI: Metals and metal products:	5	6
CPIAUCSL	CPI : All Items	5	6
CPIAPPSL	CPI : Apparel	5	6
CPITRNSL	CPI : Transportation	5	6
CPIMEDSL	CPI : Medical Care	5	6
CUSR0000SAC	CPI : Commodities	5	6
CUSR0000SAD	CPI : Durables	5	6
CUSR0000SAS	CPI : Services	5	6

Table A.1. Data Transformation (Continued)

ID	Description	Used	FRED
CPIULFSL	CPI : All Items Less Food	5	6
CUSR0000SA0L2	CPI : All items less shelter	5	6
CUSR0000SA0L5	CPI : All items less medical care	5	6
PCEPI	Personal Cons. Expend.: Chain Index	5	6
DDURRG3M086SBEA	Personal Cons. Exp: Durable goods	5	6
DNDGRG3M086SBEA	Personal Cons. Exp: Nondurable goods	5	6
DSERRG3M086SBEA	Personal Cons. Exp: Services	5	6
S&P 500	S&P's Common Stock Price Index: Composite	5	5
S&P: indust	S&P's Common Stock Price Index: Industrials	5	5
S&P div yield	S&P's Composite Common Stock: Dividend Yield	1	2
S&P PE ratio	S&P's Composite Common Stock: Price-Earnings Ratio	1	5
VIXCLSx	VIX	1	1

APPENDIX B

MAX SHARE IDENTIFICATION FOR STRUCTURAL VARS IN LEVELS: THERE IS NO FREE LUNCH

B.1 Proofs of Asymptotic Results in the Stationary Case

Proof of Theorem 2.3.1

Let Assumption (2.3.1) hold and consider the behavior of ( ) as for some finite, fixed . The asymptotic distribution can be derived from the delta method. Let $= \mathrm{vec}\,([\ _1\ ])$, one has

$$\tilde{}(\ ) := \frac{\mathrm{vec}\,(\ (\ ))}{'} = \sum_{=0}^{-1} (\ \ _{\mathrm{tr}}'\ '\ ') \frac{\mathrm{vec}\,(\ \ _{\mathrm{tr}})}{'} + \sum_{=0}^{-1} (\ _{\mathrm{tr}}'\ '\ '\ ) \frac{\mathrm{vec}\,(\ _{\mathrm{tr}}'\ ')}{'}$$

with (see Lütkepohl (2005) p.668, rules 7 and 6, respectively)

$$\frac{\mathrm{vec}\,(\ \ _{\mathrm{tr}})}{'} = (\ _{\mathrm{tr}}'\ ) \frac{\mathrm{vec}(\ )}{'}$$

$$\frac{\mathrm{vec}\,(\ _{\mathrm{tr}}'\ ')}{'} = (\ \ _{\mathrm{tr}}') \frac{\mathrm{vec}(\ ')}{'} = (\ \ _{\mathrm{tr}}') \frac{\mathrm{vec}(\ )}{'}$$

where is the ^{2} ^{2} commutation matrix such that $\mathrm{vec}(\ ') = \ \mathrm{vec}(\ )$ for any matrix. Therefore, using the Kronecker product rules and the properties of the commutation matrix, one has:[1]

$$\frac{\mathrm{vec}\,(\ (\ ))}{'} = \sum_{=0}^{-1} (\ \ _{\mathrm{tr}}'\ '\ ')(\ _{\mathrm{tr}}'\ ) \frac{\mathrm{vec}(\ )}{'} + \sum_{=0}^{-1} (\ _{\mathrm{tr}}'\ '\ '\ )(\ \ _{\mathrm{tr}}') \frac{\mathrm{vec}(\ )}{'}$$

[1] Let G be $(m \quad n)$ and F $(p \quad q)$. Then $K_{pm}(G \quad F) = (F \quad G)K_{qn}$, with K_{pm} and K_{qn} some commutation matrices.

$$= \sum_{=0}^{-1} (\,{}'_{\mathrm{tr}} \quad {}'_{\mathrm{tr}} \,{}' \quad {}') \frac{\mathrm{vec}(\quad)}{{}'}$$

$$+ \sum_{=0}^{-1} (\,{}'_{\mathrm{tr}} \,{}' \quad {}' \quad {}'_{\mathrm{tr}}) \qquad \frac{\mathrm{vec}(\quad)}{{}'}$$

$$= \sum_{=0}^{-1} (\,{}'_{\mathrm{tr}} \quad {}'_{\mathrm{tr}} \,{}' \quad {}') \frac{\mathrm{vec}(\quad)}{{}'}$$

$$+ \sum_{=0}^{-1} \qquad (\,{}'_{\mathrm{tr}} \quad {}'_{\mathrm{tr}} \,{}' \quad {}') \frac{\mathrm{vec}(\quad)}{{}'}$$

$$= \sum_{=0}^{-1} (\quad {}_2 + \qquad) (\,{}'_{\mathrm{tr}} \quad {}'_{\mathrm{tr}} \,{}' \quad {}') \frac{}{{}'}$$

Likewise, defining $\quad :=$ vech$(\quad)$,

$$(\ ) := \frac{\mathrm{vec}\,(\quad (\ ))}{{}'} = \sum_{=0}^{-1} (\qquad {}'_{\mathrm{tr}} \,{}' \quad {}' \quad) \frac{\mathrm{vec}(\ {}_{\mathrm{tr}})}{{}'}$$

$$+ \sum_{=0}^{-1} (\,{}'_{\mathrm{tr}} \,{}' \quad {}' \qquad) \frac{\mathrm{vec}(\ {}'_{\mathrm{tr}})}{{}'}$$

$$= \sum_{=0}^{-1} (\quad {}_2 + \qquad) (\qquad {}'_{\mathrm{tr}} \,{}' \quad {}' \quad) \frac{\mathrm{vec}(\ {}_{\mathrm{tr}})}{{}'}$$

We define the $(\qquad)$ matrix $\quad := (\ {}_{+1} \qquad)$ and $\quad (0) :=$ $\big((\qquad (\ ))(\ {}' \qquad (\ ))'\big)$, the contemporaneous covariance matrix of the vector process . Under Assumption (2.3.1),

$$- \begin{bmatrix} & \end{bmatrix} \qquad \left(0 \begin{bmatrix} (0)^{-1} & & 0 \\ 0 & 2 \ {}^{+} (\qquad) & {}^{+\prime} \end{bmatrix} \right)$$

where ${}^{+} := (\ {}' \qquad)^{-1} \ {}'$ is Moore-Penrose generalized inverse of the ^{2} $(\ + 1)\ \ 2$ duplication matrix. Using the Delta method,

$$- \ \mathrm{vec}\left(\widehat{\ } \ (\ ) \qquad (\ ) \right)$$

$$\left(0 \left[\;\tilde{}(\;) \quad (\;) \right] \begin{bmatrix} (0)^{-1} & 0 \\ 0 & 2 \;^{+}(\qquad) \;^{+\prime} \end{bmatrix} \begin{bmatrix} \tilde{}^{\prime} \\ {}^{\prime} \end{bmatrix} \right)$$

as stated.

Proof of Theorem 2.3.2

Suppose that the Max Share matrix ( ) is of rank . The spectral decomposition of ( ) is given by:

$$(\;) = (\;) \; (\;) \; {}^{\prime}(\;)$$

where is the diagonal matrix whose diagonal elements are the eigenvalues arranged in algebraically nonincreasing order, and is the orthogonal matrix with $^{\prime} = \mathrm{I}$ containing the associated eigenvectors. Given that the Max Share matrix is not necessarily of full rank (e.g., Case 1, Section 4), we assume that the first eigenvalues are different from zero and the last eigenvalues are equal to zero. Accordingly, the submatrix contains the eigenvectors associated with the first eigenvalues, and the submatrix $_{-}$ contains the eigenvectors associated with the last eigenvalues, so that $^{\prime} = \; ^{\prime} + \; _{-} \; ^{\prime}{}_{-}$. Additionally, can be partitioned as $= [\;_{1} \quad _{2:}\;]$, where $_{1} = (\;)$ denotes the eigenvector associated with the maximal eigenvalue when the target is the th variable. Therefore, the matrix can be written as:

$$\begin{bmatrix} & 0 \\ 0 & _{-} \end{bmatrix}$$

$$= \; ^{\prime} \; (\;) \; = \begin{bmatrix} ^{\prime} \; (\;) & ^{\prime} \; (\;) \; _{-} \\ ^{\prime}{}_{-} \; (\;) & ^{\prime}{}_{-} \; (\;) \; _{-} \end{bmatrix}$$

where $' \;\; (\,)$ $= \begin{bmatrix} {}'_1 \; (\,)_1 & {}'_1 \; (\,)_{2:} \\ {}'_{2:} \; (\,)_1 & {}'_{2:} \; (\,)_{2:} \end{bmatrix}$. Using the vectorization of the matrix , we have:

$$\mathrm{vec}\,(\quad) = \mathrm{vec}\,(\; ' \;\; (\,) \quad) = (\; ' \qquad ')\,\mathrm{vec}\,(\;\; (\,))$$

Using Theorem 2.3.1, $^{1\;2}\mathrm{vec}\left(\widehat{\;} \;\; (\,) \qquad (\,)\right) \quad \mathcal{N}(0 \quad)$, and assuming a weakly consistent estimate of the submatrix of eigenvectors , $\widehat{\;}$, the two results of Theorem 2.3.2 follow by virtue of the Slutsky theorem.

Proof of Theorem 2.3.3

Theorem 2.3.3 is an application of Theorem 4.1 and Theorem 4.2. (p. 729) of Tyler (1981) and Theorem 1 in Bura and Pfeiffer (2008). The expression of the variance-covariance matrix of the eigenvector associated to the maximal eigenvalue results from Anderson (1963).

B.2 Asymptotic Properties of the Max Share Matrix for the Bivariate DGP

We first provide some preliminary notations.

Rotating the System in Separate I(1) and I(0) Components

Some of the results in the paper rely on rotating the system into separate I(1) and I(0) components following Phillips (1998). Define $:= (\;\; _{\perp} \;\;)$, $:= \; ' \;\;$, $:= \; '$ and $:= \; ' \;\;$. Then,

$$= \sum_{=1} \quad _{-} +$$

Letting $:= \ '(\ )$, we get

$$= \quad {}_{-1} + \ ' \ (\ ) \quad {}_{-1} +$$

Furthermore, we define $:= \ (\ '_{-1} \quad '_{- \ +1})' =$ $(\ '_{-1} \quad '_{- \ +1})\ (\ {}_{-1} \quad)$ and $:= \ '(\ {}_{1} \quad {}_{-1})\ (\ {}_{-1} \quad)$ whence

$$\begin{aligned} &= \ ' \ (\ ) \\ &= \quad {}_{-1} + \quad + \end{aligned} \tag{B.1}$$

We now obtain a partition of the matrix . Under **(c)**, one gets

$$= \begin{bmatrix} \exp(\ {}^{-1} \ ) & {}'_{\perp} \\ 0_{\ \times} & + \ ' \end{bmatrix}$$

Two Random Matrix distributions

Following Phillips (1998) we define the random matrices and ${}_{\Gamma}$. Recall that $:=$ $'$ are the residuals in the separated system and define $(\ )$ as a vector of uncorrelated Brownian motions. Under assumption **(c)**, we further define ${}_{1} := {}'_{\perp} \ {}_{2}\ {}_{-1} + \ {}_{1} \ +$ ${}_{1}$, its long-run covariance matrix as , the long-run covariance matrix of ${}_{1}$ as and the correlated Brownian motions $(\ ) = \ (\ )$ and ${}_{1}(\ ) = \ (\ )$. Then, the so-called unit root matrix is given by

$$:= \int_0^1 \ (\ )\ {}_{1}(\ )' \left(\int_0^1 {}_{1}(\ )\ {}_{1}(\ )' \right)^{-1} \tag{B.2}$$

Now, under assumption **(c')**, we must also introduce the following Ornstein-Uhlenbeck process $_{\Gamma}(\ ) := \int_0 \exp((\quad)\ )\ \ _1(\ )$ and the so-called local-to-unit matrix

$$_{\Gamma} := \int_0^1 \ (\ )\ _{\Gamma}(\ )' \left(\int_0^1 \ _{\Gamma}(\ )\ _{\Gamma}(\ )' \ \right)^{-1} \tag{B.3}$$

Specific derivations for the experiments

We discuss part **(i)** of Theorem 2.3.4 (i.e., the limiting distribution of IRFs) in the special case of the DGP used in Section 2.3:

$$\begin{bmatrix} _1 \\ _2 \end{bmatrix} = \begin{bmatrix} 1 + \ _{11} & _{12} + \\ _{21} & _{22} \end{bmatrix} \begin{bmatrix} _{1\ -1} \\ _{2\ -1} \end{bmatrix} + \begin{bmatrix} _{11} & _{12} \\ _{21} & 0 \end{bmatrix} \begin{bmatrix} _{1\ -2} \\ _{2\ -2} \end{bmatrix} + \begin{bmatrix} _1 \\ _2 \end{bmatrix}$$

Equivalently, the reduced-form VECM form can be written as:

$$\begin{bmatrix} \ _1 \\ \ _2 \end{bmatrix} = \begin{bmatrix} 0 & & \\ 0 & _{22} & 1 \end{bmatrix} \begin{bmatrix} _{1\ -1} \\ _{2\ -1} \end{bmatrix} + \begin{bmatrix} _{11} & _{12} \\ _{21} & 0 \end{bmatrix} \begin{bmatrix} \ _{1\ -1} \\ \ _{2\ -1} \end{bmatrix} + \begin{bmatrix} _1 \\ _2 \end{bmatrix}$$

More generally,

$$\begin{bmatrix} \ _1 \\ \ _2 \end{bmatrix} = \begin{bmatrix} 1 & \\ 0 & _{22} \end{bmatrix} \begin{bmatrix} _{1\ -1} \\ _{2\ -1} \end{bmatrix} + \begin{bmatrix} _{11} & _{12} \\ _{21} & 0 \end{bmatrix} \begin{bmatrix} \ _{1\ -1} \\ \ _{2\ -1} \end{bmatrix} + \begin{bmatrix} _1 \\ _2 \end{bmatrix}$$

Following Phillips (1998), the system of equations admits the following alternate companion form such that $\quad = \quad {}_{-1} + \quad$ with $\quad = (\ {}_{1} \quad {}_{2} \quad {}_{1} \quad {}_{2})'$:

$$\begin{bmatrix} {}_{1} \\ {}_{2} \\ {}_{1} \\ {}_{2} \end{bmatrix} = \begin{bmatrix} 1 & & & {}_{11} & {}_{12} \\ 0 & {}_{22} & & {}_{21} & 0 \\ 0 & & & {}_{11} & {}_{12} \\ 0 & {}_{22} & 1 & {}_{21} & 0 \end{bmatrix} \begin{bmatrix} {}_{1\ -1} \\ {}_{2\ -1} \\ {}_{1\ -1} \\ {}_{2\ -1} \end{bmatrix} + \begin{bmatrix} {}_{1} \\ {}_{2} \\ {}_{1} \\ {}_{2} \end{bmatrix}$$

where $\quad = \quad '$ with $\quad = [\ {}_{2} \quad {}_{2}]$.

The (modified) companion matrix can be partitioned as follows:

$$\begin{bmatrix} \exp(\ {}^{-1}\ ) & {}_{12} \\ \begin{bmatrix} 0 \ {}_{\times} \\ \exp(\ {}^{-1}\ ) \\ 0_{(\ -1)\times} \end{bmatrix} & {}_{22} \end{bmatrix} \tag{B.4}$$

where is the number of unit root or near unit root variables, the number of stationary variable and the number of lags in the level-based specification. Note that the DGP imposes that the matrix can be either a scalar or a 2 2 matrix depending on the number of unit roots or near-unit roots. In particular, when is a matrix, the exponential function $\exp(\ )$ is understood as the matrix exponential.

As shown in Phillips (Phillips (1998), p.28), the impulse response matrices can be rewritten in terms of this companion form as follows

$$\begin{aligned} &= \quad ' \\ &= \begin{bmatrix} \exp(\ {}^{-1}\ ) & \exp(\ {}^{-1}\ )\ {}_{12}(\ + \quad + \ {}_{22}^{-1}) \\ (\ {}^{-1}) & {}_{22} + \ (\ {}^{-1}) \end{bmatrix}, \end{aligned}$$

and $= [\ _2\ 0_{2\times 2}]$ and the moving average (MA) representation of is

$$= \sum_{=0}^{-1} \quad {}' \ _{-} = \sum_{=0}^{-1} \quad _{-}$$

For $=$ for a fixed fraction 0, then where

$$= \begin{bmatrix} \exp(\quad) & \exp(\quad)\ _{12}(\qquad _{22})^{-1} \\ 0 & 0 \end{bmatrix} \quad ,$$

as because $_{22}$ has stable roots. Using an OLS-based estimation of the unrestricted VAR in levels, the ith impulse response matrix estimate is given by:

$$\widehat{\ } = \widehat{\ }\ '$$

where

$$\widehat{\ } = \begin{bmatrix} \widehat{\ } & \widehat{\ }_{12} \\ \widehat{\ }\ _2 & \widehat{\ }_{22} \end{bmatrix} \tag{B.5}$$

with

$$= \begin{bmatrix} 1 & \\ 0 & _{22} \end{bmatrix} \quad \text{and} \quad _{12} = \ _{22} = \begin{bmatrix} _{11} & _{12} \\ _{12} & 0 \end{bmatrix}$$

Let $_1$ denote the submatrix containing the first columns of (i.e., the nonstationary components of), the limit distribution is given by:

$$(\widehat{\ }_1 \qquad _1) \quad \left(\int_0^1 \qquad {}'_{\Gamma}\right)(\ \Gamma\ {}'_{\Gamma})^{-1} = \ \Gamma$$

where $\Gamma(\ ) = \int_0 \exp\ (\qquad)$ $_1$ is a vector diffusion process and $_1$ is vector of

Brownian motion (see Phillips, 1988). In particular, when the diagonal elements of are equal to zero, then $_{\Gamma}(\ )$ reduces to $_{1}(\ )$.

It follows that the expression of $\widehat{\ }$ is:

$$\widehat{\ } = \begin{bmatrix} \widehat{\ }_1 + \quad (\quad^{-1}) \quad \sum_{=0} \widehat{\ }_1^{-} \quad \widehat{\ }_{12}\widehat{\ }_{22} + \quad (\quad^{-1}) \\ (\quad^{-1}) \quad \widehat{\ }_{22} + \quad (\quad^{-1}) \end{bmatrix} \tag{B.6}$$

and, as shown by Phillips (1998),

$$\widehat{\ }_1 = [\quad + (\widehat{\ }_1 \quad)] = [\quad + \quad (\widehat{\ }_1 \quad) \quad] \quad \exp(\quad \Gamma)$$

as and $=$. Finally,

$$\widehat{\ } \quad \begin{bmatrix} \exp(\quad \Gamma) & \exp(\quad \Gamma) \ _{12}(\quad _{22})^{-1} \\ 0 & 0 \end{bmatrix}$$

and

$$\widehat{\ } \quad \begin{bmatrix} \exp(\quad \Gamma) & \exp(\quad \Gamma) \ _{12}(\quad _{22})^{-1} \\ 0 & 0 \end{bmatrix},$$

.

We now provide the complete derivations of different configurations.

- **$_1$ is (1) and $_2$ is (0) with possibly $= 0$**

  In this case $= 1$, $= 0$ and the matrix is given by (assuming that $_{11} = 0$ as in Section 5):

$$= \begin{bmatrix} 1 & {}_{12} \\ 0_{3\times 1} & {}_{22} \end{bmatrix} = \left[\begin{array}{c|cccc} 1 & & 0 & {}_{12} & \\ \hline 0 & {}_{22} & {}_{21} & 0 & \\ 0 & & 0 & {}_{12} & \\ 0 & {}_{22} & 1 & {}_{21} & 0 \end{array}\right]$$

where ${}_{12} = [\quad 0 \quad {}_{12}]$ and

$${}_{22} = \begin{bmatrix} {}_{22} & {}_{21} & 0 \\ & 0 & {}_{12} \\ {}_{22} \quad 1 & {}_{21} & 0 \end{bmatrix}$$

To determine the (random) limit, we need to compute ${}_{12}(\ {}_{3} \qquad {}_{22})^{-1}$. Using

$$(\ {}_{3} \qquad {}_{22})^{-1} = \begin{bmatrix} 1 & {}_{22} & {}_{21} & 0 \\ & & 1 & {}_{12} \\ 1 & {}_{22} & {}_{21} & 1 \end{bmatrix}^{-1}$$

$$= \frac{1}{{}_{22}} \begin{bmatrix} 1 \quad {}_{12}\ {}_{21} & {}_{21} & {}_{12}\ {}_{21} \\ {}_{12}(1 \qquad {}_{22}) & (1 \qquad {}_{22}) & {}_{12}(1 \qquad {}_{22}) \\ {}_{21} \quad (1 \qquad {}_{22}) & 0 & (1 \qquad {}_{22}) \quad {}_{21} \end{bmatrix}$$

we have

$${}_{12}(\ {}_{3} \qquad {}_{22})^{-1} = \frac{1}{{}_{22}} \begin{bmatrix} (\ (1 \qquad {}_{21}\ {}_{21}) \qquad {}_{12}((1 \qquad {}_{22}) \qquad {}_{21}\ )) \\ {}_{21} \\ (\quad {}_{12}\ {}_{21} + \ {}_{12}((1 \qquad {}_{22}) \qquad {}_{21}\ )) \end{bmatrix}'$$

$$= \frac{1}{{}_{22}} \begin{bmatrix} \quad {}_{12}(1 \qquad {}_{22}) \quad {}_{21} \qquad {}_{12}(1 \qquad {}_{22}) \end{bmatrix}$$

where $_{22} = (1 \quad _{22} \quad _{21})$. Therefore,

$$\lim_{\to\infty} \quad = \quad = \begin{bmatrix} 1 & _{12}(\ _3 \quad _{22})^{-1} \\ 0_{3\times1} & 0_{3\times3} \end{bmatrix}$$

As the impulse response horizon , the impulse response matrix of the unrestricted (reduced-form) VAR lin levels converge to :

$$\lim_{\to\infty} \quad = \quad = \quad ' = \begin{bmatrix} 1 + \frac{_{21}}{_{22}} & \frac{}{_{22}} \\ 0 & 0 \end{bmatrix}$$

It means that the only permanent impact is from both shocks on the first variable. Turning to the limiting distribution of the Max Share matrix, we first define $_\perp$, and . Taking that $'_\perp = [1\ 0]$, $' = [0\ 1]$ and $= [\ _\perp\ ]$, the permanent effect of the reduced-form innovations on the first variable is given by:

$$\begin{aligned} ' &= \ '_\perp + \ _{12}(\ _3 \quad _{22})^{-1} \begin{bmatrix} ' \\ ' \end{bmatrix} \\ &= [1\ 0] + \begin{bmatrix} \frac{_{12}(1 \quad _{22})}{_{22}} & \frac{_{21}}{_{22}} & \frac{_{12}(1 \quad _{22})}{_{22}} \end{bmatrix} \begin{bmatrix} 0 & 1 \\ 1 & 0 \\ 0 & 1 \end{bmatrix} \\ &= \begin{bmatrix} 1 + \frac{_{21}}{_{22}} & \frac{}{_{22}} \end{bmatrix} \end{aligned}$$

Finally, it involves the expression of the matrix , which is a scalar. In so doing, we derive the expression of $_1$ from the specification of $_1$, namely

$$\begin{aligned} _1 &= \quad _{2\ -1} + \ _{12} \quad _{2\ -1} + \ _1 = \ _1 \\ &= \sum_{=0}^{\infty} \quad _{-} \end{aligned}$$

where the last expression results from the moving average representation of the innovations $= (\; _1 \quad _2)'$.Then,

$$= \int_0^1 \quad (\;) \; _1(\;) \left(\int_0^1 \; _1(\;) \; _1(\;)' \quad \right)^{-1} = \frac{\int_0^1 \; _1(\;) \quad (\;)}{\int_0^1 \; _1(\;)^2}$$

where $_1$ is a scalar Brownian motion with a variance given by the long-run variance of $\sum_{=0}^{\infty} \quad _-$ and is a scalar Brownian motion with variance given by $(\; _1)$. The asymptotic distribution of $^{-1} \quad (\;)$ as with $=$ for $]0 \; 1]$ is therefore:

$$h^{-1}S_{k,T}(h) \qquad \frac{1}{f}\int_0^f \Sigma_{\text{tr}}'\beta_E \exp\left(sU'\right)\beta_\perp' e_k e_k' \beta_\perp \exp\left(sU\right)\beta_E' \Sigma_{\text{tr}} ds$$

$$\frac{1}{f}\int_0^f \Sigma_{\text{tr}}' \begin{bmatrix} 1+\frac{a_{21}\delta}{d_{22}} \\ \frac{\delta}{d_{22}} \end{bmatrix} \exp\left(sU\right) \begin{bmatrix} 1 & 0 \end{bmatrix} e_k e_k' \begin{bmatrix} 1 \\ 0 \end{bmatrix} \exp\left(sU\right) \begin{bmatrix} 1+\frac{a_{21}\delta}{d_{22}} & \frac{\delta}{d_{22}} \end{bmatrix} \Sigma_{\text{tr}} ds$$

where $_{\text{tr}}$ is the lower triangular Cholesky decomposition of $\;,\quad = \; '_{\text{tr}} \; _{\text{tr}}$, and is the first ($= 1$) or second ($= 2$) base vector of $\mathbb{R}^2$. When $= 1$, one has:

$$h^{-1}S_{1,T}(h) \qquad \frac{1}{f}\int_0^f \exp\left(2sU\right)\Sigma_{\text{tr}}' \begin{bmatrix} 1+\frac{a_{21}\delta}{d_{22}} \\ \frac{\delta}{d_{22}} \end{bmatrix} \begin{bmatrix} 1+\frac{a_{21}\delta}{d_{22}} & \frac{\delta}{d_{22}} \end{bmatrix} \Sigma_{\text{tr}} ds$$

$$\frac{1}{f}\int_0^f \exp\left(2sU\right) \begin{bmatrix} \tilde{\sigma}_{11} & \tilde{\sigma}_{21} \\ 0 & \tilde{\sigma}_{22} \end{bmatrix} \begin{bmatrix} 1+\frac{a_{21}\delta}{d_{22}} \\ \frac{\delta}{d_{22}} \end{bmatrix} \begin{bmatrix} 1+\frac{a_{21}\delta}{d_{22}} & \frac{\delta}{d_{22}} \end{bmatrix} \begin{bmatrix} \tilde{\sigma}_{11} & 0 \\ \tilde{\sigma}_{21} & \tilde{\sigma}_{22} \end{bmatrix} ds$$

$$\frac{1}{f}\int_0^f \exp\left(2sU\right) \begin{bmatrix} \tilde{\sigma}_{11}\left(1+\frac{a_{21}\delta}{d_{22}}\right)+\tilde{\sigma}_{21}\frac{\delta}{d_{22}} \\ \tilde{\sigma}_{22}\frac{\delta}{d_{22}} \end{bmatrix} \begin{bmatrix} \tilde{\sigma}_{11}\left(1+\frac{a_{21}\delta}{d_{22}}\right)+\tilde{\sigma}_{21}\frac{\delta}{d_{22}} & \tilde{\sigma}_{22}\frac{\delta}{d_{22}} \end{bmatrix} ds$$

$$\frac{1}{f}\left(2U\right)^{-1} \begin{bmatrix} \left(\tilde{\sigma}_{11}\left(1+\frac{a_{21}\delta}{d_{22}}\right)+\tilde{\sigma}_{21}\frac{\delta}{d_{22}}\right)^2 & \left(\tilde{\sigma}_{11}\left(1+\frac{a_{21}\delta}{d_{22}}\right)+\tilde{\sigma}_{21}\frac{\delta}{d_{22}}\right)\tilde{\sigma}_{22}\frac{\delta}{d_{22}} \\ \left(\tilde{\sigma}_{11}\left(1+\frac{a_{21}\delta}{d_{22}}\right)+\tilde{\sigma}_{21}\frac{\delta}{d_{22}}\right)\tilde{\sigma}_{22}\frac{\delta}{d_{22}} & \left(\tilde{\sigma}_{22}\frac{\delta}{d_{22}}\right)^2 \end{bmatrix}$$

$$\left(\exp\left(f\right) \quad 1\right).$$

where are the elements of lower triangular Cholesky decomposition of .

Accordingly, $\widehat{\;}_1 \; (\;)$ is of rank one, the second eigenvalue converges to zero and the resulting eigenvector converges to $[1 \;\; 0]'$. When $\;\; = 0$,

$$ ^{-1}\widehat{\;}_{1} \;(\;)\qquad \frac{1}{\;}(2\;\;)^{-1}\begin{bmatrix} {}^{2}_{11} & 0 \\ 0 & 0 \end{bmatrix}(\exp(\;)\quad 1) $$

- $_1$ **is** (1) **and** $_2$ **is** (1)

In this case, $\;= 2$, is a 2 2 null matrix and is given by:

$$ = \begin{bmatrix} {}_{2\times 2} & {}_{12} \\ 0_{2\times 2} & {}_{22} \end{bmatrix} = \left[\begin{array}{cc|cc} 1 & 0 & 0 & {}_{12} \\ 0 & 1 & {}_{21} & 0 \\ \hline 0 & 0 & 0 & {}_{12} \\ 0 & 0 & {}_{21} & 0 \end{array}\right] $$

Since assumption **(c)** is satisfied here, we first need to compute the expression of $_{12}(\;_2\qquad _{22})^{-1}$:

$$ (\;_2\qquad _{22})^{-1} = \begin{bmatrix} 1 & {}_{12} \\ {}_{21} & 1 \end{bmatrix}^{-1} = \frac{1}{1\qquad _{12}\;_{21}}\begin{bmatrix} 1 & {}_{12} \\ {}_{21} & 1 \end{bmatrix} $$

It implies that:

$$ _{12}(\;_2\qquad _{22})^{-1} = \frac{1}{1-\;_{12}\;_{21}}\begin{bmatrix} {}_{12}\;_{21} & {}_{12} \\ {}_{21} & {}_{12}\;_{21} \end{bmatrix} $$

and thus

$$ \lim_{\to\infty} \quad = \begin{bmatrix} {}_{2\times 2} & {}_{12}(\;_2\qquad _{22})^{-1} \\ 0_{2\times 2} & 0_{2\times 2} \end{bmatrix} $$

Capitalizing on Lemma 2.2. of Phillips (1998), one gets:

$$\lim_{\to\infty} \quad = \quad = \left[\ _2 \quad _{12} (\ _2 \quad _{22})^{-1} \ \right]$$

meaning that the only permanent impact is from both shocks on the first variable. Regarding the limiting distribution of $\ (\ )$, since is the empty matrix,

$$'_{\perp} = \begin{bmatrix} 1 & 0 \\ 0 & 1 \end{bmatrix} =$$

and the permanent effect of the reduced-form innovations on the two variables is then given by:

$$' \quad = \ '_{\perp} + \ _{12} (\ _2 \quad _{22})^{-1} \ ' = \begin{bmatrix} \frac{1}{1- \ _{12} \ _{21}} & _{12} \\ _{21} & \frac{1}{1- \ _{12} \ _{21}} \end{bmatrix}$$

Finally, starting from the (infinite) moving average representation of $_1$

$$\begin{aligned} _1 \quad &= \begin{bmatrix} _1 \\ _2 \end{bmatrix} = \begin{bmatrix} 0 & _{12} \\ _{21} & 0 \end{bmatrix} \begin{bmatrix} _{1 \ -1} \\ _{2 \ -1} \end{bmatrix} + \begin{bmatrix} _1 \\ _2 \end{bmatrix} \\ &= \sum_{=0}^{\infty} \ _1 \ _- \end{aligned}$$

where $_1 = \ _{12}$, one can define the matrix unit root distribution

$$:= \int_0^1 \ (\ ) \ '(\ ) \left(\int_0^1 \ (\ ) \ (\ )' \right)$$

where $(\ )$ is a two dimensional Brownian motion vector with covariance matrix $(1) \quad (1)'$. Using Theorem , the asymptotic distribution of $^{-1}\widehat{\ } \quad (\ )$ as with $=$ for $]0\ 1]$ is therefore

$$^{-1}\widehat{\ }\ (\ )\quad \frac{1}{}\int_0 \ {}'_{\mathrm{tr}}\ \exp(\ \ ')\ {}'_{\perp}\ \ {}'\ {}_{\perp}\exp(\ \ )\ {}'\ \ {}_{\mathrm{tr}}$$
$$\frac{1}{}\int_0 \ {}'_{\mathrm{tr}}\ \exp(\ \ ')\ \ {}'\exp(\ \ )\ {}'\ \ {}_{\mathrm{tr}}$$

- **$_1$ is (1) and $_2$ is a nearly unit-root process with possibly $=0$**

  The derivation is the same, with the exception that:

$$\Gamma := \int_0^1 \ (\ )\ \Gamma(\ )'\left(\int_0^1 \Gamma(\ )\ \Gamma(\ )'\ \right)^{-1}$$

where

$$= \begin{bmatrix} 0 & \\ 0 & \end{bmatrix}$$

This is a mixture of correlated unit root distribution and a local-to-unit root distribution.

B.3 Additional Results

We discuss the asymptotic results in the case of weakly stationary processes for the accumulated and frequency Max Share approaches mentioned in Remark 1 of the main text.

B.3.1 Asymptotic results with weakly stationary processes

Theorem B.3.1 *Let Assumption (2.3.1) hold and let* $=$ *vec* $([\ _1\ \ ])$, $=$ *vech* $(\ )$, $= (\ _{+1}\ \ )\ \ \mathbb{R}^{\ \times(\ -\ )}$, *and* $(0) := [(\ \ (\ ))(\ \ (\ ))']$. *Then, as* ,

(a) *The estimator of the accumulated Max Share weighting matrix of* $(\_\ \bar{})$*, denoted by* $\widehat{}\ (\_\ \bar{})$*, at a fixed horizon band* $[\_;\bar{}]$ *satisfies*

$$\bar{}\,vec\left(\widehat{}\ (\_\ \bar{})\quad (\_\ \bar{})\right)$$

$$\mathcal{N}\left(0\ \left[\ \tilde{}\qquad\right]\left[\begin{array}{cc}(0)^{-1} & 0\\ 0 & 2\ ^{+}(\qquad)\ ^{+\prime}\end{array}\right]\left[\begin{array}{c}\tilde{}'\\ '\end{array}\right]\right)$$

(b) *The estimator of the non-accumulated Max Share weighting matrix of* $(\_\ \bar{})$*, denoted by* $\widehat{}\ (\_\ \bar{})$*, at a given frequency band* $[\_;\bar{}]$ *satisfies*

$$\bar{}\,vec\left(\widehat{}\ (\_\ \bar{})\quad (\_\ \bar{})\right)$$

$$\mathcal{N}\left(0\ \left[\ \tilde{}\qquad\right]\left[\begin{array}{cc}(0)^{-1} & 0\\ 0 & 2\ ^{+}(\qquad)\ ^{+\prime}\end{array}\right]\left[\begin{array}{c}\tilde{}'\\ '\end{array}\right]\right)$$

where $^{+} := (\ '\quad)^{-1}\ '$ *is the Moore-Penrose generalized inverse of an appropriate* $^{2}\quad (\ +1)\ 2$ *duplication matrix, and the gradients* $\tilde{}$*,* $\ $*,* $\tilde{}$*, and are defined in the proof.*

Proof: Following Lütkepohl (2005), these results make use of the Delta method.

Proof of Theorem (B.3.1), part (a) Starting from

$$(\_\ \bar{}) = \sum_{=\_}^{\bar{}} \frac{(\ )}{'\,\texttt{MSE}(\ )}$$

one has

$$\begin{aligned}\tilde{D}_{\tilde{\alpha}} := \frac{\partial \text{vec}\left(S_k(\underline{h},\bar{h})\right)}{\partial \tilde{\alpha}} &= \sum_{h=\underline{h}}^{\bar{h}} \frac{\partial}{\partial \tilde{\alpha}}\left(\frac{1}{e_k'\texttt{MSE}(h)e_k} S_k(h)\right)\\ &= \sum_{h=\underline{h}}^{\bar{h}}\left\{\frac{1}{e_k'\texttt{MSE}(h)e_k}\frac{\partial \text{vec}\left(S_k(h)\right)}{\partial \tilde{\alpha}} + \frac{\partial \frac{1}{e_k'\texttt{MSE}(h)e_k}}{\partial \tilde{\alpha}}\quad \text{vec}\left(S_k(h)\right)\right\}\end{aligned}$$

where

$$\frac{\partial \text{vec}\left(S_k(h)\right)}{\partial \tilde{\alpha}} = \sum_{\ell=0}^{h-1} \left(I_{N^2} + K_{NN}\right)\left(\Sigma_{\text{tr}}' \quad \Sigma_{\text{tr}}' \Phi_\ell' e_k e_k'\right) \frac{\partial \Phi_\ell}{\partial \tilde{\alpha}'}.$$

$$\begin{aligned} \frac{\partial \frac{1}{e_k' \texttt{MSE}(h) e_k}}{\partial \tilde{\alpha}} &= \quad \frac{1}{\left(e_k' \texttt{MSE}(h) e_k\right)^2} \frac{\partial e_k' \texttt{MSE}(h) e_k}{\partial \tilde{\alpha}} \\ &= \sum_{\ell=0}^{h-1} e_k' \Phi_\ell \Sigma_{\text{tr}} \Sigma_{\text{tr}}' \left(K_{1N} + I_N\right)\left(I_N \quad e_k'\right) \frac{\partial \text{vec}(\Phi_\ell)}{\partial \tilde{\alpha}'}. \end{aligned}$$

On the other hand,

$$\begin{aligned} \tilde{D}_\sigma := \frac{\partial \text{vec}\left(S_k(\underline{h}, \overline{h})\right)}{\partial \sigma} &= \sum_{h=\underline{h}}^{\overline{h}} \frac{\partial}{\partial \sigma} \left(\frac{1}{e_k' \texttt{MSE}(h) e_k} S_k(h) \right) \\ &= \sum_{h=\underline{h}}^{\overline{h}} \left\{ \frac{1}{e_k' \texttt{MSE}(h) e_k} \frac{\partial \text{vec}\left(S_k(h)\right)}{\partial \sigma} + \frac{\partial \frac{1}{e_k' \texttt{MSE}(h) e_k}}{\partial \sigma} \quad \text{vec}\left(S_k(h)\right) \right\} \end{aligned}$$

where

$$\begin{aligned} \frac{\partial \text{vec}\left(S_k(h)\right)}{\partial \sigma} &= \sum_{\ell=0}^{h-1} \sum_{\ell=0}^{h-1} \left(I_{N^2} + K_{NN}\right)\left(I_N \quad \Sigma_{\text{tr}}' \Phi_\ell' e_k e_k' \Phi_\ell\right) \frac{\partial \text{vec}(\Sigma_{\text{tr}})}{\partial \sigma'} \\ \frac{\partial \frac{1}{e_k' \texttt{MSE}(h) e_k}}{\partial \sigma} &= \quad \frac{1}{\left(e_k' \texttt{MSE}(h) e_k\right)^2} \frac{\partial e_k' \texttt{MSE}(h) e_k}{\partial \sigma} \\ &= \sum_{\ell=0}^{h-1} \left(I_{N^2} + K_{NN}\right)\left(e_k' \Phi_\ell \quad e_k' \Phi_\ell \Sigma_{\text{tr}}\right) \frac{\partial \text{vec}(\Sigma_{\text{tr}})}{\partial \sigma'}. \end{aligned}$$

Using the Delta method,

$$\overline{}\ \text{vec}\left(\widehat{} \quad (\_\ \overline{}) \qquad (\_\ \overline{})\right)$$

$$\mathcal{N}\left(0 \left[\quad \tilde{} \qquad \right] \begin{bmatrix} (0)^{-1} & & 0 \\ 0 & 2 & +\left(\qquad\right) \quad +' \end{bmatrix} \begin{bmatrix} '_{\tilde{}} \\ ' \end{bmatrix}\right)$$

Remark: In the case of the estimator of $(\_\ \overline{}) = \sum_{=\_}^{-} (\ )$, denoted $\widehat{} \ (\_\ \overline{})$, one has:

$$\widehat{\tilde{S}}_{k,T}(\underline{h},\overline{h}) = \sum_{\ell=0}^{\overline{h}-1} \left(\overline{h} \quad max(\underline{h} \quad 1,\ell)\right) \Sigma_{\text{tr}}'\Phi_\ell' e_k e_k' \Phi_\ell \Sigma_{\text{tr}}$$

Suppose that $\overline{} \quad \underline{} \quad 1$ are fixed horizons. Similar algebra derivation yields

$$\tilde{D}_{\tilde{\alpha}} := \frac{\partial \text{vec}\left(\tilde{S}_k(\underline{h},\overline{h})\right)}{\partial \tilde{\alpha}} = \sum_{\ell=0}^{\overline{h}-1} \left(\overline{h} \quad max(\underline{h} \quad 1,l)\right) \left(I_{N^2} + K_{NN}\right) \left(\Sigma_{\text{tr}}' \quad \Sigma_{\text{tr}}'\Phi_\ell' e_k e_k'\right) \frac{\partial \Phi_\ell}{\partial \tilde{\alpha}'}$$

and

$$\tilde{D}_{\sigma} := \frac{\partial \text{vec}\left(\tilde{S}_k(\underline{h},\overline{h})\right)}{\partial \sigma'} = \sum_{\ell=0}^{\overline{h}-1} \left(\overline{h} \quad max(\underline{h} \quad 1,l)\right) \left(I_{N^2} + K_{NN}\right) \left(I_N \quad \Sigma_{\text{tr}}'\Phi_\ell' e_k e_k' \Phi_\ell\right) \frac{\partial \text{vec}(\Sigma_{\text{tr}})}{\partial \sigma'}.$$

Using the Delta method,

$$\overline{}\ \text{vec}\left(\widehat{} \quad (\underline{}\ \overline{}) \qquad (\underline{}\ \overline{})\right)$$
$$\mathcal{N}\left(0 \left[\quad \tilde{} \quad \right] \begin{bmatrix} (0)^{-1} & & 0 & \\ 0 & 2 & {}^{+}(\qquad) & {}^{+\prime} \end{bmatrix} \begin{bmatrix} \tilde{}' \\ ' \end{bmatrix}\right)$$

Proof of Theorem (B.3.1), part (b) In the case of the frequency Max Share approach, one has

$$(\underline{}\ \overline{}) := \int_{\in[\underline{}\ \overline{}]} {}' \ \overline{(\ {}^{-}\ )}\ {}' \quad (\ {}^{-}\ )$$
$$= \int_{\in[\underline{}\ \overline{}]} \left(\sum_{=0}^{\infty} \ {}'_{\text{tr}}\ {}' \right) {}' \left(\sum_{=0}^{\infty} \quad {}_{\text{tr}} \ {}^{-} \right)$$

We first consider the partial derivative with respect to $\ '$. To simplify notation, let $:= \quad {}_{\text{tr}}\ {}^{-}$ and $\overline{}$ its conjugate transpose. Then, taking the interchangeability of the differential operator and the integral operator,

$$\frac{\partial \text{vec}\left(S_k(\underline{\omega},\overline{\omega})\right)}{\partial \tilde{\alpha}'} = \frac{\partial}{\partial \tilde{\alpha}'} \text{vec} \int_{\omega \in [\underline{\omega},\overline{\omega}]} \left(\sum_{\ell=0}^{\infty} \overline{\delta}_\ell\right) e_k e_k' \left(\sum_{\ell=0}^{\infty} \delta_\ell\right) d\omega$$

$$= \int_{\omega \in [\underline{\omega}, \overline{\omega}]} \frac{\partial}{\partial \tilde{\alpha}'} \text{vec} \left[\left(\sum_{\ell=0}^{\infty} \overline{\delta}_\ell \right) e_k e_k' \left(\sum_{\ell=0}^{\infty} \delta_\ell \right) \right] d\omega$$

where

$$\frac{\partial}{\partial \tilde{\alpha}'} \text{vec} \left[\left(\sum_{\ell=0}^{\infty} \overline{\delta}_\ell \right) e_k e_k' \left(\sum_{\ell=0}^{\infty} \delta_\ell \right) \right] = \left(I_N \quad \sum_{\ell=0}^{\infty} \overline{\delta}_\ell e_k e_k' \right) \frac{\partial \text{vec} \left(\sum_{\ell=0}^{\infty} \delta_\ell \right)}{\partial \tilde{\alpha}'} + \left(\sum_{\ell=0}^{\infty} \delta_\ell' e_k e_k' \quad I_N \right) \frac{\partial \text{vec} \left(\sum_{\ell=0}^{\infty} \overline{\delta}_\ell e_k \right)}{\partial \tilde{\alpha}'}$$

with

$$\frac{\partial \text{vec} \left(\sum_{\ell=0}^{\infty} \delta_\ell \right)}{\partial \tilde{\alpha}'} = \sum_{\ell=0}^{\infty} \frac{\partial \text{vec} \left(\delta_\ell \right)}{\partial \tilde{\alpha}'} = \sum_{\ell=0}^{\infty} \frac{\partial \text{vec} \left(\Phi_\ell \Sigma_{\text{tr}} \right)}{\partial \tilde{\alpha}'} e^{-i\omega\ell} = \sum_{\ell=0}^{\infty} \left(\Sigma_{\text{tr}}' \quad I_N \right) \frac{\partial \text{vec} \left(\Phi_\ell \right)}{\partial \tilde{\alpha}'} e^{-i\omega\ell}$$

$$\frac{\partial \text{vec} \left(\sum_{\ell=0}^{\infty} \overline{\delta}_\ell \right)}{\partial \tilde{\alpha}'} = \sum_{\ell=0}^{\infty} \left(I_N \quad \Sigma_{\text{tr}}' \right) \frac{\partial \text{vec} \left(\Phi_\ell' \right)}{\partial \tilde{\alpha}'} e^{i\omega l} = \sum_{l=0}^{\infty} \left(I_N \quad \Sigma_{\text{tr}}' \right) K_{NN} \frac{\partial \text{vec} \left(\Phi_\ell \right)}{\partial \tilde{\alpha}'} e^{i\omega\ell}$$

Therefore

$$\frac{\partial}{\partial \tilde{\alpha}'} \text{vec} \left[\left(\sum_{\ell=0}^{\infty} \overline{\delta}_\ell \right) e_k e_k' \left(\sum_{\ell=0}^{\infty} \delta_\ell \right) \right] = \left[\left(\Sigma_{\text{tr}}' \quad \sum_{\ell=0}^{\infty} \overline{\delta}_\ell e_k e_k' \right) e^{-i\omega\ell} + \left(\sum_{\ell=0}^{\infty} \delta_\ell' e_k e_k' \quad \Sigma_{\text{tr}}' \right) K_{NN} e^{i\omega l} \right] \sum_{\ell=0}^{\infty} \frac{\partial \text{vec} \left(\Phi_\ell \right)}{\partial \tilde{\alpha}'}$$

and

$$\bar{D}_{\tilde{\alpha}} := \frac{\partial \text{vec} \left(S_k(\underline{\omega}, \overline{\omega}) \right)}{\partial \tilde{\alpha}'} = \int_{\omega \in [\underline{\omega}, \overline{\omega}]} \left(\sum_{\ell=0}^{\infty} \left[\left(\Sigma_{\text{tr}}' \quad \sum_{\tau=0}^{\infty} \overline{\delta}_\tau e_k e_k' \right) e^{-i\omega\ell} + \left(\sum_{\tau=0}^{\infty} \delta_\tau' e_k e_k' \quad \Sigma_{\text{tr}}' \right) K_{NN} e^{i\omega\ell} \right] \frac{\partial \text{vec} \left(\Phi_\ell \right)}{\partial \tilde{\alpha}'} \right) d\omega.$$

In the case of the partial derivative with respect to $'$, using Lütkepohl (2005) (p.668, rule 6), starting from

$$\frac{\partial \text{vec} \left(\Phi_l \Sigma_{\text{tr}} \right)}{\partial \sigma'} = \left(\Phi_l \quad I_K \right) \frac{\partial \text{vec} \left(\Sigma_{\text{tr}} \right)}{\partial \sigma'}$$

$$\frac{\partial \text{vec} \left(\Sigma_{\text{tr}}' \Phi_l' \right)}{\partial \sigma'} = \left(I_K \quad \Phi_l \right) \frac{\partial \text{vec} \left(\Sigma_{\text{tr}}' \right)}{\partial \sigma'} = \left(I_K \quad \Phi_l \right) K_{KK} \frac{\partial \text{vec} \left(\Sigma_{\text{tr}} \right)}{\partial \sigma'}$$

one has

$$\begin{aligned}
\frac{\partial e_k' \sum_{l=0}^{\infty} \delta_l}{\partial \sigma'} &= (I_K \quad e_k') \sum_{l=0}^{\infty} \frac{\partial \text{vec}\,(\Phi_l \Sigma_{\text{tr}})}{\partial \sigma'} e^{-i\omega l} \\
&= (I_K \quad e_k') \sum_{l=0}^{\infty} (\Phi_l \quad I_K) \frac{\partial \text{vec}\,(\Sigma_{\text{tr}})}{\partial \sigma'} e^{-i\omega l} \\
&= \sum_{l=0}^{\infty} \left(\Phi_l \quad e^{(k')}\right) \frac{\partial \text{vec}\,(\Sigma_{\text{tr}})}{\partial \sigma'} e^{-i\omega l} \\
\frac{\partial \sum_{l=0}^{\infty} \overline{\delta}_l e_k}{\partial \sigma'} &= (e_k' \quad I_K) \sum_{l=0}^{\infty} \frac{\partial \text{vec}\,(\Sigma_{\text{tr}}' \Phi_l')}{\partial \sigma'} e^{i\omega l} \\
&= (e_k' \quad I_K) \sum_{l=0}^{\infty} (I_K \quad \Phi_l)\, K_{KK} \frac{\partial \text{vec}\,(\Sigma_{\text{tr}})}{\partial \sigma'} e^{i\omega l} \\
&= \sum_{l=0}^{\infty} (e_k' \quad \Phi_l)\, K_{KK} \frac{\partial \text{vec}\,(\Sigma_{\text{tr}})}{\partial \sigma'} e^{i\omega l}
\end{aligned}$$

and thus

$$\begin{aligned}
\frac{\partial}{\partial \sigma'} \text{vec} \left[\left(\sum_{l=0}^{\infty} \overline{\delta}_l \right) e_k e_k' \left(\sum_{l=0}^{\infty} \delta_l \right) \right] &= \left(I_K \quad \sum_{\tau=0}^{\infty} \overline{\delta}_\tau e_k \right) \sum_{l=0}^{\infty} \left(\Phi_l \quad e^{(k')}\right) \frac{\partial \text{vec}\,(\Sigma_{\text{tr}})}{\partial \sigma'} e^{-i\omega l} \\
&\quad + \left(\sum_{\tau=0}^{\infty} \delta_\tau' e_k \quad I_K \right) \sum_{l=0}^{\infty} (e_k' \quad \Phi_l)\, K_{KK} \frac{\partial \text{vec}\,(\Sigma_{\text{tr}})}{\partial \sigma'} e^{i\omega l} \\
&= \sum_{l=0}^{\infty} \left[\left(\Phi_l \quad \sum_{\tau=0}^{\infty} \overline{\delta}_\tau e_k e_k' \right) e^{-i\omega l} \right. \\
&\quad \left. + \left(\sum_{\tau=0}^{\infty} \delta_\tau' e_k e_k' \quad \Phi_l \right) K_{KK} e^{i\omega l} \right] \frac{\partial \text{vec}\,(\Sigma_{\text{tr}})}{\partial \sigma'}.
\end{aligned}$$

Finally,

$$\begin{aligned}
\bar{D}_\sigma := \frac{\partial \text{vec}\,(S_k(\underline{\omega}, \overline{\omega}))}{\partial \sigma'} = \int_{\omega \in [\underline{\omega}, \overline{\omega}]} & \left(\sum_{l=0}^{\infty} \left[\left(\Phi_l \quad \sum_{\tau=0}^{\infty} \overline{\delta}_\tau e_k e_k' \right) e^{-i\omega l} \right. \right. \\
& \left. \left. + \left(\sum_{\tau=0}^{\infty} \delta_\tau' e_k e_k' \quad \Phi_l \right) K_{KK} e^{i\omega l} \right] \frac{\partial \text{vec}\,(\Sigma_{\text{tr}})}{\partial \sigma'} \right) d\omega.
\end{aligned}$$

Then, under Assumption (2.3.1),

$$\overline{} \ \text{vec} \left(\widehat{} \quad (\underline{} \ \overline{}) \qquad (\underline{} \ \overline{}) \right)$$

$$\left(0 \left[\;\tilde{}\; \right] \begin{bmatrix} (0)^{-1} & 0 \\ 0 & 2 \;+ (\qquad) \;+' \end{bmatrix} \begin{bmatrix} '\tilde{} \\ ' \end{bmatrix} \right)$$

as stated.

B.3.2 Additional Monte Carlo Results

Table B.1: Correlations corr($_1$ $_1$) and corr($_1$ $_2$)

FEV Horizon	corr($\hat{w}_{1,t}, w_{1,t}$)				corr($\hat{w}_{1,t}, w_{2,t}$)			
	Diff	Level	Levelc	Levelcb	Diff	Level	Levelc	Levelcb
	Experiment 1							
0	0.9955	0.9863	0.9863	0.9863	0.0009	0.0020	0.0020	0.0020
40	0.9955	0.9590	0.9570	0.9551	0.0031	0.0167	-0.0101	0.014
80	0.9956	0.9474	0.9368	0.9330	-0.0003	0.0106	-0.0208	0.0117
	Experiment 2							
0	0.9956	0.9880	0.9880	0.9880	-0.0016	0.0029	0.0029	0.0029
40	0.9954	0.9213	0.9128	0.9105	0.0046	-0.2337	-0.2562	-0.2477
80	0.9955	0.8927	0.8604	0.8547	0.0073	-0.2823	-0.3315	-0.3205
	Experiment 3							
	$a_{22} = 0.9$							
0	0.9916	0.9871	0.9871	0.9871	0.4e-03	0.5e-03	0.5e-03	0.5e-03
40	0.9904	0.9640	0.9612	0.9614	0.0230	-0.0715	-0.0801	-0.0639
80	0.9909	0.9614	0.9570	0.9569	0.0255	-0.0588	-0.0628	-0.0442
	$a_{22} = 0.96$							
0	0.9914	0.9866	0.9866	0.9866	-0.0001	0.0013	0.0013	0.0013
40	0.9908	0.9517	0.9470	0.9477	0.0259	-0.0993	-0.1175	-0.0932
80	0.9906	0.9437	0.9313	0.9292	0.0225	-0.0790	-0.0895	-0.0550
	$a_{22} = 0.99$							
0	0.9907	0.9855	0.9855	0.9855	-0.0032	-0.0007	-0.0007	-0.0007
40	0.9903	0.9336	0.9306	0.9300	0.0241	-0.1606	-0.1761	-0.1599
80	0.9904	0.9105	0.8933	0.8867	0.0258	-0.1361	-0.1455	-0.1133

Table B.1: Correlations corr($_1$ $_1$) and corr($_1$ $_2$)

	Experiment 4							
	$a_{22} = 0.96$							
0	0.9915	0.9879	0.9879	0.9879	-0.0048	-0.0007	-0.0007	-0.0007
40	0.9902	0.8753	0.8664	0.8634	0.0322	-0.3670	-0.3817	-0.3746
80	0.9903	0.8420	0.8116	0.8053	0.0337	-0.4091	-0.4416	-0.4280
	$a_{22} = 0.99$							
0	0.9908	0.9898	0.9898	0.9898	-0.0048	-0.0036	-0.0036	-0.0036
40	0.9901	0.7380	0.7484	0.7345	0.0375	-0.5875	-0.5741	-0.5797
80	0.9902	0.6160	0.5922	0.5567	0.0370	-0.5883	-0.5830	-0.5288

Table B.2: Correlations corr($_2$ $_1$) and corr($_2$ $_2$)

FEV Horizon	$\texttt{corr}(\hat{w}_{2,t}, w_{1,t})$				$\texttt{corr}(\hat{w}_{2,t}, w_{2,t})$			
	Diff	Level	Levelc	Levelcb	Diff	Level	Levelc	Levelcb
	Experiment 1							
0	0.0000	0.0000	0.0030	-0.0013	0.9932	0.9879	0.9879	0.98
40	-0.0022	-0.0144	0.0149	-0.0152	0.9932	0.9596	0.9575	0.9537
80	-0.0023	-0.0118	0.0216	-0.0126	0.9932	0.9478	0.9370	0.9313
	Experiment 2							
0	-0.0000	-0.0000	0.0029	0.0018	0.9934	0.9863	0.9863	0.9843
40	-0.0073	0.2357	0.2596	0.2487	0.9930	0.9195	0.9108	0.9064
80	-0.0075	0.2865	0.3403	0.3264	0.9925	0.8903	0.8577	0.8503
	Experiment 3							
	$a_{22} = 0.9$							
0	-0.0000	0.0000	0.0027	0.0020	0.9894	0.9887	0.9888	0.9867
40	-0.0253	0.0693	0.0799	0.0606	0.9882	0.9659	0.9629	0.9611
80	-0.0248	0.0592	0.0652	0.0467	0.9886	0.9626	0.9580	0.9558
	$a_{22} = 0.96$							
0	0.0000	-0.0000	0.0030	0.0020	0.9885	0.9874	0.9874	0.9854
40	-0.0244	0.1008	0.1209	0.0965	0.9880	0.9523	0.9472	0.9463

Table B.2: Correlations corr(2 1) and corr(2 2)

80	-0.0237	0.0786	0.0930	0.0568	0.9884	0.9440	0.9308	0.9267
	$a_{22} = 0.99$							
0	-0.0000	-0.0000	0.0017	0.0004	0.9875	0.9854	0.9853	0.9829
40	-0.0244	0.1622	0.1787	0.1613	0.9877	0.9337	0.9301	0.9277
80	-0.0249	0.1463	0.1585	0.1290	0.9873	0.9085	0.8903	0.8809
	Experiment 4							
	$a_{22} = 0.96$							
0	0.0000	-0.0000	0.0030	0.0020	0.9889	0.9863	0.9863	0.9843
40	-0.0328	0.3709	0.3863	0.3783	0.9874	0.8748	0.8656	0.8616
80	-0.0330	0.4154	0.4501	0.4448	0.9880	0.8421	0.8114	0.8024
	$a_{22} = 0.99$							
0	0.0000	0.0000	0.0056	-0.0024	0.9882	0.9834	0.9834	0.9815
40	-0.0377	0.5930	0.5798	0.5877	0.9870	0.7327	0.7433	0.7261
80	-0.0388	0.6765	0.6899	0.6897	0.9867	0.5989	0.5738	0.5301

Table B.3: Bias and RMSE for experiment 1

	Bias				RMSE			
IR Horizon i	Diff	Level	Pope	Bootstrap	Diff	Level	Pope	Bootstrap
	Forecast error variance horizon $h = 0$							
Shock 1 to Variable 1								
0	0.0003	0.0003	0.0048	0.0043	0.0087	0.0460	0.0458	0.0647
4	0.0236	0.0236	0.0960	0.0525	0.0526	0.1381	0.1097	0.1198
8	0.0383	0.0383	0.1762	0.0934	0.0909	0.2257	0.1633	0.1710
40	0.0663	0.0663	0.5488	0.2742	0.2672	0.6152	0.4194	0.4304
Shock 2 to Variable 1								
0	0	0	0	0	0	0	0	0
4	0.0290	0.0290	0.0058	0.0014	0.0052	0.0925	0.0902	0.0916
8	0.0488	0.0488	0.0101	0.0045	0.0089	0.1432	0.1406	0.1445
40	0.0859	0.0859	0.0203	0.0033	0.0468	0.2273	0.3049	0.3331
Shock 1 to Variable 2								

Table B.3: Bias and RMSE for experiment 1

	Bias				RMSE			
IR Horizon i	Diff	Level	Pope	Bootstrap	Diff	Level	Pope	Bootstrap
0	0.0011	0.0011	0.0004	0.0031	0.0010	0.0697	0.0699	0.0995
4	0.0329	0.0329	0.0765	0.0393	0.0342	0.1387	0.1254	0.1401
8	0.0582	0.0582	0.1378	0.0688	0.0613	0.1976	0.1655	0.1733
40	0.0429	0.0429	0.1560	0.0745	0.0701	0.2232	0.2451	0.2571
Shock 2 to Variable 2								
0	0.0048	0.0048	0.0059	0.0075	0.0146	0.0469	0.0470	0.0654
4	0.0620	0.0620	0.0630	0.0281	0.0259	0.1282	0.1182	0.1270
8	0.0936	0.0936	0.1009	0.0410	0.0311	0.1813	0.1656	0.1726
40	0.0615	0.0615	0.0768	0.0211	0.0446	0.1382	0.1980	0.2257
	Forecast error variance horizon $h = 40$							
Shock 1 to Variable 1								
0	0.0003	0.0324	0.0338	0.0403	0.0460	0.0705	0.0732	0.0911
4	0.0238	0.1019	0.0615	0.0627	0.0887	0.1426	0.1173	0.1278
8	0.0386	0.1662	0.0864	0.0842	0.1124	0.2162	0.1568	0.1649
40	0.0670	0.5111	0.2235	0.2102	0.2116	0.5856	0.3896	0.4053
Shock 2 to Variable 1								
0	0.0022	0.0144	0.0125	0.0127	0.0040	0.2290	0.2361	0.2432
4	0.0310	0.0122	0.0055	0.0133	0.0760	0.1382	0.1561	0.1632
8	0.0507	0.0108	0.0030	0.0154	0.1296	0.0688	0.0891	0.0968
40	0.0876	0.0153	0.0021	0.0177	0.2903	0.1087	0.1260	0.1343
Shock 1 to Variable 2								
0	0.0032	0.0003	0.0301	0.0032	0.0691	0.2439	0.2555	0.2660
4	0.0313	0.0668	0.0532	0.0269	0.1054	0.2404	0.2591	0.2690
8	0.0569	0.1189	0.0691	0.0428	0.1209	0.2500	0.2625	0.2719
40	0.0427	0.1436	0.0596	0.0445	0.0870	0.2191	0.2669	0.2849
Shock 2 to Variable 2								
0	0.0059	0.0416	0.0319	0.0530	0.0464	0.1346	0.1324	0.1499
4	0.0631	0.0974	0.0529	0.0675	0.1070	0.1574	0.1461	0.1592
8	0.0945	0.1305	0.0678	0.0727	0.1554	0.1813	0.1581	0.1641

Table B.3: Bias and RMSE for experiment 1

	Bias				RMSE			
IR Horizon i	Diff	Level	Pope	Bootstrap	Diff	Level	Pope	Bootstrap
40	0.0617	0.0751	0.0056	0.0239	0.1232	0.1295	0.1732	0.1922
	Forecast error variance horizon $h = 80$							
Shock 1 to Variable 1								
0	0.0024	0.0467	0.0566	0.0615	0.0468	0.0888	0.1031	0.1185
4	0.0203	0.1067	0.0733	0.0733	0.0901	0.1517	0.1347	0.1431
8	0.0353	0.1676	0.0932	0.0896	0.1162	0.2228	0.1701	0.1759
40	0.0640	0.4988	0.2091	0.1907	0.2209	0.5806	0.3937	0.4094
Shock 2 to Variable 1								
0	0.0023	0.0123	0.0191	0.0117	0.0043	0.2702	0.3015	0.3123
4	0.0320	0.0133	0.0090	0.0166	0.0788	0.1838	0.2264	0.2392
8	0.0522	0.0136	0.0014	0.0218	0.1335	0.1159	0.1606	0.1756
40	0.0909	0.0124	0.0011	0.0002	0.2949	0.0798	0.0694	0.0704
Shock 1 to Variable 2								
0	0.0014	0.0125	0.0515	0.0184	0.0676	0.2878	0.3259	0.3319
4	0.0326	0.0719	0.0674	0.0358	0.1083	0.2764	0.3180	0.3258
8	0.0576	0.1178	0.0755	0.0447	0.1243	0.2768	0.3110	0.3222
40	0.0407	0.1287	0.0403	0.0206	0.0920	0.2147	0.2766	0.3074
Shock 2 to Variable 2								
0	0.0073	0.0538	0.0507	0.0752	0.0479	0.1576	0.1696	0.1957
4	0.0640	0.1087	0.0697	0.0895	0.1096	0.1801	0.1839	0.2034
8	0.0947	0.1424	0.0856	0.0960	0.1583	0.1943	0.1800	0.1917
40	0.0588	0.0782	0.0071	0.0072	0.1292	0.1318	0.1647	0.1834

Table B.4: Bias and RMSE for experiment 2

	Bias				RMSE			
IR Horizon i	Diff	Level	Pope	Bootstrap	Diff	Level	Pope	Bootstrap
	Forecast error variance horizon $h = 0$							
Shock 1 to Variable 1								

Table B.4: Bias and RMSE for experiment 2

	Bias				RMSE			
IR Horizon i	Diff	Level	Pope	Bootstrap	Diff	Level	Pope	Bootstrap
0	0.0031	0.0065	0.0071	0.0109	0.0462	0.0468	0.0470	0.0635
4	0.0223	0.0882	0.0420	0.0435	0.0876	0.1321	0.1077	0.1151
8	0.0330	0.1562	0.0708	0.0719	0.1050	0.2058	0.1538	0.1603
40	0.0162	0.3622	0.1529	0.1599	0.1675	0.4201	0.3090	0.3188
Shock 2 to Variable 1								
0	0	0	0	0	0	0	0	0
4	0.0281	0.0049	0.0079	0.0101	0.0721	0.0918	0.0891	0.0915
8	0.0413	0.0214	0.0207	0.0249	0.1179	0.1440	0.1407	0.1466
40	0.0136	0.2495	0.1489	0.1580	0.2290	0.3345	0.3246	0.3483
Shock 1 to Variable 2								
0	0.0031	0.0003	0.0035	0.0045	0.0703	0.0710	0.0710	0.0981
4	0.0351	0.0410	0.0154	0.0120	0.1080	0.1229	0.1209	0.1356
8	0.0580	0.0722	0.0238	0.0165	0.1227	0.1607	0.1549	0.1657
40	0.0323	0.0371	0.0298	0.0442	0.0739	0.1356	0.2074	0.2277
Shock 2 to Variable 2								
0	0.0053	0.0081	0.0094	0.0110	0.0452	0.0461	0.0464	0.0637
4	0.0617	0.0880	0.0392	0.0345	0.1104	0.1452	0.1265	0.1320
8	0.0901	0.1387	0.0556	0.0464	0.1565	0.2064	0.1773	0.1824
40	0.0457	0.0864	0.0129	0.0295	0.1042	0.1525	0.2117	0.2390
	Forecast error variance horizon $h = 40$							
Shock 1 to Variable 1								
0	0.0017	0.0718	0.0804	0.0839	0.0447	0.1253	0.1351	0.1483
4	0.0204	0.1008	0.0625	0.0632	0.0877	0.1468	0.1307	0.1396
8	0.0276	0.1285	0.0483	0.0479	0.1080	0.1857	0.1442	0.1518
40	0.0013	0.2747	0.0168	0.0183	0.1824	0.3666	0.2863	0.2966
Shock 2 to Variable 1								
0	0.0073	0.2366	0.2585	0.2487	0.0099	0.3457	0.3649	0.3671
4	0.0266	0.2211	0.2525	0.2468	0.0787	0.2663	0.3021	0.3034
8	0.0333	0.2214	0.2553	0.2525	0.1248	0.2347	0.2727	0.2731

Table B.4: Bias and RMSE for experiment 2

	Bias				RMSE			
IR Horizon i	Diff	Level	Pope	Bootstrap	Diff	Level	Pope	Bootstrap
40	0.0113	0.3739	0.3458	0.3495	0.2470	0.3896	0.3691	0.3762
Shock 1 to Variable 2								
0	0.0038	0.2716	0.3003	0.2916	0.0683	0.4053	0.4312	0.4437
4	0.0293	0.2514	0.2584	0.2481	0.1045	0.3654	0.3941	0.4063
8	0.0514	0.2222	0.2089	0.1965	0.1190	0.3172	0.3452	0.3562
40	0.0267	0.0452	0.0016	0.0181	0.0779	0.1609	0.2486	0.2697
Shock 2 to Variable 2								
0	0.0087	0.0436	0.0441	0.0307	0.0459	0.1034	0.1045	0.1160
4	0.0617	0.0018	0.0528	0.0462	0.1112	0.1304	0.1470	0.1533
8	0.0867	0.0653	0.0231	0.0235	0.1567	0.1629	0.1676	0.1730
40	0.0384	0.0621	0.0429	0.0579	0.1104	0.1262	0.1992	0.2198
	Forecast error variance horizon $h = 80$							
Shock 1 to Variable 1								
0	0.0029	0.1017	0.1341	0.1393	0.0456	0.1728	0.2136	0.2317
4	0.0199	0.1196	0.1007	0.1032	0.0856	0.1688	0.1770	0.1909
8	0.0294	0.1411	0.0766	0.0777	0.1063	0.1938	0.1671	0.1779
40	0.0085	0.2662	0.0161	0.0147	0.1778	0.3701	0.2976	0.3083
Shock 2 to Variable 1								
0	0.0076	0.2880	0.3404	0.3304	0.0102	0.4043	0.4598	0.4653
4	0.0304	0.2692	0.3326	0.3263	0.0807	0.3316	0.4048	0.4102
8	0.0397	0.2634	0.3301	0.3267	0.1273	0.2935	0.3701	0.3747
40	0.0013	0.4006	0.4087	0.4114	0.2399	0.4072	0.4141	0.4175
Shock 1 to Variable 2								
0	0.0061	0.3368	0.4038	0.3911	0.0730	0.4889	0.5609	0.5747
4	0.0261	0.3041	0.3490	0.3367	0.1039	0.4369	0.5081	0.5227
8	0.0505	0.2625	0.2823	0.2694	0.1174	0.3717	0.4355	0.4496
40	0.0291	0.0535	0.0189	0.0041	0.0767	0.1644	0.2615	0.2893
Shock 2 to Variable 2								
0	0.0063	0.0423	0.0338	0.0196	0.0454	0.1043	0.1161	0.1317

Table B.4: Bias and RMSE for experiment 2

	Bias				RMSE			
IR Horizon i	Diff	Level	Pope	Bootstrap	Diff	Level	Pope	Bootstrap
4	0.0624	0.0001	0.0515	0.0435	0.1088	0.1350	0.1590	0.1670
8	0.0894	0.0673	0.0167	0.0155	0.1554	0.1663	0.1755	0.1826
40	0.0423	0.0650	0.0310	0.0455	0.1086	0.1215	0.1858	0.2063

Table B.5: Bias and RMSE for experiment 3 with $_{12} = \quad 0\ 2$, $_{22} = 0\ 99$, and $\quad = 0$

	Bias				RMSE			
IR Horizon i	Diff	Level	Pope	Bootstrap	Diff	Level	Pope	Bootstrap
	Forecast error variance horizon $h = 0$							
Shock 1 to Variable 1								
0	0.0022	0.0074	0.0073	0.0124	0.0457	0.0463	0.0462	0.0645
4	0.0237	0.0956	0.0586	0.0607	0.0879	0.1312	0.1058	0.1159
8	0.0371	0.1691	0.1019	0.1027	0.1044	0.2128	0.1610	0.1694
40	0.0904	0.5125	0.3034	0.3003	0.2173	0.5717	0.4183	0.4292
Shock 2 to Variable 1								
0	0	0	0	0	0	0	0	0
4	0.0128	0.0190	0.0096	0.0135	0.0781	0.0861	0.0814	0.0832
8	0.0306	0.0374	0.0171	0.0243	0.1077	0.1335	0.1233	0.1276
40	0.1074	0.0935	0.0473	0.0761	0.2872	0.2744	0.3167	0.3437
Shock 1 to Variable 2								
0	0.0044	0.0045	0.0061	0.0073	0.0692	0.0691	0.0692	0.0997
4	0.0540	0.0843	0.0543	0.0531	0.1295	0.1430	0.1291	0.1460
8	0.0971	0.1528	0.0944	0.0913	0.1583	0.2204	0.1875	0.1976
40	0.2155	0.3279	0.1918	0.1869	0.2644	0.4280	0.4064	0.4176
Shock 2 to Variable 2								
0	0.0063	0.0084	0.0091	0.0148	0.0472	0.0476	0.0476	0.0652
4	0.0673	0.0898	0.0529	0.0517	0.1305	0.1466	0.1301	0.1371
8	0.1290	0.1600	0.0921	0.0853	0.1905	0.2294	0.1947	0.1995
40	0.3017	0.3400	0.1468	0.1169	0.3700	0.4238	0.3866	0.4089

Table B.5: Bias and RMSE for experiment 3 with $_{12} = \quad 0\ 2$, $_{22} = 0\ 99$, and $\quad = 0$

IR Horizon i	Bias				RMSE			
	Diff	Level	Pope	Bootstrap	Diff	Level	Pope	Bootstrap
	Forecast error variance horizon $h = 40$							
Shock 1 to Variable 1								
0	0.0039	0.0609	0.0635	0.0696	0.0482	0.1092	0.1126	0.1280
4	0.0289	0.0930	0.0556	0.0613	0.0955	0.1339	0.1133	0.1227
8	0.0446	0.1567	0.0882	0.0923	0.1132	0.2033	0.1551	0.1619
40	0.1093	0.4746	0.2481	0.2456	0.2301	0.5393	0.3763	0.3865
Shock 2 to Variable 1								
0	0.0245	0.1633	0.1787	0.1617	0.0295	0.3069	0.3146	0.3154
4	0.0367	0.1523	0.1628	0.1523	0.0899	0.2115	0.2267	0.2260
8	0.0569	0.1559	0.1603	0.1531	0.1204	0.1758	0.1876	0.1860
40	0.1453	0.1543	0.1471	0.1579	0.2948	0.2055	0.2097	0.2245
Shock 1 to Variable 2								
0	0.0225	0.1932	0.2116	0.1967	0.0737	0.3558	0.3681	0.3737
4	0.0200	0.2361	0.2296	0.2144	0.1117	0.3722	0.3850	0.3892
8	0.0640	0.2727	0.2429	0.2266	0.1379	0.3935	0.4010	0.4028
40	0.1920	0.3535	0.2507	0.2358	0.2533	0.4601	0.4844	0.4932
Shock 2 to Variable 2								
0	0.0149	0.0244	0.0278	0.0156	0.0495	0.1197	0.1196	0.1324
4	0.0791	0.0372	0.0074	0.0005	0.1342	0.1526	0.1580	0.1693
8	0.1362	0.1150	0.0388	0.0386	0.1915	0.1991	0.1841	0.1930
40	0.2962	0.3172	0.1191	0.0908	0.3641	0.3990	0.3630	0.3771
	Forecast error variance horizon $h = 80$							
Shock 1 to Variable 1								
0	0.0024	0.0827	0.0993	0.1072	0.0464	0.1468	0.1718	0.1896
4	0.0299	0.1108	0.0860	0.0961	0.0910	0.1533	0.1525	0.1710
8	0.0438	0.1663	0.1095	0.1172	0.1090	0.2094	0.1777	0.1916
40	0.0990	0.4567	0.2309	0.2257	0.2293	0.5295	0.3716	0.3848
Shock 2 to Variable 1								
0	0.0250	0.1462	0.1570	0.1283	0.0294	0.3614	0.3958	0.4058

Table B.5: Bias and RMSE for experiment 3 with $_{12} = \; 0\ 2$, $_{22} = 0\ 99$, and $= 0$

	Bias				RMSE			
IR Horizon i	Diff	Level	Pope	Bootstrap	Diff	Level	Pope	Bootstrap
4	0.0379	0.1402	0.1483	0.1294	0.0879	0.2600	0.2993	0.3084
8	0.0559	0.1458	0.1470	0.1310	0.1162	0.2130	0.2492	0.2575
40	0.1338	0.1470	0.1350	0.1351	0.2889	0.1723	0.1508	0.1513
Shock 1 to Variable 2								
0	0.0250	0.1790	0.1979	0.1664	0.0772	0.4084	0.4496	0.4593
4	0.0239	0.2275	0.2219	0.1919	0.1163	0.4171	0.4618	0.4688
8	0.0688	0.2638	0.2333	0.2019	0.1422	0.4315	0.4722	0.4781
40	0.1981	0.3412	0.2304	0.1965	0.2601	0.4753	0.5356	0.5570
Shock 2 to Variable 2								
0	0.0166	0.0104	0.0244	0.0522	0.0488	0.1675	0.1908	0.2149
4	0.0800	0.0742	0.0508	0.0742	0.1352	0.2008	0.2246	0.2467
8	0.1390	0.1521	0.1005	0.1160	0.1932	0.2403	0.2427	0.2600
40	0.3029	0.3502	0.1932	0.1743	0.3733	0.4164	0.3798	0.3882

Table B.6: Bias and RMSE for experiment 3 with $_{12} = \; 0\ 2$, $_{22} = 0\ 96$, and $= 0$

	Bias				RMSE			
IR Horizon i	Diff	Level	Pope	Bootstrap	Diff	Level	Pope	Bootstrap
	Forecast error variance horizon $h = 0$							
Shock 1 to Variable 1								
0	0.0028	0.0077	0.0071	0.0122	0.0479	0.0484	0.0484	0.0638
4	0.0191	0.0866	0.0482	0.0491	0.0953	0.1263	0.1003	0.1089
8	0.0316	0.1548	0.0843	0.0831	0.1163	0.2055	0.1520	0.1590
40	0.0697	0.5125	0.2605	0.2538	0.2175	0.5824	0.4014	0.4135
Shock 2 to Variable 1								
0	0	0	0	0	0	0	0	0
4	0.0155	0.0135	0.0014	0.0076	0.0770	0.0816	0.0785	0.0800
8	0.0321	0.0272	0.0024	0.0142	0.1141	0.1269	0.1225	0.1256
40	0.0861	0.0356	0.0013	0.0393	0.2742	0.2151	0.2812	0.3032

Table B.6: Bias and RMSE for experiment 3 with $_{12} =$ $0\ 2$, $_{22} = 0\ 96$, and $= 0$

IR Horizon i	Bias Diff	Bias Level	Bias Pope	Bias Bootstrap	RMSE Diff	RMSE Level	RMSE Pope	RMSE Bootstrap
Shock 1 to Variable 2								
0	0.0015	0.0026	0.0053	0.0066	0.0676	0.0681	0.0681	0.0950
4	0.0326	0.0786	0.0422	0.0396	0.1196	0.1352	0.1210	0.1343
8	0.0589	0.1330	0.0672	0.0613	0.1304	0.1915	0.1621	0.1709
40	0.0445	0.1477	0.0640	0.0576	0.0935	0.2164	0.2415	0.2563
Shock 2 to Variable 2								
0	0.0046	0.0057	0.0072	0.0136	0.0459	0.0464	0.0464	0.0657
4	0.0528	0.0630	0.0279	0.0248	0.1203	0.1295	0.1201	0.1266
8	0.0883	0.0996	0.0403	0.0297	0.1581	0.1789	0.1645	0.1701
40	0.0640	0.0761	0.0216	0.0480	0.1299	0.1387	0.1967	0.2265
	Forecast error variance horizon $h = 40$							
Shock 1 to Variable 1								
0	0.0007	0.0400	0.0440	0.0449	0.0476	0.0811	0.0871	0.0985
4	0.0235	0.0747	0.0379	0.0388	0.0893	0.1129	0.0925	0.1037
8	0.0329	0.1296	0.0599	0.0579	0.1094	0.1763	0.1260	0.1352
40	0.0584	0.4760	0.2037	0.1900	0.2143	0.5485	0.3586	0.3795
Shock 2 to Variable 1								
0	0.0246	0.1014	0.1195	0.0948	0.0296	0.2553	0.2708	0.2667
4	0.0301	0.0968	0.1048	0.0888	0.0925	0.1595	0.1792	0.1746
8	0.0423	0.1030	0.1011	0.0898	0.1254	0.1230	0.1334	0.1291
40	0.0813	0.0894	0.0869	0.1004	0.2762	0.1347	0.1469	0.1604
Shock 1 to Variable 2								
0	0.0259	0.1204	0.1431	0.1189	0.0812	0.2918	0.3120	0.3125
4	0.0149	0.1629	0.1475	0.1235	0.1107	0.2896	0.3030	0.3047
8	0.0443	0.1943	0.1494	0.1253	0.1235	0.2970	0.3005	0.3039
40	0.0400	0.1681	0.0966	0.0832	0.0935	0.2372	0.2785	0.3007
Shock 2 to Variable 2								
0	0.0159	0.0111	0.0132	0.0035	0.0501	0.1107	0.1125	0.1264
4	0.0629	0.0422	0.0021	0.0107	0.1236	0.1268	0.1321	0.1414

Table B.6: Bias and RMSE for experiment 3 with $_{12} = \quad 0\ 2$, $_{22} = 0\ 96$, and $\quad = 0$

IR Horizon i	Bias				RMSE			
	Diff	Level	Pope	Bootstrap	Diff	Level	Pope	Bootstrap
8	0.0953	0.0881	0.0266	0.0252	0.1611	0.1604	0.1538	0.1600
40	0.0639	0.0788	0.0090	0.0330	0.1259	0.1349	0.1802	0.2095
	Forecast error variance horizon $h = 80$							
Shock 1 to Variable 1								
0	0.0025	0.0498	0.0616	0.0643	0.0469	0.0929	0.1119	0.1215
4	0.0241	0.0858	0.0549	0.0596	0.0948	0.1224	0.1112	0.1220
8	0.0345	0.1396	0.0736	0.0749	0.1174	0.1859	0.1406	0.1476
40	0.0633	0.4803	0.2039	0.1896	0.2277	0.5584	0.3744	0.3895
Shock 2 to Variable 1								
0	0.0238	0.0785	0.0907	0.0571	0.0284	0.2811	0.3156	0.3206
4	0.0280	0.0811	0.0848	0.0610	0.0931	0.1832	0.2214	0.2256
8	0.0419	0.0856	0.0784	0.0586	0.1284	0.1388	0.1704	0.1755
40	0.0859	0.0732	0.0571	0.0575	0.2830	0.1016	0.0832	0.0847
Shock 1 to Variable 2								
0	0.0214	0.1042	0.1231	0.0874	0.0752	0.3162	0.3549	0.3563
4	0.0113	0.1445	0.1261	0.0935	0.1115	0.3029	0.3342	0.3371
8	0.0417	0.1744	0.1254	0.0940	0.1242	0.3035	0.3248	0.3314
40	0.0398	0.1458	0.0635	0.0446	0.0950	0.2220	0.2791	0.3054
Shock 2 to Variable 2								
0	0.0170	0.0104	0.0193	0.0435	0.0497	0.1326	0.1499	0.1764
4	0.0626	0.0570	0.0267	0.0455	0.1254	0.1508	0.1669	0.1850
8	0.0960	0.1004	0.0475	0.0571	0.1628	0.1718	0.1703	0.1822
40	0.0648	0.0800	0.0014	0.0142	0.1298	0.1357	0.1731	0.1948

Table B.7: Bias and RMSE for experiment 4 with $_{12} = \ \ 0\ 2$, $_{22} = 0\ 99$, and $=$ $0\ 025$

	Bias				RMSE			
IR Horizon i	Diff	Level	Pope	Bootstrap	Diff	Level	Pope	Bootstrap
	Forecast error variance horizon $h = 0$							
Shock 1 to Variable 1								
0	0.0022	0.0033	0.0011	0.0074	0.0472	0.0474	0.0473	0.0638
4	0.0204	0.0483	0.0147	0.0215	0.0881	0.0946	0.0847	0.0937
8	0.0271	0.0829	0.0233	0.0321	0.0997	0.1372	0.1157	0.1239
40	0.0323	0.1534	0.0087	0.0278	0.2018	0.2784	0.2780	0.2838
Shock 2 to Variable 1								
0	0	0	0	0	0	0	0	0
4	0.0109	0.0033	0.0019	0.0034	0.0747	0.0782	0.0777	0.0799
8	0.0195	0.0061	0.0110	0.0117	0.0991	0.1169	0.1152	0.1201
40	0.0656	0.3166	0.2013	0.1797	0.2613	0.4340	0.3804	0.4027
Shock 1 to Variable 2								
0	0.0060	0.0053	0.0099	0.0049	0.0705	0.0706	0.0713	0.0963
4	0.0449	0.0345	0.0266	0.0156	0.1292	0.1174	0.1177	0.1304
8	0.0810	0.0577	0.0385	0.0204	0.1529	0.1589	0.1574	0.1648
40	0.1510	0.1062	0.0100	0.0376	0.2174	0.2444	0.2947	0.3273
Shock 2 to Variable 2								
0	0.0049	0.0097	0.0090	0.0137	0.0464	0.0472	0.0473	0.0625
4	0.0590	0.1128	0.0702	0.0635	0.1198	0.1576	0.1316	0.1319
8	0.1117	0.2025	0.1247	0.1087	0.1746	0.2534	0.2018	0.1964
40	0.2156	0.4172	0.2481	0.2100	0.3022	0.4811	0.4012	0.4001
	Forecast error variance horizon $h = 40$							
Shock 1 to Variable 1								
0	0.0026	0.2559	0.2413	0.2613	0.0490	0.3221	0.3090	0.3370
4	0.0317	0.0562	0.0267	0.0411	0.0928	0.1204	0.1173	0.1400
8	0.0432	0.0149	0.0337	0.0208	0.1107	0.1091	0.1169	0.1325
40	0.0024	0.1611	0.3621	0.3558	0.2178	0.3223	0.4579	0.4763
Shock 2 to Variable 1								

Table B.7: Bias and RMSE for experiment 4 with $_{12} = \ 0\ 2$, $_{22} = 0\ 99$, and $= 0\ 025$

	Bias				RMSE			
IR Horizon i	Diff	Level	Pope	Bootstrap	Diff	Level	Pope	Bootstrap
0	0.0379	0.5966	0.5823	0.5894	0.0423	0.6358	0.6233	0.6343
4	0.0421	0.5274	0.5328	0.5452	0.0944	0.5538	0.5599	0.5754
8	0.0490	0.5036	0.5223	0.5345	0.1185	0.5179	0.5366	0.5513
40	0.0470	0.6302	0.6173	0.6017	0.2630	0.6444	0.6338	0.6218
Shock 1 to Variable 2								
0	0.0365	0.7207	0.7032	0.7145	0.0833	0.7887	0.7732	0.7952
4	0.0064	0.6597	0.6546	0.6683	0.1210	0.7329	0.7350	0.7601
8	0.0493	0.5864	0.5923	0.6038	0.1404	0.6563	0.6741	0.6974
40	0.1440	0.2540	0.2604	0.2538	0.2128	0.3512	0.4185	0.4371
Shock 2 to Variable 2								
0	0.0232	0.0377	0.0398	0.0266	0.0517	0.1170	0.1156	0.1265
4	0.0844	0.0424	0.0786	0.0833	0.1379	0.1438	0.1641	0.1762
8	0.1360	0.0525	0.0152	0.0333	0.1929	0.1876	0.1949	0.2068
40	0.2333	0.3000	0.1319	0.0755	0.3059	0.3694	0.3448	0.3620
	Forecast error variance horizon $h = 80$							
Shock 1 to Variable 1								
0	0.0006	0.3767	0.3962	0.4356	0.0455	0.4708	0.4903	0.5344
4	0.0267	0.1517	0.1493	0.1982	0.0925	0.2836	0.3029	0.3639
8	0.0367	0.1015	0.0792	0.1316	0.1092	0.2726	0.2942	0.3586
40	0.0100	0.1190	0.3009	0.2302	0.2204	0.4426	0.5908	0.6639
Shock 2 to Variable 1								
0	0.0391	0.6824	0.6961	0.6918	0.0433	0.7306	0.7476	0.7614
4	0.0414	0.6341	0.6742	0.6855	0.0937	0.6785	0.7204	0.7441
8	0.0461	0.6179	0.6737	0.6890	0.1169	0.6521	0.7090	0.7349
40	0.0580	0.7571	0.8069	0.8207	0.2703	0.7613	0.8103	0.8254
Shock 1 to Variable 2								
0	0.0377	0.7830	0.7894	0.7495	0.0829	0.9149	0.9356	0.9473
4	0.0050	0.7347	0.7585	0.7310	0.1152	0.8591	0.9017	0.9182

Table B.7: Bias and RMSE for experiment 4 with $_{12} = \quad 0\ 2$, $_{22} = 0\ 99$, and $= 0\ 025$

	Bias				RMSE			
IR Horizon i	Diff	Level	Pope	Bootstrap	Diff	Level	Pope	Bootstrap
8	0.0481	0.6506	0.6848	0.6585	0.1342	0.7665	0.8267	0.8445
40	0.1439	0.2735	0.3040	0.2720	0.2111	0.3812	0.4988	0.5223
Shock 2 to Variable 2								
0	0.0240	0.0548	0.0765	0.1209	0.0523	0.2129	0.2314	0.2813
4	0.0849	0.0190	0.0019	0.0291	0.1401	0.1638	0.1828	0.2241
8	0.1357	0.1026	0.0560	0.0683	0.1941	0.2029	0.2065	0.2393
40	0.2314	0.3031	0.1615	0.1209	0.3066	0.3619	0.3252	0.3412

Table B.8: Bias and RMSE for experiment 4 with $_{12} = \quad 0\ 2$, $_{22} = 0\ 96$, and $= 0\ 025$

	Bias				RMSE			
IR Horizon i	Diff	Level	Pope	Bootstrap	Diff	Level	Pope	Bootstrap
	Forecast error variance horizon $h = 0$							
Shock 1 to Variable 1								
0	0.0026	0.0062	0.0067	0.0077	0.0464	0.0468	0.0468	0.0650
4	0.0232	0.0830	0.0393	0.0389	0.0865	0.1215	0.0960	0.1042
8	0.0285	0.1418	0.0638	0.0639	0.1056	0.1886	0.1391	0.1465
40	0.0081	0.3535	0.1505	0.1574	0.1837	0.4092	0.2961	0.3070
Shock 2 to Variable 1								
0	0	0	0	0	0	0	0	0
4	0.0080	0.0191	0.0144	0.0167	0.0794	0.0890	0.0844	0.0880
8	0.0145	0.0487	0.0322	0.0359	0.1139	0.1435	0.1336	0.1405
40	0.0142	0.2705	0.1533	0.1611	0.2420	0.3504	0.3229	0.3464
Shock 1 to Variable 2								
0	0.0060	0.0037	0.0070	0.0067	0.0700	0.0697	0.0698	0.0974
4	0.0381	0.0461	0.0195	0.0144	0.1171	0.1172	0.1122	0.1289
8	0.0626	0.0758	0.0273	0.0188	0.1297	0.1563	0.1467	0.1594
40	0.0364	0.0416	0.0252	0.0399	0.0790	0.1393	0.2078	0.2292

Table B.8: Bias and RMSE for experiment 4 with $_{12} =$ 0 2, $_{22} = 0$ 96, and $=$ 0 025

	Bias				RMSE			
IR Horizon i	Diff	Level	Pope	Bootstrap	Diff	Level	Pope	Bootstrap
Shock 2 to Variable 2								
0	0.0061	0.0087	0.0099	0.0145	0.0447	0.0453	0.0455	0.0660
4	0.0540	0.0844	0.0365	0.0341	0.1207	0.1417	0.1247	0.1301
8	0.0884	0.1329	0.0519	0.0448	0.1592	0.1996	0.1731	0.1766
40	0.0514	0.0908	0.0125	0.0278	0.1083	0.1545	0.2133	0.2344
	Forecast error variance horizon $h = 40$							
Shock 1 to Variable 1								
0	0.0030	0.1183	0.1273	0.1316	0.0442	0.1760	0.1873	0.2015
4	0.0282	0.0555	0.0181	0.0221	0.0955	0.1052	0.0957	0.1116
8	0.0335	0.0836	0.0091	0.0125	0.1145	0.1466	0.1184	0.1302
40	0.0144	0.2577	0.0074	0.0137	0.1943	0.3492	0.2706	0.2794
Shock 2 to Variable 1								
0	0.0330	0.3729	0.3866	0.3802	0.0378	0.4425	0.4568	0.4592
4	0.0314	0.3291	0.3525	0.3504	0.0947	0.3550	0.3834	0.3859
8	0.0337	0.3306	0.3549	0.3541	0.1244	0.3373	0.3655	0.3668
40	0.0040	0.4318	0.4140	0.4156	0.2416	0.4426	0.4301	0.4347
Shock 1 to Variable 2								
0	0.0312	0.4303	0.4507	0.4429	0.0812	0.5288	0.5501	0.5573
4	0.0069	0.3712	0.3792	0.3716	0.1097	0.4547	0.4800	0.4874
8	0.0350	0.3151	0.3116	0.3028	0.1191	0.3881	0.4145	0.4211
40	0.0259	0.0666	0.0378	0.0244	0.0821	0.1735	0.2574	0.2772
Shock 2 to Variable 2								
0	0.0213	0.0677	0.0635	0.0523	0.0516	0.1040	0.1039	0.1125
4	0.0660	0.0360	0.0861	0.0820	0.1301	0.1349	0.1633	0.1691
8	0.0927	0.0339	0.0510	0.0531	0.1616	0.1593	0.1831	0.1906
40	0.0448	0.0594	0.0486	0.0655	0.1111	0.1242	0.2060	0.2325
	Forecast error variance horizon $h = 80$							
Shock 1 to Variable 1								

Table B.8: Bias and RMSE for experiment 4 with $\ _{12} = \ 0\ 2$, $\ _{22} = 0\ 96$, and $\ = 0\ 025$

	Bias				RMSE			
IR Horizon i	Diff	Level	Pope	Bootstrap	Diff	Level	Pope	Bootstrap
0	0.0039	0.1529	0.1833	0.1915	0.0479	0.2257	0.2615	0.2790
4	0.0306	0.0717	0.0469	0.0544	0.0972	0.1267	0.1292	0.1497
8	0.0381	0.0943	0.0305	0.0375	0.1159	0.1584	0.1368	0.1576
40	0.0252	0.2477	0.0011	0.0069	0.1890	0.3480	0.2800	0.3017
Shock 2 to Variable 1								
0	0.0331	0.4169	0.4501	0.4424	0.0380	0.4939	0.5348	0.5378
4	0.0362	0.3663	0.4118	0.4091	0.0950	0.4054	0.4623	0.4670
8	0.0412	0.3632	0.4104	0.4090	0.1233	0.3808	0.4381	0.4420
40	0.0105	0.4482	0.4556	0.4571	0.2317	0.4529	0.4590	0.4607
Shock 1 to Variable 2								
0	0.0321	0.4897	0.5384	0.5293	0.0813	0.6000	0.6584	0.6687
4	0.0137	0.4231	0.4596	0.4515	0.1089	0.5160	0.5767	0.5867
8	0.0432	0.3583	0.3809	0.3721	0.1214	0.4377	0.4959	0.5054
40	0.0319	0.0802	0.0684	0.0573	0.0791	0.1774	0.2707	0.2913
Shock 2 to Variable 2								
0	0.0221	0.0552	0.0391	0.0266	0.0515	0.1149	0.1224	0.1387
4	0.0715	0.0246	0.0665	0.0613	0.1320	0.1359	0.1625	0.1707
8	0.1008	0.0486	0.0268	0.0278	0.1668	0.1639	0.1809	0.1892
40	0.0519	0.0658	0.0270	0.0439	0.1092	0.1179	0.1835	0.2117

B.3.3 Additional Empirical Results

We consider a reduced-form VAR with five (log-) variables for the US economy from 1959Q1 to 2019Q4:

$$= (\ \log \mathbf{TFP} \quad \log \mathbf{IST} \quad \log \quad \log \quad \log \ )'$$

We employ a first-difference transformation for the first three variables of the unrestricted VAR model, while leaving the last two variables unchanged (see Section 5). Our identification approach assumes two sources of persistent fluctuations in the system, which we define as TFP and IST permanent shocks. Using the methodology outlined in Section 5, we apply the Max Share approach of Francis et al. (2014) to sequentially identify two structural permanent shocks. The forecast error variance horizon is truncated at $= 80$ quarters. We then contrast these results with those obtained from a VAR *in levels*.

Importantly, each structural shock (i.e., TFP and IST permanent shocks) is identified under two different orderings: (1) The permanent TFP shock is identified first, followed by the IST permanent shock; and (2) the permanent IST shock is identified first, followed by the TFP permanent shock. This allows us to identify two sets of permanent TFP (and IST) shocks and compare the corresponding structural impulse response functions across both specifications.

Figure B.1 presents the impulse response functions (top panel) and the forecast error variance shares (bottom panel) for each structural permanent TFP shock on each variable, comparing both identification order strategies for the VAR *in levels* and *in first-differences*. Three points are worth commenting on. First, the impulse response functions (IRFs) and forecast error variance decomposition (FEVD) shares for TFP shocks exhibit significant differences based on the identification order of structural shocks. For example, while both orderings suggest that a TFP shock generally increases hours worked (except at the initial impact), the VAR *in levels* shows a markedly different response and attributes a considerably larger share of the variance in hours worked to TFP shocks. Specifically, TFP shocks account for nearly 60% of the variance in hours worked after 10 quarters when identified first, but only 25% when identified second. This suggests that when TFP shocks are identified first, they appear to be the primary drivers of fluctuations in hours worked, a conclusion that becomes less pronounced when TFP shocks are identified second.

Second, results for the *first-difference* VAR specification are nearly identical and thus are robust regardless of the identification order. Third, consistent with our Monte Carlo simulation findings, there is a substantial discrepancy between the structural impulse responses estimated from the VAR *in levels* and those from the *first-difference* VAR, irrespective of the identification order.

Figure B.2 illustrates the impulse response functions (top panel) and the forecast error variance shares (bottom panel) for each structural permanent IST shock on each variable, comparing both identification order strategies for the VAR *in levels* and *in first-differences*. The differences are even more pronounced with IST shocks, as depicted in Figure 2. When using the VAR *in levels*, hours worked tend to decline for several quarters following an IST shock, particularly when the shock is identified conditionally on the TFP shock. In contrast, if IST shocks are identified first, they account for a substantial portion of the fluctuations in hours worked and consumption. However, when IST shocks are identified second, their influence on these fluctuations is markedly diminished. This discrepancy suggests that in the second identification scheme, IST shocks may not be a primary driver of business cycles.

These results highlight the sensitivity of structural identification when using an unrestricted VAR in levels and thus the importance of considering stationary transformations to assess the reliability of structural shock estimates.

Figure B.1: TFP Shock

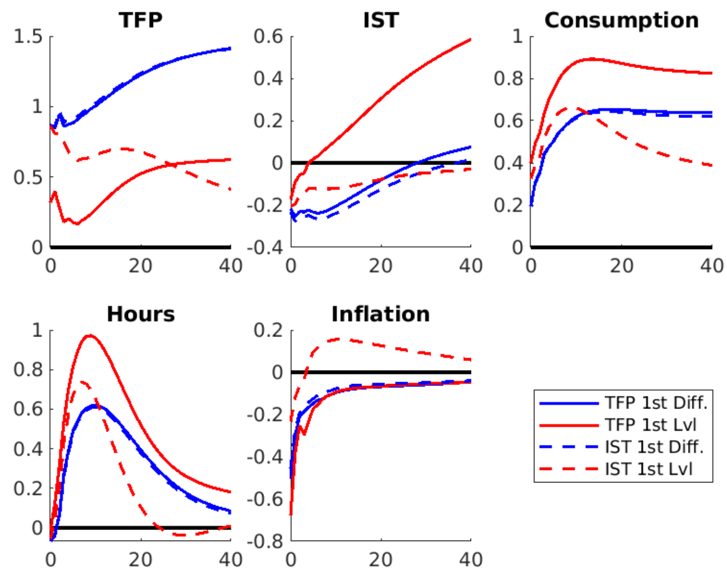

(a) Impulse Responses

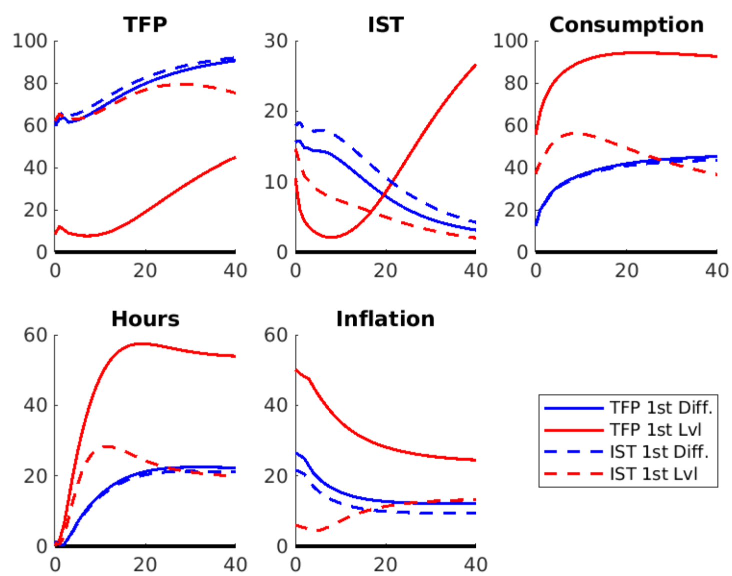

(b) Variance Decomposition

Notes: (1) The first three (log-) variables—total factor productivity, inverse of the real price of investment and real consumption per capita—enter in first-difference in the unrestricted reduced-form VAR. (2) Red color corresponds to level-based estimates. Blue color corresponds to "first-difference" estimates. (3) A solid line indicates the TFP shock is identified before the IST shock. A dashed line indicates the IST shock is identified before the TFP shock.

Figure B.2: IST Shock

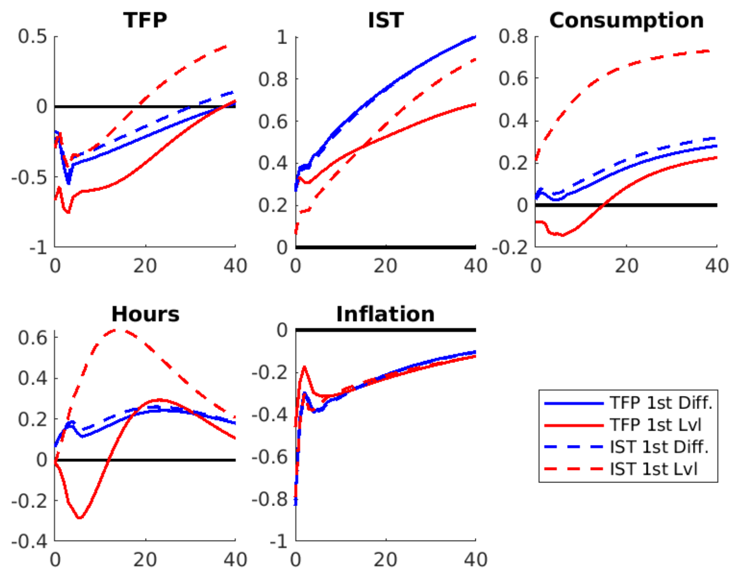

(a) Impulse Responses

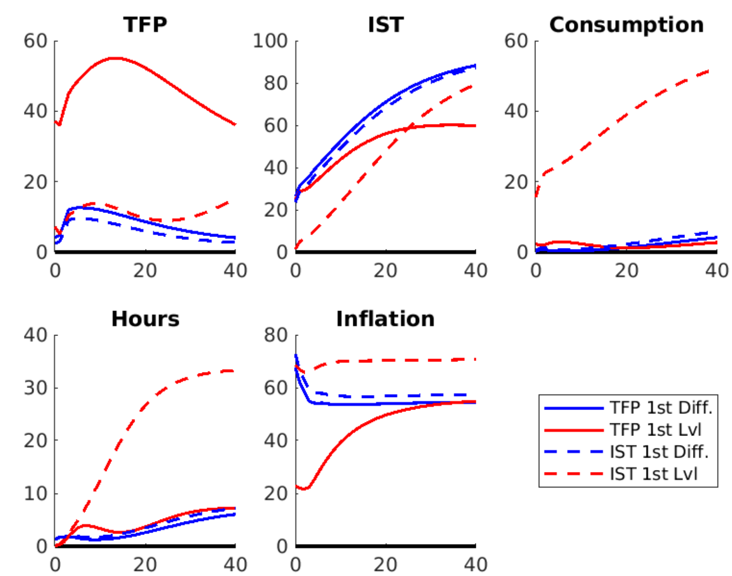

(b) Variance Decomposition

Notes: (1) The first three (log-) variables—total factor productivity, inverse of the real price of investment and real consumption per capita—enter in first-difference in the unrestricted reduced-form VAR. (2) Red color corresponds to level-based estimates. Blue color corresponds to "first-difference" estimates. (3) A solid line indicates the TFP shock is identified before the IST shock. A dashed line indicates the IST shock is identified before the TFP shock.

B.3.4 Additional Figures

Figure B.3: Impulse response effects of the first structural shock based on a *non-accumulated* Max-Share identification with $= 0$ (experiment 2)

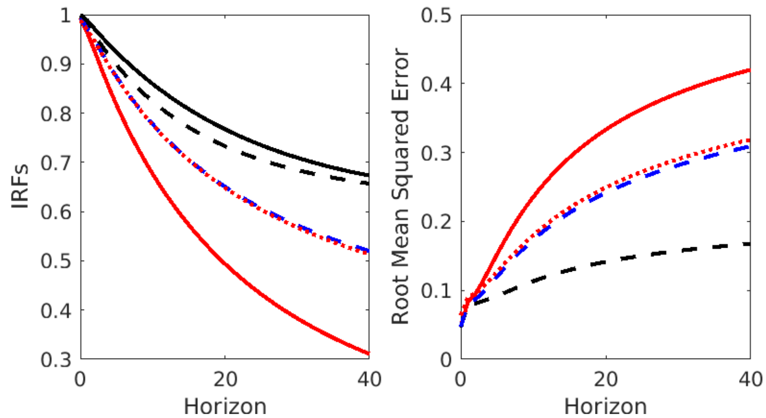

(a) Variable 1

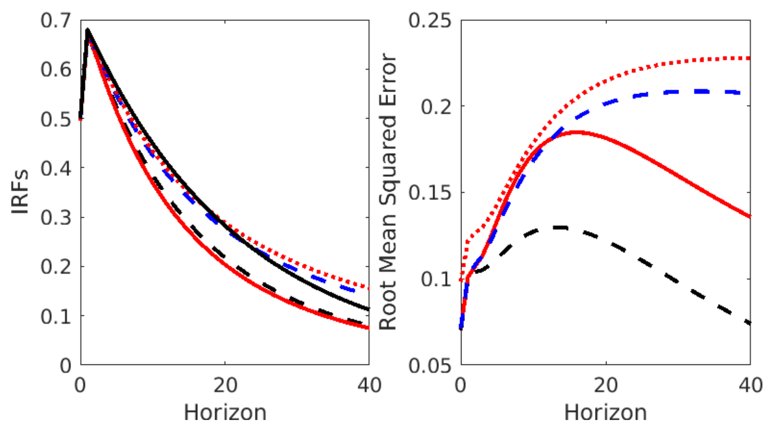

(b) Variable 2

The black solid line represents the true IRF, $\texttt{IRF}_{11,i}$ and $\texttt{IRF}_{21,i}$ for $i = 0,$ $, 40$, whereas the dashed line, the red solid line, the blue dashed line, and the red dotted line represent the average IRF estimates, $\overline{\texttt{IRF}}_{11,i}(0)$ and$\overline{\texttt{IRF}}_{11,i}(0)$, inherited from the first-difference specification, the level specification, the bias-correction method of Pope, and a bootstrap procedure, respectively.

Figure B.4: Impulse response effects of the first structural shock based on a *non-accumulated* Max-Share identification with $= 80$ (experiment 2)

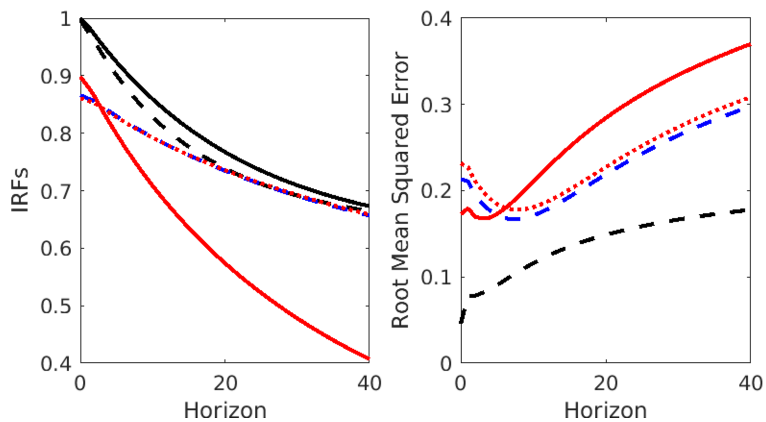

(a) Variable 1

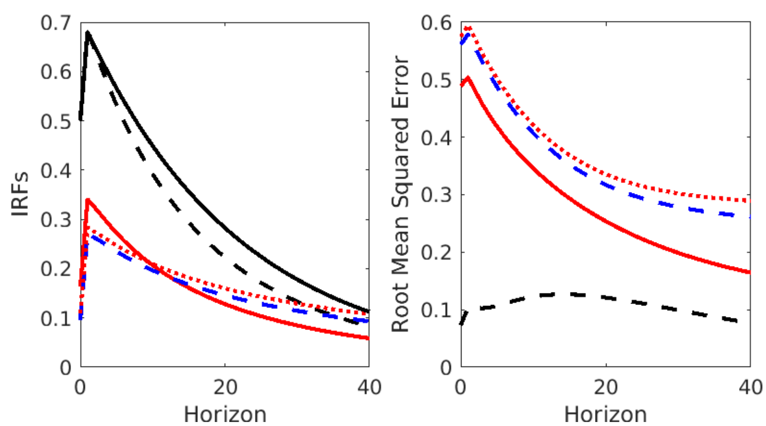

(b) Variable 2

The black solid line represents the true IRF, $\mathtt{IRF}_{11,i}$ and $\mathtt{IRF}_{21,i}$ for $i = 0, \quad , 40$, whereas the dashed line, the red solid line, the blue dashed line, and the red dotted line represent the average IRF estimates, $\overline{\mathtt{IRF}}_{11,i}(0)$ and$\overline{\mathtt{IRF}}_{11,i}(0)$, inherited from the first-difference specification, the level specification, the bias-correction method of Pope, and a bootstrap procedure, respectively.

APPENDIX C

A LARGE CANADIAN DATABASE FOR MACROECONOMIC ANALYSIS

C.1 Additional Results

C.1.1 Seasonal adjustments

The series under investigation is split into 12 subsamples, each consisting of $(\quad)_{=1}^{12}$ observations specific to a given month. Under the null hypothesis of no seasonal behavior, these subsamples must have the same mean. The Kruskal-Wallis test (Kruskal and Wallis (1952)) offers a non-parametric approach to test this hypothesis. In each subsample, observations are assigned a rank following their relative magnitudes. If is the total number of observations, the Kruskal-Wallis statistic is given by:

$$= \frac{12}{(\quad + 1)} \sum_{=1}^{12} \left(\frac{\sum_{=1}^{j}}{\qquad} \right)^2 \quad 3(\quad + 1) \qquad {}^2(12 \quad 1) \tag{C.1}$$

C.1.2 Factors' interpretation over time

Here, we study the factor interpretation through time by estimating the factor model recursively since 1990M12. The resulting time series form the basis of the heatmaps shown in Figures C.3 and C.4. For convenience, variables are grouped in categories, the exact composition of which are given in the data appendix. Tables C.2 and C.3 offer a more granular look in the interpretation and stability of factors, reporting the top ten series in terms of average squared loadings over subperiods. The subperiods have been chosen to match visual changes in some of the heatmaps, facilitating the parallel between the two.

The first factor weighs heavily and constantly on production variables. The factor appears overall very stable and this can be confirmed by the ranking of series in three selected subperiods reproduced in Table C.2. The second factor is clearly related to

Table C.1: Kruskal-Wallis Rank Sum Test Results

Series	**Unajusted**		**Ajusted**	
	chi-squared	p-value	chi-squared	p-value
Unemployment duration				
Canada	239.6419	0	0.8426	1
New Foundland	57.6381	0	1.9380	0.9987
Prince Edward Island	216.5544	0	1.7885	0.9991
Nova Scotia	131.6689	0	1.9556	0.9986
New Brunswick	75.7492	0	1.4571	0.9997
Quebec	76.0553	0	0.9038	1
Ontario	171.9024	0	0.3691	1
Manitoba	74.1367	0	0.8112	1
Saskatchewan	93.2069	0	2.2827	0.9972
Alberta	92.7645	0	3.5774	0.9807
British Columbia	87.9181	0	0.9468	1
Initial claims				
Canada	309.4079	0	0.6171	1
New Foundland	387.0221	0	0.8858	1
Prince Edward Island	416.8684	0	0.5220	1
Nova Scotia	382.3249	0	0.3162	1
New Brunswick	425.1459	0	0.3084	1
Quebec	317.1152	0	1.8707	0.9989
Ontario	254.3162	0	0.4762	1
Manitoba	279.2051	0	0.3161	1
Saskatchewan	288.7726	0	0.5814	1
Alberta	74.4530	0	0.3275	1
British Columbia	213.2004	0	0.7640	1

money and credit measures, even though few price and production series gain importance since 2010. The third factor used to be linked to international flows until 2003 but then turns to production and inflation series. The case of the fourth factor is interesting since it drastically changed since 2000, going from credit and house prices to exchange rates and stock returns.

Of course, further factors are harder to interpret given the natural ordering of importance of principal components. Nevertheless, there are some interesting patterns in

Figure C.1: Seasonal adjustment of unemployment duration

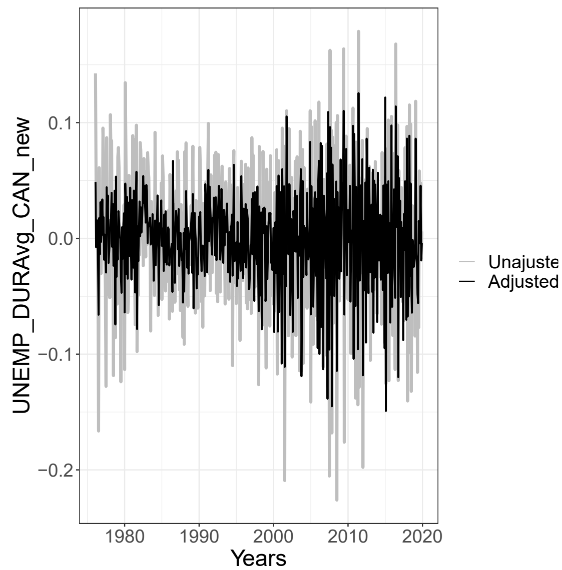

(a) Canada

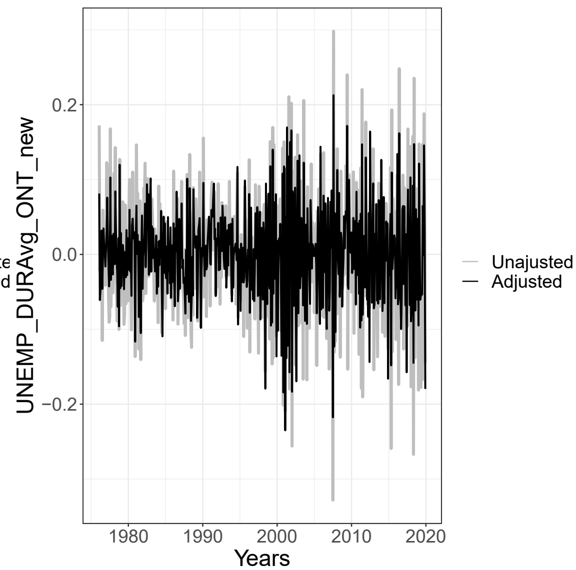

(b) Ontario

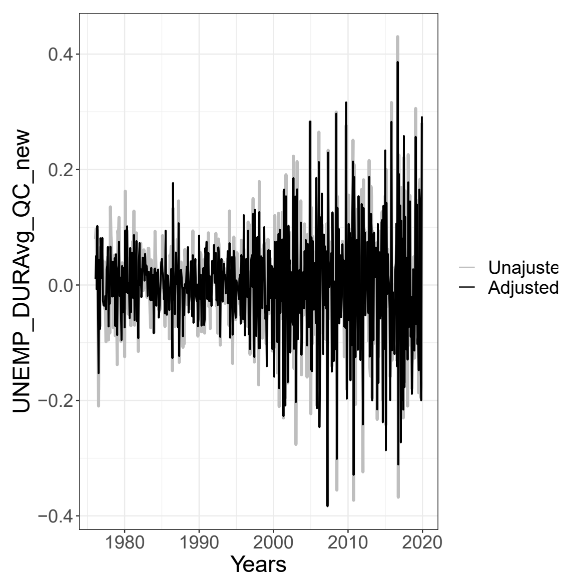

(c) Québec

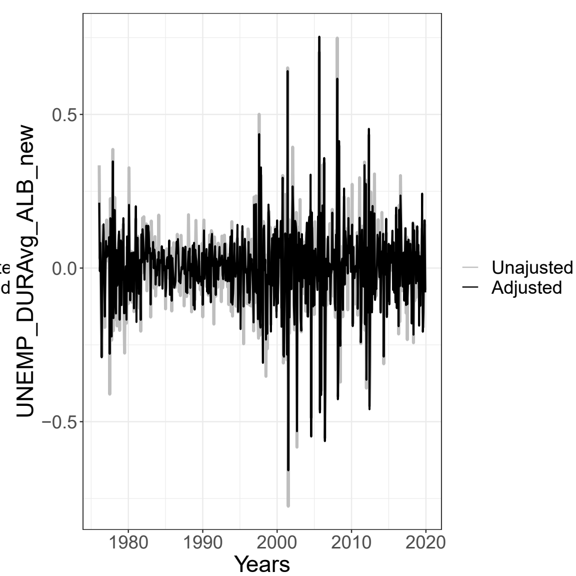

(d) Alberta

factors 5 and 6. The former captures movements in orders until 2003, then is related to stock market and finally it mostly loads on labor market and money / credit. The

Figure C.2: Seasonal adjustment of initial claims

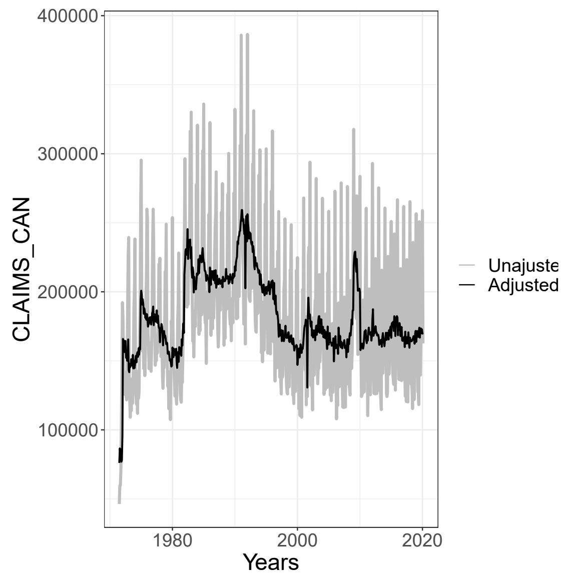

(a) Canada

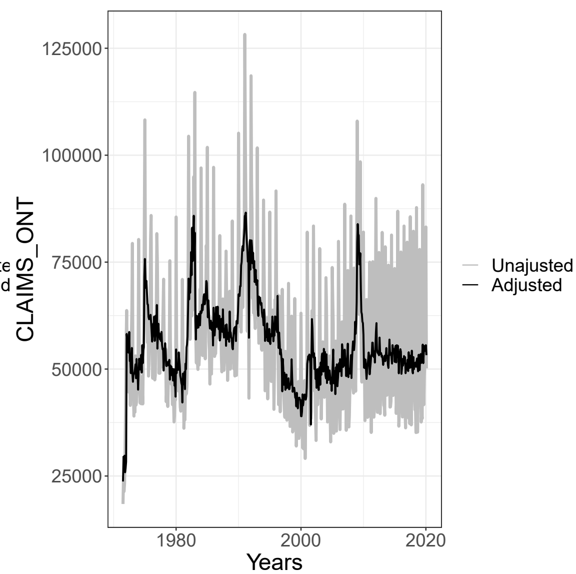

(b) Ontario

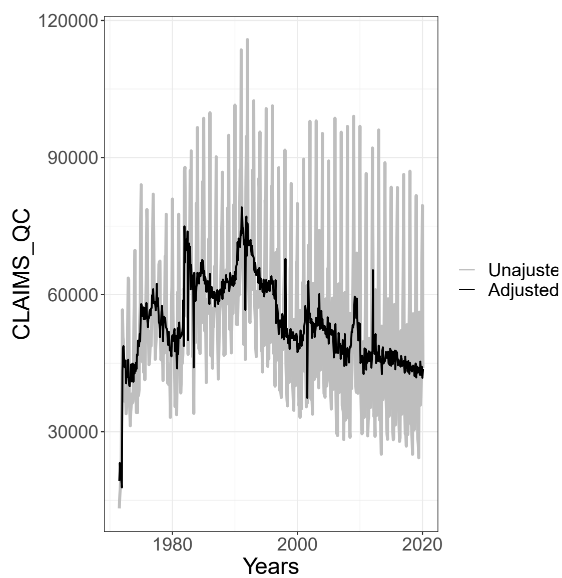

(c) Québec

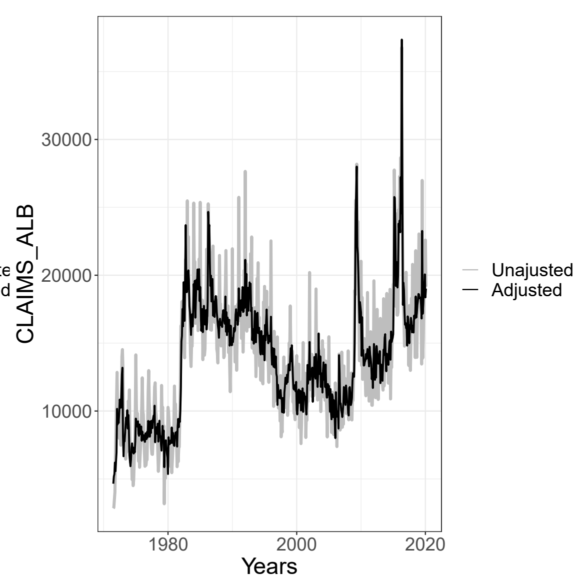

(d) Alberta

latter has almost the opposite behaviour, but ends up being related to inflation and few international flows. The remaining factors are hard to interpret over time.

Figure C.3: Heatmaps for factors 1 to 4

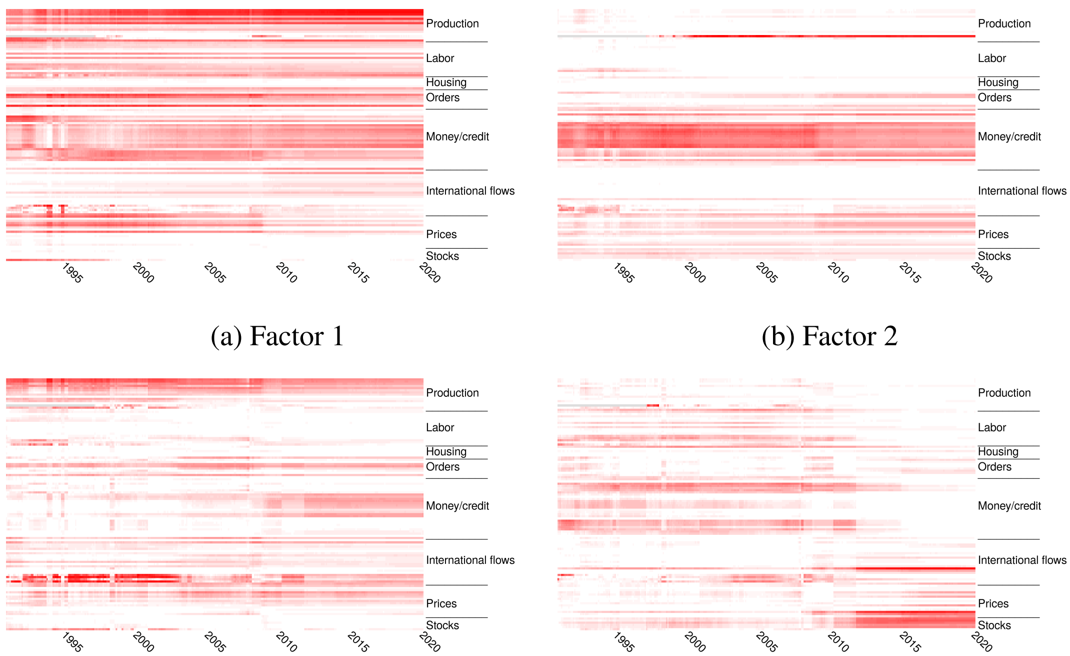

(a) Factor 1

(b) Factor 2

(c) Factor 3

(d) Factor 4

Note: Factors and loadings are estimated recursively using an expanding window. Displayed shades of red capture squared loadings.

Figure C.4: Heatmaps for factors 5 to 8

(a) Factor 5

(b) Factor 6

(c) Factor 7

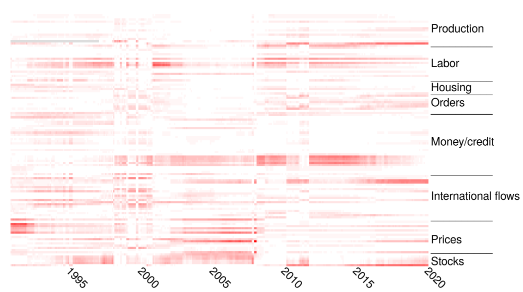

(d) Factor 8

Note: Factors and loadings are estimated recursively using an expanding window. Displayed shades of red capture squared loadings.

Table C.2: Top ten explained series for factors 1 to 4

Factor 1		
1991M1-2005M1	2005M1-2010M1	2010M1-2019M12
DUR_INV_RAT_new	BSI_new	BSI_new
MANU_INV_RAT_new	GDP_new	GDP_new
BSI_new	GPI_new	GPI_new
GPI_new	IP_new	IP_new
DM_new	DUR_INV_RAT_new	DM_new
GDP_new	DM_new	EMP_CAN
IP_new	MANU_INV_RAT_new	DUR_INV_RAT_new
EMP_CAN	EMP_CAN	MANU_INV_RAT_new
N_DUR_INV_RAT_new	N_DUR_INV_RAT_new	TBILL_3M
CPI_MINUS_FEN_CAN	CPI_MINUS_FEN_CAN	TBILL_6M
Factor 2		
1991M1-2005M1	2005M1-2010M1	2010M1-2019M12
TBILL_6M	GOV_AVG_1_3Y	G_AVG_10p.TBILL_3M
GOV_AVG_1_3Y	TBILL_6M	CRED_T
TBILL_3M	TBILL_3M	CRE_BUS
BANK_RATE_L	PC_PAPER_3M	G_AVG_5.10.Bank_rate
PC_PAPER_3M	GOV_AVG_3_5Y	TBILL_6M
GOV_AVG_3_5Y	BANK_RATE_L	GOV_AVG_1_3Y
MORTG_1Y	GOV_AVG_5_10Y	PC_PAPER_3M
MORTG_5Y	MORTG_5Y	TBILL_3M
GOV_AVG_5_10Y	MORTG_1Y	BANK_RATE_L
Factor 3		
1991M1-2005M1	2005M1-2010M1	2010M1-2019M12
CAN_SEC_NETFLOW	GDP_new	GDP_new
CAN_US_SEC_NETFLOW	GPI_new	BSI_new
GDP_new	BSI_new	CPI_MINUS_FOO_CAN
BSI_new	IP_new	GPI_new
CAN_EQTY_NETFLOW	CPI_MINUS_FOO_CAN	N_DUR_INV_RAT_new
GPI_new	N_DUR_INV_RAT_new	GOV_AVG_1_3Y
SPI_new	Exp_BP_new	CAN_US_SEC_NETFLOW
IP_new	MANU_INV_RAT_new	PC_PAPER_3M
CPI_MINUS_FOO_CAN	Imp_BP_new	TBILL_6M
N_DUR_INV_RAT_new	DUR_INV_RAT_new	TBILL_3M
Factor 4		
1991M1-2005M1	2005M1-2010M1	2010M1-2019M12
CRED_T	CRED_T	USDCAD_new
CRED_HOUS	CRED_HOUS	IPPI_MOTOR_CAN
NHOUSE_P_CAN	NHOUSE_P_CAN	TSX_LO
G_AVG_1.3.Bank_rate	CRED_CONS	TSX_CLO
UNEMP_DURAvg_CAN_new	EMP_CAN	TSX_HI
CRED_MORT	G_AVG_1.3.Bank_rate	IPPI_MACH_CAN
USDCAD_new	CAN_US_SEC_NETFLOW	SP500
G_AVG_3.5.Bank_rate	G_AVG_3.5.Bank_rate	DJ_CLO
CRED_CONS	G_AVG_5.10.Bank_rate	JPYCAD_new
EMP_CAN	CRED_MORT	WTISPLC

Note: Factor loadings estimated recursively with an expanding window. Rankings are based on mean squared loadings over the indicated period.

Table C.3: Top ten explained series for factors 5 to 8

Factor 5		
1991M1-2005M1	2005M1-2010M1	2010M1-2019M12
DUR_N_ORD_new	SP500	UNEMP_DURAvg_CAN_new
MANU_UNFIL_new	DJ_CLO	CRED_T
DUR_UNFIL_new	TSX_LO	CRED_HOUS
MANU_N_ORD_new	USDCAD_new	G_AVG_1.3.Bank_rate
GOOD_HRS_CAN	TSX_CLO	G_AVG_3.5.Bank_rate
CAN_US_SEC_NETFLOW	TSX_HI	CLAIMS_CAN
CAN_EQTY_NETFLOW	IPPI_MOTOR_CAN	G_AVG_5.10.Bank_rate
WT_new	IPPI_CAN	NHOUSE_P_CAN
FOR_SEC_NETFLOW	CAN_SEC_NETFLOW	CRED_MORT
Imp_BP_new	CAN_US_SEC_NETFLOW	G_AVG_10p.TBILL_3M
Factor 6		
1991M1-2005M1	2005M1-2010M1	2010M1-2019M12
DJ_CLO	MANU_UNFIL_new	IPPI_ENER_CAN
SP500	DUR_UNFIL_new	IPPI_CAN
TSX_LO	DUR_N_ORD_new	CAN_US_SEC_NETFLOW
TSX_CLO	DUR_TOT_INV_new	CAN_EQTY_NETFLOW
TSX_HI	MANU_TOT_INV_new	CPI_GOO_CAN
MANU_UNFIL_new	OIL_ALB_new	CAN_SEC_NETFLOW
DUR_UNFIL_new	MANU_N_ORD_new	CPI_MINUS_FOO_CAN
DUR_N_ORD_new	OIL_CAN_new	CPI_ALL_CAN
MANU_TOT_INV_new	DJ_CLO	MANU_TOT_INV_new
IPPI_CAN	SP500	WTISPLC
Factor 7		
1991M1-2005M1	2005M1-2010M1	2010M1-2019M12
Exp_BP_new	IPPI_ENER_CAN	G_AVG_1.3.Bank_rate
Imp_BP_new	WTISPLC	DJ_CLO
DUR_TOT_INV_new	EX_TRANSP_BP_new	SP500
EX_TRANSP_BP_new	CAN_EQTY_NETFLOW	G_AVG_3.5.Bank_rate
MANU_TOT_INV_new	CAN_SEC_NETFLOW	IPPI_ENER_CAN
IMP_TRANSP_BP_new	CAN_US_SEC_NETFLOW	EOIL_BP_new
OIL_CAN_new	EX_ENER_BP_new	WTISPLC
OIL_ALB_new	EOIL_BP_new	TBILL_6M.Bank_rate
TBILL_6M.Bank_rate	IMP_TRANSP_BP_new	EX_ENER_BP_new
IPPI_METAL_CAN	Exp_BP_new	EX_TRANSP_BP_new
Factor 8		
1991M1-2005M1	2005M1-2010M1	2010M1-2019M12
UNEMP_DURA_1.4_CAN	IPPI_ENER_CAN	OIL_ALB_new
CPI_GOO_CAN	CPI_GOO_CAN	OIL_CAN_new
UNEMP_CAN	G_AVG_1.3.Bank_rate	G_AVG_1.3.Bank_rate
CPI_ALL_CAN	CPI_ALL_CAN	EOIL_BP_new
IPPI_CAN	G_AVG_3.5.Bank_rate	EMP_MANU_CAN
EX_TRANSP_BP_new	G_AVG_5.10.Bank_rate	EX_ENER_BP_new
EMP_MANU_CAN	CPI_MINUS_FOO_CAN	TBILL_6M.Bank_rate
USDCAD_new	WTISPLC	G_AVG_3.5.Bank_rate
SP500	TBILL_6M.Bank_rate	UNEMP_CAN
TSX_CLO	G_AVG_10p.TBILL_3M	G_AVG_5.10.Bank_rate

Note: Factor loadings estimated recursively with an expanding window. Rankings are based on mean squared loadings over the indicated period.

C.1.3 Forecasting results: rolling window

Table C.4: Forecasting real activity

	Industrial Production				Employment				Unemployment			
Models	h=1	h=3	h=6	h=12	h=1	h=3	h=6	h=12	h=1	h=3	h=6	h=12
AR,BIC (RMSE)	0.010	0.006	0.005	0.004	0.002	0.001	0.001	0.001	0.186	0.111	0.093	0.083
ARDI,BIC	0.96**	0.90***	0.97	0.91**	0.97	0.98	1.00	1.00	0.96**	0.88**	0.85***	0.91**
Elastic-Net-X	0.95**	0.91***	0.96	1.03	1.00	1.08*	1.11**	1.22***	1.02	0.94	0.96	1.15***
Ridge-X	0.95***	0.93***	0.92***	0.95	1.02	1.04	1.05	1.02	0.97*	0.90***	0.89***	0.97
Lasso-X	0.94***	0.92***	0.94**	1.00	0.99	1.02	1.06*	1.23***	0.99	0.96	0.98	1.12**
Adaptive-Lasso-X	0.95***	0.92***	0.93**	1.00	0.99	1.01	1.07*	1.21***	1.00	0.95	0.95	1.10**
RF-X	0.95***	0.95**	0.99	0.92**	0.99	1.00	1.03	1.04	0.95***	0.93**	0.98	1.04
ARDI,Elastic-Net	0.96**	0.93***	0.95*	1.11	0.99	1.04	1.00	1.06	1.00	0.90**	0.92*	0.98
ARDI,Ridge	0.97***	0.97*	0.97**	1.08	1.05	1.10*	1.02	1.09	0.98*	0.91***	0.89***	0.92*
ARDI,Lasso	0.96***	0.93***	0.93**	0.89**	0.98	1.00	1.04	1.04	0.99	0.92**	0.91**	1.06
ARDI,Adaptive-Lasso	0.96**	0.95**	0.93**	0.89**	0.98*	0.99	1.01	1.01	0.99	0.90**	0.90***	1.10
RFARDI	0.96***	0.94***	0.94***	0.92***	0.99	1.04	1.04	1.04	0.97**	0.93*	0.92***	0.97
T-CSR5	0.95***	0.92***	0.96	0.92**	0.97*	0.95*	0.96*	1.00	0.97*	0.92**	0.90***	0.96
T-CSR10	0.95***	0.92***	0.99	1.00	0.99	0.96	0.96	1.02	0.97	0.92**	0.89***	1.01
T-CSR20	0.97	0.96	1.07	1.16**	1.04*	1.01	1.01	1.09	1.00	0.98	0.93	1.15*

Note: See table 3.3.

Table C.5: Forecasting inflation

	CPI				Core CPI			
Models	h=1	h=3	h=6	h=12	h=1	h=3	h=6	h=12
AR,BIC (RMSE)	0.004	0.002	0.002	0.001	0.003	0.002	0.001	0.001
ARDI,BIC	0.99	0.99	1.04	0.83**	0.99	0.97	0.98	0.90
Elastic-Net-X	0.96***	0.94***	1.04	1.04	0.93***	0.94**	1.09*	1.03
Ridge-X	0.98**	0.97***	0.99	0.82**	0.97	1.01	0.97	0.94
Lasso-X	0.96***	0.95***	1.03	0.93	0.94***	0.96	1.10**	0.99
Adaptive-Lasso-X	0.96***	0.94***	1.02	0.95	0.94***	0.97*	1.10**	0.97
RF-X	0.95***	0.95***	0.98	0.87***	0.93***	0.94**	1.00	0.87**
ARDI,Elastic-Net	0.98*	0.99	1.13*	0.98	0.95***	0.94**	0.96	1.01
ARDI,Ridge	0.99	0.98***	1.03	0.98	0.99	1.04**	1.07***	0.97**
ARDI,Lasso	1.00	0.97*	1.09*	0.84**	0.96***	0.99	1.00	0.93
ARDI,Adaptive-Lasso	0.99	0.98*	1.12*	0.86**	0.96**	0.99	0.99	0.93
RFARDI	0.98**	0.94***	0.95	0.90***	0.95***	0.96	0.91*	0.91**
T-CSR5	0.97*	0.97	1.01	0.90**	0.95***	0.95*	1.03	0.97
T-CSR10	0.99	1.01	1.06	0.88**	0.97**	0.97	1.09*	1.02
T-CSR20	1.02	1.05	1.19***	0.92	1.01	1.01	1.17**	1.12

Note: See table 3.3.

Table C.6: Forecasting credit markets

	Total Credit				Business Credit				Consumption Credit			
Models	h=1	h=3	h=6	h=12	h=1	h=3	h=6	h=12	h=1	h=3	h=6	h=12
AR,BIC (RMSE)	0.002	0.001	0.001	0.002	0.003	0.002	0.002	0.002	0.003	0.002	0.002	0.003
ARDI,BIC	1.04**	1.04*	1.03	0.97	1.00	1.03	0.99	1.00	1.04**	1.04*	1.02	1.04
Elastic-Net-X	1.01	0.99	1.18***	1.24***	0.98	0.95*	1.04	1.12*	1.06**	1.10**	1.10*	1.15***

Table C.6: Forecasting credit markets

	Total Credit				Business Credit				Consumption Credit			
Models	h=1	h=3	h=6	h=12	h=1	h=3	h=6	h=12	h=1	h=3	h=6	h=12
Ridge-X	1.08**	1.09*	1.27***	1.30***	1.01	1.05	1.13**	1.07	1.12***	1.13***	1.14***	1.13***
Lasso-X	1.02	0.98	1.16***	1.22***	1.01	0.92**	1.01	1.12*	1.09**	1.09**	1.10*	1.16***
Adaptive-Lasso-X	1.04	1.01	1.16***	1.23***	1.00	0.95*	1.04	1.13*	1.09**	1.11**	1.10*	1.15***
RF-X	1.00	1.09*	1.22**	1.28***	1.00	1.06*	1.18***	1.18**	1.02	1.08*	1.16**	1.23***
ARDI,Elastic-Net	1.03*	1.01	1.07**	1.19**	1.00	0.98	0.94*	1.13	1.08***	1.03	1.02	1.10
ARDI,Ridge	1.28***	1.15***	1.31***	1.26***	1.10***	1.18**	1.11**	1.02	1.24***	1.34***	1.24***	1.15***
ARDI,Lasso	1.04*	0.98	1.02	1.20***	1.00	0.93*	0.93**	1.03	1.07***	1.09**	1.00	1.03
ARDI,Adaptive-Lasso	1.02	0.99	1.03	1.23***	1.00	0.93*	0.93*	1.10*	1.08***	1.03	1.02	1.05
RFARDI	1.01	1.06*	1.18***	1.15***	0.98	1.01	1.12***	1.09**	1.02	1.04	1.05	1.08**
T-CSR5	1.00	0.95**	0.96*	1.10**	0.98*	0.93***	0.90***	0.95*	0.97	0.96**	0.96*	1.00
T-CSR10	1.04**	0.99	1.00	1.22***	1.02	0.96*	0.90***	1.01	1.01	0.99	0.98	1.03
T-CSR20	1.13***	1.10**	1.13**	1.39***	1.08***	1.01	0.95*	1.15**	1.07**	1.10**	1.06	1.07

Note: See table 3.3.

Table C.7: Forecasting the housing market

	Housing starts				Building Permits			
Models	h=1	h=3	h=6	h=12	h=1	h=3	h=6	h=12
AR,BIC (RMSE)	0.090	0.041	0.027	0.018	0.078	0.033	0.021	0.014
ARDI,BIC	1.00	1.05*	1.03	1.06	1.02**	1.03*	1.03***	1.06**
Elastic-Net-X	1.11***	1.03*	1.06**	1.23***	1.14***	1.06*	1.09***	1.22***
Ridge-X	1.07***	1.02	1.01	1.18***	1.10***	1.05**	1.07**	1.12***
Lasso-X	1.05**	1.04*	1.01	1.18**	1.07***	1.04	1.07**	1.26***
Adaptive-Lasso-X	1.05***	1.02	1.02	1.08**	1.08***	1.04*	1.04*	1.14**
RF-X	1.06***	1.02	1.04**	1.06**	1.07***	1.04*	1.07**	1.04
ARDI,Elastic-Net	1.05***	1.03	1.05***	1.09**	1.08***	1.03	1.11**	1.22**
ARDI,Ridge	1.07***	1.02	1.00	1.05**	1.10***	1.04*	1.06**	1.04
ARDI,Lasso	1.04***	1.02	1.04*	1.10***	1.06***	1.04**	1.05*	1.19**
ARDI,Adaptive-Lasso	1.03**	1.01	1.03**	1.13***	1.06***	1.03*	1.08**	1.20**
RFARDI	1.07***	1.03	1.02	1.04**	1.07***	1.04*	1.07**	1.04
T-CSR5	1.02	1.06	1.04	1.08*	1.02	1.03	1.03	1.06*
T-CSR10	1.05**	1.10**	1.08**	1.17**	1.05***	1.06**	1.08**	1.15**
T-CSR20	1.08***	1.20***	1.25***	1.40**	1.12***	1.13***	1.18***	1.40**

Note: See table 3.3.

Figure C.5: Forecasting performance over time: fluctuation test

Note: The figure shows the Giacomini-Rossi fluctuation test for best RMSPE models against the ARD benchmark. Solide lines correspond to 10% critical value.

C.1.4 Impulse response functions

Figure C.6 show the main results for the aggregate series when considering observations from 1981M01 to 2015M10. When looking at inflation and unemployment one pattern emerge, monetary shocks have larger effects in central Canada (Québec and Ontario) than in the prairies, British-Columbia and New Foundland. The effect on inflation is slowly decaying as one move west and the shape of the IRFs for unemployment follow a hump shape in Québec and Ontario while it's less clear in the other provinces. Unemployment in Alberta and British Columbia eventually rises but the effect in Manitoba and Saskatchewan are quite small and counterintuitive with reductions in unemployment after around two years. We can also see a similar pattern for total employment but in this case Manitoba joins Québec and Ontario with decreases in employment following a monetary policy shock. Atlantic provinces are affected the most by the shock. In Québec and Ontario housing starts drops while it takes more time in Alberta and British-Columbia and we see the opposite in Manitoba and Saskatchewan with an increase in housing starts. As for housing prices, they clearly decrease in Ontario, Alberta and British-Columbia but increases in Québec before starting to decrease after 30 months. Manitoba and Saskatchewan have again their own specific patterns with increases in housing prices.

Figure C.7 reports same IRFs but estimated since inflation targeting. Using only the inflation targeting (IT) period we find similar results to those of Champagne and Sekkel (2018) when looking specifically at Canada. Figure C.8 shows that monetary policy shocks in Canada have smaller effects in the IT period than in the entire period. While prices dropped by 2% in the full sample they only drop by around 0.7 % in the post-1992 estimation.[1] The differences for unemployment are even more important as the shocks no longer have a significant effect using in the IT period. This suggests that monetary policy have become more effective since inflation targeting (Boivin and Giannoni, 2006). We find similar results for the provinces but again there are important differences. Monetary policy continued to have significant effects on prices in Québec and Ontario but not in the other provinces. The effect on unemployment is interesting as Ontario's unemployment rate is no longer affected by monetary policy shocks but Québec's and Manitoba's are.

---

[1]We also find smaller effects of monetary policy shocks in the post-1992 period for price components.

Figure C.6: Impulse response functions of aggregate series - 1981m1-2015m10

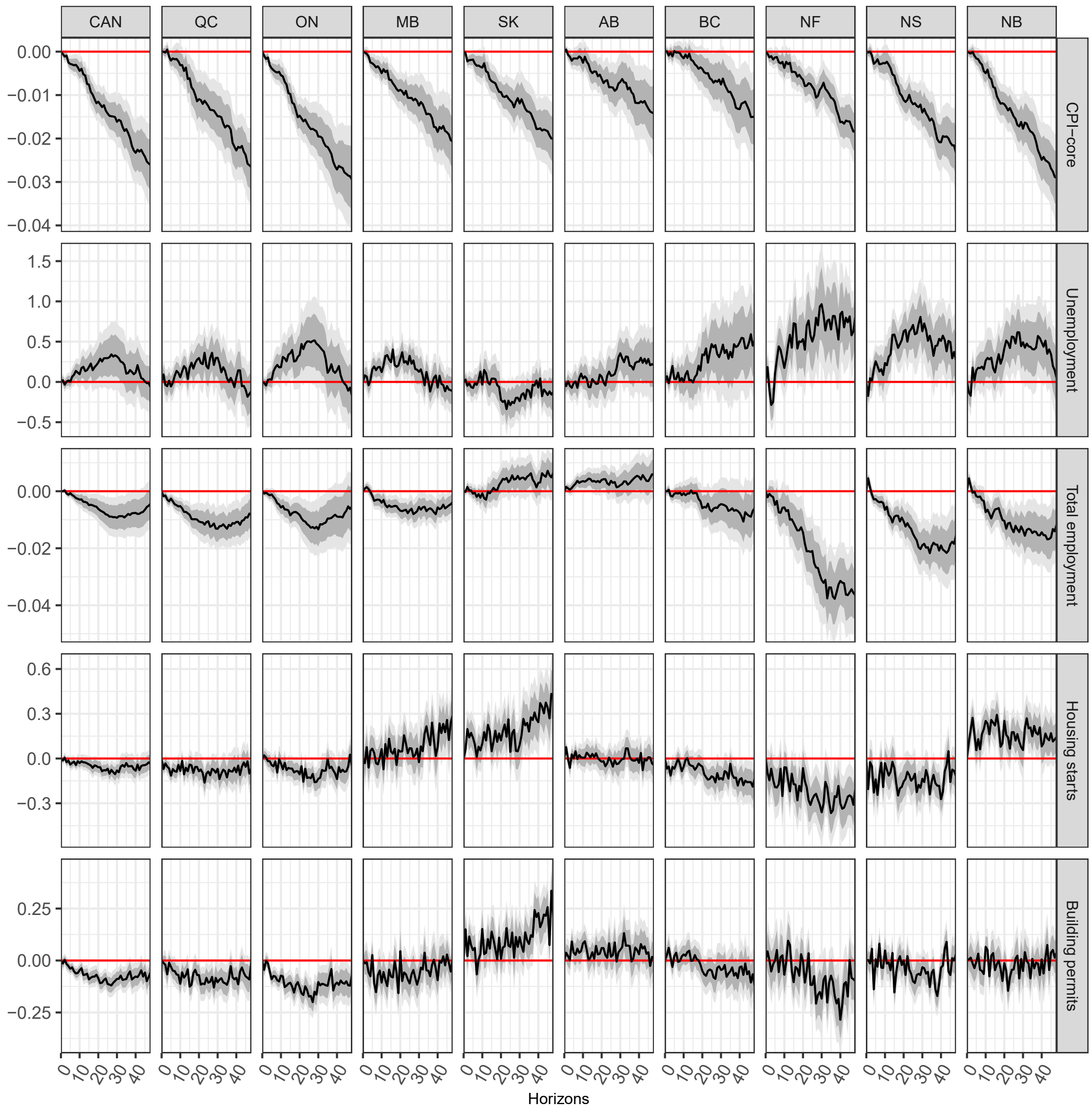

Note: Dark and light gray shades are 68% and 90% confidence bands constructed using HAC standard errors.

Figure C.7: Impulse response functions of aggregate series - 1992m1-2015m10

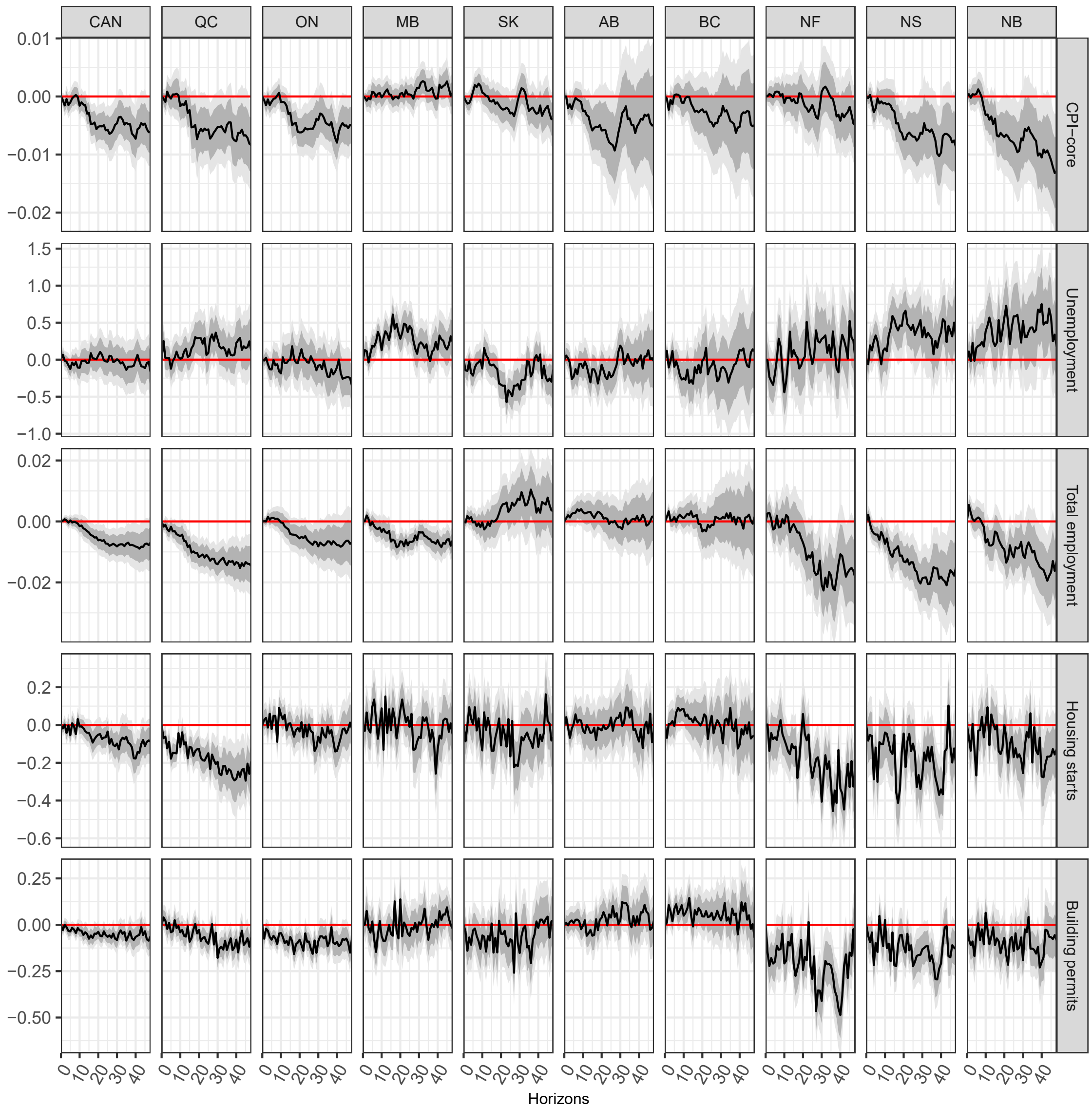

Note: Dark and light gray shades are 68% and 90% confidence bands constructed using HAC standard errors.

Figure C.8: Comparison of IRFs: full sample versus IT period

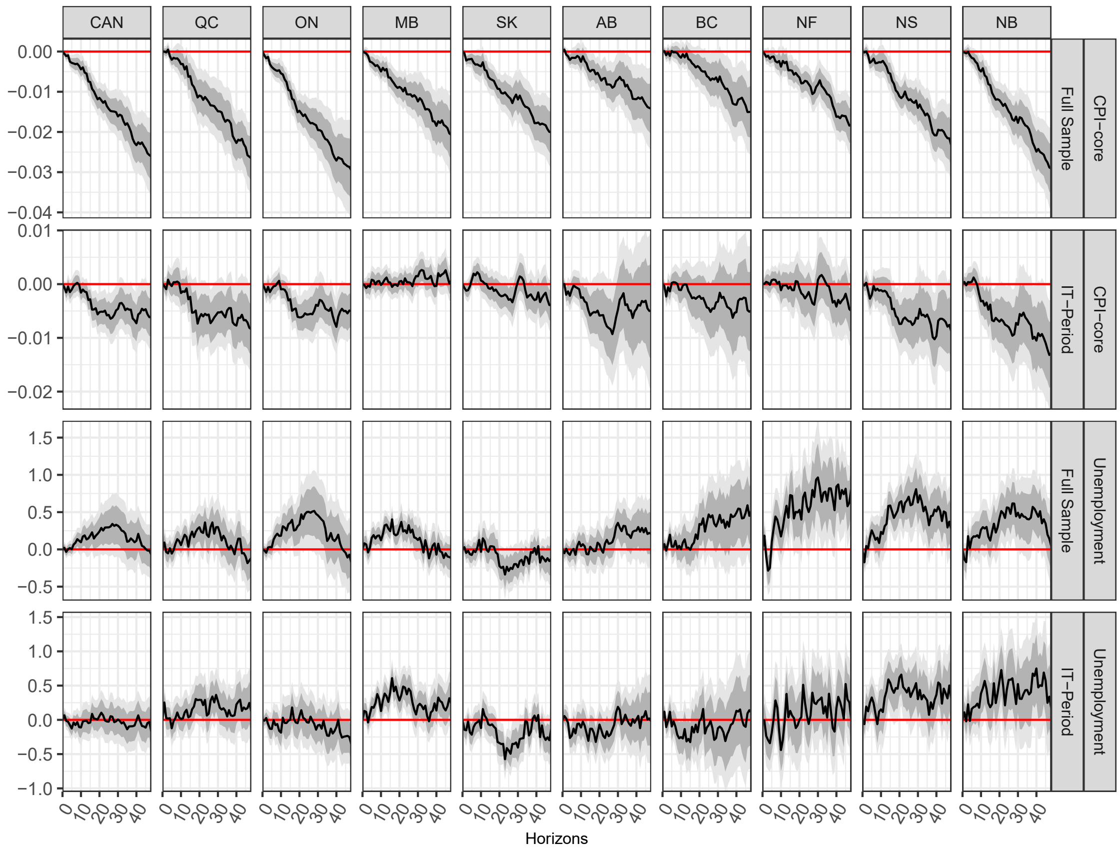

Note: Dark and light gray shades are 68% and 90% confidence bands constructed using HAC standard errors.

Figure C.9: Comparison of IRFs: CPI - full sample

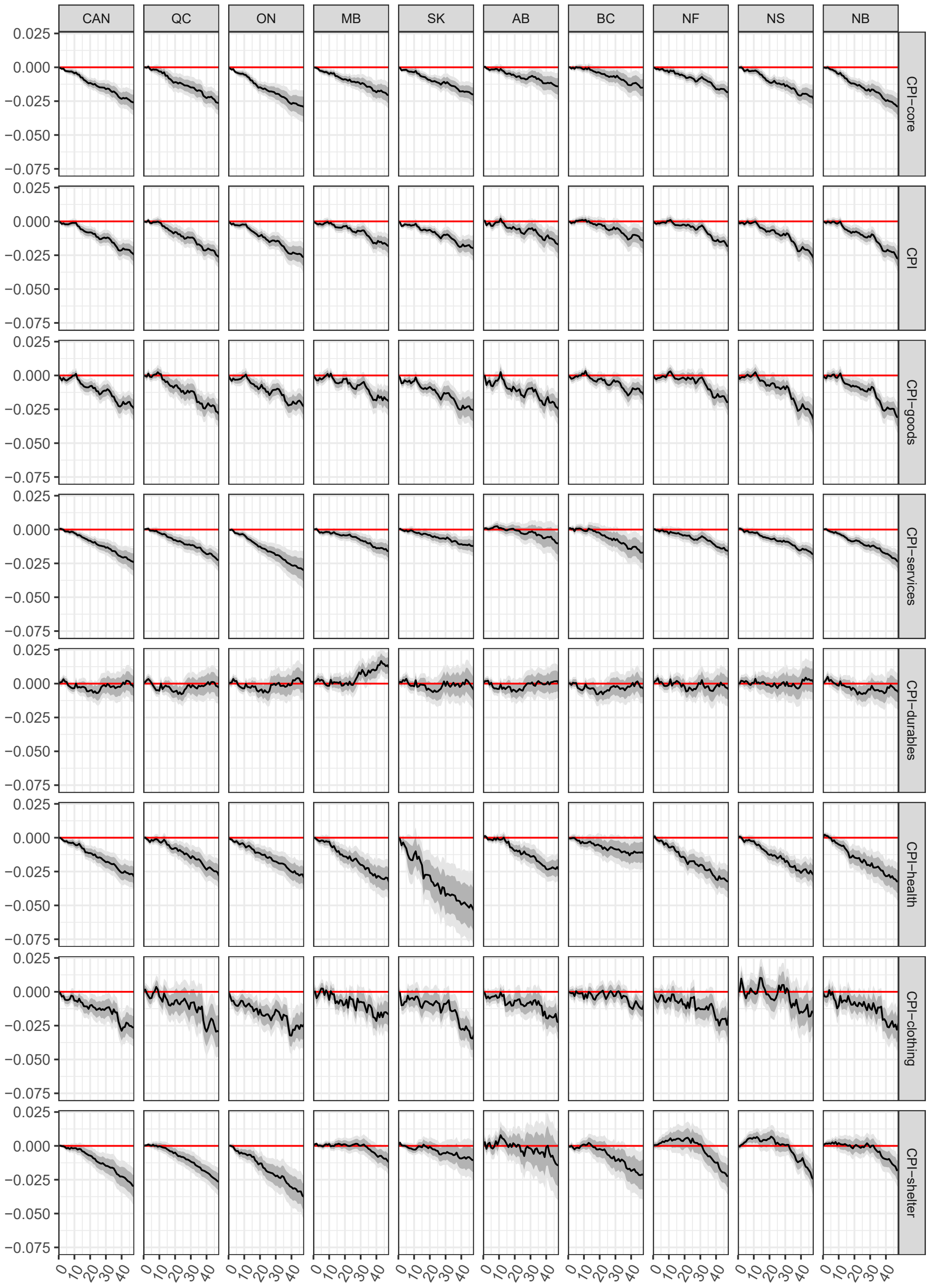

Note: Dark and light gray shades are 68% and 90% confidence bands constructed using HAC standard errors.

Figure C.10: Comparison of IRFs: CPI - IT period

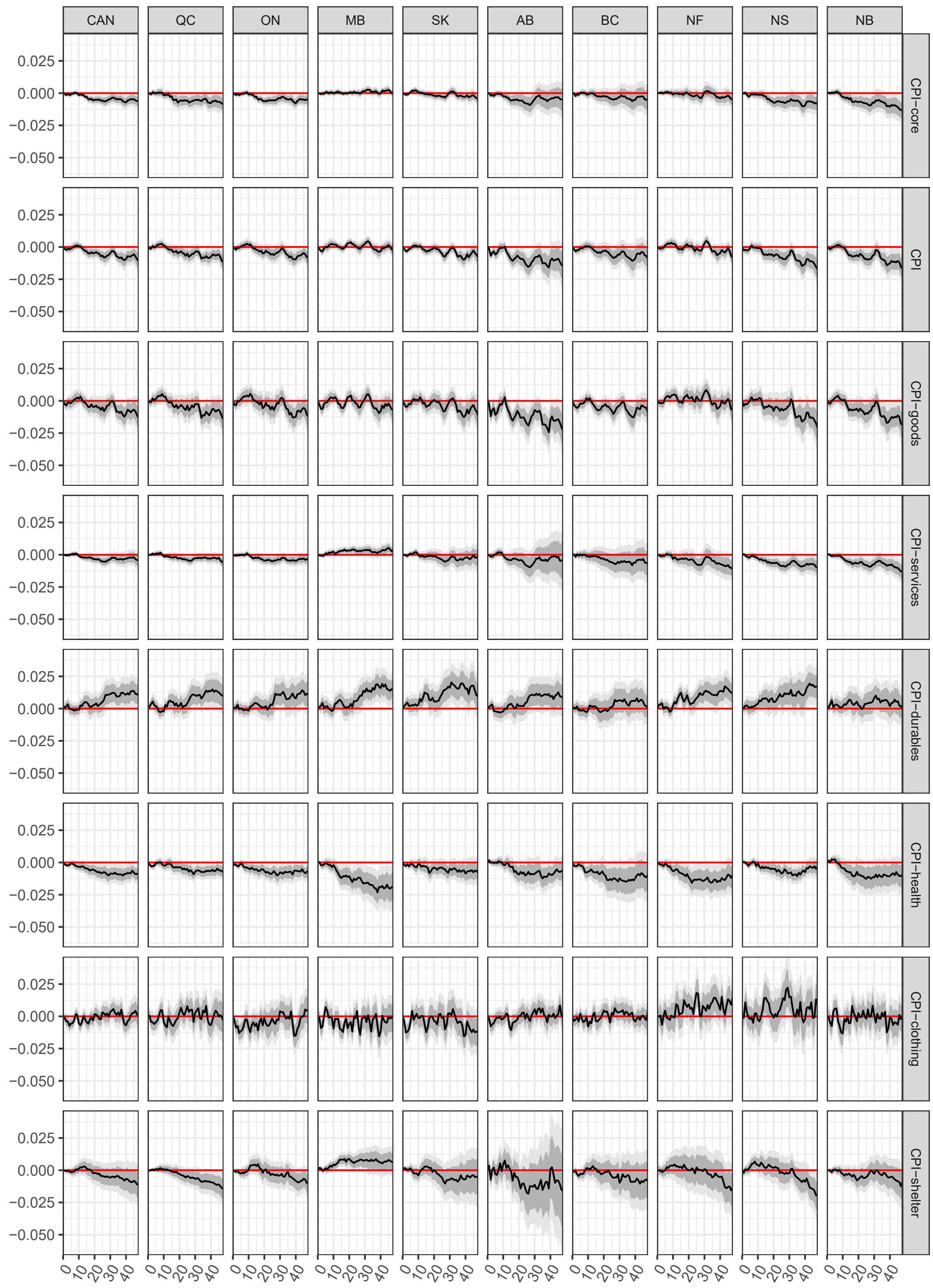

Note: Dark and light gray shades are 68% and 90% confidence bands constructed using HAC standard errors.

Figure C.11: Comparison of IRFs: EMP - full sample

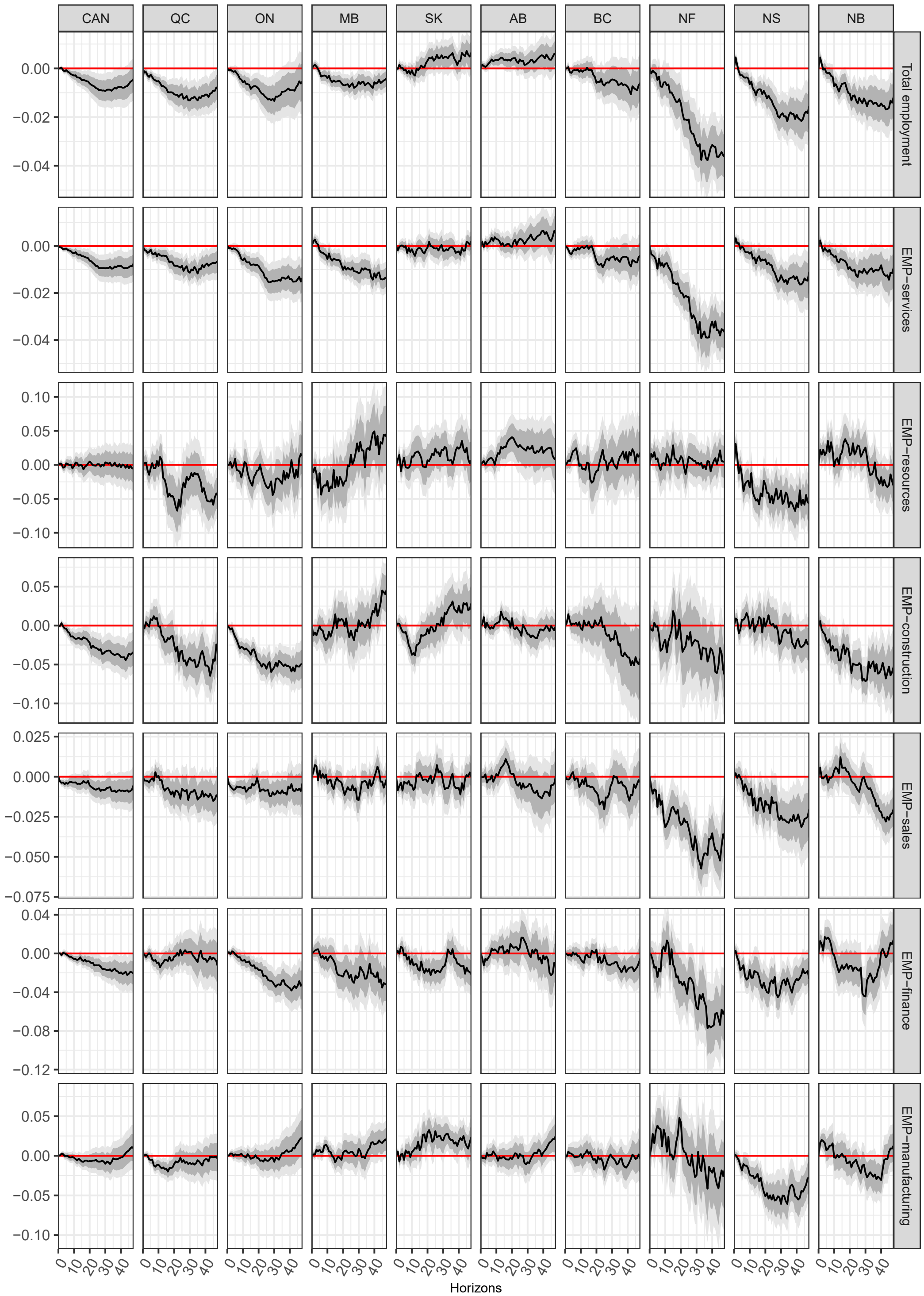

Note: Dark and light gray shades are 68% and 90% confidence bands constructed using HAC standard errors.

Figure C.12: Comparison of IRFs: EMP - IT period

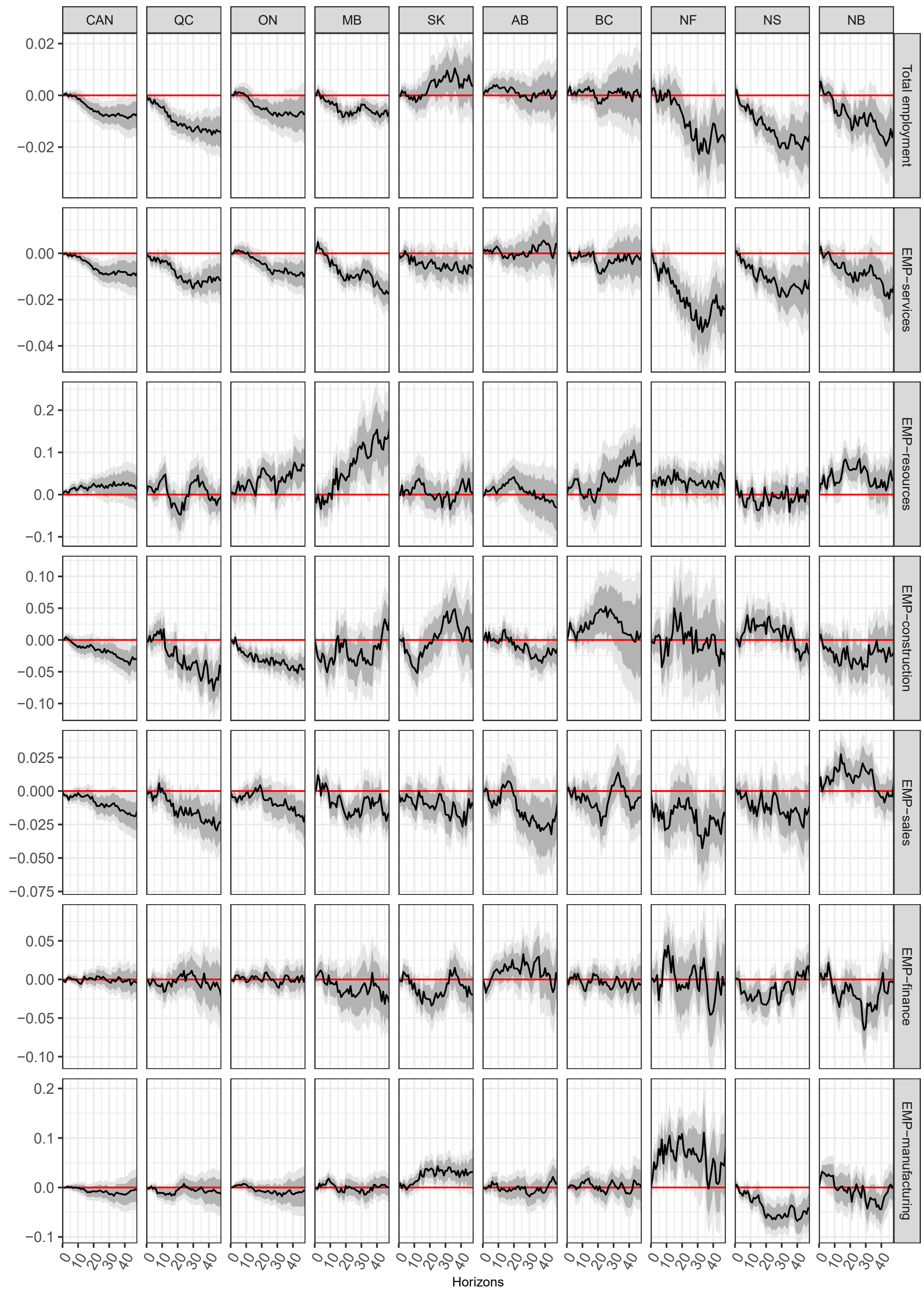

Note: Dark and light gray shades are 68% and 90% confidence bands constructed using HAC standard errors.

C.2 Data Set

The transformation codes are: 1 - no transformation; 2 - first difference; 4 - logarithm; 5 - first difference of logarithm. Vector(1) and Vector(2) indicate StatCan vectors. When different series are needed to construct an indicator of interest because of the break indicated by column Date, Vector(1) is the most recent series. Some variables are taken from the Federal Reserve of St-Louis Economic Data Base (FRED), from the Bank of Canada (BoC) and Yahoo Finance.

No	Variable	Description	Region	Vector(1)	Vector(2)	Date	T-code
		PRODUCTION					
1	GDP_new	GDP total	CAN	v41881478	v65201483	1997M1	5
2	BSI_new	GDP business	CAN	v41881479	v65201486	2007M1	5
3	GPI_new	GDP goods	CAN	v41881485	v65201484	1997M1	5
4	SPI_new	GDP services	CAN	v41881486	v65201485	1997M1	5
5	IP_new	GDP industrial production	CAN	v41881487	v65201492	1997M1	5
6	NDM_new	GDP non durable goods	CAN	v41881488	v65201493	1997M1	5
7	DM_new	GDP durables	CAN	v41881489	v65201494	1997M1	5
8	OILP_new	GDP mining, petrol and gas	CAN	v41881501	v65201509	1997M1	5
9	CON_new	GDP construction	CAN	v41881523	v65201531	1997M1	5
10	RT_new	GDP retail trade	CAN	v41881688	v65201641	1997M1	5
11	WT_new	GDP wholesale trade	CAN	v41881689	v65201631	1997M1	5
12	PA_new	GDP public administration	CAN	v41881775	v65201749	1997M1	5
13	FIN_new	GDP finance and insurance	CAN	v41881725	v65201680	1997M1	5
14	OIL_CAN_new	Crude oil production (Cubic meters)	CAN	v17948	v107757044	2016M1	5
15	OIL_ALB_new	Crude oil production (ALB) (Cubic meters)	ALB	v18050	v107757710	2016M1	5
		LABOR MARKET					
16	EMP_CAN	Employment total	CAN	v24793			5
17	EMP_SERV_CAN	Employment services	CAN	v2057610			5
18	EMP_FOR_OIL_CAN	Employment forestry, fishing, mining, oil and gas	CAN	v2057606			5
19	EMP_CONS_CAN	Employment construction	CAN	v2057608			5
20	EMP_SALES_CAN	Employment sales (wholesale and retail trade)	CAN	v2057611			5
21	EMP_FIN_CAN	Employment finance, insurance and real estate	CAN	v2057613			5
22	EMP_MANU_CAN	Employment manufacturing	CAN	v2057609			5
23	EMP_PART_CAN	Employment part time	CAN	v2062813			5
24	UNEMP_CAN	Unemployment rate LRUNTTTTCAM156S	CAN	(FRED)	v2062815	1976M1	2
25	UNEMP_DURA_1-4_CAN	Unemployment duration (1-4 weeks)	CAN	v1078667742			5
26	UNEMP_DURA_5-13_CAN	Unemployment duration (5-13 weeks)	CAN	v1078667850			5
27	UNEMP_DURA_14-25_CAN	Unemployment duration (14-24 weeks)	CAN	v1078667958			5
28	UNEMP_DURA_27+_CAN	Unemployment duration (27+ weeks)	CAN	v1078668066			5
29	UNEMP_DURAvg_CAN_new	Unemployment average duration	CAN	v3433887	v1078668391	1997M1	5
30	CLAIMS_CAN	Employment insurance initial claims, Allowed	CAN	v383942			1
31	TOT_HRS_CAN	Hours worked total	CAN	v4391505			5
32	GOOD_HRS_CAN	Hours worked goods	CAN	v4391507			5
		HOUSING AND CONSTRUCTION					
33	NHOUSE_P_CAN	New housing price index, Total (house and land)	CAN	v111955442			5
34	hstart_CAN_new	Housing starts (units)	CAN	v730413	v52300157	1990M1	5
35	build_Total_CAN_new	Building permits (tous)	CAN	v42061	v121293395	2011M1	5
36	build_Ind_CAN_new	Building permits (industries)	CAN	v42064	v121301795	2011M1	5
37	build_Comm_CAN_new	Building permits (commerce)	CAN	v42065	v121304915	2011M1	5

No	Variable	Description	Region	Vector(1)	Vector(2)	Date	T-code
		MANUFACTURING, SALES AND INVENTORIES					
38	MANU_N_ORD_new	Manufacturing new orders (total)	CAN	v723019	v800913	1992M1	5
39	MANU_UNFIL_new	Manufacturing unfilled orders (total)	CAN	v723313	v803189	1992M1	5
40	MANU_TOT_INV_new	Manufacturing inventories (total)	CAN	v724933	v803227	1992M1	5
41	MANU_INV_RAT_new	Manufacturing inventories to shipments ratio (total)	CAN	v725059	v803313	1992M1	1
42	N_DUR_INV_RAT_new	Manufacturing inventories to shipments ratio (durables)	CAN	v725060	v803314	1992M1	1
43	DUR_N_ORD_new	Manufacturing new orders (durables)	CAN	v723034	v800926	1992M1	5
44	DUR_UNFIL_new	Manufacturing unfilled orders (durables)	CAN	v723328	v803202	1992M1	5
45	DUR_TOT_INV_new	Manufacturing inventories (durables)	CAN	v724948	v803240	1992M1	5
46	DUR_INV_RAT_new	Manufacturing inventories to shipments ratio (durables)	CAN	v725074	v803326	1992M1	1
		MONEY AND CREDIT					
47	M3	M3 (gross)	CAN	v41552794			5
48	M2p	M2+ (gross)	CAN	v41552798			5
49	M_BASE1	Monetary base	CAN	v37145			5
50	CRED_T	Total credit	CAN	v36414			5
51	CRED_HOUS	Household credit	CAN	v36415			5
52	CRED_MORT	Mortgage credit	CAN	v36416			5
53	CRED_CONS	Consumption credit	CAN	v36417			5
54	CRE_BUS	Business credit	CAN	v36418			5
55	BANK_RATE_L	Bank rate	CAN	v122550			2
56	PC_PAPER_1M	Corporate paper rate (1 month)	CAN	v122509	IIROC	2019M1	2
57	PC_PAPER_3M	Corporate paper rate (3 months)	CAN	v122491	IIROC	2019M1	2
58	GOV_AVG_1_3Y	Governmental bonds (average rate) (1-3 years)	CAN	v122558			2
59	GOV_AVG_3_5Y	Governmental bonds (average rate) (3-5 years)	CAN	v122485			2
60	GOV_AVG_5_10Y	Governmental bonds (average rate) (5-10 years)	CAN	v122486			2
61	GOV_AVG_10pY	Governmental bonds (average rate) (10+ years)	CAN	v122487			2
62	MORTG_1Y	Mortgage rate (1 year) BoC	CAN	v122520	(V80691333)	2019M10	2
63	MORTG_5Y	Mortgage rate (5 years) BoC	CAN	v122521	(V80691335)	2019M10	2
64	TBILL_3M	Treasury bills (3 months)	CAN	v122541			2
65	TBILL_6M	Treasury bills (6 months)	CAN	v122552			2
66	PC_3M-Bank_rate	Corporate paper rate (3 months) - Bank rate	CAN	Difference			1
67	G_AVG_1-3-Bank_rate	Government bonds (1-3 years) - Bank rate	CAN	Difference			1
68	G_AVG_3-5-Bank_rate	Government bonds (3-5 years) - Bank rate	CAN	Difference			1
69	G_AVG_5-10-Bank_rate	Government bonds (5-10 years) - Bank rate	CAN	Difference			1
70	TBILL_6M-Bank_rate	Treasury bond (6 months) - Bank rate	CAN	Difference			1
71	G_AVG_10p-TBILL_3M	Government Bonds (10+ years) - TBILL_3M	CAN	Difference			1
		INTERNATIONAL TRADE AND FLOWS					
72	RES_TOT	Total Canada's official international reserves	CAN	v122396			5
73	RES_USD	Canadian USD reserves	CAN	v122398			5
74	RES_IMF	Canadian reserve position at the IMF	CAN	v122401			5
75	Imp_BP_new	Imports total	CAN	v183406	v1001826653	1988M1	5
76	IOIL_BP_new	Imports oil	CAN	v183426	v1001826667	1988M1	5
77	Exp_BP_new	Exports total	CAN	v191490	v1001827265	1988M1	5
78	EOIL_BP_new	Exports oil	CAN	v191516	v1001827279	1988M1	5
79	EX_ENER_BP_new	Export energy products	CAN	v191516	v1001827278	1988M1	5
	(Sum)	Export energy products	CAN	v191517	v1001827278	1988M1	
	(Sum)	Export energy products	CAN	v191504	v1001827278	1988M1	
	(Sum)	Export energy products	CAN	v191533	v1001827278	1988M1	
80	EX_MINER_BP_new	Exports non-metallic ores	CAN	v191511	v1001827292	1988M1	5
	(Sum)	Exports non-metallic ores	CAN	v191512	v1001827292	1988M1	
	(Sum)	Exports non-metallic ores	CAN	v191513	v1001827292	1988M1	
	(Sum)	Exports non-metallic ores	CAN	v191514	v1001827292	1988M1	
	(Sum)	Exports non-metallic ores	CAN	v191515	v1001827292	1988M1	
	(Sum)	Exports non-metallic ores	CAN	v191508	v1001827292	1988M1	
81	EX_METAL_BP_new	Exports metal and other mineral products	CAN	v191522	v1001827303	1988M1	5
	(Sum)	Exports metal and other mineral products	CAN	v191523	v1001827303	1988M1	

No	Variable	Description	Region	Vector(1)	Vector(2)	Date	T-code
	(Sum)	Exports metal and other mineral products	CAN	v191524	v1001827303	1988M1	
	(Sum)	Exports metal and other mineral products	CAN	v191525	v1001827303	1988M1	
	(Sum)	Exports metal and other mineral products	CAN	v191526	v1001827303	1988M1	
	(Sum)	Exports metal and other mineral products	CAN	v191527	v1001827303	1988M1	
	(Sum)	Exports metal and other mineral products	CAN	v191528	v1001827303	1988M1	
	(Sum)	Exports metal and other mineral products	CAN	v191529	v1001827303	1988M1	
	(Sum)	Exports metal and other mineral products	CAN	v191531	v1001827303	1988M1	
	(Sum)	Exports metal and other mineral products	CAN	v191532	v1001827303	1988M1	
	(Sum)	Exports metal and other mineral products	CAN	v191535	v1001827303	1988M1	
82	EX_IND_EQUIP_BP_new	Exports industrial machinery, pieces and equipment	CAN	v191545	v1001827350	1988M1	5
	(Sum)	Exports industrial machinery, pieces and equipment	CAN	v191549	v1001827350	1988M1	
	(Sum)	Exports industrial machinery, pieces and equipment	CAN	v191556	v1001827350	1988M1	
83	EX_TRANSP_BP_new	Exports motor vehicules and parts	CAN	v191550	v1001827369	1988M1	5
	(Sum)	Exports motor vehicules and parts	CAN	v191551	v1001827369	1988M1	
	(Sum)	Exports motor vehicules and parts	CAN	v191552	v1001827369	1988M1	
84	EX_CONS_BP_new	Exports consumption goods	CAN	v191492	v1001827385	1988M1	5
	(Sum)	Exports consumption goods	CAN	v191534	v1001827385	1988M1	
	(Sum)	Exports consumption goods	CAN	v191547	v1001827385	1988M1	
85	IMP_METAL_BP_new	Imports metal and other mineral products	CAN	v183446	v1001826691	1988M1	5
	(Sum)	Imports metal and other mineral products	CAN	v183447	v1001826691	1988M1	
	(Sum)	Imports metal and other mineral products	CAN	v183448	v1001826691	1988M1	
	(Sum)	Imports metal and other mineral products	CAN	v183435	v1001826691	1988M1	
	(Sum)	Imports metal and other mineral products	CAN	v183436	v1001826691	1988M1	
	(Sum)	Imports metal and other mineral products	CAN	v183439	v1001826691	1988M1	
86	IMP_IND_EQUIP_BP_new	Imports industrial machinery, pieces and equipment	CAN	v183450	v1001826738	1988M1	5
	(Sum)	Imports industrial machinery, pieces and equipment	CAN	v183461	v1001826738	1988M1	
	(Sum)	Imports industrial machinery, pieces and equipment	CAN	v183465	v1001826738	1988M1	
	(Sum)	Imports industrial machinery, pieces and equipment	CAN	v183466	v1001826738	1988M1	
	(Sum)	Imports industrial machinery, pieces and equipment	CAN	v183467	v1001826738	1988M1	
	(Sum)	Imports industrial machinery, pieces and equipment	CAN	v183468	v1001826738	1988M1	
87	IMP_TRANSP_BP_new	Imports motor vehicules and parts	CAN	v183469	v1001826757	1988M1	5
	(Sum)	Imports motor vehicules and parts	CAN	v183470	v1001826757	1988M1	
	(Sum)	Imports motor vehicules and parts	CAN	v183471	v1001826757	1988M1	
88	IMP_CONS_BP_new	Imports consumption goods	CAN	v183457	v1001826773	1988M1	5
	(Sum)	Imports consumption goods	CAN	v183458	v1001826773	1988M1	
	(Sum)	Imports consumption goods	CAN	v183459	v1001826773	1988M1	
	(Sum)	Imports consumption goods	CAN	v183460	v1001826773	1988M1	
	(Sum)	Imports consumption goods	CAN	v183462	v1001826773	1988M1	
	(Sum)	Imports consumption goods	CAN	v183463	v1001826773	1988M1	
89	USDCAD_new	Exchange rate CADUSD	CAN	v37426	v111666275	2017M1	5
90	JPYCAD_new	Exchange rate CADJPY	CAN	v37456	v111666258	2017M1	5
91	GBPCAD_new	Exchange rate CADGBP	CAN	v37430	v111666274	2017M1	5
92	CAN_EQTY_NETFLOW	Canadian equity and investment fund shares, net flows	CAN	v61916203			1
93	CAN_SEC_NETFLOW	Canadian securities, Net flows	CAN	v61915649			1
94	FOR_SEC_NETFLOW	Foreign securities, Net flows	CAN	v61915715			1
95	CAN_US_SEC_NETFLOW	Canadian securities, United States, Net flows	CAN	v61915862			1
		PRICES					
96	CPI_ALL_CAN	Consumption price index (CPI) (all)	CAN	v41690973			5
97	CPI_SHEL_CAN	CPI (shelter)	CAN	v41691050			5
98	CPI_CLOT_CAN	CPI (clothing and footwear)	CAN	v41691108			5
99	CPI_HEA_CAN	CPI (health and personal care)	CAN	v41691153			5
100	CPI_MINUS_FOO_CAN	CPI (all minus food)	CAN	v41691232			5
101	CPI_MINUS_FEN_CAN	CPI (all minus food and energy)	CAN	v41691233			5
102	CPI_GOO_CAN	CPI (durable goods)	CAN	v41691223			5
103	CPI_DUR_CAN	CPI (goods)	CAN	v41691222			5
104	CPI_SERV_CAN	CPI (services)	CAN	v41691230			5

No	Variable	Description	Region	Vector(1)	Vector(2)	Date	T-code
105	IPPI_CAN	Industrial production price index (IPPI) (all)	CAN	v79309114			5
106	IPPI_ENER_CAN	IPPI (energy)	CAN	v79309126			5
107	IPPI_WOOD_CAN	IPPI (wood)	CAN	v79309124			5
108	IPPI_METAL_CAN	IPPI (metal and construction materials)	CAN	v79309129			5
109	IPPI_MOTOR_CAN	IPPI (motor vehicles and parts)	CAN	v79309130			5
110	IPPI_MACH_CAN	IPPI (industrial machinery and equipment)	CAN	v79309131			5
111	WTISPLC	Petroleum price Western Intermediate (WTI) (FRED)		WTISPLC			5
		STOCK MARKETS					
112	TSX_HI	Toronto Stock Exchange (high)		v122618			5
113	TSX_LO	Toronto Stock Exchange (low)		v122619			5
114	TSX_CLO	Toronto Stock Exchange (close)		v122620			5
115	DJ_CLO	Dow Jones index (close)		v37416	DJI (YAHOO!)		5
116	SP500	Standard and Poor's (500) index (YAHOO)		GSPC			5
		PROVINCIAL / REGIONAL SERIES					
		HOUSING AND CONSTRUCTION					
117	NHOUSE_P_NF	New housing price index, Total (house and land)	NF	v111955448			5
118	NHOUSE_P_PEI	New housing price index, Total (house and land)	PEI	v111955454			5
119	NHOUSE_P_NS	New housing price index, Total (house and land)	NS	v111955460			5
120	NHOUSE_P_NB	New housing price index, Total (house and land)	NB	v111955466			5
121	NHOUSE_P_QC	New housing price index, Total (house and land)	QC	v111955472			5
122	NHOUSE_P_ONT	New housing price index, Total (house and land)	ONT	v111955490			5
123	NHOUSE_P_MAN	New housing price index, Total (house and land)	MAN	v111955526			5
124	NHOUSE_P_SAS	New housing price index, Total (house and land)	SAS	v111955532			5
125	NHOUSE_P_ALB	New housing price index, Total (house and land)	ALB	v111955541			5
126	NHOUSE_P_BC	New housing price index, Total (house and land)	BC	v111955550			5
127	hstart_NF_new	Housing starts (units)	NF	v730402	v52300159	1990M1	2
128	hstart_PEI_new	Housing starts (units)	PEI	v730403	v52300160	1990M1	2
129	hstart_NS_new	Housing starts (units)	NS	v730404	v52300161	1990M1	5
130	hstart_NB_new	Housing starts (units)	NB	v730405	v52300162	1990M1	2
131	hstart_QC_new	Housing starts (units)	QC	v730406	v52300163	1990M1	5
132	hstart_ONT_new	Housing starts (units)	ONT	v730407	v52300164	1990M1	5
133	hstart_MAN_new	Housing starts (units)	MAN	v730409	v52300166	1990M1	2
134	hstart_SAS_new	Housing starts (units)	SAS	v730410	v52300167	1990M1	5
135	hstart_ALB_new	Housing starts (units)	ALB	v730411	v52300168	1990M1	5
136	hstart_BC_new	Housing starts (units)	BC	v730412	v52300169	1990M1	5
137	build_Total_NF_new	Building permits (tous)	NF	v42094	v121314755	2011M1	5
138	build_Ind_NF_new	Building permits (industries)	NF	v42097	v121323155	2011M1	2
139	build_Comm_NF_new	Building permits (commerce)	NF	v42098	v121326275	2011M1	5
140	build_Total_PEI_new	Building permits (tous)	PEI	v42106	v121336115	2011M1	5
141	build_Ind_PEI_new	Building permits (industries)	PEI	v42109	v121344515	2011M1	2
142	build_Comm_PEI_new	Building permits (commerce)	PEI	v42110	v121347635	2011M1	5
143	build_Total_NS_new	Building permits (tous)	NS	v42112	v121357475	2011M1	5
144	build_Ind_NS_new	Building permits (industries)	NS	v42115	v121365875	2011M1	5
145	build_Comm_NS_new	Building permits (commerce)	NS	v42116	v121368995	2011M1	5
146	build_Total_NB_new	Building permits (tous)	NB	v42118	v121378835	2011M1	5
147	build_Ind_NB_new	Building permits (industries)	NB	v42122	v121387235	2011M1	2
148	build_Comm_NB_new	Building permits (commerce)	NB	v42123	v121390355	2011M1	5
149	build_Total_QC_new	Building permits (tous)	QC	v42163	v121400195	2011M1	5
150	build_Ind_QC_new	Building permits (industries)	QC	v42166	v121408595	2011M1	5
151	build_Comm_QC_new	Building permits (commerce)	QC	v42167	v121411715	2011M1	5
152	build_Total_ONT_new	Building permits (tous)	ONT	v42199	v121421555	2011M1	5
153	build_Ind_ONT_new	Building permits (industries)	ONT	v42202	v121429955	2011M1	5
154	build_Comm_ONT_new	Building permits (commerce)	ONT	v42203	v121433075	2011M1	5
155	build_Total_MAN_new	Building permits (tous)	MAN	v42124	v121442915	2011M1	5
156	build_Ind_MAN_new	Building permits (industries)	MAN	v42128	v121451315	2011M1	5
157	build_Comm_MAN_new	Building permits (commerce)	MAN	v42129	v121454435	2011M1	5

No	Variable	Description	Region	Vector(1)	Vector(2)	Date	T-code
158	build_Total_SAS_new	Building permits (tous)	SAS	v42130	v121464275	2011M1	5
159	build_Ind_SAS_new	Building permits (industries)	SAS	v42133	v121472675	2011M1	5
160	build_Comm_SAS_new	Building permits (commerce)	SAS	v42134	v121475795	2011M1	5
161	build_Total_ALB_new	Building permits (tous)	ALB	v42136	v121485635	2011M1	5
162	build_Ind_ALB_new	Building permits (industries)	ALB	v42139	v121494035	2011M1	5
163	build_Comm_ALB_new	Building permits (commerce)	ALB	v42140	v121497155	2011M1	5
164	build_Total_BC_new	Building permits (tous)	BC	v42250	v121506995	2011M1	5
165	build_Ind_BC_new	Building permits (industries)	BC	v42253	v121515395	2011M1	5
166	build_Comm_BC_new	Building permits (commerce)	BC	v42254	v121518515	2011M1	5
		LABOR MARKET					
167	EMP_NF	Employment total	NF	v2057622			5
168	EMP_SERV_NF	Employment services	NF	v2057629			5
169	EMP_FOR_OIL_NF	Employment forestry, fishing, mining, oil and gas	NF	v2057625			5
170	EMP_CONS_NF	Employment construction	NF	v2057627			5
171	EMP_SALES_NF	Employment sales (wholesale and retail trade)	NF	v2057630			5
172	EMP_FIN_NF	Employment finance, insurance and real estate	NF	v2057632			5
173	EMP_MANU_NF	Employment manufacturing	NF	v2057628			5
174	EMP_PEI	Employment total	PEI	v2057641			5
175	EMP_SERV_PEI	Employment services	PEI	v2057648			5
176	EMP_FOR_OIL_PEI	Employment forestry, fishing, mining, oil and gas	PEI	v2057644			5
177	EMP_CONS_PEI	Employment construction	PEI	v2057646			5
178	EMP_SALES_PEI	Employment sales (wholesale and retail trade)	PEI	v2057649			5
179	EMP_FIN_PEI	Employment finance, insurance and real estate	PEI	v2057651			5
180	EMP_MANU_PEI	Employment manufacturing	PEI	v2057647			5
181	EMP_NS	Employment total	NS	v2057660			5
182	EMP_SERV_NS	Employment services	NS	v2057667			5
183	EMP_FOR_OIL_NS	Employment forestry, fishing, mining, oil and gas	NS	v2057663			5
184	EMP_CONS_NS	Employment construction	NS	v2057665			5
185	EMP_SALES_NS	Employment sales (wholesale and retail trade)	NS	v2057668			5
186	EMP_FIN_NS	Employment finance, insurance and real estate	NS	v2057670			5
187	EMP_MANU_NS	Employment manufacturing	NS	v2057666			5
188	EMP_NB	Employment total	NB	v2057679			5
189	EMP_SERV_NB	Employment services	NB	v2057686			5
190	EMP_FOR_OIL_NB	Employment forestry, fishing, mining, oil and gas	NB	v2057682			5
191	EMP_CONS_NB	Employment construction	NB	v2057684			5
192	EMP_SALES_NB	Employment sales (wholesale and retail trade)	NB	v2057687			5
193	EMP_FIN_NB	Employment finance, insurance and real estate	NB	v2057689			5
194	EMP_MANU_NB	Employment manufacturing	NB	v2057685			5
195	EMP_QC	Employment total	QC	v2057698			5
196	EMP_SERV_QC	Employment services	QC	v2057705			5
197	EMP_FOR_OIL_QC	Employment forestry, fishing, mining, oil and gas	QC	v2057701			5
198	EMP_CONS_QC	Employment construction	QC	v2057703			5
199	EMP_SALES_QC	Employment sales (wholesale and retail trade)	QC	v2057706			5
200	EMP_FIN_QC	Employment finance, insurance and real estate	QC	v2057708			5
201	EMP_MANU_QC	Employment manufacturing	QC	v2057704			5
202	EMP_ONT	Employment total	ONT	v2057717			5
203	EMP_SERV_ONT	Employment services	ONT	v2057724			5
204	EMP_FOR_OIL_ONT	Employment forestry, fishing, mining, oil and gas	ONT	v2057720			5
205	EMP_CONS_ONT	Employment construction	ONT	v2057722			5
206	EMP_SALES_ONT	Employment sales (wholesale and retail trade)	ONT	v2057725			5
207	EMP_FIN_ONT	Employment finance, insurance and real estate	ONT	v2057727			5
208	EMP_MANU_ONT	Employment manufacturing	ONT	v2057723			5
209	EMP_MAN	Employment total	MAN	v2057736			5
210	EMP_SERV_MAN	Employment services	MAN	v2057743			5
211	EMP_FOR_OIL_MAN	Employment forestry, fishing, mining, oil and gas	MAN	v2057739			5
212	EMP_CONS_MAN	Employment construction	MAN	v2057741			5

No	Variable	Description	Region	Vector(1)	Vector(2)	Date	T-code
213	EMP_SALES_MAN	Employment sales (wholesale and retail trade)	MAN	v2057744			5
214	EMP_FIN_MAN	Employment finance, insurance and real estate	MAN	v2057746			5
215	EMP_MANU_MAN	Employment manufacturing	MAN	v2057742			5
216	EMP_SAS	Employment total	SAS	v2057755			5
217	EMP_SERV_SAS	Employment services	SAS	v2057762			5
218	EMP_FOR_OIL_SAS	Employment forestry, fishing, mining, oil and gas	SAS	v2057758			5
219	EMP_CONS_SAS	Employment construction	SAS	v2057760			5
220	EMP_SALES_SAS	Employment sales (wholesale and retail trade)	SAS	v2057763			5
221	EMP_FIN_SAS	Employment finance, insurance and real estate	SAS	v2057765			5
222	EMP_MANU_SAS	Employment manufacturing	SAS	v2057761			5
223	EMP_ALB	Employment total	ALB	v2057774			5
224	EMP_SERV_ALB	Employment services	ALB	v2057781			5
225	EMP_FOR_OIL_ALB	Employment forestry, fishing, mining, oil and gas	ALB	v2057777			5
226	EMP_CONS_ALB	Employment construction	ALB	v2057779			5
227	EMP_SALES_ALB	Employment sales (wholesale and retail trade)	ALB	v2057782			5
228	EMP_FIN_ALB	Employment finance, insurance and real estate	ALB	v2057784			5
229	EMP_MANU_ALB	Employment manufacturing	ALB	v2057780			5
230	EMP_BC	Employment total	BC	v2057793			5
231	EMP_SERV_BC	Employment services	BC	v2057800			5
232	EMP_FOR_OIL_BC	Employment forestry, fishing, mining, oil and gas	BC	v2057796			5
233	EMP_CONS_BC	Employment construction	BC	v2057798			5
234	EMP_SALES_BC	Employment sales (wholesale and retail trade)	BC	v2057801			5
235	EMP_FIN_BC	Employment finance, insurance and real estate	BC	v2057803			5
236	EMP_MANU_BC	Employment manufacturing	BC	v2057799			5
237	UNEMP_NF	Unemployment rate	NF	v2063004			2
238	UNEMP_PEI	Unemployment rate	PEI	v2063193			2
239	UNEMP_NS	Unemployment rate	NS	v2063382			2
240	UNEMP_NB	Unemployment rate	NB	v2063571			2
241	UNEMP_QC	Unemployment rate	QC	v2063760			2
242	UNEMP_ONT	Unemployment rate	ONT	v2063949			2
243	UNEMP_MAN	Unemployment rate	MAN	v2064138			2
244	UNEMP_SAS	Unemployment rate	SAS	v2064327			2
245	UNEMP_ALB	Unemployment rate	ALB	v2064516			2
246	UNEMP_BC	Unemployment rate	BC	v2064705			2
247	EMP_PART_NF	Employment part time	NF	v2063002			5
248	EMP_PART_PEI	Employment part time	PEI	v2063191			5
249	EMP_PART_NS	Employment part time	NS	v2063380			5
250	EMP_PART_NB	Employment part time	NB	v2063569			5
251	EMP_PART_QC	Employment part time	QC	v2063758			5
252	EMP_PART_ONT	Employment part time	ONT	v2063947			5
253	EMP_PART_MAN	Employment part time	MAN	v2064136			5
254	EMP_PART_SAS	Employment part time	SAS	v2064325			5
255	EMP_PART_ALB	Employment part time	ALB	v2064514			5
256	EMP_PART_BC	Employment part time	BC	v2064703			5
257	UNEMP_DURAvg_NF_new	Unemployment average duration	NF	v3434211	v1078669579		5
258	UNEMP_DURAvg_PEI_new	Unemployment average duration	PEI	v3434535	v1078670767		5
259	UNEMP_DURAvg_NS_new	Unemployment average duration	NS	v3434859	v1078671955		5
260	UNEMP_DURAvg_NB_new	Unemployment average duration	NB	v3435183	v1078673143		5
261	UNEMP_DURAvg_QC_new	Unemployment average duration	QC	v3435507	v1078674331		5
262	UNEMP_DURAvg_ONT_new	Unemployment average duration	ONT	v3435831	v1078675519		5
263	UNEMP_DURAvg_MAN_new	Unemployment average duration	MAN	v3436155	v1078676707		5
264	UNEMP_DURAvg_SAS_new	Unemployment average duration	SAS	v3436479	v1078677895		5
265	UNEMP_DURAvg_ALB_new	Unemployment average duration	ALB	v3436803	v1078679083		5
266	UNEMP_DURAvg_BC_new	Unemployment average duration	BC	v3437127	v1078680271		5
267	CLAIMS_NF	Employment insurance initial claims, Allowed	NF	v383943			1
268	CLAIMS_PEI	Employment insurance initial claims, Allowed	PEI	v383948			1

No	Variable	Description	Region	Vector(1)	Vector(2)	Date	T-code
269	CLAIMS_NS	Employment insurance initial claims, Allowed	NS	v383949			1
270	CLAIMS_NB	Employment insurance initial claims, Allowed	NB	v383950			1
271	CLAIMS_QC	Employment insurance initial claims, Allowed	QC	v383951			1
272	CLAIMS_ONT	Employment insurance initial claims, Allowed	ONT	v383952			1
273	CLAIMS_MAN	Employment insurance initial claims, Allowed	MAN	v383953			1
274	CLAIMS_SAS	Employment insurance initial claims, Allowed	SAS	v383954			1
275	CLAIMS_ALB	Employment insurance initial claims, Allowed	ALB	v383955			1
276	CLAIMS_BC	Employment insurance initial claims, Allowed	BC	v383944			1
		MANUFACTURING, SALES AND INVENTORIES					
277	MANU_NF_new	Manufacturing new orders (total)	NF	v727515	v803786	1992M1	5
278	DUR_NF_new	Manufacturing new orders (durables)	NF	v727527	v803799	1992M1	5
279	MANU_PEI_new	Manufacturing new orders (total)	PEI	v727539	v804246	1992M1	5
280	DUR_PEI_new	Manufacturing new orders (durables)	PEI	v727551	v804259	1992M1	5
281	MANU_NS_new	Manufacturing new orders (total)	NS	v727563	v804706	1992M1	5
282	DUR_NS_new	Manufacturing new orders (durables)	NS	v727577	v804719	1992M1	5
283	MANU_NB_new	Manufacturing new orders (total)	NB	v727591	v805166	1992M1	5
284	DUR_NB_new	Manufacturing new orders (durables)	NB	v727605	v805179	1992M1	5
285	MANU_QC_new	Manufacturing new orders (total)	QC	v727617	v805626	1992M1	5
286	DUR_QC_new	Manufacturing new orders (durables)	QC	v727632	v805639	1992M1	5
287	MANU_ONT_new	Manufacturing new orders (total)	ONT	v727646	v806086	1992M1	5
288	DUR_ONT_new	Manufacturing new orders (durables)	ONT	v727661	v806099	1992M1	5
289	MANU_MAN_new	Manufacturing new orders (total)	MAN	v727675	v806546	1992M1	5
290	DUR_MAN_new	Manufacturing new orders (durables)	MAN	v727689	v806559	1992M1	5
291	MANU_SAS_new	Manufacturing new orders (total)	SAS	v727703	v807006	1992M1	5
292	DUR_SAS_new	Manufacturing new orders (durables)	SAS	v727716	v807019	1992M1	5
293	MANU_ALB_new	Manufacturing new orders (total)	ALB	v727729	v807466	1992M1	5
294	DUR_ALB_new	Manufacturing new orders (durables)	ALB	v727743	v807479	1992M1	5
295	MANU_BC_new	Manufacturing new orders (total)	BC	v727756	v807928	1992M1	5
296	DUR_BC_new	Manufacturing new orders (durables)	BC	v727770	v807941	1992M1	5
		PRICES					
297	CPI_ALL_NF	Consumption price index (CPI) (all)	NF	v41691244			5
298	CPI_SHEL_NF	CPI (shelter)	NF	v41691277			5
299	CPI_CLOT_NF	CPI (clothing and footwear)	NF	v41691304			5
300	CPI_HEA_NF	CPI (health and personal care)	NF	v41691328			5
301	CPI_MINUS_FOO_NF	CPI (all minus food)	NF	v41691368			5
302	CPI_MINUS_FEN_NF	CPI (all minus food and energy)	NF	v41691369			5
303	CPI_GOO_NF	CPI (goods)	NF	v41691363			5
304	CPI_DUR_NF	CPI (durable goods)	NF	v41691364			5
305	CPI_SERV_NF	CPI (services)	NF	v41691367			5
306	CPI_ALL_PEI	Consumption price index (CPI) (all)	PEI	v41691379			5
307	CPI_SHEL_PEI	CPI (shelter)	PEI	v41691412			5
308	CPI_CLOT_PEI	CPI (clothing and footwear)	PEI	v41691439			5
309	CPI_HEA_PEI	CPI (health and personal care)	PEI	v41691462			5
310	CPI_MINUS_FOO_PEI	CPI (all minus food)	PEI	v41691502			5
311	CPI_MINUS_FEN_PEI	CPI (all minus food and energy)	PEI	v41691503			5
312	CPI_GOO_PEI	CPI (goods)	PEI	v41691497			5
313	CPI_DUR_PEI	CPI (durable goods)	PEI	v41691498			5
314	CPI_SERV_PEI	CPI (services)	PEI	v41691501			5
315	CPI_ALL_NS	Consumption price index (CPI) (all)	NS	v41691513			5
316	CPI_SHEL_NS	CPI (shelter)	NS	v41691546			5
317	CPI_CLOT_NS	CPI (clothing and footwear)	NS	v41691573			5
318	CPI_HEA_NS	CPI (health and personal care)	NS	v41691597			5
319	CPI_MINUS_FOO_NS	CPI (all minus food)	NS	v41691637			5
320	CPI_MINUS_FEN_NS	CPI (all minus food and energy)	NS	v41691638			5
321	CPI_GOO_NS	CPI (goods)	NS	v41691632			5
322	CPI_DUR_NS	CPI (durable goods)	NS	v41691633			5

No	Variable	Description	Region	Vector(1)	Vector(2)	Date	T-code
323	CPI_SERV_NS	CPI (services)	NS	v41691636			5
324	CPI_ALL_NB	Consumption price index (CPI) (all)	NB	v41691648			5
325	CPI_SHEL_NB	CPI (shelter)	NB	v41691681			5
326	CPI_CLOT_NB	CPI (clothing and footwear)	NB	v41691708			5
327	CPI_HEA_NB	CPI (health and personal care)	NB	v41691732			5
328	CPI_MINUS_FOO_NB	CPI (all minus food)	NB	v41691772			5
329	CPI_MINUS_FEN_NB	CPI (all minus food and energy)	NB	v41691773			5
330	CPI_GOO_NB	CPI (goods)	NB	v41691767			5
331	CPI_DUR_NB	CPI (durable goods)	NB	v41691768			5
332	CPI_SERV_NB	CPI (services)	NB	v41691771			5
333	CPI_ALL_QC	Consumption price index (CPI) (all)	QC	v41691783			5
334	CPI_SHEL_QC	CPI (shelter)	QC	v41691816			5
335	CPI_CLOT_QC	CPI (clothing and footwear)	QC	v41691844			5
336	CPI_HEA_QC	CPI (health and personal care)	QC	v41691868			5
337	CPI_MINUS_FOO_QC	CPI (all minus food)	QC	v41691908			5
338	CPI_MINUS_FEN_QC	CPI (all minus food and energy)	QC	v41691909			5
339	CPI_GOO_QC	CPI (goods)	QC	v41691903			5
340	CPI_DUR_QC	CPI (durable goods)	QC	v41691904			5
341	CPI_SERV_QC	CPI (services)	QC	v41691907			5
342	CPI_ALL_ONT	Consumption price index (CPI) (all)	ONT	v41691919			5
343	CPI_SHEL_ONT	CPI (shelter)	ONT	v41691952			5
344	CPI_CLOT_ONT	CPI (clothing and footwear)	ONT	v41691980			5
345	CPI_HEA_ONT	CPI (health and personal care)	ONT	v41692004			5
346	CPI_MINUS_FOO_ONT	CPI (all minus food)	ONT	v41692044			5
347	CPI_MINUS_FEN_ONT	CPI (all minus food and energy)	ONT	v41692045			5
348	CPI_GOO_ONT	CPI (goods)	ONT	v41692039			5
349	CPI_DUR_ONT	CPI (durable goods)	ONT	v41692040			5
350	CPI_SERV_ONT	CPI (services)	ONT	v41692043			5
351	CPI_ALL_MAN	Consumption price index (CPI) (all)	MAN	v41692055			5
352	CPI_SHEL_MAN	CPI (shelter)	MAN	v41692088			5
353	CPI_CLOT_MAN	CPI (clothing and footwear)	MAN	v41692116			5
354	CPI_HEA_MAN	CPI (health and personal care)	MAN	v41692140			5
355	CPI_MINUS_FOO_MAN	CPI (all minus food)	MAN	v41692180			5
356	CPI_MINUS_FEN_MAN	CPI (all minus food and energy)	MAN	v41692181			5
357	CPI_GOO_MAN	CPI (goods)	MAN	v41692175			5
358	CPI_DUR_MAN	CPI (durable goods)	MAN	v41692176			5
359	CPI_SERV_MAN	CPI (services)	MAN	v41692179			5
360	CPI_ALL_SAS	Consumption price index (CPI) (all)	SAS	v41692191			5
361	CPI_SHEL_SAS	CPI (shelter)	SAS	v41692224			5
362	CPI_CLOT_SAS	CPI (clothing and footwear)	SAS	v41692252			5
363	CPI_HEA_SAS	CPI (health and personal care)	SAS	v41692276			5
364	CPI_MINUS_FOO_SAS	CPI (all minus food)	SAS	v41692316			5
365	CPI_MINUS_FEN_SAS	CPI (all minus food and energy)	SAS	v41692317			5
366	CPI_GOO_SAS	CPI (goods)	SAS	v41692311			5
367	CPI_DUR_SAS	CPI (durable goods)	SAS	v41692312			5
368	CPI_SERV_SAS	CPI (services)	SAS	v41692315			5
369	CPI_ALL_ALB	Consumption price index (CPI) (all)	ALB	v41692327			5
370	CPI_SHEL_ALB	CPI (shelter)	ALB	v41692360			5
371	CPI_CLOT_ALB	CPI (clothing and footwear)	ALB	v41692387			5
372	CPI_HEA_ALB	CPI (health and personal care)	ALB	v41692411			5
373	CPI_MINUS_FOO_ALB	CPI (all minus food)	ALB	v41692451			5
374	CPI_MINUS_FEN_ALB	CPI (all minus food and energy)	ALB	v41692452			5
375	CPI_GOO_ALB	CPI (goods)	ALB	v41692446			5
376	CPI_DUR_ALB	CPI (durable goods)	ALB	v41692447			5
377	CPI_SERV_ALB	CPI (services)	ALB	v41692450			5
378	CPI_ALL_BC	Consumption price index (CPI) (all)	BC	v41692462			5

No	Variable	Description	Region	Vector(1)	Vector(2)	Date	T-code
379	CPI_SHEL_BC	CPI (shelter)	BC	v41692495			5
380	CPI_CLOT_BC	CPI (clothing and footwear)	BC	v41692523			5
381	CPI_HEA_BC	CPI (health and personal care)	BC	v41692547			5
382	CPI_MINUS_FOO_BC	CPI (all minus food)	BC	v41692587			5
383	CPI_MINUS_FEN_BC	CPI (all minus food and energy)	BC	v41692588			5
384	CPI_GOO_BC	CPI (goods)	BC	v41692582			5
385	CPI_DUR_BC	CPI (durable goods)	BC	v41692583			5
386	CPI_SERV_BC	CPI (services)	BC	v41692586			5

BIBLIOGRAPHY

Acemoglu, D. and Scott, A. (1997). Asymmetric business cycles: Theory and time-series evidence i. *Journal of Monetary Economics*, *40*, 501–533.

Adams, P. A., Adrian, T., Boyarchenko, N. and Giannone, D. (2021). Forecasting macroeconomic risks. *International Journal of Forecasting*, *37*, 1173–1191. http://dx.doi.org/10.1016/j.ijforecast.2021.01.003

Adrian, T. and Boyarchenko, N. (2012). Intermediary leverage cycles and financial stability. Retrieved from http://hdl.handle.net/10419/62944

Adrian, T., Boyarchenko, N. and Giannone, D. (2019). Vulnerable growth. *The American Economic Review*, *109*, 1263–1289. http://dx.doi.org/10.1257/aer.20161923

Ahn, S. C. and Horenstein, A. R. (2013). Eigenvalue ratio test for the number of factors. *Econometrica*, *81*, 1203–1227. http://dx.doi.org/10.3982/ECTA8968

Aiyagari, S. R. and Gertler, M. (1999). "overreaction" of asset prices in general equilibrium. *Review of Economic Dynamics*, *2*, 3–35. http://dx.doi.org/10.1006/redy.1998.0053

Alessi, L., Barigozzi, M. and Capasso, M. (2010). Improved penalization for determining the number of factors in approximate factor models. *Statistics and Probability Letters*, *80*, 1806–1813. http://dx.doi.org/10.1016/j.spl.2010.08.005

Amengual, D. and Watson, M. W. (2007). Consistent estimation of the number of dynamic factors in a large n and t panel. *Journal of Business and Economic Statistics*, *25*, 91–96. http://dx.doi.org/10.1198/073500106000000585

Amisano, G. and Giannini, C. (1997). *From VAR models to Structural VAR models*, (pp. 1–28). Springer Berlin Heidelberg

Anderson, T. W. (1963). Asymptotic theory for principal component analysis. *The Annals of Mathematics and Statistics*, *34*, 122–148.

Angeletos, G.-M., Collard, F. and Dellas, H. (2020). Business cycle anatomy.

Angrist, J., Chernozhukov, V. and Fernández-Val, I. (2006). Quantile regression under misspecification, with an application to the u.s. wage structure. *Econometrica*, *74*, 539–563. http://dx.doi.org/10.1111/j.1468-0262.2006.00671.x

Azzalini, A. and Capitanio, A. (2003). Distributions generated by perturbation of symmetry with emphasis on a multivariate skew t-distribution. *Journal of the Royal Statistical Society B*, *65*, 367–389. Retrieved from https://academic.oup.com/jrsssb/article/65/2/367/7092856

Bai, J. and Ng, S. (2002). Determining the number of factors in approximate factor models. *Econometrica*, *70*, 191–221. http://dx.doi.org/10.1111/1468-0262.00273

Bai, J. and Ng, S. (2007). Determining the number of primitive shocks in factor models. *Journal of Business and Economic Statistics*, *25*, 52–60. http://dx.doi.org/10.1198/073500106000000413

Bai, J. and Ng, S. (2008). Forecasting economic time series using targeted predictors. *Journal of Econometrics*, *146*, 304–317. http://dx.doi.org/10.1016/j.jeconom.2008.08.010

Barsky, R. B., Basu, S. and Lee, K. (2015). *Whither news shocks?*, volume 29. http://dx.doi.org/10.1086/680625

Barsky, R. B., House, C. L. and Kimball, M. S. (2007). Sticky-price models and durable goods. *American Economic Review*, *97*, 984–998. http://dx.doi.org/10.1257/aer.97.3.984

Barsky, R. B. and Sims, E. R. (2011). News shocks and business cycles. *Journal of Monetary Economics*, *58*, 273–289. http://dx.doi.org/10.1016/j.jmoneco.2011.03.001. Retrieved from http://dx.doi.org/10.1016/j.jmoneco.2011.03.001

Bedock, N. and Stevanovic, D. (2017). An empirical study of credit shock transmission in a small open economy. *Canadian Journal of Economics*, *50*, 541–570. http://dx.doi.org/10.1111/caje.12269

Benhima, K. and Cordonier, R. (2022). News, sentiment and capital flows. *Journal of International Economics*, *137*, 1–33. http://dx.doi.org/10.1016/j.jinteco.2022.103621

Benigno, P. and Eggertsson, G. B. (2023). It's baaack: The surge in inflation in the 2020s and the return of the non-linear phillips curve.

Bernanke, B. S. (1983). Irreversibility, uncertainty, and cyclical investment. *Source: The Quarterly Journal of Economics*, *98*, 85–106. Retrieved from https://www.jstor.org/stable/1885568?seq=1&cid=pdf-

Bernanke, B. S. (1986). Alternative explanations of the money-income correlation. *Carnegie Rochester Conference Series on Public Policy*, *25*, 49–99.

Bernanke, B. S., Boivin, J. and Eliasz, P. (2005). Measuring the effects of monetary policy: A factor-augmented vector autoregressive (favar) approach. *Quarterly Journal of Economics*, *120*, 387–422.

Boivin, J. and Giannoni, M. P. (2006). Has monetary policy become more effective? *Review of Economics and Statistics*, *88*, 445–462. http://dx.doi.org/10.1162/rest.88.3.445

Boivin, J., Giannoni, M. P. and Stevanovic, D. (2010). Monetary transmission in a small open economy: More data, fewer puzzles.

Boivin, J., Giannoni, M. P. and Stevanović, D. (2020). Dynamic effects of credit shocks in a data-rich environment. *Journal of Business and Economic Statistics*, *38*, 272–284. http://dx.doi.org/10.1080/07350015.2018.1497507

Boivin, J. and Ng, S. (2005). Understanding and comparing factor-based forecasts. *International Journal of Central Banking*, *1*, 117–151. Retrieved from http://www.nber.org/papers/w11285

Boivin, J. and Ng, S. (2006). Are more data always better for factor analysis? *Journal of Econometrics*, *132*, 169–194. http://dx.doi.org/10.1016/j.jeconom.2005.01.027

Bouakez, H., Chihi, F. and Normandin, M. (2014). Measuring the effects of fiscal policy. *Journal of Economic Dynamics and Control*, *47*, 123–151. http://dx.doi.org/10.1016/j.jedc.2014.08.004

Bouakez, H. and Kemoe, L. (2023). News shocks, business cycles, and the disinflation puzzle. *Journal of Money, Credit and Banking*, *55*, 2115–2151. http://dx.doi.org/10.1111/jmcb.12939

Bouakez, H. and Normandin, M. (2010). Fluctuations in the foreign exchange market: How important are monetary policy shocks? *Journal of International Economics*, *81*, 139–153. http://dx.doi.org/10.1016/j.jinteco.2009.11.007

Breiman, L. (2001). Random forests. *Machine Learning*, *45*, 5–32. http://dx.doi.org/10.1201/9780367816377-11

Brownlees, C. and Souza, A. B. (2021). Backtesting global growth-at-risk. *Journal of Monetary Economics*, *118*, 312–330. http://dx.doi.org/10.1016/j.jmoneco.2020.11.003

Brunnermeier, M. K. and Sannikov, Y. (2014). A macroeconomic model with a financial sector. *American Economic Review*, *104*, 379–421. http://dx.doi.org/10.1257/aer.104.2.379

Bura, E. and Pfeiffer, R. (2008). On the distribution of the left singular vectors of a random matrix and its applications. *Statistics and Probability Letters*, *78*, 2275–2280. http://dx.doi.org/10.1016/j.spl.2008.01.097

Caldara, D., Cascaldi-Garcia, D., Cuba-Borda, P. and Loria, F. (2021). Understanding growth-at-risk: A markov-switching approach.

Cantelmo, A. and Melina, G. (2018). Monetary policy and the relative price of durable goods. *Journal of Economic Dynamics and Control*, *86*, 1–48. http://dx.doi.org/10.1016/j.jedc.2017.10.006

Carriero, A., Clark, T. E. and Marcellino, M. (2020). Capturing macroeconomic tail risks with bayesian vector autoregressions. http://dx.doi.org/10.26509/frbc-wp-202002r. Retrieved from https://doi.org/10.26509/frbc-wp-202002r.

Carriero, A., Clark, T. E. and Marcellino, M. (2021). Using time-varying volatility for identification in vector autoregressions: An application to endogenous uncertainty. *Journal of Econometrics*, *225*, 47–73. http://dx.doi.org/10.1016/j.jeconom.2021.07.001

Carriero, A., Clark, T. E. and Marcellino, M. (2022). Specification choices in quantile regression for empirical macroeconomics specification choices in quantile regression for empirical macroeconomics. http://dx.doi.org/

10.26509/frbc-wp-202225. Retrieved from https://doi.org/10.26509/frbc-wp-202225.

Carriero, A. and Volpicella, A. (2024). Max share identification of multiple shocks: An application to uncertainty and financial conditions. *Journal of Business and Economic Statistics*, pp. 1–13. http://dx.doi.org/10.1080/07350015.2024.2316829

Champagne, J., Poulin-Bellisle, G. and Sekkel, R. (2018). The real-time properties of the bank of canada's staff output gap estimates. *Journal of Money, Credit and Banking*, *50*, 1167–1188. http://dx.doi.org/10.1111/jmcb.12493

Champagne, J., Poulin-Bellisle, G. and Sekkel, R. (2020). Introducing the bank of canada staff economic projections database. *Journal of Applied Econometrics*, *35*, 114–129. http://dx.doi.org/10.1002/jae.2744

Champagne, J. and Sekkel, R. (2018). Changes in monetary regimes and the identification of monetary policy shocks: Narrative evidence from canada. *Journal of Monetary Economics*, *99*, 72–87. http://dx.doi.org/10.1016/j.jmoneco.2018.06.002

Chan, J. C. and Eisenstat, E. (2018). Bayesian model comparison for time-varying parameter vars with stochastic volatility. *Journal of Applied Econometrics*, *33*, 509–532. http://dx.doi.org/10.1002/jae.2617

Chan, J. C. C. and Hsiao, C. Y. L. (2014). *Estimation of Stochastic Volatility Models with Heavy Tails and Serial Dependence*, (pp. 155–176). John Wiley and Sons Inc.

Chavleishvili, S., Engle, R. F., Fahr, S., Kremer, M., Manganelli, S., Schwaab, B. and Bank., E. C. (2021). The risk management approach to macro-prudential policy.

Chavleishvili, S. and Manganelli, S. (2021). Forecasting and stress testing with quantile vector autoregression

Chen, K. and Wemy, E. (2015). Investment-specific technological changes: The source of long-run tfp fluctuations. *European Economic Review*, *80*, 230–252. http://dx.doi.org/10.1016/j.euroecorev.2015.10.002

Chen, L., Dolado, J. J. and Gonzalo, J. (2021). Quantile factor models. *Econometrica*, *89*, 875–910. http://dx.doi.org/10.3982/ecta15746

Chernozhukov, V., Fernández-Val, I. I. and Kaji, T. (2017). *Extremal Quantile Regression*, (pp. 333–362). CRC Press, (1st éd.).

Chevillon, G., Mavroeidis, S. and Zhan, Z. (2020). Robust inference in structural vector autoregressions with long-run restrictions. *Econometric Theory*, *36*, 86–121. http://dx.doi.org/10.1017/S0266466619000045

Cho, J. S., Kim, T. H. and Shin, Y. (2015). Quantile cointegration in the autoregressive distributed-lag modeling framework. *Journal of Econometrics*, *188*, 281–300. http://dx.doi.org/10.1016/j.jeconom.2015.05.003. Retrieved from http://dx.doi.org/10.1016/j.jeconom.2015.05.003

Christoffersen, P. (2004). Backtesting value-at-risk: A duration-based approach. *Journal of Financial Econometrics*, *2*, 84–108. http://dx.doi.org/10.1093/jjfinec/nbh004

Christoffersen, P., Hahn, J. and Inoue, A. (2001). Testing and comparing value-at-risk measures. *Journal of Empirical Finance*, *8*, 325–342. http://dx.doi.org/10.1016/S0927-5398(01)00025-1

Christoffersen, P. F. and Diebold, F. X. (1998). Cointegration and long-horizon forecasting. *Journal of Business and Economic Statistics*, *16*, 450–458. http://dx.doi.org/10.2307/1392613

Cogley, T. and Sargent, T. J. (2005). Drifts and volatilities: Monetary policies and outcomes in the post wwii us. *Review of Economic Dynamics*, *8*, 262–302. http://dx.doi.org/10.1016/j.red.2004.10.009

Cooley, T. F. and Leroy, S. F. (1985). Atheoretical macroeconometrics: A critique. *Journal of Monetary Economics*, *16*, 283–308. http://dx.doi.org/10.1016/0304-3932(85)90038-8

Coulombe, P. G., Leroux, M., Stevanovic, D. and Surprenant, S. (2021a). Macroeconomic data transformations matter. *International Journal of Forecasting*, *37*, 1338–1354. http://dx.doi.org/10.1016/j.ijforecast.2021.05.005

Coulombe, P. G., Leroux, M., Stevanovic, D. and Surprenant, S. (2022). How is machine learning useful for macroeconomic forecasting? *Journal of Applied Econometrics*, *37*, 920–964. http://dx.doi.org/10.1002/jae.2910

Coulombe, P. G., Marcellino, M. and Stevanović, D. (2021b). Can machine learning catch the covid-19 recession? *National Institute Economic Review*, *256*, 71–109. http://dx.doi.org/10.1017/nie.2021.10

Cross, P. and Bergevin, P. (2012). Turning points: Business cycles in canada since 1926.

de la Escosura, L. P. (2016). Mismeasuring long-run growth: the bias from splicing national accounts—the case of spain. *Cliometrica*, *10*, 251–275. http://dx.doi.org/10.1007/s11698-015-0131-4

Dedola, L. and Lippi, F. (2005). The monetary transmission mechanism: Evidence from the industries of five oecd countries. *European Economic Review*, *49*, 1543–1569. http://dx.doi.org/10.1016/j.euroecorev.2003.11.006

DiCecio, R. and Owyang, M. (2012). Identifying technology shocks in the frequency domain

Diebold, F. X. and Mariano, R. S. (1995). Comparing predictive accuracy. *Journal of Business and Economic Statistics*, *13*, 253–263. http://dx.doi.org/10.1080/07350015.1995.10524599

Dieppe, A., Francis, N. and Kindberg-Hanlon, G. (2021). The identification of dominant macroeconomic drivers: Coping with confounding shocks.

Dominguez-Torres, H. and Hierro, L. A. (2019). The regional effects of monetary policy: A survey of the empirical literature. *Journal of Economic Surveys*, *33*, 604–638. http://dx.doi.org/10.1111/joes.12288

Dufour, J.-M. (2006). Monte carlo tests with nuisance parameters: A general approach to finite-sample inference and nonstandard asymptotics. *Journal of Econometrics*, *133*, 443–477. http://dx.doi.org/10.1016/j.jeconom.2005.06.007

Dufour, J.-M. and Renault, E. (1998). Short run and long run causality in time series: Theory. *Econometrica*, *66*, 1099–1125.

Elder, J. R. and Serletis, A. (2010). Oil price uncertainty. *Journal of Money, Credit and Banking*, *42*, 1137–1159. http://dx.doi.org/10.1111/j.1538-4616.2010.00323.x

Elliott, G., Gargano, A. and Timmermann, A. (2013). Complete subset regressions. *Journal of Econometrics*, *177*, 357–373. http://dx.doi.org/10.1016/j.jeconom.2013.04.017

Engle, R. F. and Manganelli, S. (2004). Caviar: Conditional autoregressive value at risk by regression quantiles. *Journal of Business and Economic Statistics*, *22*, 367–381. http://dx.doi.org/10.1198/073500104000000370

Erceg, C. and Levin, A. (2006). Optimal monetary policy with durable consumption goods. *Journal of Monetary Economics*, *53*, 1341–1359. http://dx.doi.org/10.1016/j.jmoneco.2005.05.005

Estrella, A. and Mishkin, F. S. (1998). Predicting u.s. recessions: Financial variables as leading indicators. *Review of Economics and Statistics*, *80*, 45–61. http://dx.doi.org/10.1162/003465398557320

Fares, J. and Srour, G. (2001). The monetary transmission mechanism at the sectoral level.

Faust, J. (1998). The robustness of identified var conclusions about money. In *Carnegie-Rochester Conference Series on Public Policy*, volume 49, pp. 207–244.

Fernald, J. G. (2014). A quarterly, utilization-adjusted series on total factor productivity

Figueres, J. M. and Jarociński, M. (2020). Vulnerable growth in the euro area: Measuring the financial conditions. *Economics Letters*, *191*. http://dx.doi.org/10.1016/j.econlet.2020.109126

Fisher, J. D. M. (2006). The dynamic effects of neutral and investment-specific technology shocks. *Journal of Political Economy*, *114*, 413–451. http://dx.doi.org/10.1086/505048

Forni, M., Gambetti, L. and Sala, L. (2014). No news in business cycles. *Economic Journal*, *124*, 1168–1191. http://dx.doi.org/10.1111/ecoj.12111

Forni, M., Gambetti, L. and Sala, L. (2021). Downside and upside uncertainty shocks.

Francis, N. and Kindberg-Hanlon, G. (2022). Signing out confounding shocks in variance-maximizing identification methods. *AEA Papers and Proceedings*, *112*, 476–480. http://dx.doi.org/10.1257/pandp.20221046

Francis, N., Owyang, M. T., Roush, J. E. and DiCecio, R. (2014). A flexible finite-horizon alternative to long-run restrictions with an application to technology shocks. *Review of Economics and Statistics*, *96*, 638–647. http://dx.doi.org/10.1162/REST_a_00406

Fève, P. and Guay, A. (2019). Sentiments in svars. *The Economic Journal*, *129*, 877–896. http://dx.doi.org/10.1111/ecoj.12580

Gaglianone, W. P., Lima, L. R., Linton, O. and Smith, D. R. (2011). Evaluating value-at-risk models via quantile regression. *Journal of Business and Economic Statistics*, *29*, 150–160. http://dx.doi.org/10.1198/jbes.2010.07318

Galbraith, J. W. and Tkacz, G. (2007). How far can forecasting models forecast? forecast content horizons for some important macroeconomic variables.

Gali, J. (1999). Technology, employment, and the business cycle: Do technology shocks explain aggregate fluctuations? *American Economic Review*, *89*, 249–271. http://dx.doi.org/10.1257/aer.89.1.249

Giacomini, R. and Rossi, B. (2010). Forecast comparisons in unstable environments. *Journal of Applied Econometrics*, *25*, 595–620. http://dx.doi.org/10.1002/jae

Giglio, S., Kelly, B. and Pruitt, S. (2016). Systemic risk and the macroeconomy: An empirical evaluation. *Journal of Financial Economics*, *119*, 457–471. http://dx.doi.org/10.1016/j.jfineco.2016.01.010

Gneiting, T. and Raftery, A. E. (2007). Strictly proper scoring rules, prediction, and estimation. *Journal of the American Statistical Association*, *102*, 359–378. http://dx.doi.org/10.1198/016214506000001437

Gneiting, T. and Ranjan, R. (2011). Comparing density forecasts using thresholdand quantile-weighted scoring rules. *Journal of Business and Economic Statistics*, *29*, 411–422. http://dx.doi.org/10.1198/jbes.2010.08110

Gospodinov, N. (2010). Inference in nearly nonstationary svar models with long-run identifying restrictions. *Journal of Business and Economic Statistics*, *28*, 1–12. http://dx.doi.org/10.1198/jbes.2009.08116

Gospodinov, N., Herrera, A. M. and Pesavento, E. (2013). Unit roots, cointegration, and pretesting in var models. *Advances in Econometrics*, *32*, 81–115. http://dx.doi.org/10.1108/S0731-9053(2013)0000031003

Gospodinov, N., Maynard, A. and Pesavento, E. (2011). Sensitivity of impulse responses to small low-frequency comovements: Reconciling the evidence on the effects of technology shocks. *Journal of Business and Economic Statistics*, *29*, 455–467. http://dx.doi.org/10.1198/jbes.2011.10042

Gosselin, M.-A. and Tkacz, G. (2001). Evaluating factor models: An application to forecasting inflation in canada.

Hallin, M. and Liška, R. (2007). Determining the number of factors in the general dynamic factor model. *Journal of the American Statistical Association*, *102*, 603–617. http://dx.doi.org/10.1198/016214506000001275

Hallin, M. and Werker, B. J. (2006). Comment. *Journal of the American Statistical Association*, *101*, 996–998. http://dx.doi.org/10.1198/016214506000000546

Hastie, T., Tibshirani, R. J. and Friedman, J. (2009). *The Elements of Statistical Learning: Data Mining, Interference, and Prediction* (second éd.). Springer Science & Business Media. http://dx.doi.org/10.1007/978-1-4419-9863-7_941

Hoerl, A. E. and Kennard, R. W. (1970). Ridge regression: Biased estimation for nonorthogonal problems. *Technometrics*, *12*, 55–67. http://dx.doi.org/10.1080/00401706.1970.10488634

Inoue, A. and Kilian, L. (2002a). Bootstrapping autoregressive processes with possible unit roots. *Econometrica*, *70*, 377–391.

Inoue, A. and Kilian, L. (2002b). Bootstrapping smooth functions of slope parameters and innovation variances in var models. *International Economic Review*, *43*, 309–332.

Iseringhausen, M. (2021). A time-varying skewness model for growth-at-risk. http://dx.doi.org/10.2852/176745

Jansen, D. W., Kishan, R. P. and Vacaflores, D. E. (2013). Sectoral effects of monetary policy: The evidence from publicly traded firms. *Southern Economic Journal*, *79*, 946–970. http://dx.doi.org/10.4284/0038-4038-2011.040

Johansen, S. (1995). *Likelihood-based inference in cointegrated vector autoregressive models*. Oxford University Press on Demand.

Kilian, L. (1998a). Small-sample confidence intervals for impulse response functions. *Review of Economics and Statistics*, *80*, 218–230. http://dx.doi.org/10.1162/003465398557465

Kilian, L. (1998b). Small-sample confidence intervals for impulse response functions. *The Review of Economics and Statistics*, *80*, 218–230.

Kilian, L. (2013). *Structural Vector Autoregressions*, (pp. 515–554). Edward Elgar.

Kilian, L. and Lütkepohl, H. (2017). *Structural Vector Autoregressive Analysis*. Cambridge University Press.

Kilian, L., Plante, M. and Richter, A. W. (2023). Estimating macroeconomic news and surprise shocks.

Kim, S., Shephard, N. and Chib, S. (1998). Stochastic volatility : Likelihood inference and comparison with arch models. *Review of Economic Studies*, *65*, 361–393.

King, R. G., Plosser, C. I., Stock, J. H. and Watson, M. W. (1991). Stochastic trends and economic fluctuations. *The American Economic Review*, *81*, 819–840.

Kipriyanov, A. (2022). Comparison of models for growth-at-risk forecasting. Retrieved from https://ssrn.com/abstract=4115853

Koenker, R. and Bassett, G. (1978). Regression quantiles. *Econometrica*, *46*, 33. http://dx.doi.org/10.2307/1913643

Koenker, R. and Machado, J. A. (1999). Goodness of fit and related inference processes for quantile regression. *Journal of the American Statistical Association*, *94*, 1296–1310. http://dx.doi.org/10.1080/01621459.1999.10473882

Koenker, R. and Xiao, Z. (2004). Unit root quantile autoregression inference. *Journal of the American Statistical Association*, *99*, 775–787. http://dx.doi.org/10.1198/016214504000001114

Koenker, R. and Xiao, Z. (2006). Rejoinder. *Journal of the American Statistical Association*, *101*, 1002–1006. http://dx.doi.org/10.1198/016214506000000726

Kotchoni, R., Leroux, M. and Stevanovic, D. (2019). Macroeconomic forecast accuracy in a data-rich environment. *Journal of Applied Econometrics*, *34*, 1050–1072. http://dx.doi.org/10.1002/jae.2725

Kronick, J. and Ambler, S. (2019). Do demographics affect monetary policy transmission in canada? *International Journal of Finance and Economics*, *24*, 787–811. http://dx.doi.org/10.1002/ijfe.1691

Kruskal, W. H. and Wallis, W. A. (1952). Use of ranks in one-criterion variance analysis. *Journal of the American Statistical Association*, *47*, 583–621. http://dx.doi.org/10.1080/01621459.1952.10483441

Kupiec, P. H. (1995). Techniques for verifying the accuracy of risk measurement models. *Journal of Derivatives*, *3*, 73–84.

Kurmann, A. and Otrok, C. (2013). News shocks and the slope of the term structure of interest rates: Reply. *American Economic Review*, *103*, 2612–2632. http://dx.doi.org/10.1257/aer.20161946

Kurmann, A. and Sims, E. R. (2021). Revisions in utilization-adjusted tfp and robust identification of news shocks. *The Review of Economics and Statistics*, *0*, 1–45. http://dx.doi.org/10.1162/rest_a_00896

Leamer, E. E. (2015). Housing really is the business cycle: What survives the lessons of 2008–09? *Journal of Money, Credit and Banking*, *47*, 43–50. http://dx.doi.org/10.1111/jmcb.12189

Levchenko, A. A. and Pandalai-Nayar, N. (2020). Tfp, news, and sentiments: The international transmission of business cycles. *Journal of the European Economic Association*, *18*, 302–341. http://dx.doi.org/10.1093/jeea/jvy044

Liang, C. and Schienle, M. (2019). Determination of vector error correction models in high dimensions. *Journal of Econometrics*, *208*, 418–441. http://dx.doi.org/10.1016/j.jeconom.2018.09.018

Liao, Z. and Phillips, P. C. B. (2015). Automated estimation of vector error correction models. *Econometric Theory*, *31*, 581–646. http://dx.doi.org/10.1017/S026646661500002X

Loria, F., Matthes, C. and Zhang, D. (2023). Modeling the macroeconomy in risky times.

López-Salido, D. and Loria, F. (2020). Inflation at risk

Lütkepohl, H. (2005). *A New Introduction to Multiple Time Series*. Springer-Verlag. Retrieved from https://www.m-culture.go.th/mculture_th/download/king9/Glossary_about_HM_King_Bhumibol_Adulyadej's_Funeral.pdf

Lütkepohl, H. and Velinov, A. (2016). Structural vector autoregressions: Checking identifying long-run restrictions via heteroskedasticity. *Journal of Economic Surveys*, *30*, 377–392. http://dx.doi.org/10.1111/joes.12100

Manzan, S. (2015). Forecasting the distribution of economic variables in a data-rich environment. *Journal of Business and Economic Statistics*, *33*, 144–164. http://dx.doi.org/10.1080/07350015.2014.937436

Manzan, S. and Zerom, D. (2013). Are macroeconomic variables useful for forecasting the distribution of u.s. inflation? *International Journal of Forecasting*, *29*, 469–478. http://dx.doi.org/10.1016/j.ijforecast.2013.01.005

McCracken, M. and Ng, S. (2020). Fred-qd: A quarterly database for macroeconomic research. http://dx.doi.org/10.3386/w26872

McCracken, M. W. and Ng, S. (2016). Fred-md: A monthly database for macroeconomic research. *Journal of Business and Economic Statistics*, *34*, 574–589. http://dx.doi.org/10.1080/07350015.2015.1086655

McDonald, R. and Siegel, D. (1986). The value of waiting to invest. *Source: The Quarterly Journal of Economics*, *101*, 707–728. Retrieved from https://about.jstor.org/terms

Medeiros, M. C., Vasconcelos, G. F., Álvaro Veiga and Zilberman, E. (2019). Forecasting inflation in a data-rich environment: The benefits of machine learning methods. *Journal of Business and Economic Statistics*, *0*, 1–45. http://dx.doi.org/10.1080/07350015.2019.1637745. Retrieved from https://doi.org/10.1080/07350015.2019.1637745

Micossi, S. (2015). The monetary policy of the european central bank.

Mihov, I. (2001). Monetary policy implementation and transmission in the european monetary union. *Economic Policy*, pp. 369–406.

Mincer, J. A. and Zarnowitz, V. (1969). *The Evaluation of Economic Forecasts and Expectations*, (pp. 3–46). NBER.

Montes-Rojas, G. (2021). Estimating impulse-response functions for macroeconomic models using directional quantiles. *Journal of Time Series Econometrics*, pp. 1–27. http://dx.doi.org/10.1080/15551020902995363

Moran, K., Stevanovic, D. and Touré, A. K. (2022). Macroeconomic uncertainty and the covid-19 pandemic: Measure and impacts on the canadian economy. *Canadian Journal of Economics/Revue canadienne d'économique*, *55*, 379–405. http://dx.doi.org/10.1111/caje.12551

Moreno, A. D. L. F. (2014). A "mixed" splicing procedure for economic time series. *Estadistica Espanola*, *56*, 107–121.

Mumtaz, H., Pinter, G. and Theodoridis, K. (2018). What do vars tell us about the impact of a credit supply shock? *International Economic Review*, *59*, 625–646. http://dx.doi.org/10.1111/iere.12282

Mumtaz, H. and Theodoridis, K. (2023). The federal reserve's implicit inflation target and macroeconomic dynamics: An svar analysis. *International Economic Review*, *64*, 1749–1775. http://dx.doi.org/10.1111/iere.12638

Normandin, M. and Phaneuf, L. (2004). Monetary policy shocks: Testing identification conditions under time-varying conditional volatility. *Journal of Monetary Economics*, *51*, 1217–1243. http://dx.doi.org/10.1016/j.jmoneco.2003.11.002

Onatski, A. (2010). Determining the number of factors from empirical distribution of eigenvalues. *Review of Economics and Statistics*, *92*, 1004–1016. http://dx.doi.org/10.1162/REST_a_00043

Peersman, G. and Smets, F. (2005). The industry effects of monetary policy in the euro area. *The Economic Journal*, *115*, 319–342. http://dx.doi.org/10.1111/j.1468-0297.2005.00991.x

Phillips, P. C. B. (1998). Impulse response and forecast error variance asymptotics in nonstationary vars. *Journal of Econometrics*, *83*, 21–56. http://dx.doi.org/10.1016/S0304-4076(97)00064-X

Plagborg-Moller, M., Reichlin, L., Ricco, G. and Hasenzagl, T. (2020). When is growth at risk? *Brookings Papers on Economic Activity*, pp. 167–213. http://dx.doi.org/10.2307/26996625

Plagborg-Møller, M. and Wolf, C. K. (2019). Local projections and vars estimate the same impulse responses.

Pope, A. L. (1990). Biases of estimators in multivariate non-gaussian autoregressions. *Journal of Time Series Analysis*, *11*, 249–258.

Primiceri, G. E. (2005). Time varying structural vector autoregressions and monetary policy. *Review of Economic Studies*, *72*, 821–852. Retrieved from https://academic.oup.com/restud/article/72/3/821/1556589

Romer, C. D. and Romer, D. H. (2004). A new measure of monetary shocks: Derivation and implications. *American Economic Review*, *90*, 429–457.

Ruzicka, J. (2021). Dynamic quantile causal inference and forecasting. pp. 1–149.

Serletis, A. and Gogas, P. (2014). Divisia monetary aggregates, the great ratios, and classical money demand functions. *Journal of Money, Credit and Banking*, *46*, 229–241. http://dx.doi.org/10.1111/jmcb.12103

Sims, C. A. (1980a). Comparison of interwar and postwar business cycles: Monetarism reconsidered. *American Economic Review*, *70*, 250–257.

Sims, C. A. (1980b). Macroeconomics and reality. *Econometrica*, *48*, 1–48. http://dx.doi.org/10.2307/2223855

Sims, C. A., Stock, J. H. and Watson, M. W. (1990). Inference in linear time series models with some unit roots. *Econometrica*, *58*, 113. http://dx.doi.org/10.2307/2938337

Stevanovic, D. (2015). Factor-augmented autoregressive distributed lag model with macroeconomic applications.

Sties, M. (2017). Forecasting recessions in a big data environment. pp. 1–88.

Stock, J. and Watson, M. (1998). A comparison of linear and nonlinear univariate models for forecasting macroeconomic time series. http://dx.doi.org/10.3386/w6607

Stock, J. H. and Watson, M. W. (2002a). Forecasting using principal components from a large number of predictors. *Journal of the American Statistical Association*, *97*, 1167–1179. http://dx.doi.org/10.1198/016214502388618960

Stock, J. H. and Watson, M. W. (2002b). Macroeconomic forecasting using diffusion indexes. *Journal of Business and Economic Statistics*, *20*, 147–162. http://dx.doi.org/10.1198/073500102317351921

Stock, J. H. and Watson, M. W. (2016). *Dynamic Factor Models, Factor-Augmented Vector Autoregressions, and Structural Vector Autoregressions in Macroeconomics*, (pp. 415–526). North-Holland.

Takongmo, C. O. M. and Stevanovic, D. (2016). Selection of the number of factors in presence of structural instability: A monte carlo study. *L'Actualité économique*, *91*, 177–233. http://dx.doi.org/10.7202/1036919ar

Tibshirani, R. J. (1996). Regression shrinkage and selection via the lasso. *Journal of the Royal Statistical Society: Series B (Methodological)*, *58*, 267–288.

Tyler, D. E. (1981). Asymptotic inference for eigenvectors. *Annals of Statistics*, *9*, 725–736.

Uhlig, H. (2003). What moves real gnp?

Uhlig, H. (2004). Do technology shocks lead to a fall in total hours worked? *Journal of the European Economic Association*, *2*, 361–371. http://dx.doi.org/10.1162/154247604323068050

Whelan, K. (2002). A guide to us chain aggregated nipa data. *Review of Income and Wealth*, *48*, 217–233.

White, H., Kim, T.-H. and Manganelli, S. (2015). Var for var: Measuring tail dependence using multivariate regression quantiles. *Journal of Econometrics*, *187*, 169–188. http://dx.doi.org/10.1016/j.jeconom.2015.02.004

Xiao, Z. (2009). Quantile cointegrating regression. *Journal of Econometrics*, *150*, 248–260. http://dx.doi.org/10.1016/j.jeconom.2008.12.005

Zeev, N. B. and Khan, H. (2015). Investment-specific news shocks and u.s. business cycles. *Journal of Money, Credit and Banking*, *47*, 1443–1464. http://dx.doi.org/10.1111/jmcb.12250

Zou, H. (2006). The adaptive lasso and its oracle properties. *Journal of the American Statistical Association*, *101*, 1418–1429. http://dx.doi.org/10.1198/016214506000000735

Zou, H. and Hastie, T. (2005). Regularization and variable selection via the elastic net. *Journal of the Royal Statistical Society Series B: Statistical Methodology*, *67*, 301–320. http://dx.doi.org/10.1111/j.1467-9868.2005.00503.x

Òscar Jordà (2005). Estimation and inference of impulse responses by local projections. *American Economic Review*, *95*, 161–182. http://dx.doi.org/10.1257/0002828053828518